Stabilization of 3D DNA Nanostructures for *In Vivo* Applications and Developing an Assay to Estimate Stability

by

Saswata Banerjee

A Dissertation Presented in Partial Fulfillment
of the Requirements for the Degree
Doctor of Philosophy

Approved March 2018 by the
Graduate Supervisory Committee:

Hao Yan, Co-Chair
Yan Liu
Austen Angell
Neal Woodbury

ARIZONA STATE UNIVERSITY

May 2018

ABSTRACT

Though DNA nanostructures (DNs) have become interesting subjects of drug delivery, *in vivo* imaging and biosensor research, however, for real biological applications, they should be 'long circulating' in blood. One of the crucial requirements for DN stability is high salt concentration (like ~5–20 mM Mg^{2+}) that is unavailable in a cell culture medium or in blood. Hence DNs denature promptly when injected into living systems. Another important factor is the presence of nucleases that cause fast degradation of unprotected DNs. The third factor is 'opsonization' which is the immune process by which phagocytes target foreign particles introduced into the bloodstream. The primary aim of this thesis is to design strategies that can improve the *in vivo* stability of DNs, thus improving their pharmacodynamics and biodistribution.

Several strategies were investigated to address the three previously mentioned limitations. The first attempt was to study the effect length and conformation of polyethylene glycol (PEG) on DN stability. DNs were also coated with PEG-lipid and human serum albumin (HSA) and their stealth efficiencies were compared. The findings reveal that both PEGylation and albumin coating enhance low salt stability, increase resistance towards nuclease action and reduce uptake of DNs by macrophages. Any protective coating around a DN increases its hydrodynamic radius, which is a crucial parameter influencing their clearance. Keeping this in mind, intrinsically stable DNs that can survive low salt concentration without any polymer coating were built. Several DNA compaction agents and DNA binders were screened to stabilize DNs in low magnesium

conditions. Among them arginine, lysine, bis-lysine and hexamine cobalt showed the potential to enhance DN stability.

This thesis also presents a sensitive assay, the Proximity Ligation Assay (PLA), for the estimation of DN stability with time. It requires very simple modifications on the DNs and it can yield precise results from a very small amount of sample. The applicability of PLA was successfully tested on several DNs ranging from a simple wireframe tetrahedron to a 3D origami and the protocol to collect *in vivo* samples, isolate the DNs and measure their stability was developed.

To

Dibbendu

Apu

ACKNOWLEDGEMENTS

This section of my thesis, with an obvious intrinsicality of being lengthy and thankful, should undoubtedly begin with my advisors Dr. Hao Yan and Dr. Yan Liu. They have been amazingly helpful, patient and encouraging through the period of my doctoral research. It is for them that I have had the opportunity to explore, learn and contemplate over serious matters of science independently. A stride towards this degree, in particular, in not only about unimpeded funds and research ideas, but something more, like an unspoken vibe of assurance from the advisor in times of struggle, which I received whenever required. Thank you, Hao. Thanks, Yan.

I would also like to thank Dr. Milan Stojanovic and his research group at Columbia University with whom I had been collaborating almost since the beginning of my Ph.D. Milan has taught me how to develop a deep and multi-directional view towards a problem and to look for intelligent and simple solutions employing basic knowledge. I am especially thankful to Dr. Nenad Milosavic from the Stojanovic group who has been my closest collaborator through these years. Thanks Nenad for your time, energy and spirit on our projects and also for the long hours of discussion on an often irksome skype!

Apu, Subhasish, Mamoni, Pishimoni, Baba, Ma, Buru and Moni, thank you for being with and within me. You have inspirited each and every attempt of mine and accepted even the most trivial achievement ceremoniously. I and Dibbendu started this journey amidst molecules and equations together. Without him, I would have halted somewhere in the midway. Each and every moment I feel to be in harmony with this dearest friend of mine. My hours of darkness have always been enlightened by Raju and Rivu. At this

juncture, how could I forget Subhradeep and Sweta who had always stood firm by me, unquestionably, in times of sorrow and delight? You have filled my life with a divine fragrance and an eternal light. I owe a lot to you. Thanking you all in words is like drenching a river with her own waters! I also remember my teachers Mr. Debasish Mondal and Dr. Chandan Saha, who had instilled in me the affection for chemistry. Without them, unguided and confused, I might have traversed some other path leading to a completely different story of life.

I would like to express my gratitude towards the committee members Dr. Neal Woodbury and Dr. Austen Angell and eventually, I want to thank all the members of the Center for Molecular Design and Biomimetics who had made my journey of doctoral research smooth and lively. Among my research group members, I would specially mention Swarup, who has always been extremely helpful, supportive and caring as a colleague, friend and dear brother. I will, forever, remember our long discussions and moments of precious silence, debates over matters of science, politics and philanthropy, and the joyful outings, that have wrapped past few years my stay in Tempe with homely warmth. Thank you, Swarup.

TABLE OF CONTENTS

Page

LIST OF TABLES x

LIST OF FIGURES xi

CHAPTER

1 OVERVIEW OF DRUG DELIVERY SYSTEMS AND DNA NANOSTRUCTURES 1

1.1 Introduction to Drug Delivery Systems (DDSs) 1

1.1.1 DDS 1

1.1.2 Advanced DDS 1

1.1.3 Enhanced Permeability and Retention (EPR) effect and Targeting DDS 4

1.2 Properties of an Efficient DDS 6

1.3 Polyethylene Glycol (PEG) and its Effect on *In Vivo* Lifetime of Nanocarriers 7

1.4 DNA Nanotechnology 8

1.5 DNs in Nanomedicine 9

1.6 Stability of DNs 10

1.7 Overview of the Projects 12

1.8 References 18

2 EFFECT OF PEG LENGTH AND CONFORMATION AND PEG- LIPID COATING ON STABILITY AND CELLULAR UPTAKE OF DNA NANOSTRUCTURES 23

CHAPTER Page

2.1 Abstract 23

2.2 Introduction 24

2.3 Results and Discussion 27

2.3.1 Building PEG-conjugated DNs 27

2.3.2 Stability in Physiological Conditions 29

2.3.3 Confocal Microscopy 32

2.3.4 Uptake of DNs by Macrophages 36

2.3.4.1 Cellular Uptake without Plasma or Clusterin Incubation 36

2.3.4.2 Effects of Plasma and Clusterin Incubation 40

2.3.4.3 Effect of PEG-lipid Coating 43

2.4 Conclusion 45

2.5 References 47

3 ENHANCING LOW SALT STABILITY OF DNA NANOSTRUCTURES USING FREE STABILIZING AGENTS 50

3.1 Abstract 50

3.2 Introduction 50

3.3 Results and Discussion 55

3.3.1 Designing the DNs 55

3.3.2 Screening of Stabilizing Agents 56

3.3.3 Estimation of Stability Enhancement 60

3.3.4 Combination of Stabilizing Agents 63

3.3.5 Melting Temperature of DNs 66

CHAPTER Page

3.4 Conclusion 67

3.5 References 69

4 BUILDING ALBUMIN-COATED DNA NANOSTRUCTURES FOR *IN VIVO* APPLICATIONS 71

4.1 Abstract 72

4.2 Introduction 74

4.3 Results and Discussion 74

4.3.1 Building the DNs 74

4.3.2 Synthesis of Albumin Attracting Molecule (AAM) 76

4.3.3 Conjugation of Serum Albumin to DNA 77

4.3.4 Coating DNA Nanostructures with Serum Albumin 78

4.3.5 Stability of Albumin-coated Structures in Physiological Conditions ..79

4.3.6 Confocal Microscopy 81

4.3.7 Cellular Uptake of Albumin-coated DNs 86

4.4. Conclusion 88

4.5 References 89

5 PROXIMITY LIGATION ASSAY TO ESTIMATE THE STABILITY OF DNA NANOSTRUCTURES 91

5.1 Abstract 91

5.2 Introduction 92

5.3 Results and Discussion 97

5.3.1 PLA on Antennae with Phosphodiester Backbone 97

CHAPTER Page

5.3.2 PLA on Antennae with Phosphorothioate Backbone.....100

5.3.3 Time vs Stability studies *In Vitro* 101

5.3.4 Time vs Stability Studies *In Vivo*.....103

5.4 Conclusion 105

5.5 References.....106

6 SUMMARY AND FUTURE DIRECTIONS.....107

6.1 Summary.....107

6.2 Future Directions 108

REFERENCES 113

APPENDIX

A SUPPLEMENTAL INFORMATION FOR CHAPTER 2.....124

B SUPPLEMENTAL INFORMATION FOR CHAPTER 3.....171

C SUPPLEMENTAL INFORMATION FOR CHAPTER 4.....216

D SUPPLEMENTAL INFORMATION FOR CHAPTER 5.....264

LIST OF TABLES

Table Page

1. List of Potential Stabilizing Agents Screened.....57

2. Maximum Concentration of Each Stabilizing Agent that Allow the Formation of DN1.....59

3. Concentration Titration of Combination of Stabilizing Agents.....64

LIST OF FIGURES

Figure Page

1.1. Schematics of a Targeted DDS 2

1.2. Some Common Carriers used in Nanomedicine 4

1.3. Different Types of PEGs. a) Linear, and b) Branched 8

1.4. Effects on PEGylation and PEG-lipid Conjugation on Stability and Cellular Uptake of DNs. 13

1.5. Enhancing Stability of DNA Nanostructures in Low Salt Conditions by Using Free Stabilizing Agents.....15

1.6. Albumin Attracting Molecule (AAM) 16

1.7. Coating DNA Nanostructures with Serum Albumin to Enhance Stability and Reduce Uptake by Macrophages 16

1.8 Proximity Ligation Assay on DNs.....17

2.1. a) Td b) DNO 28

2.2. Stability of Td in DMEM Supplemented with 10% FBS. A) Plotting Concentration of Td and Different PEG-coated Tds with Time B) Comparison of Half-Lives of Bare Td and Different PEG-coated Tds.....30

2.3. Stability of DNO in DMEM Supplemented with 10% FBS. A) Plotting Concentration of DNO And Different PEG-coated DNOs with Time B) Comparison of Half-Lives of DNO and Different PEG-coated DNOs 31

Figure Page

2.4. Confocal Microscopy Images Of RAW Cells Incubated with Alexa Fluor 488 Labeled Td Followed by DNase Treatment. The Cell Membranes Were Stained with CellTracker CM-Dil Dye 33

2.5 Z-Stacked Confocal Microscopy Images Of RAW Cells Incubated With Alexa Fluor 488 Labeled Td Followed by DNase Treatment.....34

2.6. Confocal Microscopy Images of RAW Cells Incubated with Alexa Fluor 488 Labeled Td–5L Followed by DNase Treatment 34

2.7. Z-Stacked Confocal Microscopy Images of RAW Cells Incubated With Alexa Fluor 488 Labeled Td Followed by DNase Treatment 35

2.8. Confocal Microscopy Images of RAW Cells Incubated with Alexa Fluor 488 Labeled Td–5L Followed by DNase Treatment 35

2.9. Z-Stacked Confocal Microscopy Images of RAW Cells Incubated With Alexa Fluor488 Labeled Td Followed by DNase Treatment 36

2.10. Comparing Fluorescence Intensity of DNase Treated and Untreated Controls 37

2.11. Comparing Fluorescence Intensities from Internalized Linear PEG-coated DNs 38

2.12. Effect of PEG Branching on Cellular Uptake of DNs. a) Td b) DNO 39

Figure Page

2.13. Effect of Plasma and Clusterin Incubation on Cellular Uptake of Bare DNs. a) Td b) DNO.....40

2.14. Effect of Plasma and Clusterin Incubation on Cellular Uptake of Linear PEG-coated DNs. a) Td b) DNO.....41

2.15. Effect of Plasma and Clusterin Incubation on Cellular Uptake of Branched PEG-coated DNs. a) Td b) DNO 43

2.16. Effect of PEG-Lipid Coating on Cellular Uptake of DNs. a) Td b) DNO 45

3.1. DNA Nanostructures Studied. a) DN1 b) DN2 c) DN3.....55

3.2. Comparison of DN1 Half-Lives Formed with and without Free Stabilizing Agents 61

3.3. Comparison of Half-Lives of All Three DNs Formed with and without Free Stabilizing Agents.....62

3.4. Comparison of DN1 Half-Lives Formed with Single and Combined Stabilizing Agents 64

3.5. Comparison of DN2 Half-Lives Formed with Single and Combined Stabilizing Agents 65

3.6. Comparison of DN3 Half-Lives Formed With Single and Combined Stabilizing Agents 65

Figure Page

3.7. Melting Temperatures of Three DNs When Formed with Different Stabilizing Agents and Their Combinations 66

4.1. Albumin Attracting Molecule (SP141C) 74

4.2. a) Td b) DNO 75

4.3. Scheme Showing the Synthesis of AAM (SP141C).....76

4.4. HSA Binding of S5-AAM 78

4.5. HSA Coating of a) Td b) DNO 79

4.6. Time vs Stability of a) Bare Td b) HSA-coated Td 80

4.7. Half-Lives of Coated and Uncoated DNs 80

4.8. Confocal Microscopy Images of RAW Cells Incubated with Alexa Fluor 488 Labeled Td 83

4.9. Z-Stacked Confocal Microscopy Images of RAW Cells Incubated with Alexa Fluor 488 Labeled Td.....83

4.10. Confocal Microscopy Images of RAW Cells Incubated with Alexa Fluor 488 Labeled Td Followed by DNase Treatment.....85

4.11. Z-Stacked Confocal Microscopy Images of RAW Cells Incubated With Alexa Fluor 488 Labeled Td Followed by DNase Treatment 84

4.12. Confocal Microscopy Images of RAW Cells Incubated with Alexa Fluor 488

Figure Page

Labeled HSA-Coated Td.....84

4.13. Z-Stacked Confocal Microscopy Images of RAW Cells Incubated With Alexa Fluor 488 Labeled HSA-coated Td.....85

4.14. Confocal Microscopy Images of RAW Cells Incubated With Alexa Fluor 488 Labeled HSA-coated Td. The Cells were Treated with DNase after Incubation 85

4.15. Z-Stacked Confocal Microscopy Images of RAW Cells Incubated with Alexa Fluor 488 Labeled HSA-coated Td. The Cells were Treated with DNase after Incubation. 86

4.16. Comparing Fluorescence Intensity of DNase Treated and Untreated Controls.....87

4.17. Cellular Uptake of Bare and Albumin-coated DNs.....90

5.1. Proximity Ligation Assay Design on a DNA Tetrahedron.....96

5.2. PLA on TdP2. 97

5.3. PLA on TdP4. 98

5.4. a) TD b) DNC. 99

5.5. PLA on TDP24. 100

5.6. PLA on DNC with Various Inter-antennae Distances. 100

Figure Page

5.7. Comparison of PLA Results Obtained from A) TdS2 And B) DNCS2. 101

5.8. PLA Results From *In Vitro* TdP2 Samples. a) Particles/μL Plotted with Time b) Comparison of Half-lives. 103

5.9. Time vs Stability Curve for TdP2 from *In Vivo* Sample. 104

5.10. Time vs Stability Curve for TdS2 from *In Vivo* Sample. 104

CHAPTER 1

DRUG DELIVERY SYSTEMS AND DNA NANOSTRUCTURES

1.1 Introduction to Drug Delivery Systems (DDS)

1.1.1 DDS

The application of nanotechnology in medicine has opened up a new arena of research called 'nanomedicine' and in the recent years this field has given an emphasis on development of drug-loaded nanocarriers like the nanoparticles (NPs), liposomes and micelles. These nanocarriers, commonly termed as DDS, are being developed to combat serious threats like neurodegenerative disorders, cancer, *etc*. In principle, DDS alter several of the pharmacological properties of the conventional 'free' drugs. They are designed to improve the pharmacokinetics and biodistribution of drug molecules associated to them. In addition, they often act as drug reservoirs enabling sustained release of the drugs *in vivo*.

1.1.2 Advanced DDS

The advanced DDS have two basic features: they can target drugs to specific sites inside the body and the release rates of the drug from the vehicle can be precisely controlled for prolonged time. There has been remarkable advancement in the research and marketing of advanced DDS in the past few decades. They improve drug delivery by allowing the following features: a) keeping drug levels in a therapeutically desirable range inside the body continuously, b) allowing usage of a decreased amount of drug in comparison to previous methods in use, c) reduce number of dosages

and allow less invasive dosing, d) reduction of harmful side effects by targeted to the desired sites, and e) making possible the administration of less stable (low in vivo half-lives) drugs.[1]

The nanoparticulate systems used for drug delivery have diameters from 1 to 1000 nm and they are made up of a variety of materials like inorganic materials, polymers, and lipids. Hence they have varying physiochemical properties and are suited to different applications.

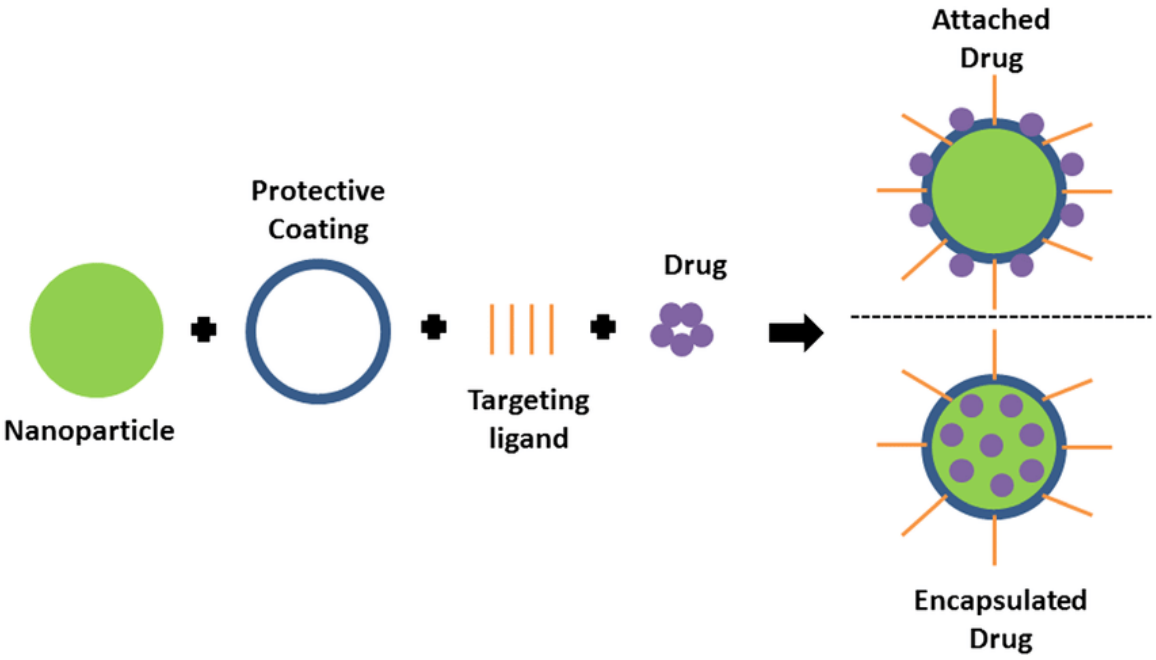

***Figure 1.1*:** Schematics of a targeted DDS.[2] Two different strategies for cargo loading are shown.

However, most of the DDS currently approved for parenteral administration can be classified into two groups: a) polymer based systems, and b) lipid based systems. The lipid based systems are the liposomes and different lipid-based formulations while the polymer based systems are mostly drug molecules conjugated to PEG. One well known DDS available in market is a PEGylated liposomal doxorubicin (Doxil / Caelyx). These polymer based colloidal systems have drawn much interest due to reasons like the flexibility in macromolecular synthetic methods, the

incredible diversity of polymers with respect to their nature, composition, properties and scopes (ease and diversity) of functionalization.[3]

The mechanisms by which these DDS deliver the drugs are basically of three types: a) diffusion of drug molecules from the system, b) cleavage of drug from DDS or a chemical or enzymatic degradation of the delivery system, and c) activation of the system by solvent. A combined functioning of these three mechanisms is also possible.

A. Polymer based DDS

The polymer based DDS can be classified into three major types: a) polymeric micelles, b) polymersomes, and c) NPs. Polymeric micelles are formed by self-assembly of amphiphilic block copolymers in aqueous solution.[4] They are a combination of hydrophobic core and hydrophilic outer shell. Hydrophobic drugs are contained in the core that is stabilized by the hydrophilic shell.[5] Till date, micelles are the most advanced nanoparticulate systems for clinical trials.[6] They have shown considerable efficacy to deliver DNA and hydrophobic drugs and they can be functionalized by a number of ligands.[7] In the nanoparticle DDS the drug molecules are dissolved, dispersed or chemically conjugated to the constituent polymer chains.[8] The method of preparation governs whether the NP will be a nanocapsule (vesicular systems) or a nanosphere (matrix-like system). Polymersomes are the biomimetic analogs of phospholipids and the membrane is the primary feature of these nanocarriers. They confer the advantage of encapsulation of both hydrophilic and hydrophobic molecules in their aqueous cavities and membranes respectively.[9]

B. Lipid based DDS

Lipid bilayer vesicles were originally developed as a trial to mimic biological membranes.[10] Encapsulating drugs inside a vesicle instead of attaching them to a polymer chain provides the advantage of higher drug-loading capacity. Their internal aqueous compartment can be loaded with hydrophilic payloads while the phospholipid bilayer membrane can carry the hydrophobic drugs. The application of liposomes to deliver anticancer drugs is now well-established. In solid tumors the vasculature becomes leaky and the lymphatic drainage become defective, thus allowing the stealth liposomes to accumulate in them. The nanometer sized liposomes that contain doxorubicin in their aqueous compartment (Doxil, Caelyx and Myocet) are employed for Kaposi's sarcoma, ovarian cancer, and multiple myeloma.[11-14]

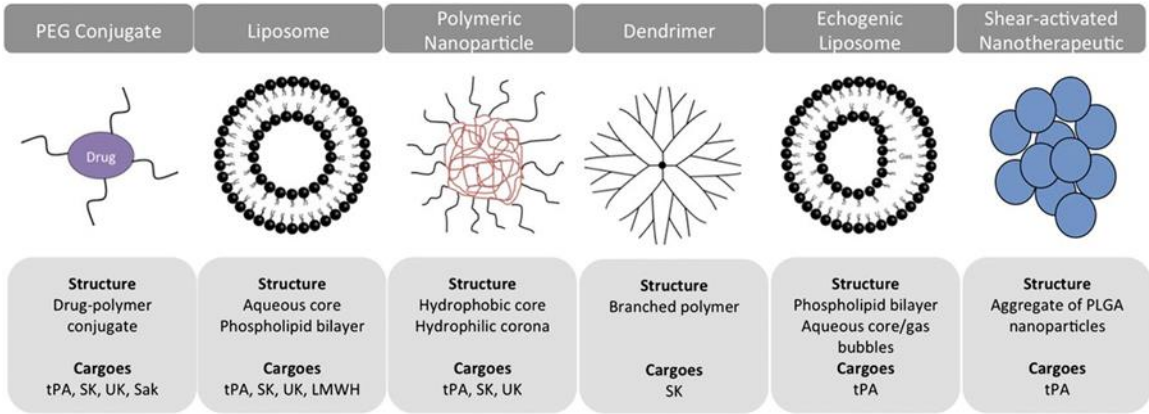

***Figure 1.2*:** Some common carriers used in nanomedicine. (These carriers have specially been tested for *in vivo* delivery of anti-thrombin agents.)[15]

1.1.3 Enhanced Permeability and Retention (EPR) Effect and Targeting DDS

Paul Enrich was awarded the Nobel Prize in medicine in 1908 as he put forward the concept of ‘magic bullet’, which is a drug that can reach and destroy the diseased cells selectively without causing any harm to the normal healthy cells.[16] This concept led to the development of targeted

nanocarriers. The fundamental aim of drug delivery is to enhance the drug concentration in the diseased site with a simultaneous reduction in the systemic exposure.[17] Several drug delivery methods have been formulated to achieve this aim, some of the most important being micelles, liposomes, antibody-directed enzyme-prodrug therapy[18], photodynamic therapy[19], affinity targeting[20], and macromolecular drug carriers.[21,22] In case of treating tumors, most of these DDS exploit the characteristic pathophysiology of the tumor vasculature. In 1920, it was found that unlike normal tissue, tumors have a high density of dilated and poorly differentiated blood vessels. These vessels have an unordered architecture and aberrant branching.[23-26] This leads to hindered functions of the tumor vasculature like enhanced permeability than normal blood vessels and increased concentration of plasma proteins in tumor tissues in comparison to the normal ones.[27-36] In addition to this there is a lack of functional lymphatic vessels in the tumor resulting in a decreased rate of clearance. Maeda and colleagues named this as the enhanced permeability and retention (EPR) effect, [37-39] which is responsible for the enhanced passive accumulation of intravenously administered macromolecules in tumors. The EPR effect is the key behind the technique of passive tumor targeting. Understanding the concept of EPR makes it clear why the PEGylation strategy is so effective in treating certain tumors. Covalent conjugation of PEG chains to nanocarriers increases circulation times, thus increasing its opportunity to reach the desired site.

However, there are instances where the vascular permeability is low like in pancreatic cancers. Also there is the phenomenon of accelerated blood clearance[40] arising from the phenomenon that repeated administering of PEGylated liposomes lead to the production of anti-PEG immunoglobulin-M induced by the first injection. Hence the liposomes are cleared off from the circulation quickly. These two situations set the basis for development of targeted drug delivery

systems that can recognize certain cells or tissues. The ligand-conjugated liposomes developed in 1980 provide the first examples of targeted DDS.[41]

1.2 Properties of an Efficient DDS

There are several factors that have to be considered for designing a DDS applicable to a particular disease, some of the very crucial ones being: a) stability b) solubility c) size (molecular weight) d) charge e) potency f) circulation time g) targeting ability h) loading mechanism i) protection of the drug molecule from premature metabolism, and j) drug release profile.

Stability of the DDS is of obvious importance and both liposomes and polymer based systems have demonstrated sufficient *in vivo* stability for real life applications. Polymers like PEG have enough *in vivo* solubility to be used as efficient DDS. The solubility of liposomes can be modified by conjugating PEG chains of varying lengths on the surface.

The size and surface charge of the nanocarriers govern the efficiency of drug delivery and determine the pathway of cellular uptake for liposomes[42], polymeric NPs[43,44], gold NPs[45], and silica NPs[46] by altering the particle adhesion and their interaction with cells[47]. He and co-workers found that murine macrophages engulf NPs with high surface charge and large particle size more efficiently.[48] Their study also showed that slightly negatively charged NPs of size 150 nm show enhanced accumulation in tumor. In addition to accumulation profiles, particle size is a significant factor in determining the *in vivo* life time of the nanocarriers. It has been found that cell membranes have a higher concentration of negative charge, so positively charged peptides (the cell penetrating peptides (CPPs)) have been used for building targeted DDS. The CPPs are less than 30 amino acids

in length and have a net positive charge. Liposomes are often conjugated with CPPs, which assist in the transfer of cargos into the cells.[49]

The amount of carriers to be used for the delivery of a certain amount of drug depends largely on the drug potency.[11] Lesser the number of drug molecules that the DDS can carry, the higher the potency of the drug must be. In cases such as immunoconjugates and immonotoxins, the DDS can carry only a few number of molecules and the polymer conjugates can carry few tens of molecules, in these cases the drug molecules should have higher potencies for delivering therapeutically relevant amounts of drug.[20]

Circulation time of a nanocarrier is simultaneously governed by several factors like its stability under physiological conditions, solubility, size etc. In order to increase circulation time, the carrier has to be prevented from opsonization. PEGylation of drug delivery vehicles has emerged as a successful strategy to render them long circulating.

1.3 Polyethylene glycol (PEG) and Its Effect on I*n Vivo* Lifetime of Nanocarriers

In 1977 Abuchowski and co-workers demonstrated that bovine serum albumin (BSA) when covalently conjugated to methoxypolyethylene glycols of 1900 and 5000 Daltons (PEG1900, PEG5000) loses immunogenicity and its half-life is circulation is enhanced.[50] During the very short period of 1990-91, there were several reports showing that PEG can be used to increase circulation times of liposomes.[51-54] Different researchers have proposed different hypotheses to explain the effect of PEG in rendering nanocarriers long circulating. According to Ilium and co-workers surface hydrophobicity plays a major role in the phagocytosis of NPs by mononuclear phagocyte system (MPS) and they demonstrated that hydrophilic coatings with poloxamers reduced MPS

uptake of colloidal particles.[55] The ether oxygen of $(CH2—CH2—O)_n$ units of PEG, being capable of hydrogen bonding with water, can also result in the formation of a highly hydrophilic surface in aqueous solution. There are hypotheses that this hydration forms of a polymer brush that extends outwards from the liposome surface, thus resulting in steric stabilization of the liposomes by bringing down attractive forces and enhancing repulsive forces at the liposome surface.[56-59] Lasic and co-workers presented a more detailed explanation about the theory of steric stabilization.[56,60,61]

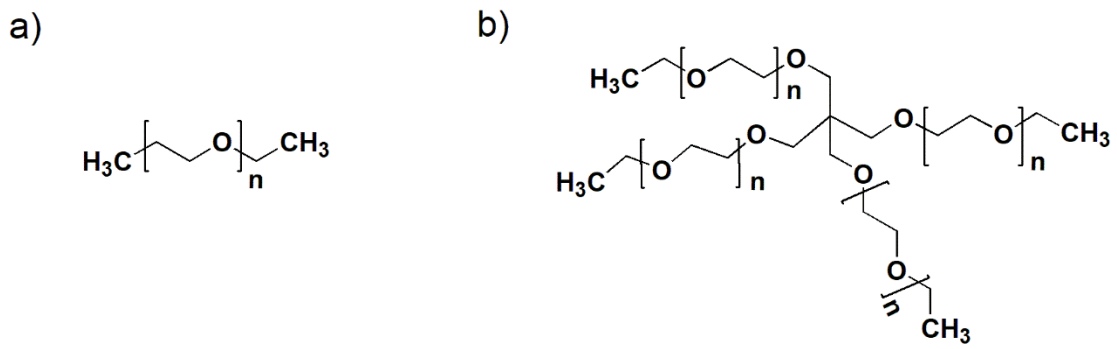

Figure 1.3: Different types of PEGs. a) Linear, and b) branched.

1.4 DNA Nanotechnology

DNA, the carrier of our genetic information, is undoubtedly one of the most widely studied biopolymers. Owing to its highly predictable base pairing, chemical stability and biocompatibility, it has become an interesting candidate for building nanometer-sized 2D and 3D structures of varying shapes, sizes and complexities.[62-65] DNA nanotechnology[66] is primarily concerned with building up novel DNs with interesting properties and look for their realistic applications. DNs can be designed to have very sophisticated capabilities like mechanical[67] and logic gating[68], which is not possible with structures build from other known nanomaterials. The excellent strategy put forward by Paul K. Rothemund in 2006, known as the 'DNA Origami'[69] has made the formation

of complex 3D structures very convenient using a single stranded long scaffold and few hundreds of smaller single stranded DNA (staples). Moreover, the distance between two consecutive bases on the phosphate backbone of a single stranded DNA being 0.34 nm and due to the availability of a library of chemical modifications separately on each base, DNA allows precise modifications every 0.34 nm long its length. This makes DNs very suitable platforms for precise spatial arrangements of interesting molecules like aptamers[70], antibodies[71], fluorophores[72], metal NPs and quantum dots[73], etc. In addition to this, reconfigurable DNs can be built and their dynamics can be controlled by external stimuli like a single stranded DNA (strand displacement), small molecule and light. All these attributes make DNs promising candidates for applications in nanoplasmonics, biosensors and drug delivery.

1.5 DNs in Nanomedicine

Nanomedicine uses nanosized materials to build platforms for gene and drug delivery.[74] With respect to size, DNs are potential candidates as cellular transport occurs at nanometer length-scale.[75] The multivalence of DNA, the diverse nature of functionalizations available and the compatibility of biological systems have drawn considerable attention of the nanomedicine researchers and DNs have been used as drug delivery vehicles in a number of reports. Douglas and co-workers have built a nanorobot that can release Fab antibody fragments in the presence of target cells.[76] A DNA tetrahedron was employed by Anderson and co-workers for *in vivo* delivery of small interfering RNA to target and suppress gene expression in a mouse model.[77] The DNs have also demonstrated their potential to serve as platforms for synthetic vaccines. Fan, Huang and co-workers assembled a multivalent DNA tetrahedron for noninvasive delivery of immunostimulatory CpG oligonucleotides.[78] Yan, Chang and co-workers have employed a DNA tetrahedron for

coassembly of model antigens and CpG with precise control over the valency and spatial arrangement of each constituent.[79]

DNs have also been employed to carry drug molecules *in vivo* either by intercalation into the carrier DNA helix or by attachment through chemical conjugation. Huang and co-workers demonstrated the application of aptamer-conjugated DNA icosahedral NPs as carriers of doxorubicin for cancer therapy.[80] In 2012, Ding and co-workers constructed 2- and 3-D doxorubicin-loaded DNs, the loading being through intercalation, and their construct showed prominent cytotoxicity to regular human breast adenocarcinoma cancer cells (MCF 7) and also to doxorubicin-resistant cancer cells.[81] In the same year, Högberg and co-workers developed DNA origami delivery systems for cancer therapy having tunable release properties.[82] Their aim was the optimal delivery of anthracycline doxorubicin (Dox) to human breast cancer cells. With varying degrees of global twists, the amounts of DN relaxation also varied. They tuned the DN design to control the encapsulation efficiency and release rate of Dox, increase the cytotoxicity and decrease the intracellular elimination rate of Dox in comparison to the free drug molecule.

1.6 Stability of DNs

Formation of DNs require a high concentration (~5-20 mM) of divalent magnesium ions in the annealing buffer and this concentration increases with rise in packing density of the structure. In absence of sufficient Mg^{2+} concentration, the phosphate backbones of DNA strands being negatively charged repel each other and thus prevent formation of packed structures. Positively charged Mg^{2+} ions screen the negative charges on the phosphodiester backbone and allow two DNA strands to come closer and form DNs. For 3D DNs at least 16 mM Mg^{2+} is required. The

physiological concentration of Mg^{2+} is almost tenfold lower than that required for formation of 3D DNs and this is a major factor limiting stability of DNs *in vivo*.

When administered in blood, DNs have to encounter nucleases that degrade them rapidly. Even in cell culture medium supplemented with fetal bovine serum, the life time of DNs is considerably reduced due to the presence of the nucleases. Protection from the nucleases is a crucial issue that needs to be addressed in order to use the DNs for *in vivo* applications.

In addition to these two issues, there is another limitation posed on the *in vivo* fate of DNs by opsonization. As soon as NPs are introduces in circulation, a series pf chemical-physical interactions are established between their surfaces and the various components of the physiological medium like phospholipids, DNA, proteins etc. Hence, NPs lose their 'synthetic identity' in no time and a new interface termed as the 'bio-nano interface' is developed around it. This interface is actually responsible for the biological fate of injected NPs.[75] DNs are also opsonized like other NPs and opsonins on their surface are promptly recognized and sequestered by macrophages. An efficient DDS based on DNs has to be retained in circulation for a minimum period of time to exert their effect. Exerting their effect might require pre-requisites like unloading of the drug from the vehicle through diffusion, hydrolysis of some covalent bond *etc*. If prior to this the delivery vehicle is removed by the excretory system, the drug will require a) a higher dosage, and / or b) very frequent dosages. Hence, to improve *in vivo* lifetime of DNs, they have to be protected beforehand, so that they can avoid rapid opsonization followed by clearance from blood in the spleen and liver.

Few reports have been published with investigations on the stability of DNs under physiological conditions. In 2014, Perrault and coworkers reported that while the denaturation of the DNs due to low salt conditions was dependent on design and time, the degradation by nucleases

is not time dependent.[83] Very recently in 2017, Shih and coworkers reported an oligolysine coating that can be applied over the DNs via electrostatic adsorption and this coating can protect them from low salt denaturation and nuclease degradation for prolonged hours.[84] However, the detailed study on how the PEG coating affects the stability of DNs and their uptake by macrophages still remains to be done.

1.7 Overview of the projects in this thesis

1.7.1 Effect of PEG Length and Conformation and PEG-lipid on Stability and Cellular Uptake of DNA Nanostructures

The conventional method of forming PEG-coated DNs is to pre-PEGylate a certain number of staples before annealing, mix them with the non-PEGylated staples and m13 scaffold and then subject the mixture to the annealing program. But PEG chains often hinder base pair recognition and thus render the DN formation kinetically demanding leading to the formation of deformed structures. So we PEGylated pre-formed DNs decorated by strained alkyne moiety (DBCO) on the surface employing the copper-free click reaction.

Then we studied the effect of three different linear PEGs of molecular weights 2 kD, 5 kD and 10 kD on the stability of two different DNs in the cell culture medium supplemented with 10% fetal bovine serum (FBS). We also investigated the effect of PEG branching on uptake of DNs by macrophages. In addition to PEG, we investigated the effect of PEG-lipid coating on the cellular uptake of DNs by macrophages. There has been reports that PEGylation alters the composition of the outer protein corona of a NP when it is introduced in blood.[85,86] It is this protein corona that affects cellular uptake of NPs. It has also been reported that the clusterin protein plays an important

role in reducing the uptake of the NPs.[87] In order to investigate this effect on DNs, we incubated PEGylated DNs with human serum and clusterin protein separately before studying cellular uptake. We found that increasing the PEG length (from 2–10 kD) led to enhancement of stability in low salt conditions and also enhanced resistance towards nucleases. The cellular uptake is also reduced as the PEG length increases. Branched PEG reduces the cellular uptake further in comparison to the linear polymers of same molecular weight. The PEG-lipid coating reduces the cellular uptake more efficiently than the only PEG polymer of equal molecular weight. Incubation with clusterin further reduces the DN uptake by macrophages; the branched PEGs being most efficient for allowing deposition of clusterin on the DN surface.

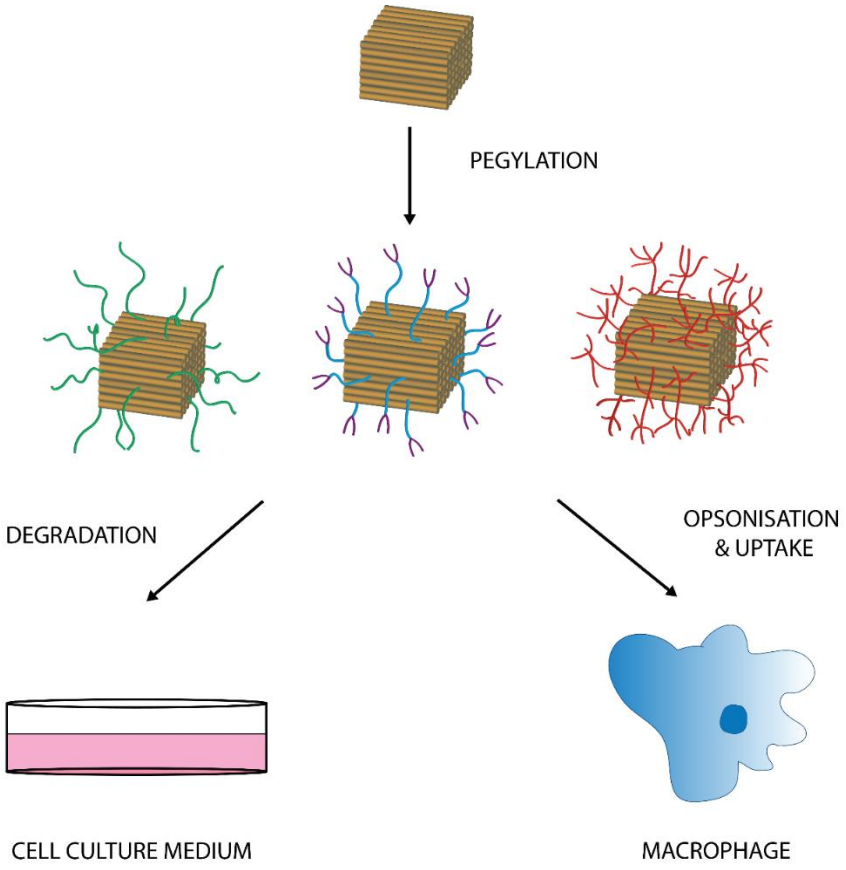

***Figure 1.4**:* Effects on PEGylation and PEG-lipid conjugation on stability and cellular uptake of DNs.

1.7.2 Enhancing Stability of DNA Nanostructures in Low Salt Conditions by Using Free Stabilizing Agents

After screening several molecules (free, not covalently conjugated to the structures) that are DNA compaction agents or DNA binders or intercalators and studying their effect on stability of 3D DNs, we found that four of them, namely arginine, lysine, bis-lysine and hexamine cobalt, can provide stability to the DNs under low salt conditions. We studied the extent of stability enhancement by using transmission electron microscopy (counting intact DNA structures using 30 nM gold NPs as internal standards), and time vs fluorescence assay. We also found that the stabilizing agents enhance the thermodynamic stability of the DNs as is reflected in their increase in melting points.

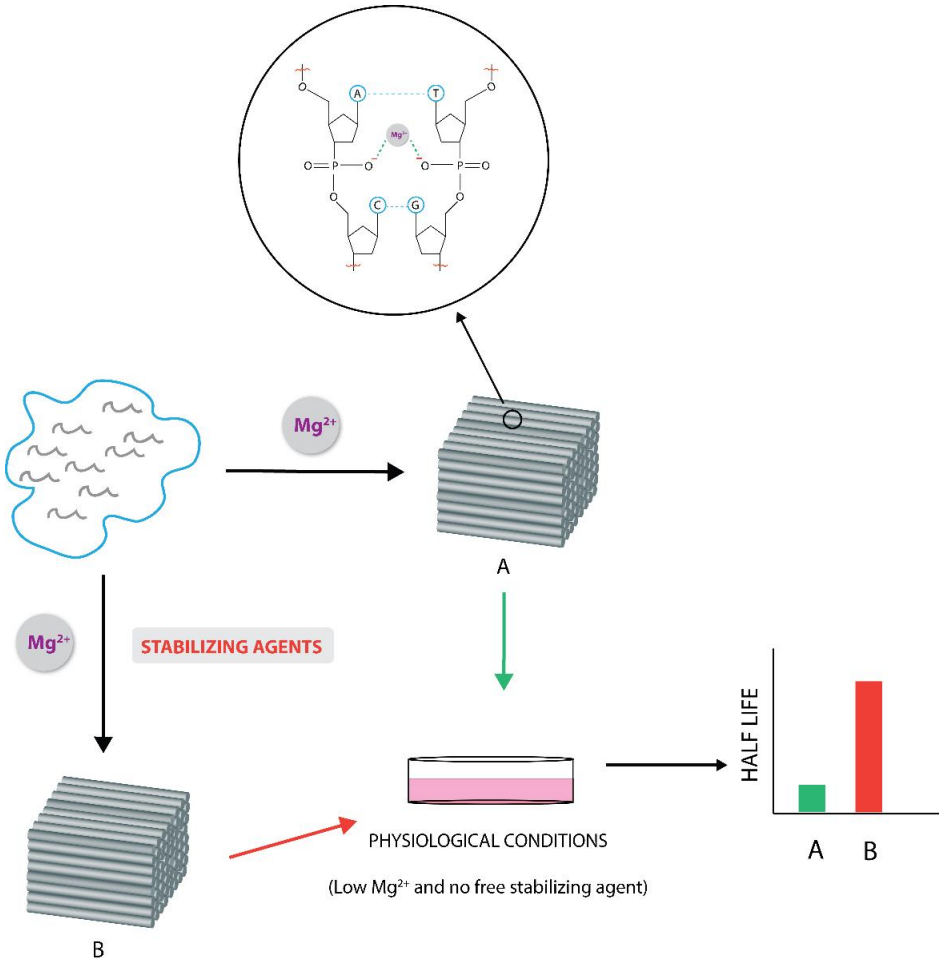

Figure 1.5: Enhancing stability of DNA nanostructures in low salt conditions by using free stabilizing agents.

1.7.3 Building Albumin-coated DNA Nanostructures for *In Vivo* Applications

Albumins are among the very common proteins found in serum. We hypothesized that if we can coat DNs with serum albumin then they would be able to maintain structural integrity in low salt conditions and also be able to avoid prompt degradation by nucleases. In addition, as their surfaces are coated by a protein familiar to the opsonins, the albumin-coated DNs will have delayed recognition by opsonins, leading to increase in their circulation times in blood. For coating DNs

we coated the DN surfaces with an albumin attracting molecule (figure 1.6) and then incubated them with normal HSA.

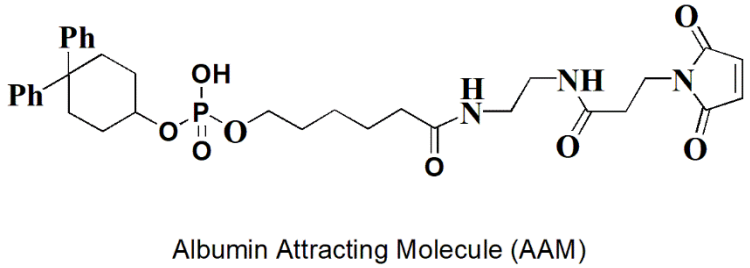

Figure 1.6: Albumin attracting molecule (AAM).

The albumin coated structures showed reduced uptake by murine macrophages and in addition to this they are found to be more resistant toward nuclease degradation (tested in the DMEM cell culture medium containing 10% FBS).

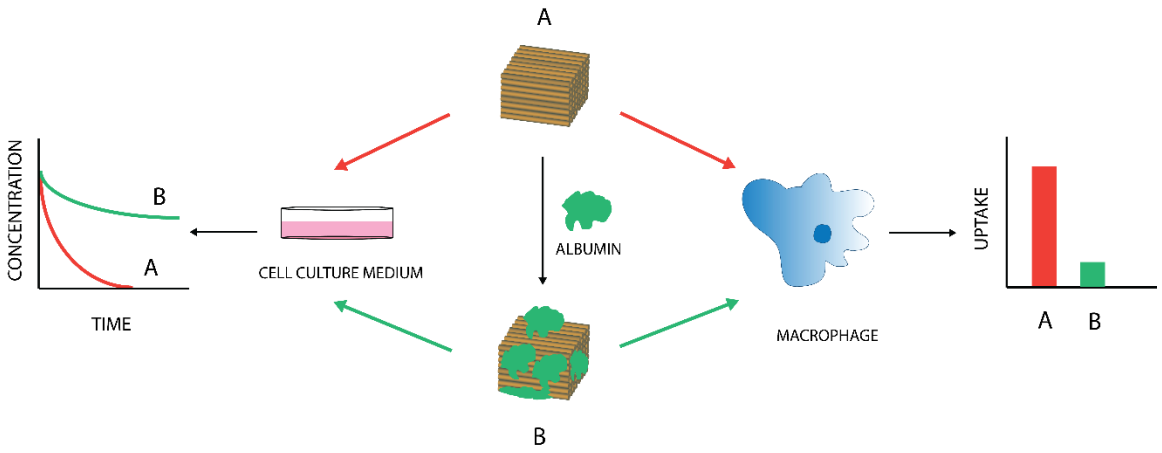

Figure 1.7: Coating DNA nanostructures with serum albumin to enhance stability and reduce uptake by macrophages.

1.7.4 Proximity ligation assay (PLA) to estimate stability of DNA Nanostructures

PLA is a well-known method for stability estimation of protein molecules. We applied that concept and studied the stability of a wireframe DNA tetrahedron (Td) reported by Tuberfield and co-workers. We developed a sensitive assay that can estimate the number of intact DNs even after administering them in blood. We subjected the Td under various conditions (buffer containing 16 mM Mg^{2+}, DMEM, DMEM containing 10% FBS and human serum and estimated the half-lives of the Td in these media. The results obtained from PLA showed matched with those obtained from electrophoretic gels. We also injected two different Tds, one having antennae pair with phosphodiester backbone and the other having antennae pair with phosphorothioate backbone, in mice and estimated their half-lives applying the PLA.

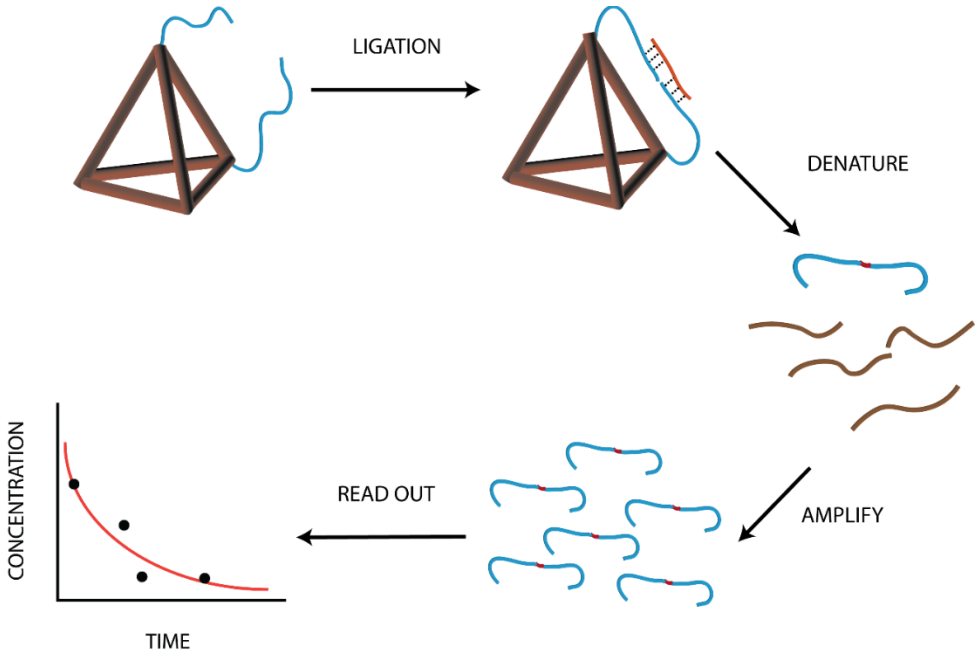

Figure 1.8: Proximity Ligation Assay on DNs.

1.8 References

1. Langer, R. In *Nature* 1998; Vol. 392, p 5.
2. McNamara, K.; Tofail, S. A. *Advances in Physics: X* **2017**, *2*, 54.
3. Nicolas, J.; Mura, S.; Brambilla, D.; Mackiewicz, N.; Couvreur, P. *Chemical Society Reviews* **2013**, *42*, 1147.
4. Peer, D.; Karp, J. M.; Hong, S.; Farokhzad, O. C.; Margalit, R.; Langer, R. *Nature nanotechnology* **2007**, *2*, 751.
5. Adams, M. L.; Lavasanifar, A.; Kwon, G. S. *Journal of pharmaceutical sciences* **2003**, *92*, 1343.
6. Oerlemans, C.; Bult, W.; Bos, M.; Storm, G.; Nijsen, J. F. W.; Hennink, W. E. *Pharmaceutical research* **2010**, *27*, 2569.
7. Kedar, U.; Phutane, P.; Shidhaye, S.; Kadam, V. *Nanomedicine: Nanotechnology, Biology and Medicine* **2010**, *6*, 714.
8. Hillaireau, H.; Couvreur, P. *Cellular and Molecular Life Sciences* **2009**, *66*, 2873.
9. Battaglia, G.; Ryan, A. J. *Journal of the American Chemical Society* **2005**, *127*, 8757.
10. Bangham, A. D. *BioEssays* **1995**, *17*, 1081.
11. Allen, T. M.; Cullis, P. R. *Science* **2004**, *303*, 1818.
12. Barenholz, Y. C. *Journal of controlled release* **2012**, *160*, 117.
13. Minisini, A. M.; Andreetta, C.; Fasola, G.; Puglisi, F. *Expert review of anticancer therapy* **2008**, *8*, 331.
14. Verma, S.; Dent, S.; Chow, B. J.; Rayson, D.; Safra, T. *Cancer treatment reviews* **2008**, *34*, 391.
15. Greineder, C. F.; Howard, M. D.; Carnemolla, R.; Cines, D. B.; Muzykantov, V. R. *Blood* **2013**, *122*, 1565.
16. Strebhardt, K.; Ullrich, A. *Nature Reviews Cancer* **2008**, *8*, 473.
17. Dreher, M. R.; Liu, W.; Michelich, C. R.; Dewhirst, M. W.; Yuan, F.; Chilkoti, A. *Journal of the National Cancer Institute* **2006**, *98*, 335.
18. Senter, P. D.; Springer, C. J. *Advanced drug delivery reviews* **2001**, *53*, 247.

19. Vrouenraets, M. B.; Visser, G.; Snow, G.; Van Dongen, G. *Anticancer research* **2003**, *23*, 505.
20. Allen, T. M. *Nature Reviews Cancer* **2002**, *2*, 750.
21. Kopeček, J.; Kopečková, P.; Minko, T.; Lu, Z.-R. *European Journal of Pharmaceutics and Biopharmaceutics* **2000**, *50*, 61.
22. Duncan, R. *Nature reviews Drug discovery* **2003**, *2*, 347.
23. Lewis, W. H. *Bull Johns Hopkins Hosp* **1927**, *41*, 156.
24. Sandison, J. *Developmental Dynamics* **1928**, *41*, 475.
25. 窶; deAG, B. *AJR Am J Roentgenol1939*, *42*, 891.
26. Algire, G. H.; Chalkley, H. W.; Earle, W. R.; Legallais, F. Y.; Park, H. D.; Shelton, E.; Schilling, E. L. **1950**.
27. Duran-Reynals, F. *The American Journal of Cancer* **1939**, *35*, 98.
28. Babson, A. L.; Winnick, T. *Cancer Research* **1954**, *14*, 606.
29. Busch, H.; Greene, H. S. *The Yale journal of biology and medicine* **1955**, *27*, 339.
30. Dewey, W. C. *American Journal of Physiology--Legacy Content* **1959**, *197*, 423.
31. Song, C. W.; Levitt, S. H. *Cancer research* **1971**, *31*, 587.
32. Underwoodand, J.; Carr, I. *The Journal of pathology* **1972**, *107*, 157.
33. Peterson, H.-I.; Appelgren, K. *European Journal of Cancer (1965)* **1973**, *9*, 543.
34. Heuser, L. S.; Miller, F. N. *Cancer* **1986**, *57*, 461.
35. Gerlowski, L. E.; Jain, R. K. *Microvascular research* **1986**, *31*, 288.
36. Dvorak, H. F.; Nagy, J. A.; Dvorak, J.; Dvorak, A. *The American journal of pathology* **1988**, *133*, 95.
37. Matsumura, Y.; Maeda, H. *Cancer research* **1986**, *46*, 6387.
38. Maeda, H.; Matsumura, Y. *Critical reviews in therapeutic drug carrier systems* **1989**, *6*, 193.
39. Maeda, H.; Seymour, L. W.; Miyamoto, Y. *Bioconjugate chemistry* **1992**, *3*, 351.
40. Ishida, T.; Kiwada, H. *International journal of pharmaceutics* **2008**, *354*, 56.
41. Elsabahy, M.; Wooley, K. L. *Chemical Society Reviews* **2012**, *41*, 2545.

42. Chono, S.; Tanino, T.; Seki, T.; Morimoto, K. *Journal of pharmacy and pharmacology* **2007**, *59*, 75.

43. Win, K. Y.; Feng, S.-S. *Biomaterials* **2005**, *26*, 2713.

44. Foged, C.; Brodin, B.; Frokjaer, S.; Sundblad, A. *International journal of pharmaceutics* **2005**, *298*, 315.

45. Chithrani, B. D.; Ghazani, A. A.; Chan, W. C. *Nano lett* **2006**, *6*, 662.

46. Lu, F.; Wu, S. H.; Hung, Y.; Mou, C. Y. *Small* **2009**, *5*, 1408.

47. Lee, K. D.; Nir, S.; Papahadjopoulos, D. *Biochemistry* **1993**, *32*, 889.

48. He, C.; Hu, Y.; Yin, L.; Tang, C.; Yin, C. *Biomaterials* **2010**, *31*, 3657.

49. Zorko, M.; Langel, Ü. *Advanced drug delivery reviews* **2005**, *57*, 529.

50. Abuchowski, A.; Van Es, T.; Palczuk, N.; Davis, F. *Journal of Biological Chemistry* **1977**, *252*, 3578.

51. Allen, T.; Redemann, C.; Yau-Young, A.; Hansen, C. In *Proceedings, 10th International Biophysics Congress, International Union of Pure and Applied Biophysics* 1990, p 312.

52. Woodle, M.; Newman, M.; Collins, L.; Martin, F. In *Biophysical Journal*; BIOPHYSICAL SOCIETY 9650 ROCKVILLE PIKE, BETHESDA, MD 20814-3998: 1990; Vol. 57, p A261.

53. Klibanov, A. L.; Maruyama, K.; Torchilin, V. P.; Huang, L. *FEBS letters* **1990**, *268*, 235.

54. Blume, G.; Cevc, G. *Biochimica et Biophysica Acta (BBA)-Biomembranes* **1990**, *1029*, 91.

55. Ilium, L.; Hunneyball, I.; Davis, S. *International journal of pharmaceutics* **1986**, *29*, 53.

56. Woodle, M. C.; Lasic, D. D. *Biochimica et Biophysica Acta (BBA)-Reviews on Biomembranes* **1992**, *1113*, 171.

57. Needham, D.; Hristova, K.; McIntosh, T.; Dewhirst, M.; Wu, N.; Lasic, D. *Journal of Liposome Research* **1992**, *2*, 411.

58. Needham, D.; McIntosh, T.; Lasic, D. *Biochimica et Biophysica Acta (BBA)-Biomembranes* **1992**, *1108*, 40.

59. Woodle, M.; Collins, L.; Sponsler, E.; Kossovsky, N.; Papahadjopoulos, D.; Martin, F. *Biophysical journal* **1992**, *61*, 902.

60. Lasic, D. D.; Woodle, M. C.; Papahadjopoulos, D. *Journal of Liposome Research* **1992**, *2*, 335.

61. Lasic, D.; Martin, F.; Gabizon, A.; Huang, S.; Papahadjopoulos, D. *Biochimica et Biophysica Acta (BBA)-Biomembranes* **1991**, *1070*, 187.

62. Douglas, S. M.; Dietz, H.; Liedl, T.; Högberg, B.; Graf, F.; Shih, W. M. *Nature* **2009**, *459*, 414.

63. Dietz, H.; Douglas, S. M.; Shih, W. M. *Science* **2009**, *325*, 725.

64. Han, D.; Pal, S.; Nangreave, J.; Deng, Z.; Liu, Y.; Yan, H. *Science* **2011**, *332*, 342.

65. Liedl, T.; Högberg, B.; Tytell, J.; Ingber, D. E.; Shih, W. M. *Nature nanotechnology* **2010**, *5*, 520.

66. Seeman, N. C. *Annual review of biochemistry* **2010**, *79*, 65.

67. Mao, C.; Sun, W.; Shen, Z.; Seeman, N. C. *Nature* **1999**, *397*, 144.

68. Seelig, G.; Soloveichik, D.; Zhang, D. Y.; Winfree, E. *science* **2006**, *314*, 1585.

69. Rothemund, P. W. *Nature* **2006**, *440*, 297.

70. Liu, Y.; Lin, C.; Li, H.; Yan, H. *Angewandte Chemie* **2005**, *117*, 4407.

71. He, Y.; Tian, Y.; Ribbe, A. E.; Mao, C. *Journal of the American Chemical Society* **2006**, *128*, 12664.

72. Dutta, P. K.; Varghese, R.; Nangreave, J.; Lin, S.; Yan, H.; Liu, Y. *Journal of the American Chemical Society* **2011**, *133*, 11985.

73. Schreiber, R.; Do, J.; Roller, E.-M.; Zhang, T.; Schüller, V. J.; Nickels, P. C.; Feldmann, J.; Liedl, T. *Nature nanotechnology* **2014**, *9*, 74.

74. Langer, R. *Nature* **1998**, *392*, 5.

75. Pozzi, D.; Colapicchioni, V.; Caracciolo, G.; Piovesana, S.; Capriotti, A. L.; Palchetti, S.; De Grossi, S.; Riccioli, A.; Amenitsch, H.; Laganà, A. *Nanoscale* **2014**, *6*, 2782.

76. Douglas, S. M.; Bachelet, I.; Church, G. M. *Science* **2012**, *335*, 831.

77. Lee, H.; Lytton-Jean, A. K.; Chen, Y.; Love, K. T.; Park, A. I.; Karagiannis, E. D.; Sehgal, A.; Querbes, W.; Zurenko, C. S.; Jayaraman, M. *Nature nanotechnology* **2012**, *7*, 389.

78. Li, J.; Pei, H.; Zhu, B.; Liang, L.; Wei, M.; He, Y.; Chen, N.; Li, D.; Huang, Q.; Fan, C. *ACS nano* **2011**, *5*, 8783.

79. Liu, X.; Xu, Y.; Yu, T.; Clifford, C.; Liu, Y.; Yan, H.; Chang, Y. *Nano letters* **2012**, *12*, 4254.

80. Chang, M.; Yang, C.-S.; Huang, D.-M. *ACS nano* **2011**, *5*, 6156.

81. Jiang, Q.; Song, C.; Nangreave, J.; Liu, X.; Lin, L.; Qiu, D.; Wang, Z.-G.; Zou, G.; Liang, X.; Yan, H. *Journal of the American Chemical Society* **2012**, *134*, 13396.

82. Zhao, Y.-X.; Shaw, A.; Zeng, X.; Benson, E.; Nyström, A. M.; Högberg, B. r. *ACS nano* **2012**, *6*, 8684.

83. Aggarwal, P.; Hall, J. B.; McLeland, C. B.; Dobrovolskaia, M. A.; McNeil, S. E. *Advanced drug delivery reviews* **2009**, *61*, 428.

84. Du, H.; Chandaroy, P.; Hui, S. W. *Biochimica et Biophysica Acta (BBA)-Biomembranes* **1997**, *1326*, 236.

85. Schöttler, S.; Becker, G.; Winzen, S.; Steinbach, T.; Mohr, K.; Landfester, K.; Mailänder, V.; Wurm, F. R. *Nature nanotechnology* **2016**, *11*, 372.

CHAPTER 2

EFFECT OF PEG LENGTH AND CONFORMATION AND PEG-LIPID COATING ON STABILITY AND CELLULAR UPTAKE OF DNA NANOSTRUCTURES

2.1 Abstract

DNA nanostructures (DNs) have become candidates of extreme interest in therapeutics and diagnostics during the last few decades, because of their ease of formation, precise control over shapes, sizes and sites of modification, and dynamic attributes responsive to simple stimuli. However enhancing the stability of DNs in low salt conditions, resisting nuclease degradation and reducing their opsonization while in circulation are crucial factors for making them suitable for *in vivo* applications. Polyethylene glycol (PEG) is widely being used as a biocompatible 'stealth' polymer that can render drug carriers like liposome long circulating. Here we studied the effect of PEG and PEG-lipid coating on the stability and macrophage uptake of DNs. We varied the length and branching of the PEG chains and studied their influence on cellular uptake. We found that increasing chain length provide higher stabilization towards low salt conditions and enhanced resistance to nuclease degradation. Branching has no observable effect on these two aspects, while higher branching showed higher efficiency towards reducing macrophage uptake of DNs in comparison to their linear isomers. We also tested the effect of plasma and clusterin incubation of the structures prior to incubation with the macrophages. Clusterin incubation highly reduces the uptake, the effect being most pronounced in case of the branched PEG-coated DNs.

2.2 Introduction

In the past few decades a significant progress has been made in nanotechnology research, as a result of which diverse nanoscopic particles with different kinds of constitution and morphology have been developed for nanomedicinal applications like tissue regeneration, *in vivo* imaging and drug delivery.[1] Paralleled with the flourishment of DNA nanotechnology, the pool of potential nanomedicine candidates have been largely enriched. This fascinating branch of nanotechnology can build biocompatible nanoscale objects with diverse structural and functional features and precisely defined modifications using DNA as the building material.[2-7] These DNA nanostructures (DNs) can be engineered employing known biochemical methods and they can demonstrate controlled dynamics in response to stimuli like small DNA strand (fuels),[8-10] pH,[11,12] enzymatic reaction, and temperature. For these myriad abilities coupled with biodegradability and biocompatibility, DNs have also been employed for biomedical applications like biosensing, *in vivo* delivery of nucleic acids like siRNAs[13], building synthetic vaccines[14] and drug delivery.[15-18]

In the current stage of development, however, *in vivo* applications of DNs are limited by certain factors, among which three are the most important. The first one is requirement of high concentration of divalent cations like Mg^{2+} (~5–20 nM) for DN formation. These ions screen negative charges on phosphodiester backbone and allows DNA single strands to come closer during DN formation. But such a high concentration of divalent ions is not available in physiological conditions like cell culture medium and blood.[19] Hence when incubated with cell culture medium or administered in circulation, the structures unfold and lose their structural integrity, a process the rapidity of which is

proportional to the packing density of the DN. The second important factor is degradation by the nucleases in both cell culture medium (supplemented with 10% FBS) and blood.[20-23] Thus, the protection of DNs from nuclease degradation before they can be employed for any tissue culture experiments or *in vivo* injections is a crucial requirement for successful nanomedicinal applications. The third element of concern is opsonization, an immune process by which a foreign particle entering bloodstream is identified to macrophages of the mononuclear phagocytic system (MPS). Various components of the complement system like C3, C4 and C5, immunoglobulins, laminin, C-reactive protein, type I collagen, fibronectin and several other proteins are known as opsonins.[24] Macrophages do not possess the capability to recognize NPs directly, but they can identify the opsonin tags attached to their surfaces.[25] The opsonins promptly bind to injected nanoparticles (NPs), leading to their recognition by macrophages which eliminate the particle from circulation within seconds of intravenous administration.[26] This phenomenon leads to severe reduction of circulation lifetime of NPs. When a NP is injected into a physiological fluid like blood, the proteins from the medium quickly adsorb on the NP surface and form a protein corona around the NP.[27] There has been several reports that claim this protein shell is actually responsible for the biological fate of NPs.[28-30]

Among the several strategies devised to camouflage NPs from macrophages until they are done performing their desired roles *in vivo*, the most common is grafting of 'stealth polymer' polyethylene glycol (PEG) to NP surfaces.[31] Reports are abundant where PEG and its various derivative have been employed to make polymeric NPs and liposomes 'long circulating' in the circulation. The exact and complete mechanism of opsonization and its

reduction by grafted PEG chains have not been yet revealed. Initially it was thought that PEG chains sterically hinder the attachment of opsonins on NP surface by creating a surface-random cloud, and thus hampers the formation of the protein corona around NPs. This reduces aggregation and receptor-mediated recognition of NPs eventually improving their pharmacokinetics (PK).[32-36]

A recent report have shown that surface PEGs lead to an alternation in the composition of the protein corona formed as soon as NPs enter the bloodstream and this is actually responsible for the reduced uptake of PEGylated NPs by the MPS. This group has also found an increased abundance of the clusterin protein in the protein corona around PEGylated NPs, from which they investigated the role of clusterin in reducing phagocytosis of injected NPs.[37] Another paper in 2013 reported that the conformation of surface PEGs influence the formation of protein corona around single-walled carbon nanotubes (SWCNTs).[30]

There has been attempts to render DNs long circulating by encapsulating them in liposomes or forming an oligolysine-PEG coating around them.[38,39] Both of these strategies have become successful to enhance the low salt stability of DNs and also to provide protection against nucleases. But these strategies require synthesis of specific polymers to coat DNs. Moreover encapsulation of DNs within a liposome raises the obvious question that why we cannot use a liposome directly instead of forming it around a DN. However, a detailed study on how PEGylation affects the stability of DNs in physiological conditions and their uptake by the MPS, was missing till date. We have attempted to pursue that investigation. We studied the effect of both PEG lengths and conformations (linear or

branched) on their circulation lifetime. In addition to simple PEGs, we also conjugated a PEG-lipid to DN surface and studied its efficacy. In addition, we have also studied how incubation with plasma and clusterin protein separately affects internalization of different PEGylated DNs.

We designed two DNs: a tetrahedron (Td) and an 8x8 layered structure (DNO), and covalently attached PEG chains of varying lengths and conformation on their surface. Higher PEG chain lengths provide enhanced protection to the DNs against degradation in physiological conditions. Branching of PEG chain does not provide any additional stability in comparison to the linear isomers. However, they show higher efficiency in reducing macrophage uptake of DNs than the corresponding linear chains. We conjugated a 2 kD PEG-lipid on DN surfaces and that reduced the uptake with greater efficiency than the corresponding linear and even the 4 arm PEG isomer. Incubation of bare DNs with plasma increased their cellular uptake, while incubation with clusterin reduced the same. Branched PEGs, especially those having higher molecular weights, have pronounced effect on reduction of cellular uptake when the DNs were pre-incubated with clusterin.

2.3 Results and Discussion

2.3.1 Building PEG-conjugated DNs

In order to compare results and establish the generality of our findings, we conducted studies using two DNs: a DNA tetrahedron (Td) and an 8x8 DNA origami (DNO) designed in the square lattice motif of caDNAno. Td being a comparatively hollower structure more resembling a wireframe DN than a densely packed DNA origami,

the divalent cation requirement should be lesser while the scope for nuclease action should be higher. Exactly the reverse is expected to be true for densely packed DNO.

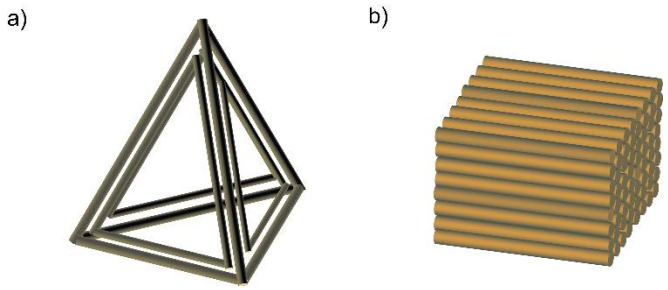

Figure 2.1*:* a) Td b) DNO.

The common method to form simple DNs with PEG coating is to select a certain number of staples, conjugate PEG to them, and then mix them with the other normal staples prior to annealing. But from our experiments, we found that the PEG chains probably hamper the base pair recognition during the process of annealing, an effect which becomes increasingly pronounced in larger and tightly packed DNs like DNA origami resulting in highly compromised yields. So we chose to PEGylate pre-formed DNs.

The schematic representation of Td shows that each structure is comprised of four symmetric units capable of inter-unit assembly through sticky end hybridization. Three strands on each of the constituent units were modified with a single stranded handle. Hence, a complete Td had 12 DNA handles and each handle was hybridized with a complimentary strand containing a reactive alkyne group (DBCO) to which PEG-azide can be conjugated via copper-free click reaction. Similarly, in case of DNO, 24 surface staples were selected and their amine versions (single strand with a terminal amine) were conjugated to DBCO. Thus we obtained DNO decorated with 24 reactive DBCOs on the surface. This DNO was

reacted with different PEGs having terminal azides to yield pegylated DNOs as required for further experiments. Formation of the pegylated structures (both Td and DNO) was confirmed by agarose gel electrophoresis.

2.3.2 Stability in Physiological Conditions

DMEM supplemented with 10% fetal bovine serum is a very common medium used for *in vitro* cell culture. This medium provides an excellent environment to study the stability of DNs in physiological conditions. Mg^{2+} content of DMEM is ~0.8 mM and it contains more than 256U/L of DNase I activity.[22] Hence, when incubated with DMEM + 10% FBS, DNs experience loss in structural integrity both due to low salt concentration as well as nuclease mediated degradation. We studied stability of bare and PEG-coated DNs in this medium. We incubated each structure separately and monitored their stability via gel electrophoresis. DNO being a densely packed structure had considerably lower half-life in the medium (~39 minutes) than Td (~5 h). On studying PEG-coated DNs we found that increase in the length of linear PEG chains positively contribute towards enhancing DN stability. The half-life of Td was almost doubled by 10 kD linear PEG coating while the effect is almost 2.5 fold for DNO. However, branched PEGs or DSPE-PEG did not provide any higher stability to the tested structures over their linear isomers.

a)

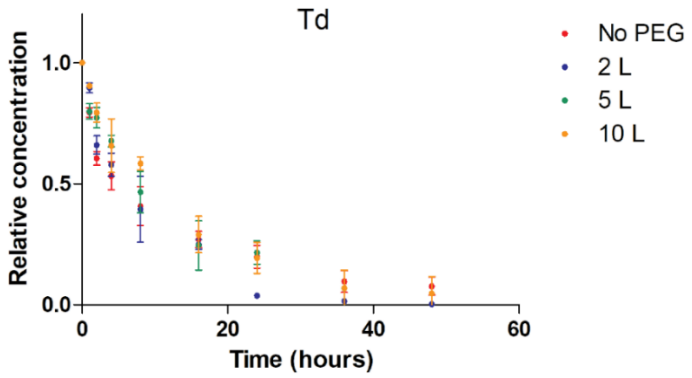

b)

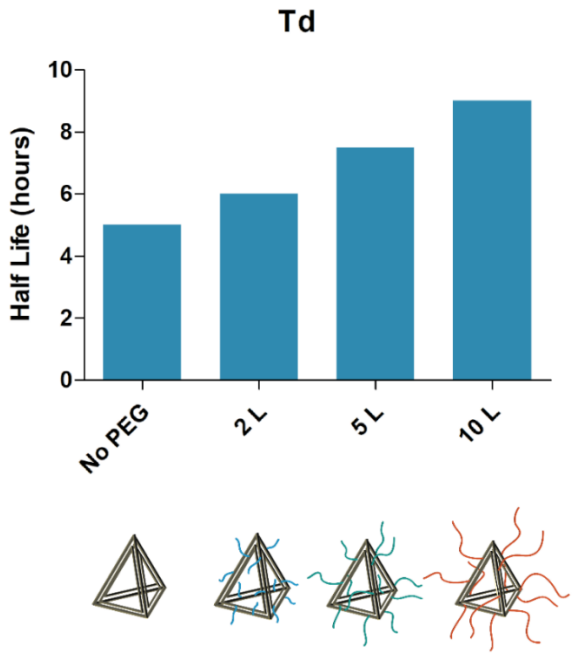

Figure 2.2: Stability of Td in DMEM supplemented with 10% FBS. a) Plotting concentration of Td and different PEG coated Tds with time b) comparison of half-lives of bare Td and different PEG-coated Tds.

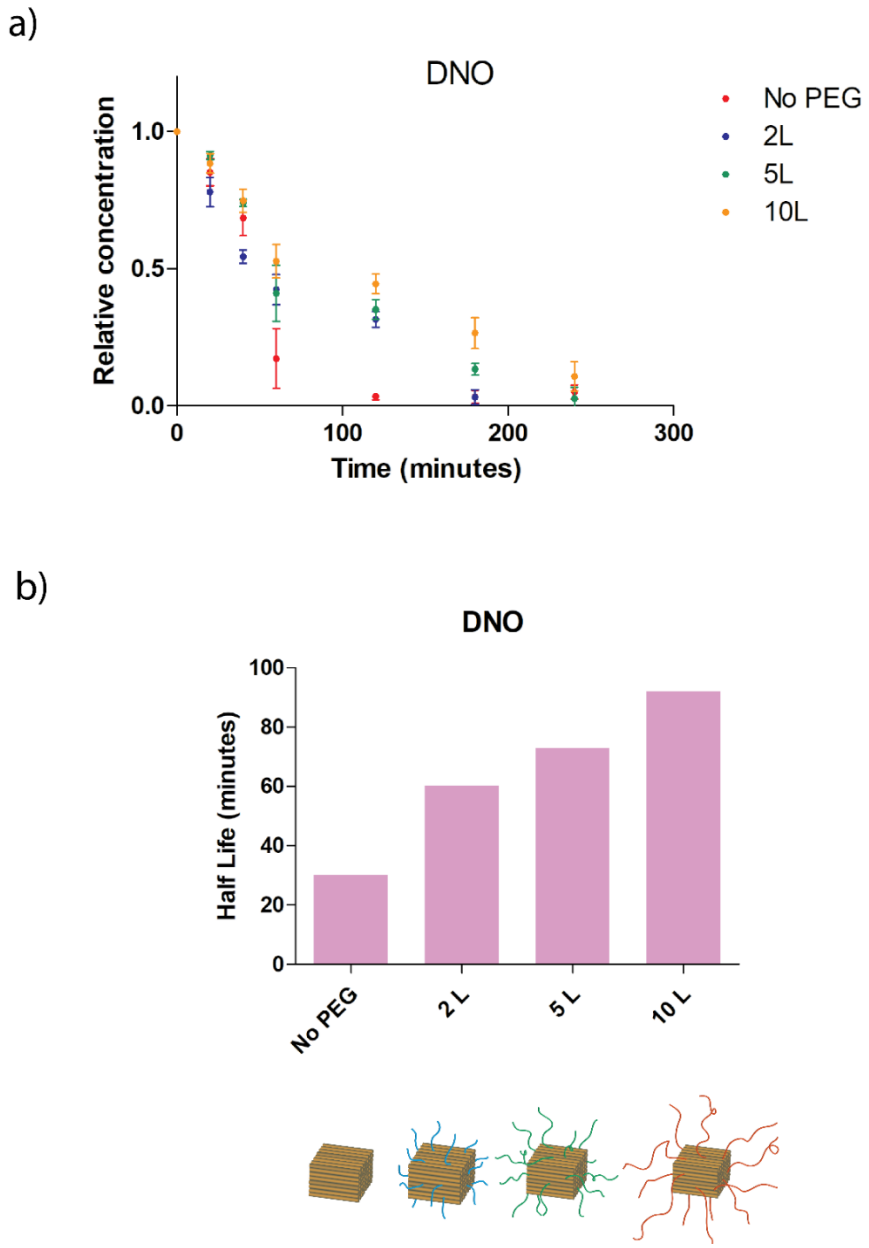

Figure 2.3: Stability of DNO in DMEM supplemented with 10% FBS. a) Plotting concentration of DNO and different PEG coated DNOs with time b) comparison of half-lives of DNO and different PEG-coated DNOs.

2.3.3 Confocal Microscopy

A probability of the DNs being attached to the cell surface without being internalized and thus giving false positive was very feasible. We used confocal microscopy to visualize the internalization of bare and coated DNs. The Alexa fluor 488 labeled DNs show green fluorescence when excited at 488 nm. To show co-localization we stained the cell membranes with CellTracker CM-Dil dye (553/570 nm). In addition to imaging cells directly after incubation, we also studied batches treated with DNase after incubation, such that any DNA or DN sticking to the surface was degraded by the nuclease. The images for DNase treated RAW cells after incubation with Td, Td–5L and Td–2 –lip are shown below. DNs coated with DSPE-PEG might have higher tendencies to stay stuck to the phospholipid bilayer instead of entering the cytoplasm. Also, the protein corona formed on the DNs after incubation with plasma and clusterin might cause them to be attached to the cell surface. We investigated all the situations and confirmed the internalization of structures in all cases. The confocal and z-stacked images with orthogonal sectioning are provided in the supplemental information.

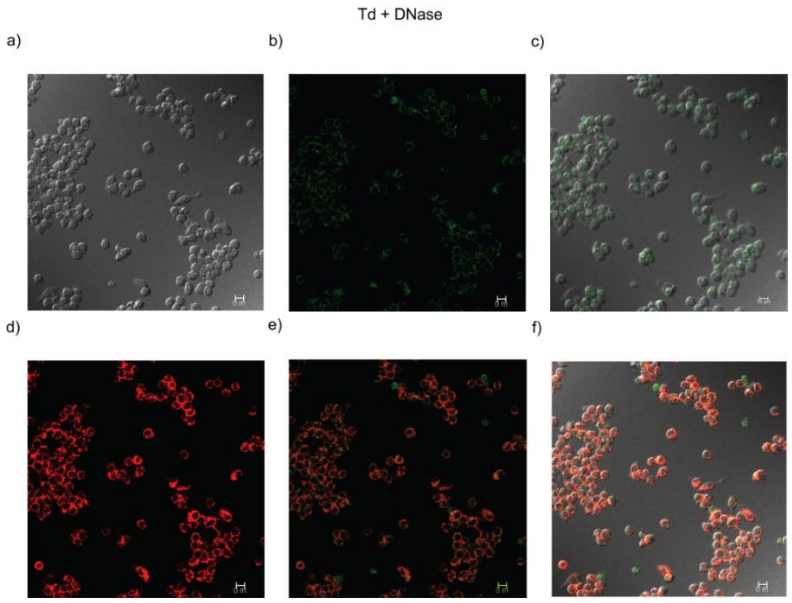

Figure 2.4*:* Confocal microscopy images of RAW cells incubated with Alexa fluor 488 labeled Td followed by DNase treatment. The cell membranes were stained with CellTracker CM-Dil dye. a) Bright field image b) green fluorescence from internalized Td c) overlay of bright field and green fluorescence d) red fluorescence from CellTracker CM-Dil dye e) overlay of green and red fluorescence f) overlay of bright field, green and red fluorescence.

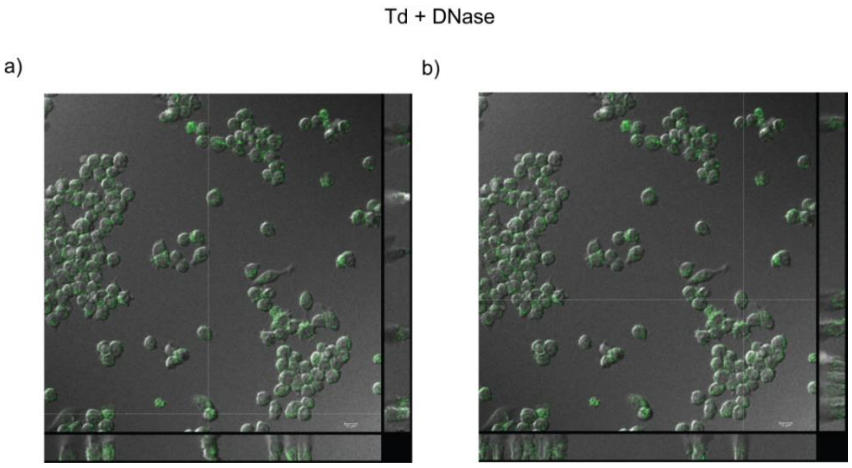

Figure 2.5: Z-stacked confocal microscopy images of RAW cells incubated with Alexa fluor 488 labeled Td followed by DNase treatment. The crosshairs indicate orthogonal sectioning. The bottom and right panels show the sectioned planes and confirm that fluorescent particles (green) are located inside the cells and not merely attached to the cell membrane.

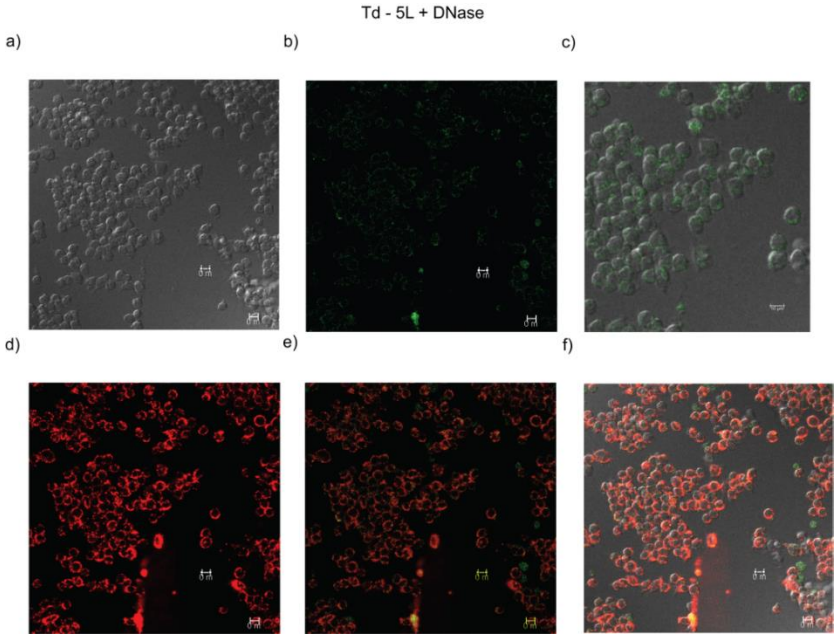

Figure 2.6: Confocal microscopy images of RAW cells incubated with Alexa fluor 488 labeled Td–5L followed by DNase treatment. The cell membranes were stained with CellTracker CM-Dil dye. a) Bright field image b) green fluorescence from internalized Td–5L c) overlay of bright field and green fluorescence d) red fluorescence from CellTracker CM-Dil dye e) overlay of green and red fluorescence f) overlay of bright field, green and red fluorescence.

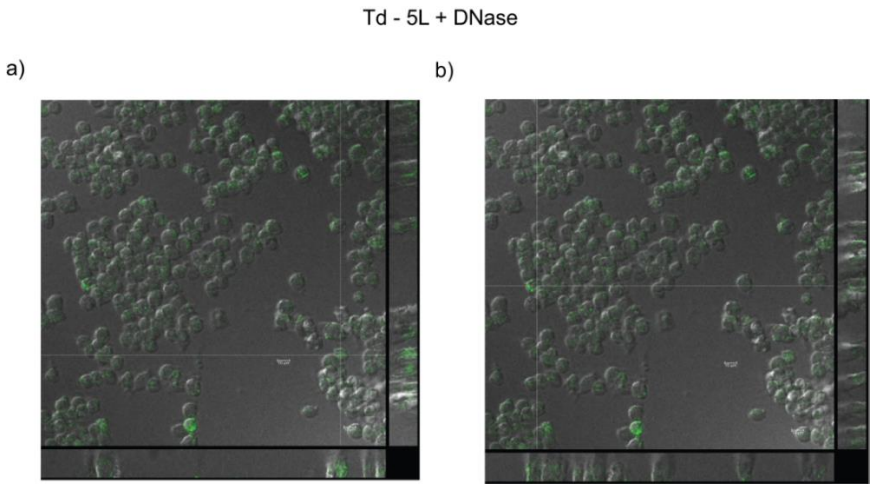

Figure 2.7*:* Z-stacked confocal microscopy images of RAW cells incubated with Alexa fluor488 labeled Td and then treated with DNase.

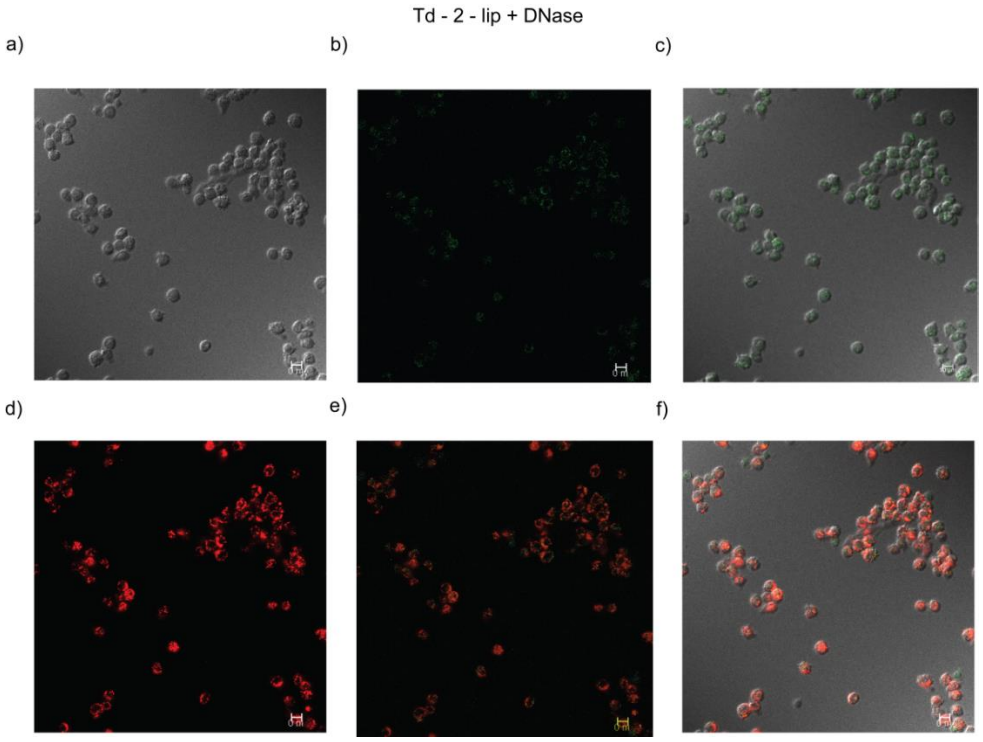

Figure 2.8*:* Confocal microscopy images of RAW cells incubated with Alexa fluor 488 labeled Td–5L followed by DNase treatment. The cell membranes were stained with

CellTracker CM-Dil dye. A) Bright field image b) green fluorescence from internalized Td–2-lip c) overlay of bright field and green fluorescence d) red fluorescence from CellTracker CM-Dil dye e) overlay of green and red fluorescence f) overlay of bright field, green and red fluorescence.

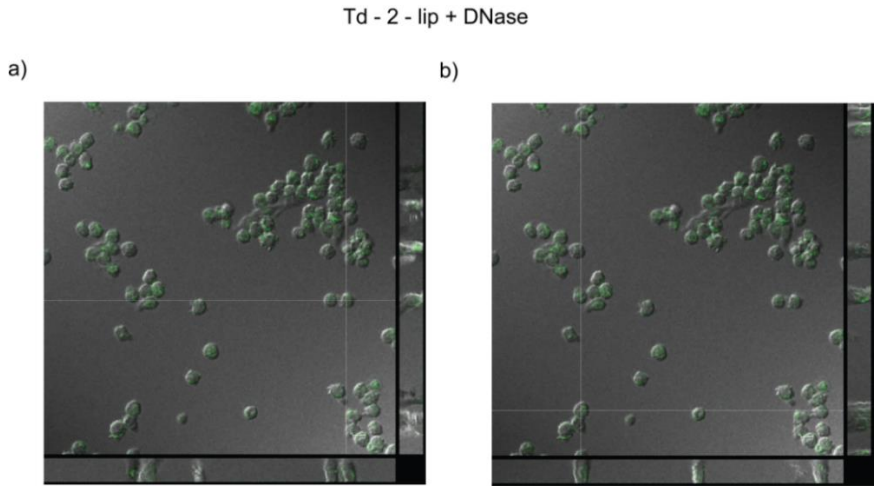

Figure 2.9*:* Z-stacked confocal microscopy images of RAW cells incubated with Alexa fluor488 labeled Td and then treated with DNase.

2.3.4 Uptake of DNs by Macrophages

2.3.4.1 Cellular uptake without plasma or clusterin incubation

Stealth polymers like PEG enhance the circulation lifetime of nanocarriers by ambushing them from the MPS, thus avoiding their clearance by the immune system. Macrophages play an active role in clearing foreign particles from the blood. Thus, if DNs are to serve as successful drug delivery vehicles, they have to be protected from recognition by the macrophages. To investigate how recognition by macrophages in altered by PEG

coating on DNs, we studied their internalization into a murine macrophage cell line, RAW264.7.

The S4 strand of Td labeled with Alexa fluor 488 was used as a control. The other controls were both bare Td and DNO, each labeled with 12 dye molecules. In order to mitigate the probability of fluorescence contribution from DNs sticking to cell surfaces, after incubation with dye-labeled DNA, bare Td and bare DNO, we treated the cells with DNase and measured their fluorescence. They acted as another set of controls. Comparing the fluorescence, it was found that there was almost no difference between the DNase treated and untreated controls. This confirmed that all the results obtained are from actually internalized structures and not mere DNs sticking to the cell surface. However, the data presented here are all from DNase treated cells.

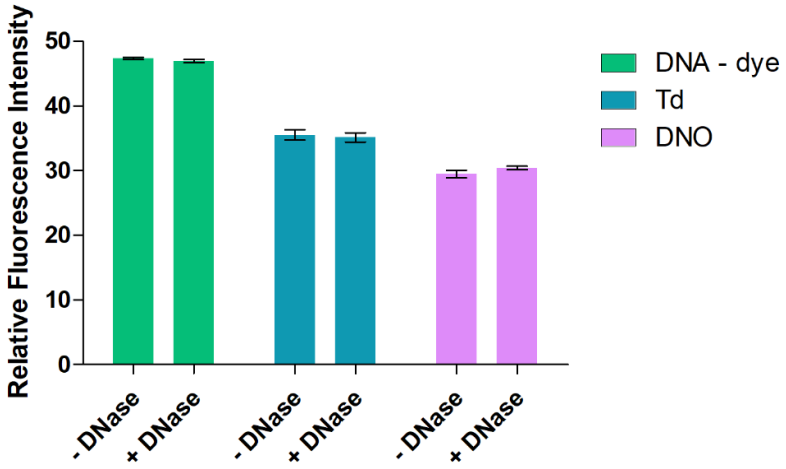

Figure 2.10*:* Comparing fluorescence intensity of DNase treated and untreated controls.

When the cellular uptake of DNs coated with linear PEGs was studied, we found that the uptake is inversely related to the length of PEG chains, which is in agreement with

our prediction. Looking carefully at the values, we can see that a 2L coting does not reduce the uptake of DNO to an extent similar to Td. This might be because the amount of coverage conferred to DNO by 2L is insignificant as it has a much higher size than Td. But the effect of 5L coating on DNO was much pronounced. Again, we note that the extent of decrease from 5L to 10L is higher in case of DNO than Td. This probably implies that a shift from 5L to 10L coating in Td does not improve the amount of coverage much. 12 5L PEG might be able to provide a decent ambush around the smaller Td structures. But, the same shift decently enhances the coverage of larger DNO that is reflected in the higher reduction of macrophage uptake.

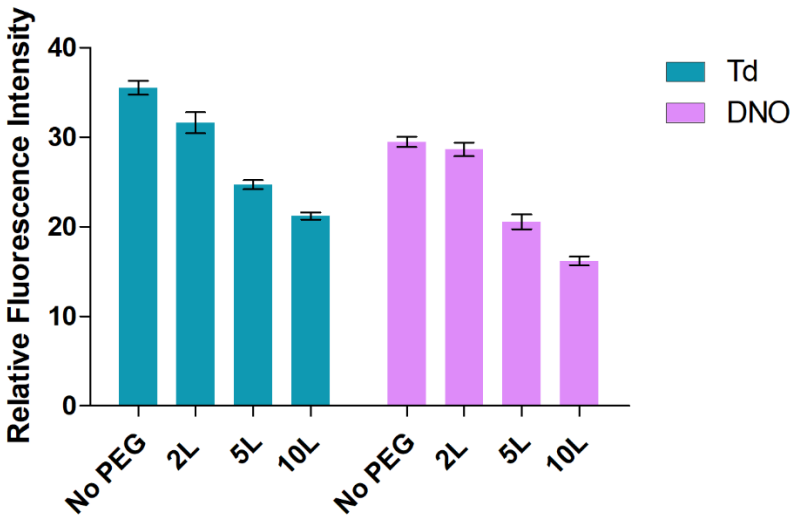

Figure 2.11*:* Comparing fluorescence intensities from internalized linear PEG coated DNs.

After studying the effect of linear PEGs, we directed our attention to investigate the effect of PEG conformation on cellular uptake. Both Td and DNO were coated with a 4 arm 2 kD PEG (2-4 arm), a 4 arm 10 kD PEG (10-4 arm) and an 8 arm 10 kD PEG. The data shows considerable decrease in uptake of DNO when an 8 arm 10 kD PEG is used

instead of the linear isomer. However the decrease is not that prominent for Td probably because 12 10 kD linear PEG chains were enough to give the structure a sufficient coverage.

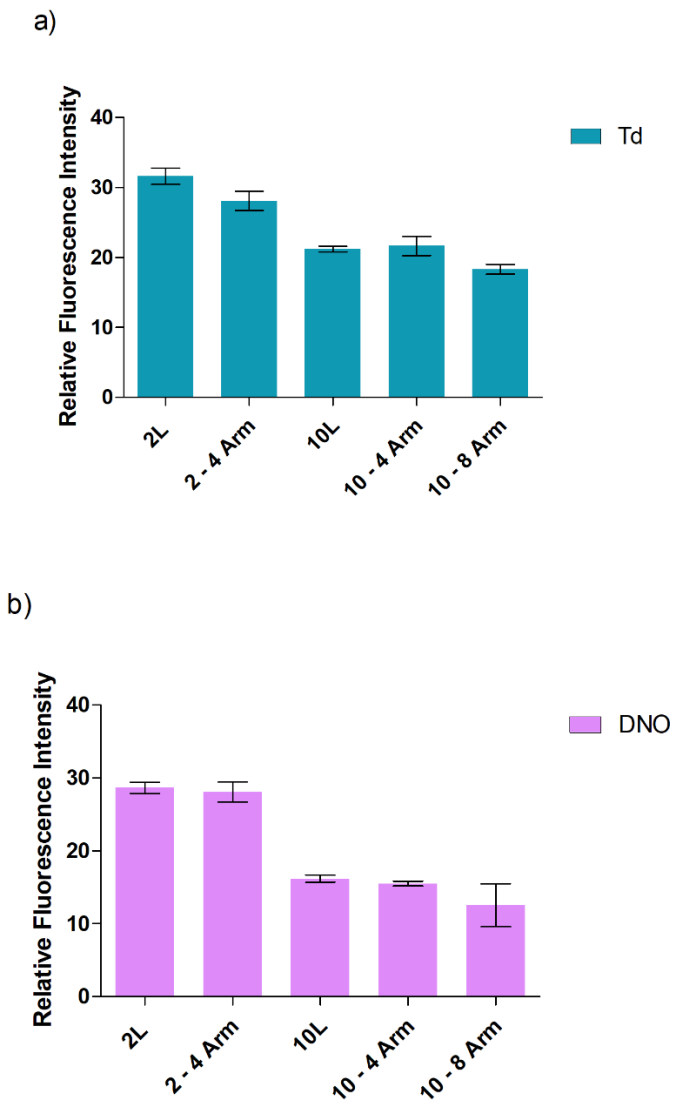

Figure 2.12*:* Effect of PEG branching on cellular uptake of DNs. a) Td b) DNO.

2.3.4.2 Effects of plasma and clusterin Incubation

In 2016, Wurm and coworkers analyzed the protein corona formed over nanoparticles when they are subjected to plasma and found that PEG coating does not inhibit the formation corona, but they change its composition relative to the uncoated particles.[37] The corona with altered composition is responsible for determining their extent of uptake by the macrophages. They also found a higher percentage of clusterin protein in the PEG coated NPs. As the cellular internalization of NPs depends on the material of the core, we decided to study how plasma and clusterin incubation of bare and PEG-coated DNs influence their internalization by macrophages. We found that incubation with mouse plasma had almost no effect on the uptake of bare Td but the same was increased in case of bare DNO. On the other hand, clusterin incubation marked decreased the uptake of both the structures.

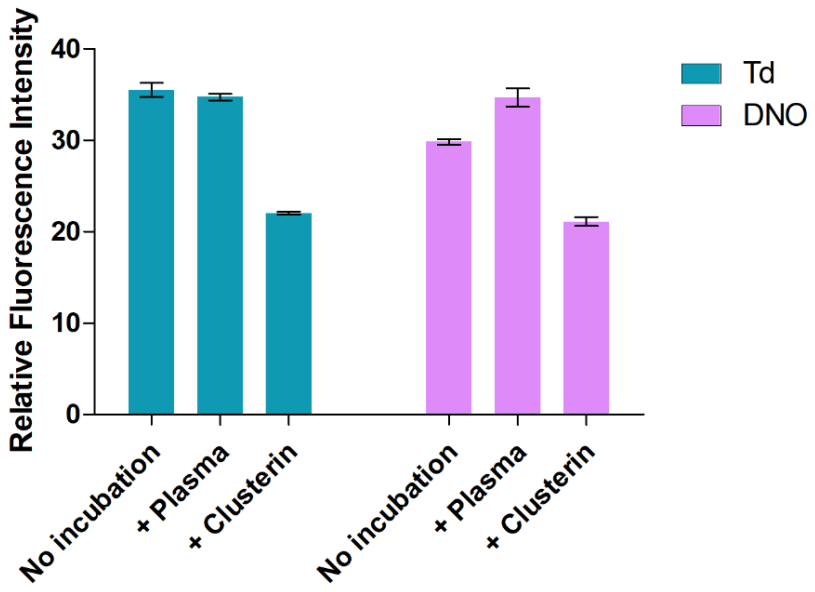

Figure 2.13*:* Effect of plasma and clusterin incubation on cellular uptake of bare DNs. a) Td b) DNO.

After studying the bare structures we looked at the effect of plasma and clusterin incubation on PEG coated DNs. Figure 2.14 shows the effect of linear PEG chains on cellular uptake of plasma and clusterin incubated structures. From the plots we can find two noteworthy trends. First, plasma incubation of bare structures had almost no influence on the uptake, but the same reduced the uptake of coated DNs to various extents. And second, clusterin incubation always brought about reduction in internalization.

a)

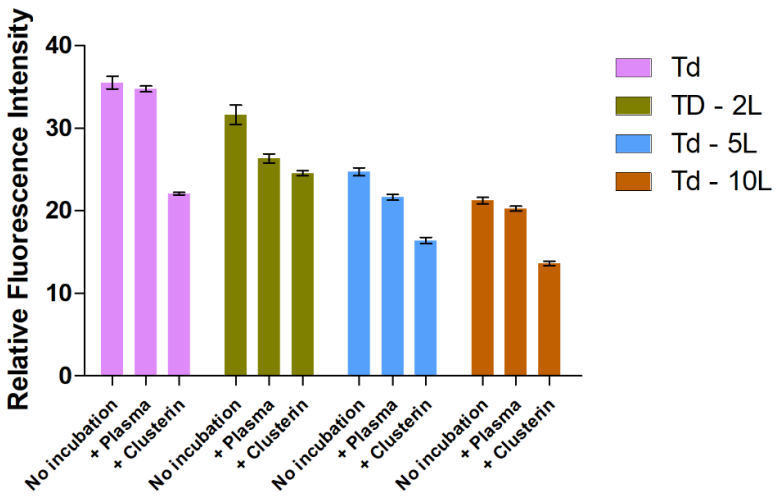

b)

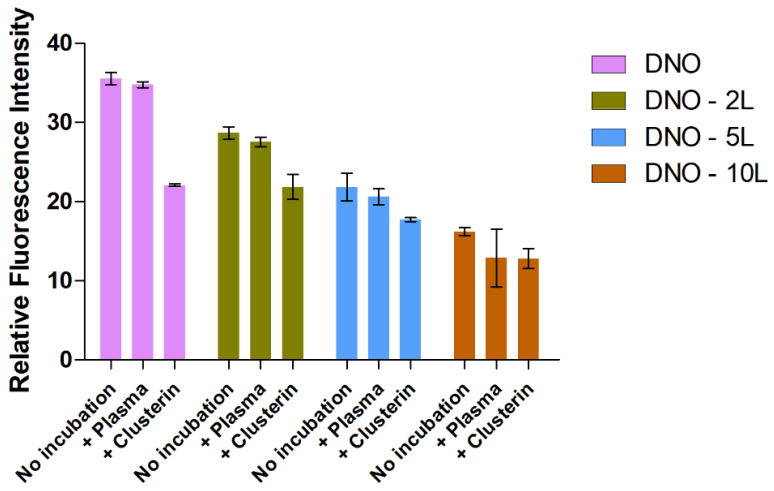

Figure 2.14*:* Effect of plasma and clusterin incubation on cellular uptake of linear PEG coated DNs. a) Td b) DNO.

Branching of the PEG chains showed a dramatic effect on the internalization of DNs when they are incubated with clusterin. And this effect was pronounced in case of higher chain lengths (i.e., higher in 10 kD branched PEG than 2 kD branched PEG). This is probably due to the fact that branching provides a higher coverage and this attracts more clusterin to deposit around the structure, thus reducing engulfment by macrophages.

a)

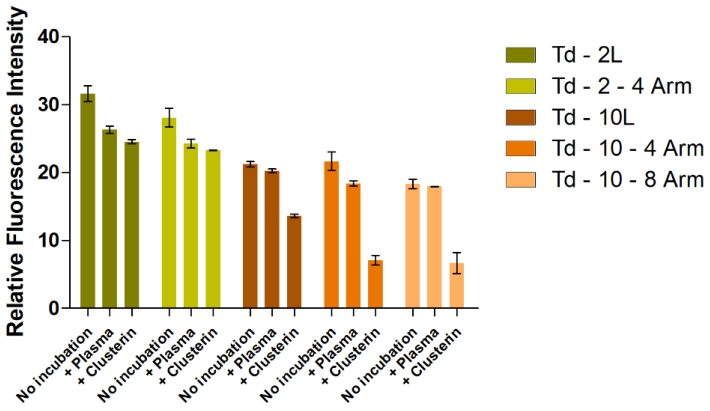

b)

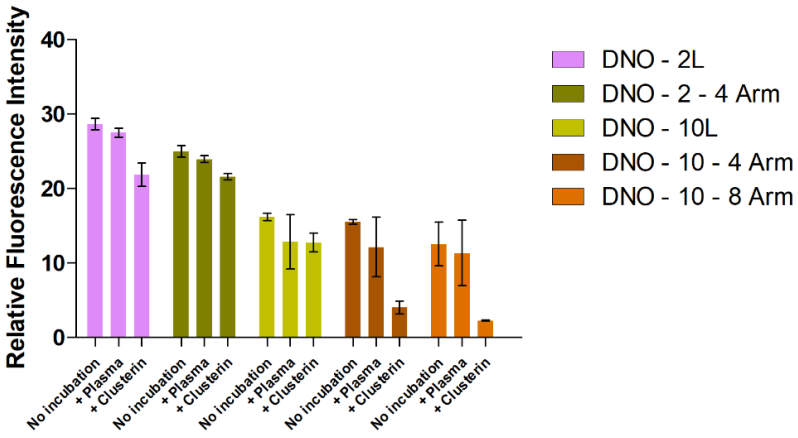

Figure 2.15*:* Effect of plasma and clusterin incubation on cellular uptake of branched PEG coated DNs. a) Td b) DNO.

2.3.5.3 Effect of PEG-lipid coating

The cell membrane being a phospholipid bilayer, might not recognize another lipid-coated article as a candidate for prompt internalization – this was the rationale behind choosing the DSPE-PEG (2 kD) coating. Without any plasma or clustering incubation, the

DSPE-PEG coating indeed reduced the uptake of DNs, ~35% for Td and ~40% in case of DNC. But clusterin incubation did not reflect any consistent trend as was observed in case of the PEG coatings. This is probably due to the fact clusterin deposition is no more the key component in the protein corona formed over DSPE-PEG coating, and hence its deposition did reflect any significant reduction in the internalization of DNs by macrophages. However, this issue requires a separate investigation where the protein corona around a PEG-lipid coated DN would be analyzed meticulously and a detailed profile of the corona constituents would be built.

a)

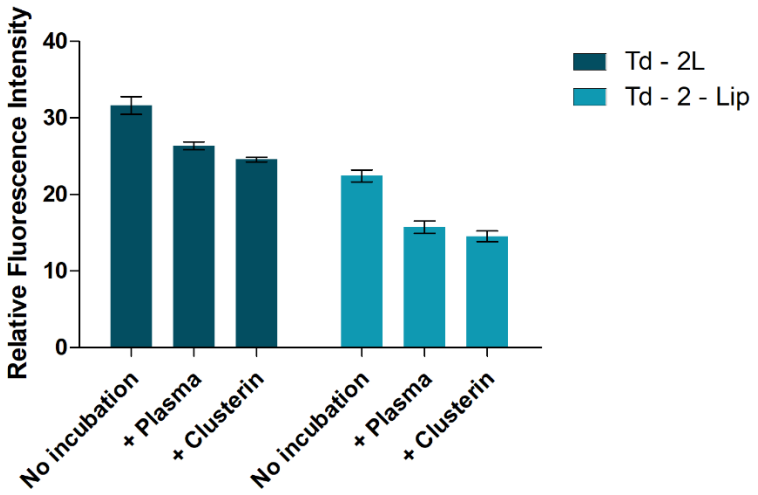

b)

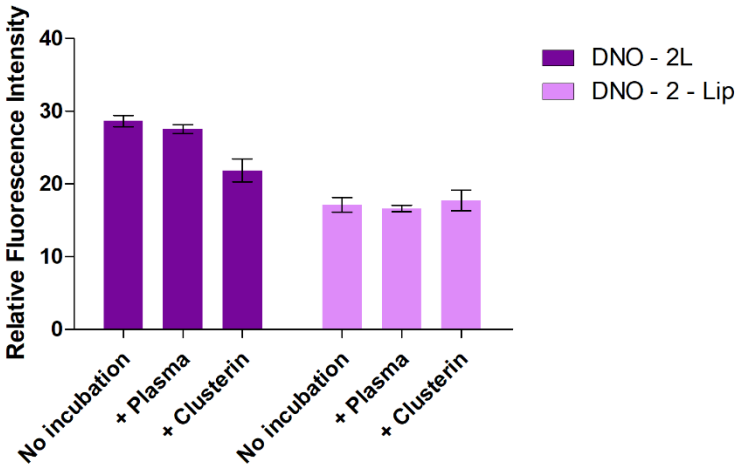

Figure 2.16: Effect of PEG-lipid coating on cellular uptake of DNs. a) Td b) DNO.

2.4 Conclusion

We reported the effect PEG coating on the stability and macrophage internalization by macrophages. In this study, the aspects of PEG length and conformation have been studied and increased chain length has demonstrated increased resistance towards low salt denaturation and nuclease attack. Also, higher chain lengths reduce the cellular uptake of the DNs more in comparison to the shorter ones. But from careful analysis of the results, it is clear that without considering length or extent of branching as isolated parameters, the ideal parameter for consideration would be 'surface coverage' of the DN under study. PEG branching has shown its effect on reducing cellular uptake of structures, but the amount of reduction differs in case of Td and DNO. This observation, again, points to the issue of surface coverage. Higher coverage makes the DNs more efficient in avoiding recognition by the MPS. This might be due to the fact that higher coverage allows enhanced deposition of clusterin, incubation with which prior to cellular internalization has demonstrated

prominent effects. The findings definitely open up a new direction of investigation where covalent conjugation of clusterin to DNs could be employed to reduce the cellular uptake. Another interesting observation is the results from DSPE-PEG coating, which indicates, not clusterin but some other blood component is also playing a crucial role in reducing clearance of DNs in circulation.

2.5 References

1. Riehemann, K.; Schneider, S. W.; Luger, T. A.; Godin, B.; Ferrari, M.; Fuchs, H. *Angewandte Chemie International Edition* **2009**, *48*, 872.
2. Rothemund, P. W. *Nature* **2006**, *440*, 297.
3. Douglas, S. M.; Dietz, H.; Liedl, T.; Högberg, B.; Graf, F.; Shih, W. M. *Nature* **2009**, *459*, 414.
4. Dietz, H.; Douglas, S. M.; Shih, W. M. *Science* **2009**, *325*, 725.
5. Han, D.; Pal, S.; Nangreave, J.; Deng, Z.; Liu, Y.; Yan, H. *Science* **2011**, *332*, 342.
6. Wei, B.; Dai, M.; Yin, P. *Nature* **2012**, *485*, 623.
7. Ke, Y.; Ong, L. L.; Shih, W. M.; Yin, P. *science* **2012**, *338*, 1177.
8. Andersen, E. S.; Dong, M.; Nielsen, M. M.; Jahn, K.; Subramani, R.; Mamdouh, W.; Golas, M. M.; Sander, B.; Stark, H.; Oliveira, C. L. *Nature* **2009**, *459*, 73.
9. Goodman, R. P.; Heilemann, M.; Doose, S.; Erben, C. M.; Kapanidis, A. N.; Turberfield, A. J. *Nature nanotechnology* **2008**, *3*, 93.
10. Liu, M.; Fu, J.; Hejesen, C.; Yang, Y.; Woodbury, N. W.; Gothelf, K.; Liu, Y.; Yan, H. *Nature communications* **2013**, *4*, 2127.
11. Modi, S.; Swetha, M.; Goswami, D.; Gupta, G. D.; Mayor, S.; Krishnan, Y. *Nature nanotechnology* **2009**, *4*, 325.
12. Liu, D.; Balasubramanian, S. *Angewandte Chemie International Edition* **2003**, *42*, 5734.
13. Lee, H.; Lytton-Jean, A. K.; Chen, Y.; Love, K. T.; Park, A. I.; Karagiannis, E. D.; Sehgal, A.; Querbes, W.; Zurenko, C. S.; Jayaraman, M. *Nature nanotechnology* **2012**, *7*, 389.
14. Liu, X.; Xu, Y.; Yu, T.; Clifford, C.; Liu, Y.; Yan, H.; Chang, Y. *Nano letters* **2012**, *12*, 4254.
15. Douglas, S. M.; Bachelet, I.; Church, G. M. *Science* **2012**, *335*, 831.
16. Lu, C.-H.; Willner, B.; Willner, I. *ACS nano* **2013**, *7*, 8320.
17. Campolongo, M. J.; Tan, S. J.; Xu, J.; Luo, D. *Advanced drug delivery reviews* **2010**, *62*, 606.
18. Zhao, Y.-X.; Shaw, A.; Zeng, X.; Benson, E.; Nyström, A. M.; Högberg, B. r. *ACS nano* **2012**, *6*, 8684.
19. Jahnen-Dechent, W.; Ketteler, M. *Clinical kidney journal* **2012**, *5*, i3.

20. Mei, Q.; Wei, X.; Su, F.; Liu, Y.; Youngbull, C.; Johnson, R.; Lindsay, S.; Yan, H.; Meldrum, D. *Nano letters* **2011**, *11*, 1477.

21. Conway, J. W.; McLaughlin, C. K.; Castor, K. J.; Sleiman, H. *Chemical Communications* **2013**, *49*, 1172.

22. Hahn, J.; Wickham, S. F.; Shih, W. M.; Perrault, S. D. *ACS nano* **2014**, *8*, 8765.

23. Surana, S.; Bhatia, D.; Krishnan, Y. *Methods* **2013**, *64*, 94.

24. Johnson, R. J. In *Biomaterials Science (Third Edition)*; Elsevier: 2013, p 533.

25. Frank, M. M.; Fries, L. F. *Immunology today* **1991**, *12*, 322.

26. Dunn, S. E.; Brindley, A.; Davis, S. S.; Davies, M. C.; Illum, L. *Pharmaceutical research* **1994**, *11*, 1016.

27. Tenzer, S.; Docter, D.; Kuharev, J.; Musyanovych, A.; Fetz, V.; Hecht, R.; Schlenk, F.; Fischer, D.; Kiouptsi, K.; Reinhardt, C. *Nature nanotechnology* **2013**, *8*, 772.

28. Aggarwal, P.; Hall, J. B.; McLeland, C. B.; Dobrovolskaia, M. A.; McNeil, S. E. *Advanced drug delivery reviews* **2009**, *61*, 428.

29. Monopoli, M. P.; Åberg, C.; Salvati, A.; Dawson, K. A. *Nature nanotechnology* **2012**, *7*, 779.

30. Sacchetti, C.; Motamedchaboki, K.; Magrini, A.; Palmieri, G.; Mattei, M.; Bernardini, S.; Rosato, N.; Bottini, N.; Bottini, M. *ACS nano* **2013**, *7*, 1974.

31. Owens III, D. E.; Peppas, N. A. *International journal of pharmaceutics* **2006**, *307*, 93.

32. Klibanov, A. L.; Maruyama, K.; Torchilin, V. P.; Huang, L. *FEBS letters* **1990**, *268*, 235.

33. Woodle, M. C.; Lasic, D. D. *Biochimica et Biophysica Acta (BBA)-Reviews on Biomembranes* **1992**, *1113*, 171.

34. Needham, D.; McIntosh, T.; Lasic, D. *Biochimica et Biophysica Acta (BBA)-Biomembranes* **1992**, *1108*, 40.

35. Du, H.; Chandaroy, P.; Hui, S. W. *Biochimica et Biophysica Acta (BBA)-Biomembranes* **1997**, *1326*, 236.

36. Price, M.; Cornelius, R.; Brash, J. *Biochimica et Biophysica Acta (BBA)-Biomembranes* **2001**, *1512*, 191.

37. Schöttler, S.; Becker, G.; Winzen, S.; Steinbach, T.; Mohr, K.; Landfester, K.; Mailänder, V.; Wurm, F. R. *Nature nanotechnology* **2016**, *11*, 372.

38. Perrault, S. D.; Shih, W. M. *ACS nano* **2014**, *8*, 5132.

39. Ponnuswamy, N.; Bastings, M. M.; Nathwani, B.; Ryu, J. H.; Chou, L. Y.; Vinther, M.; Li, W. A.; Anastassacos, F. M.; Mooney, D. J.; Shih, W. M. *Nature communications* **2017**, *8*, 15654.

CHAPTER 3

ENHANCING LOW SALT STABILITY OF DNA NANOSTRUCTURES USING FREE STABILIZING AGENTS

3.1 Abstract

Stability of the DNs is a crucial factor determining their suitability for *in vivo* applications. The formation of DNs require a very high concentration of divalent magnesium and this concentration is not available in physiological fluids like blood. Hence when injected in a living system, the DNs rapidly unfold and thus their lifetime becomes extremely reduced. In this project we screened several DNA compaction agents, intercalators and groove binders and only four of them, arginine, lysine, bis-lysine and hexamine cobalt, were able to enhance the stability of DNs in low salt condition. Bis-lysine was found to be the most stabilizing. The enhancement of stability was studied by counting the number of intact structures via transmission electron microscopy using 30 nm gold NPs as internal standards. In addition to studying the effect of single agents, we also studied the efficacy of their combinations. Hexamine cobalt in combination with bis-lysine demonstrated the highest efficacy. Through melting point studies we also confirmed that the stabilizing agents enhance the thermodynamic stability of the DNs which is reflected by the increase in their melting points when formed in presence of the four stabilizing agents.

3.2 Introduction

Because of its versatility and functionality, DNA has contributed largely to bridge the gap between material science and biology. DNA nanotechnology, a burgeoning field

of research for the past few decades, have used DNA as a structural nanoscale material and has provided an easy and convenient method to produce nanoscale 2D and 3D structures of diverse shapes, sizes and complexities[1-4] that would not be possible with any other known nanomaterial. The DNA origami method[5] has become a very popular choice to build 3D DNs owing to its convenience and robustness. The intrinsic biocompatibility and nanosize of the DNs has made them obvious choices for various biological applications. In addition to this, as the DNs allow very precise organization of functional molecules like fluorophores[6], quantum dots[7], aptamers[8], antibodies[9], etc. on them with excellent control over number, position and architecture, and the dynamics of reconfigurable and dynamic DNs can be controlled by stimuli like a single stranded DNA (fuel), small molecules, or light, they have become candidates of interest in the fields of biomimicking, nanoelectronics, biosensors and nanomedicine.[10-13]

The multivalence of DNA, the diverse nature of functionalizations available and the compatibility of biological systems have drawn considerable attention of the nanomedicine researchers and the DNs have been used as drug delivery vehicles in a number of reports. Douglas and co-workers build a nanorobot that can release Fab antibody fragments in the presence of target cells.[14] A DNA tetrahedron was employed by Anderson and co-workers for *in vivo* delivery of small interfering RNA in order to target and suppress gene expression in a mouse model.[15] The DNs have also demonstrated their potential to serve as platforms for synthetic vaccines. Fan, Huang and co-workers assembled a multivalent DNA tetrahedron for noninvasive delivery of immunostimulatory CpG oligonucleotides.[16] Yan, Chang and co-workers have employed a DNA tetrahedron for

coassembly of model antigens and CpG with precise control over the valency and spatial arrangement of each constituent.[17]

DNs have also been employed to carry drug molecules *in vivo* either by intercalation into the carrier DNA helix or by attachment through chemical conjugation. Huang and co-workers demonstrated the application of aptamer-conjugated DNA icosahedral NPs as carriers of doxorubicin for cancer therapy.[18] In 2012, Ding and co-workers constructed 2- and 3-D doxorubicin-loaded DNs, the loading being through intercalation, and they demonstrated that their construct showed prominent cytotoxicity to regular human breast adenocarcinoma cancer cells (MCF 7) and also to doxorubicin-resistant cancer cells.[19] In the same year Högberg and co-workers developed DNA origami delivery systems for cancer therapy that have tunable release properties.[20] Their aim was the optimal delivery of anthracycline doxorubicin (Dox) to human breast cancer cells. As they designed different DNs having varying degrees of global twists, hence the amounts of relaxation of the structures also varied. They tuned the DN design to control the encapsulation efficiency and release rate of Dox and also increase the cytotoxicity and decrease the intracellular elimination rate of Dox in comparison to the free drug molecule.

However, all the DNs used as the delivery vehicles are very simple structures, either 2D or wireframe or single layer DNA origamis. There are several concerns while using these structures like drug potencies and leakage. Simple wireframe structures offer limited number of valencies, so when the drug needs to be chemically conjugated, the amount of carrier to be administered will be quite high. And, as the drug delivery vehicles reported do not provide encapsulation of the drug molecules, they might leak while being circulated

and exert non-specific effects. The application of densely packed 3D origamis are limited by the shorter *in vivo* lifetimes. *In vivo* stability of a DN is a function of several factors, the important ones being low salt denaturation, nuclease degradation and opsonization.

The basic principles underlying the attempts to address these issues could be summarized as: a) increase low salt stability by replacing divalent magnesium with other positively charged species that are either available in the blood, or that can adhere to the DNs even after administering, b) coat DNs with protective layers that can minimize their exposure to nucleases, and c) avoid immune recognition. Several attempts have been reported to increase the lifetime of DNs in circulation. Being inspired by the natural particle systems like viruses, Shih and co-workers demonstrated membrane encapsulation of DNs in order to achieve enhanced circulation times.[21] They encapsulated DNs with PEGylated lipids and achieved a twofold lower immune activation and 17 fold higher pharmacokinetic bioavailability. In 2014, Perrault and co-workers addressed the instability of DNs in tissue culture, which is basically a combination of low salt and nuclease degradation effects.[22] They systematically studied the sensitivity of DNA nanostructures to cation depletion and effect of nucleases in cell culture medium. Shih and co-workers further reported a oligolysine-based coating that can protect nanostructures from low-salt denaturation and nuclease degradation.[23]

In this project we have focused on enhancing the stability of DNs in low magnesium buffers. The strategies reported till date that aim at enhancing the DN lifetime in low salt conditions require coating by some special polymers or lipids, either covalently conjugated or electrostatically anchored to the DN surface. These modifications increase the net

hydrodynamic radius of the structures, alter their shapes and surface properties and thus might alter their excretory and cellular uptake profiles.[24] It has been reported that nanomaterials of same geometric shape but different dimensions have varying rates of uptake by cells. For spherical gold NPs, silica NPs, single-walled carbon nanotubes and quantum dots, a 50 nm diameter is of optimal value that can maximize the rate of cellular uptake and intracellular concentration in certain mammalian cells.[25-27] Not only the shape and size but also the composition of the nanomaterial is a significant factor that influences the uptake of nanomaterials. It has been found that both 50 nm carbon nanotube and gold NPs have endocytosis rates of 10^{-3} min^{-1} and 10^{-6} min^{-1}, respectively. The observed difference of 1000-fold might arise from the difference of the intrinsic properties of carbon and gold.

Our aim was to use free stabilizing agents that could be added to the mixture of DNA strands prior to annealing of a particular structure. To look for the potential stabilizing agents we turned our attention towards the natural DNA compaction agents. There are certain molecules like polyamines that can bring about DNA compaction by binding electrostatically to the DNA double helix. Borrowing this concept, we tried to combat the low salt instability of DNs by forming them in the presence of simple amino acids like arginine and lysine, their low molecular weight polymers, and spremine. In addition we also used some intercalators and groove binders to test if they can contribute towards the stability enhancement of DNs under low magnesium conditions.

3.3 Results and Discussion

3.3.1 Designing the DNs

We chose three different structures (DN1, DN2 and DN3) for this project. DN1 is a hollow cage closed on all sides, DN2 is a densely packed 8x8 structure, and DN3 is a hollow cage open on two ends. DN1 and DN2 are designed in the square lattice motif while DN3 is designed in the honey-comb motif of the caDNAno software. The rationale for choosing these three structures lies in the difference of their packing densities. The stability dependence on divalent magnesium (and also on the stabilizing agents) should be a function of the packing density as more densely packed structures would require higher concentration of cations to screen the negative charge on the phosphodiester backbone of the DNA strands.

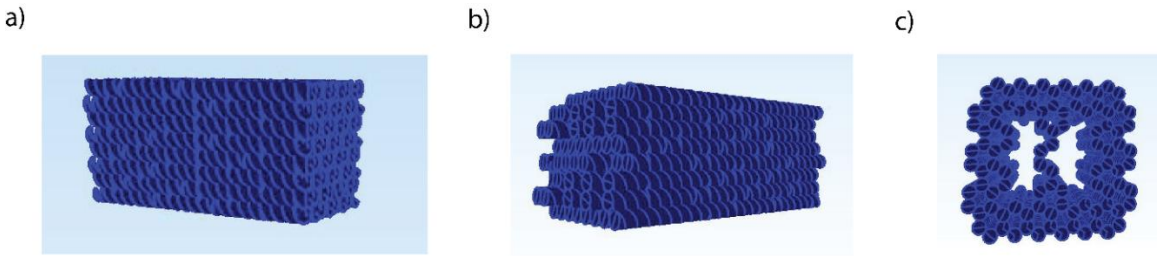

Figure 3.1: DNA nanostructures studied. a) DN1 b) DN2 c) DN3.

3.3.2 Screening of Stabilizing Agents

We screened ten different materials that can act as potential stabilizing agents (table 3.1). Different concentrations of aqueous solutions of these agents were added to the annealing mixture of DN1 (5 nM m13, 10X staples) making the final stabilizing agent

concentrations 1 uM, 10 uM, 50 uM, 100 uM, 500 uM, 1 mM and 1.5 mM. The resulting structures were imaged using TEM. From the results a table (3.2) was built showing the maximum amount of stabilizing agent that allowed the formation of complete DNs.

Table 3.1 List of potential stabilizing agents screened.

Nature of Interaction	Potential Stabilizing Agents
Electrostatic Interaction	Arginine 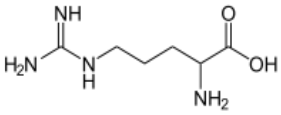 Lysine 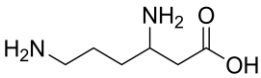 Hexamine Cobalt 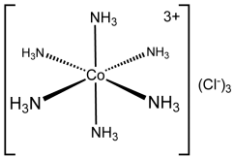 Glyoxyl-derived lysine dimer trifluoroacetate salt 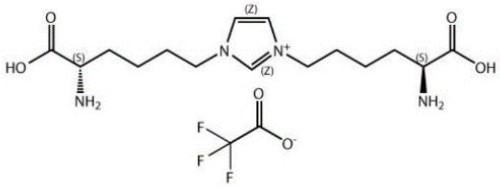
Groove Binder	Spermine 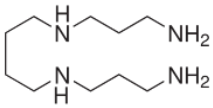 Hoechst Dye 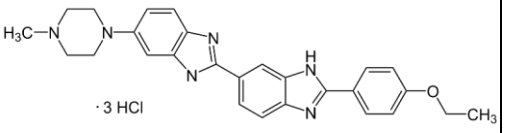 Netropsin 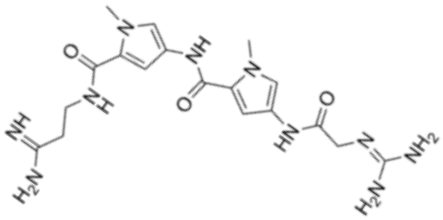

Intercalators	Thiaozle Orange 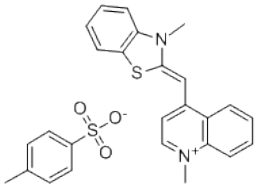 YOYO 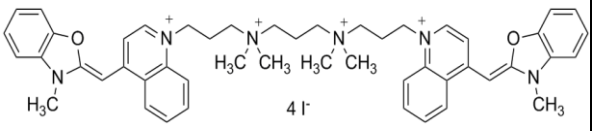
Dual interaction (Groove binding + intercalation)	DAPI 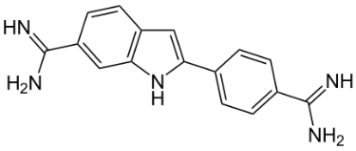

Table 3.2 Maximum concentration of each stabilizing agents that allow the formation of DN1.

Stabilizing agent	Maximum concentration of stabilizing agent that allowed formation of DN1 (mM)
Arginine / Lysine	1.0
Lysine	1.0
Bis-lysine	0.7
Spermine	0.1
Thiazole Orange	0.01
Hoechst Dye	0.01
Netropsin	0.01
DAPI	0.01
Hexamine Cobalt	0.01
YOYO	0.001

DN1 was annealed with the highest tolerable concentration of the free stabilizing agents in 1X 3D buffer containing 16 mM Mg^{2+}. Then we exchanged the annealing buffer with 1X physiological buffer and imaged the structures every 20 minutes. The images showed that out of the ten potential stabilizing agents only five are able to confer stability to the structures in low salt conditions. They are arginine, lysine, bis-lysine, hexamine cobalt and thiazole orange. Unlike the first four promising stabilizing agents, thiazole orange is not innocuous, so we discontinued using thiazole orange for further studies.

From the nature of the molecules that conferred enhanced stability to the DN in low salt conditions, it is prominent that four bind to the DNA electrostatically, while only thiazole orange is an intercalator. Probably, the ionic stabilizing agents are least demanding in terms of structural integrity than the other class of molecules studied. The other intercalator studied was YOYO that is a much larger molecule that thiazole orange. It is probable that it caused much higher deformation of the double helices than thiazole orange, and hence DN1 could be formed only in the presence of 1 μM YOYO, the least in the series.

3.3.3 Estimation of Stability Enhancement

The most commonly known method for estimating the stability of DNs is studying their mobility on electrophoretic gels. This method is not very sensitive and does not yield very accurate conclusions mainly because of three reasons. While studying stability in low salt conditions it might happen that some structures are partially deformed or unfolded but still they might have the same mobility on an electrophoretic gel. The second point is running through an agarose gel under a certain voltage is quite a harsh treatment that might itself bring about degradation of some structures. And the last, during the running time the structures might get degraded. Keeping these in mind we employed a different strategy to estimate the stability enhancement. After forming the DNs with and without the potential stabilizing agents, we subjected them to low magnesium buffer and then made TEM samples at different time points. While preparing TEM samples, 30 nm gold nanoparticles (AuNPs) were used as internal standards. We counted only the intact structures from TEM images and plotted the number of DNs per 100 AuNPs. While counting the intact images

from TEM images we can have a better idea about the intactness of the structures and exclude any deformed and/or degraded structures. This might be a better strategy to approach towards accurateness.

From the counting results we obtained the half-lives of each DN following the procedure explained in supplementary information S3.7. Figure 3.2 shows the half-lives of DN1 formed with maximum concentration of the stabilizing agents as mentioned in table 3.2. On comparing the values with the half-life of normal DN1, we see that bis-lysine provided the highest stabilization in absence of high magnesium in the buffer. With bis-lysine, the half-life of DN1 was increased almost three fold than the bare DN1. This increase is significant when looked at perspective of *in vivo* delivery as we need the carriers to be stable in circulation not for ever but for a therapeutically relevant length of time. The stabilizations conferred by arginine and lysine were almost same, lysine being slightly higher in efficiency.

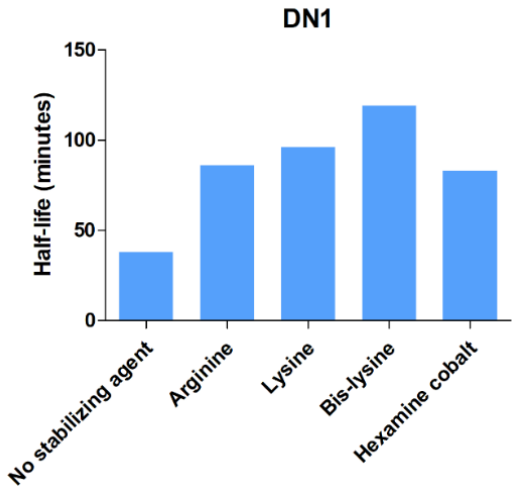

Figure 3.2: Comparison of half-lives of DN1 formed with and without free stabilizing agents.

Figure 3.3 depicts the half-lives of all three DNs formed with and without stabilizing agents. Bis-lysine always provided the highest stabilization irrespective of the structure studied. It is to be noted that the half-life of DN3 is the highest among the three structures followed by DN1 and then DN2. This could probably be explained by looking at their designs. DN3 was designed in the honeycomb motif of the caDNAno while the other two were designed using the square lattice motif. The former motif being more porous than the later, leads to less denser packing of the DNs. Hence the requirement of stabilizing cations was lesser for DN3 than the other two. While designing DN1, a cavity was intentionally left inside the structure. Conceptually, it can be said that if the cavity of DN1 is filled with densely packed DNA layers, we arrive at DN2. From this it is pretty obvious that DN1 had the highest packing density among the three DNs and this was reflected in the half-lives of the normal structures and the stabilized ones as well.

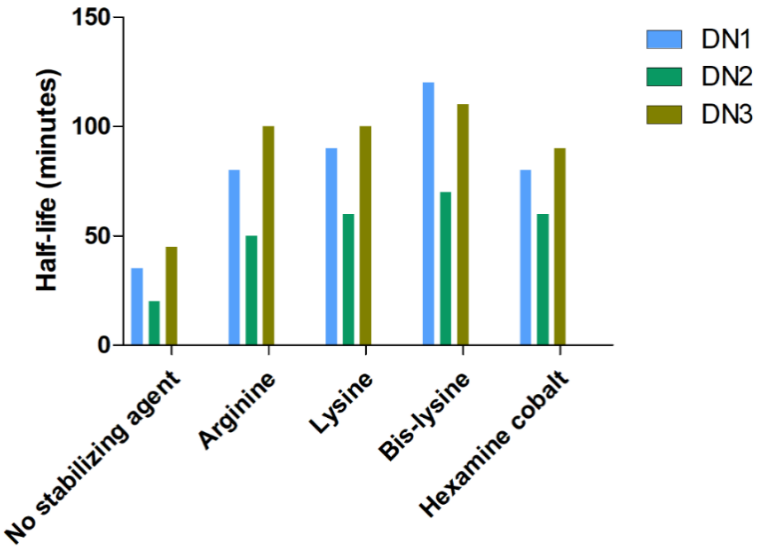

Figure 3.3: Comparison of half-lives of all three DNs formed with and without free stabilizing agents.

Being encouraged by the higher efficiency of lysine dimer in stabilizing structures we studied pentamer, decamer and higher polymers of lysine. But their presence in the annealing solution in concentrations as low as 100 nM did not allow the formation of well-defined structures. Those who are formed were either deformed, or incomplete or the yields were highly compromised. High degree of aggregation was observed in most of the cases.

3.3.4 Combination of Stabilizing Agents

After testing the stabilizing agents separately, we attempted to study the effect of their combination. The rationale behind this was that the different stabilizing agents might bind to different domains of a DNs thus providing additive stability to the structures, the following combinations were studied: a) arginine + lysine b) arginine + bis-lysine c) arginine + hexamine cobalt, d) lysine + hexamine cobalt, and e) bis-lysine + hexamine cobalt. Concentration titrations were also performed in a way similar to the single stabilizing agents and DN1 was used as the test structure. The results obtained are summarized in table 3.3.

Table 3.3 Concentration titration of combination of stabilizing agents

Combination	Maximum concentrations of combination of stabilizing agents that allowed formation of DN1 (mM)
Arginine + Lysine	0.5 + 0.6
Arginine + Bis-lysine	0.5 + 0.4
Arginine + Hexamine cobalt	0.5 + 0.0075
Lysine + Hexamine cobalt	0.5 + 0.0075
Bis-lysine + Hexamine cobalt	0.3 + 0.0075

Figures 3.4, 3.5 and 3.6 show the comparison of half-lives of DN1, DN2 and DN3 respectively formed with the single and selected combination of stabilizing agents.

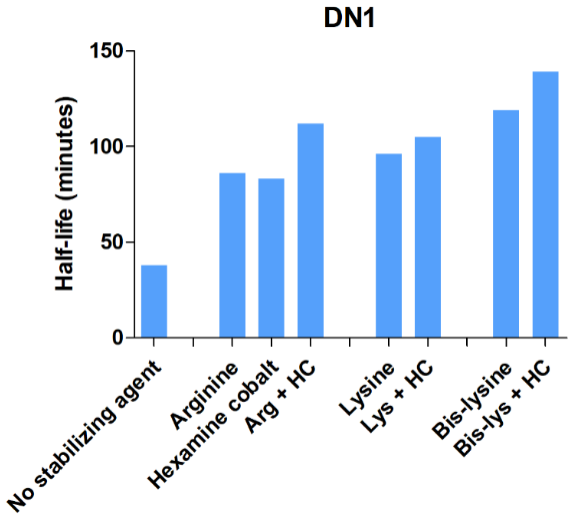

Figure 3.4: Comparison of half-lives of DN1 formed with single and combined stabilizing agents.

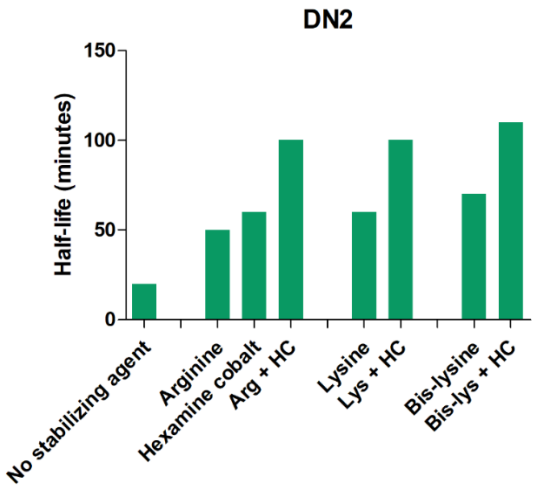

Figure 3.5: Comparison of half-lives of DN2 formed with single and combined stabilizing agents.

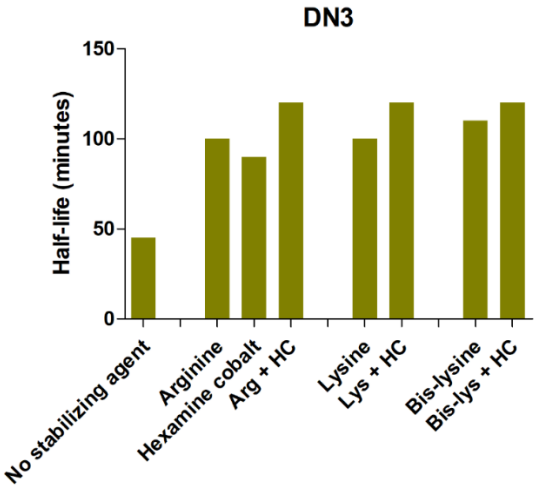

Figure 3.6: Comparison of half-lives of DN3 formed with single and combined stabilizing agents.

In all three cases, hexamine cobalt when combined with arginine, lysine and bis-lysine conferred the highest stabilization. But a combination of arginine and lysine (data not shown) did not enhance stability over any one of the amino acids. This might be an

indication that hexamine binds to different domains of the DNs than arginine and lysine and thus when used in combination the stabilization from each agent was added. However, this aspect requires further study to be confirmed and put in further applications.

3.3.5 Melting Temperature of DNs

All the stabilizing agents used in this study bind to the DNs electrostatically and have demonstrated stability enhancement effects in low salt conditions. In order to find out whether this enhancement is thermodynamic in nature we studied the melting temperatures of each DN formed with each stabilizing agent (or their chosen combination) following the procedure described in the supplementary information.

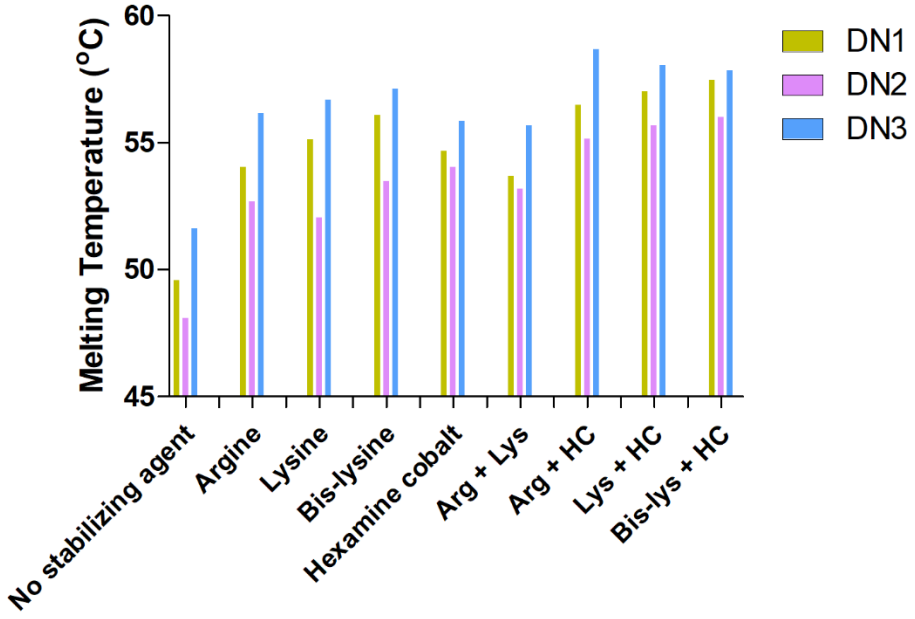

Figure 3.7: Melting temperatures of three DNs when formed with different stabilizing agents and their combinations.

Figure 3.7 compares the melting temperatures of the three DNs formed will all the stabilizing agents (single and combinations). It is evident that the stabilizing agents confer thermodynamic stabilization to the DNs that is reflected in their higher melting temperatures in comparison to the normal DNs. It is to be noted that the agent providing highest stability singularly (bis-lysine) makes the DN the most stable thermodynamically and similar is the effect of the most stabilizing combination (i.e., bis-lysine + hexamine cobalt).

3.4 Conclusion

From the screening of the potential stabilizing agents, we found that the molecules that bind electrostatically with the DNA double helix are the least demanding in terms of forming DNs and they confer the maximum stabilization. This can be explained primary by two rationale. First, probably they bring about the least deformation among the batch of stabilizing agents screened in this study. The other molecules bring about deformation of the DNA double helix to an extent such that formation of well-defined DNs are not possible. So when they are present in higher concentration in the annealing buffer, the DNs are not formed or form in deformed manner. The second reason behind the efficiency of the stabilizing agents in the dissociation kinetics of the molecules with DNA. The more they are retained inside the structure, the more they are able to screen the negative charge of the phosphodiester backbone and maintain the dense packing of the DNs.

We have presented the results from the bis-lysine in this paper. But we have also studied pentamers and decamers of both arginine and lysine and they generally do not allow the formation of structures even at a concentration as low as 1.0 uM. This strengthens the

probability that if the stabilizing agents present in the annealing buffer deform the shaped of the DNA double helix beyond a certain extent, the DNs would not form.

In this study we have tested a certain number of potential stabilizing agents in a particular range of concentration and some limited number of their combinations. This study shows the promise that smart DNs that are intrinsically stable under low salt conditions can be made by forming them with simple stabilizing agents. A wide range of DNA compacting and complexing agents in different concentrations and combinations can be studied in order to search for better and more effective stabilizing agents. They can eliminate the need of any special polymer coating on the DNs to make them stable under physiological conditions, thus alleviating the scope of an increased hydrodynamic radius and unknown immune activations while in circulation.

3.5 References

1. Seeman, N. C. *Annual review of biochemistry* **2010**, *79*, 65.
2. Douglas, S. M.; Dietz, H.; Liedl, T.; Högberg, B.; Graf, F.; Shih, W. M. *Nature* **2009**, *459*, 414.
3. Dietz, H.; Douglas, S. M.; Shih, W. M. *Science* **2009**, *325*, 725.
4. Han, D.; Pal, S.; Nangreave, J.; Deng, Z.; Liu, Y.; Yan, H. *Science* **2011**, *332*, 342.
5. Rothemund, P. W. *Nature* **2006**, *440*, 297.
6. Dutta, P. K.; Varghese, R.; Nangreave, J.; Lin, S.; Yan, H.; Liu, Y. *Journal of the American Chemical Society* **2011**, *133*, 11985.
7. Schreiber, R.; Do, J.; Roller, E.-M.; Zhang, T.; Schüller, V. J.; Nickels, P. C.; Feldmann, J.; Liedl, T. *Nature nanotechnology* **2014**, *9*, 74.
8. Liu, Y.; Lin, C.; Li, H.; Yan, H. *Angewandte Chemie* **2005**, *117*, 4407.
9. He, Y.; Tian, Y.; Ribbe, A. E.; Mao, C. *Journal of the American Chemical Society* **2006**, *128*, 12664.
10. Zhang, F.; Nangreave, J.; Liu, Y.; Yan, H. *Journal of the American Chemical Society* **2014**, *136*, 11198.
11. Chhabra, R.; Sharma, J.; Liu, Y.; Rinker, S.; Yan, H. *Advanced drug delivery reviews* **2010**, *62*, 617.
12. Lu, C.-H.; Willner, B.; Willner, I. *ACS nano* **2013**, *7*, 8320.
13. Campolongo, M. J.; Tan, S. J.; Xu, J.; Luo, D. *Advanced drug delivery reviews* **2010**, *62*, 606.
14. Douglas, S. M.; Bachelet, I.; Church, G. M. *Science* **2012**, *335*, 831.
15. Lee, H.; Lytton-Jean, A. K.; Chen, Y.; Love, K. T.; Park, A. I.; Karagiannis, E. D.; Sehgal, A.; Querbes, W.; Zurenko, C. S.; Jayaraman, M. *Nature nanotechnology* **2012**, *7*, 389.
16. Li, J.; Pei, H.; Zhu, B.; Liang, L.; Wei, M.; He, Y.; Chen, N.; Li, D.; Huang, Q.; Fan, C. *ACS nano* **2011**, *5*, 8783.
17. Liu, X.; Xu, Y.; Yu, T.; Clifford, C.; Liu, Y.; Yan, H.; Chang, Y. *Nano letters* **2012**, *12*, 4254.
18. Chang, M.; Yang, C.-S.; Huang, D.-M. *ACS nano* **2011**, *5*, 6156.

19. Jiang, Q.; Song, C.; Nangreave, J.; Liu, X.; Lin, L.; Qiu, D.; Wang, Z.-G.; Zou, G.; Liang, X.; Yan, H. *Journal of the American Chemical Society* **2012**, *134*, 13396.

20. Zhao, Y.-X.; Shaw, A.; Zeng, X.; Benson, E.; Nyström, A. M.; Högberg, B. r. *ACS nano* **2012**, *6*, 8684.

21. Perrault, S. D.; Shih, W. M. *ACS nano* **2014**, *8*, 5132.

22. Hahn, J.; Wickham, S. F.; Shih, W. M.; Perrault, S. D. *ACS nano* **2014**, *8*, 8765.

23. Ponnuswamy, N.; Bastings, M. M.; Nathwani, B.; Ryu, J. H.; Chou, L. Y.; Vinther, M.; Li, W. A.; Anastassacos, F. M.; Mooney, D. J.; Shih, W. M. *Nature Communications* **2017**, *8*.

24. Albanese, A.; Tang, P. S.; Chan, W. C. *Annual review of biomedical engineering* **2012**, *14*, 1.

25. Chithrani, B. D.; Chan, W. C. *Nano lett* **2007**, *7*, 1542.

26. Lu, F.; Wu, S. H.; Hung, Y.; Mou, C. Y. *Small* **2009**, *5*, 1408.

27. Jin, H.; Heller, D. A.; Sharma, R.; Strano, M. S. *Acs Nano* **2009**, *3*, 149.

CHAPTER 4

BUILDING SERUM ALBUMIN-COATED DNA NANOSTRUCTURES FOR *IN VIVO* APPLICATIONS

4.1 Abstract

Stabilization of DNA nanostructures (DNs) in physiological conditions is a threshold that must be crossed if DNA nanotechnology has to make successful contributions in the field of therapeutics and diagnostics. The factors limiting the *in vivo* stability of DNs are low salt conditions, degradation from nucleases and opsonization. Opsonization is the immune process that renders a foreign particle recognizable to the macrophages of the mononuclear phagocyte system (MPS) and bring about rapid clearance of the injected particles. Albumin proteins are one of the most abundant proteins in blood and if we can coat the DNs with serum albumin before injection, they might void recognition by the macrophages. We tested this hypothesis by ornamenting two DNs with a albumin attracting molecule reported earlier and incubated them with human serum albumin (HSA). On studying the cellular uptake of HSA coated DNs, it was found that they showed a lower uptake than the uncoated structures. We also studied if this coating can render the DNs more stable in a cell culture medium that provides both the physiological conditions of low salt and presence of nucleases. The time vs stability results demonstrated that HSA coating was able to enhance the lifetimes of DNs.

4.2 Introduction

From being simply a structural arena of research exploring the 3D design space of nanoscale objects and building nanostructures of increasingly diverse shapes, sizes and dynamics,[1-4] DNA nanotechnology has shown tremendous potential in biomedical applications like biosensing,[5,6] building synthetic vaccines[7,8], nucleic acid delivery[9] and drug delivery[10,11] in the past few decades. However for delivering cargo in a living system the DNA nanostructures (DNs) have to be stable in physiological conditions. Lower half-life of a drug requires high-frequency dosing in order to provide a sustained dosing effect. So half-life extension strategies have to be implemented on the DNs for improving their circulatory abilities for successful biomedicinal applications.

There has been continuing attempts to comprehend the instability of DNs in physiological conditions and to come up with strategies overcoming the limitations. In 2014, Perrault and coworkers reported that while the denaturation of the DNs due to low salt conditions was dependent on design and time, the degradation by nucleases is not dependent on time.[12] Being inspired by virus capsules, the same group came up with a strategy to encapsulate DNA nanostructures into liposome and achieved higher lifetimes in circulation.[13] In 2017, Shih and coworkers reported an oligolysine coating that can be applied over the DNs via electrostatic adsorption and this coating can protect them from low salt denaturation and nuclease degradation for prolonged hours.[14] However, researchers have now directed their attention towards using proteins that are abundant in blood for coating DNs to make them stable in vivo. The most abundant protein in human blood is the 66 kDa human serum albumin that comprises 50–60% of the total serum

proteins.[15] The half-life of HSA in circulation is around 19 days[16] that makes it a promising candidate to be explored for half-life enhancement strategies. The high binding capacity, high bioavailability and low cost has made HSA a candidate of interest in drug delivery. In addition to all these advantages, it has also been found that HSA accumulates in solid tumors and is retailed due to EPR effect.[17] FDA has already given approval to drugs encapsulated in albumin NPs that can be used for cancer treatment. Abraxane, currently available in the market, is being used to treat lung, breast and pancreatic cancers.[18] This drug is actually an albumin paclitaxel NPs.

Not many reports are available in the literature that have studied the applicability of HSA in nucleic acid delivery and therapeutics. In 2003, Manoharan and coworkers explored this strategy and conjugated ibuprofen to an antisense oligonucleotide, the oligo being itself bound to HSA with micromolar affinity.[19] Recently in 2017, Lacroix and coworkers applied the strategy of HSA conjugation to improve the pharmacokinetics and biodistribution of DNs.[15] They conjugated dendritic alkyl chains to a very simple DN and showed that it can bind to HSA with a Kd of ~5 nM. They also showed that HSA conjugation enhances the lifetime of the DN in cell culture medium supplemented with 10% FBS.

In our work we employed the albumin-binding molecule tags reported by Huang and coworkers in 2012.[20] They have attached albumin binding molecule tags to compstatin, a 13-residue cyclic peptide that interacts with the complement component C3 and also with its activation fragment C3b and thus inhibits complement activation.[21,22] In this project, we used the molecule tag used by Huang and coworkers and attached it with a single stranded

DNA which , in turn, was attached to DNA handles protruded out from two DNs. The azide version of the albumin binding molecule tag that we used is shown in figure 4.1.

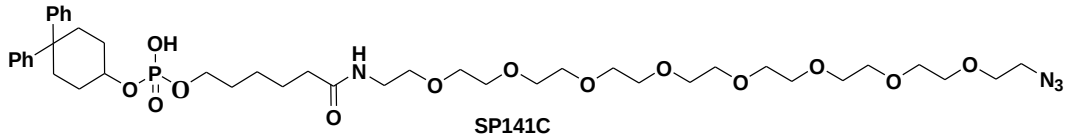

Figure 4.1: Albumin attracting molecule (SP141C).

In comparison to the work done by Lacroix and coworkers, we dealt more complex DNs that are more demanding with respect to salt concentration and are expected to unfold quite rapidly when injected. Our results confirm successful attachment of HSA to the two DNs we used and conjugation to the albumin considerably enhanced their half-lives in a cell culture medium supplemented with 10% FBS. Our findings also show that HSA coated DNs showed reduced uptakes by murine macrophages in comparison to the non-coated structures.

4.3 Results and Discussion

4.3.1 Building the DNs

In order to compare results and establish the generality of our findings, we conducted studies using two DNs: a DNA tetrahedron (Td) and an 8x8 DNA origami (DNO) designed in the square lattice motif of caDNAno. The tetrahedron (Td) we used (with some modifications) have been employed by Chang, Yang and coworkers in 2012 for building up a DNA platform for synthetic vaccines.[8] The schematic representation (S 4.3.2.1) shows that each Td is comprised of four symmetric units capable of inter-unit

assembly through sticky end hybridization. Three strands on each of the constituent units were modified with a single stranded handle. Hence, a complete Td had 12 DNA handles and each handle was hybridized to S5-AAM to which HSA can be attached. Similarly, in case of DNO 24 surface staples were selected and their ends protruding outside were extended leading to 24 handles that can be hybridized to S5-AAM. (Structural details for both Td and DNO are provided in S4.3).

Td being a comparatively hollower structure more resembling a wireframe DN than a densely packed DNA origami, the divalent cation requirement should be lesser while the scope for nuclease action should be higher. Exactly the reverse is expected to be true for densely packed DNO that was designed in the square lattice motif of caDNAno. It requires high magnesium concentration in medium for being stable. Employing both of them for the experiments, we can get a better idea regarding the efficiency of our HSA-coating strategy to enhance the stability of DNA nanostructures in physiological conditions.

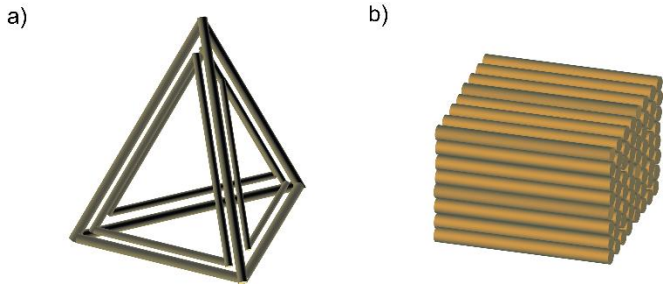

Figure 4.2*:* a) Td b) DNO.

4.3.2 Synthesis of Albumin Attracting Molecule (AAM)

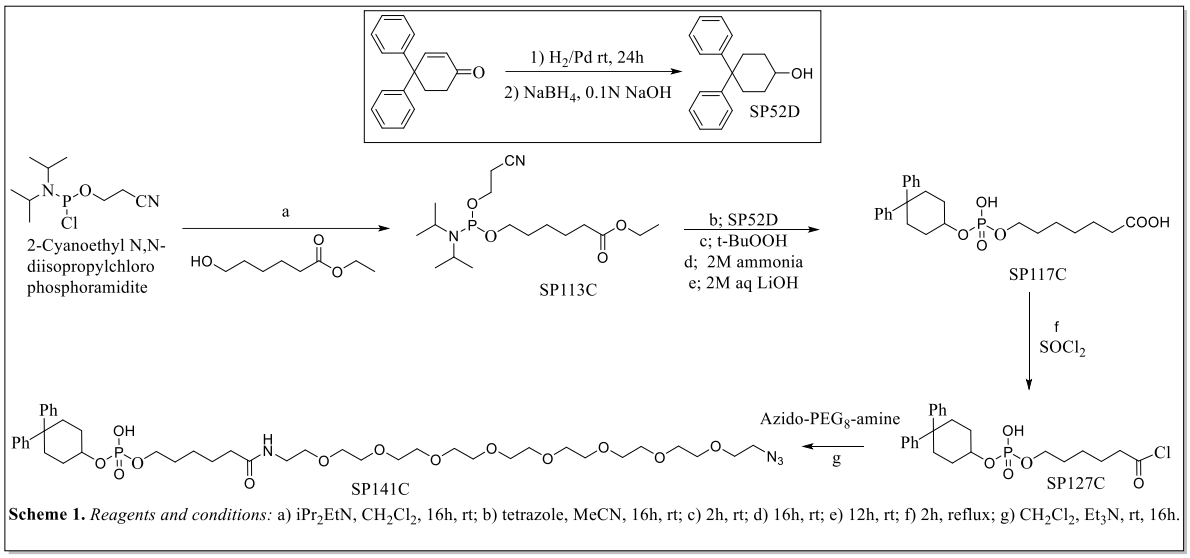

Figure 4.3: Scheme showing the synthesis of AAM (SP141C).

The molecule was synthesized by Dr. Stevan Pecic from the Stojanvic group at Columbia University. In order to prepare the albumin-attracting molecule SP141C, we employed synthetic approach that involves 5 synthetic transformations altogether (Scheme 1). According to previously published procedure, we first synthesized the intermediate 4,4-diphenylcyclohexanol, SP52D by a hydrogenation and reduction with sodium borohydride of commercially available starting material 4,4-diphenyl-2-cyclohexen-1-one in one pot. This reaction provided the intermediate molecule SP52D in 84% yield.[23] We then coupled commercially available ethyl 6-hydroxyhexanoate with 2-cyanoethyl *N*,*N*-diisopropyl-chlorophosphoramidite, which furnished phosphoramidite SP113C. In the next step, we coupled SP113C with the intermediate molecule SP52D, followed by oxidation with tert-butyl hydroperoxide in order to obtain the phosphodiester. Subsequently, the cyanoethyl protecting group was removed using ammonia in methanol and the ethyl ester cleaved with

lithium hydroxide to the get the free acid SP117C. This carboxylic acid was then converted to the acid chloride SP127C by refluxing with thionyl chloride, and finally coupled to the amino terminus of the commercially available azido-$(PEG)_8$-amine in order to get the final product SP141C.

4.3.3 Conjugation of Serum Albumin to DNA

AAM was synthesized with an azide terminal so that it can be conjugated to a DNA strand containing a strained alkyne (DBCO) via copper uncatalyzed click reaction. We conjugated the amine functionality of a DNA strand (S5) with DBCO-NHS ester (supplementary information 4.5) and obtained the DNA-DBCO. This strand was reacted with different equivalents of AAM at room temperature for 6 h and mass spectrometry of the click-conjugated product was recorded. It was found that a S5-DBCO: AAM ratio of 1:2.5 yielded a S5-AAM product (S 4.6). The S5-AAM thus obtained was reacted with increasing equivalents of HSA and a characterization gel showed a 1:5 ratio of S5-AAM: HSA led to decent conversion to S5-HSA (S4.7).

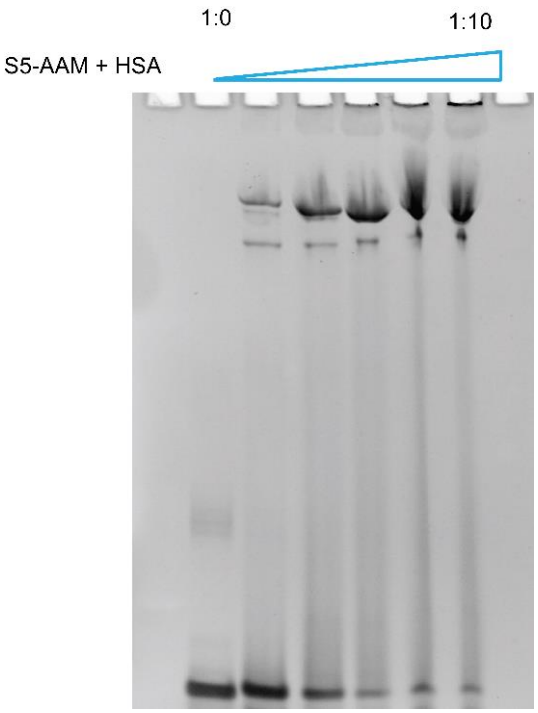

Figure 4.4: HSA binding of S5-AAM.

4.3.4 Coating DNA nanostructures with serum albumin

Both Td and DNO were mixed with 5 fold equivalents of S5-AAM when S5 hybridized with the handles on Td and DNO. When incubated with 5 equivalents of HSA for 4 h, the DNs got coated with HSA was demonstrated by agarose gel characterizations. For confirming that the DNs were bound to HAS we added excess of anti-HAS antibody to an aliquot from each of the HSA coated DNs. A prominent gel shift showed that the DNs were indeed coated with albumin. A mixture of DNs decorated with AAM and anti-HSA antibody was used as control that showed same mobility as the corresponding DNs on agarose gel.

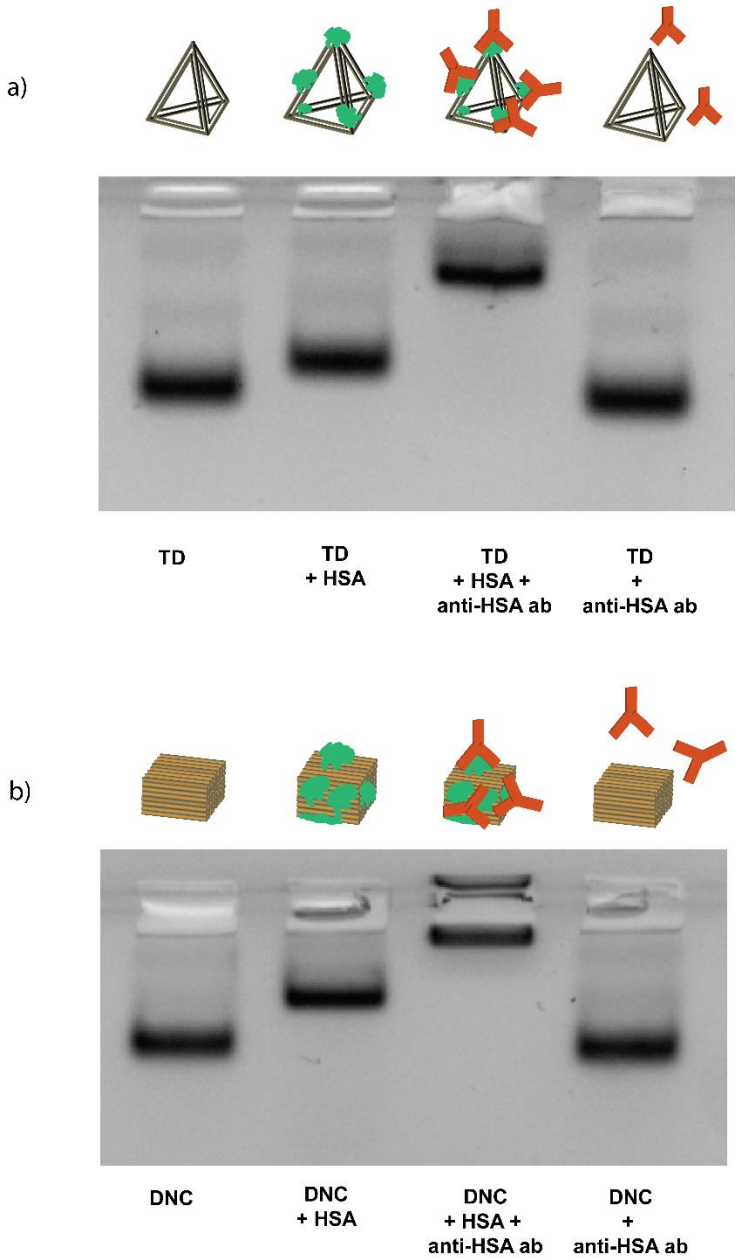

Figure 4.5: HSA coating of a) Td b) DNO.

4.3.5 Stability of Albumin-coated Structures in Physiological Conditions

The DNA nanostructures require high magnesium concentration (~5–20 mM) to preserve their structural integrity. But this amount of magnesium is not available in the

physiological fluids or cell culture medium. Hence the structures degrade when incubated with cells or injected in a living body. In addition to the low salt denaturation, nucleases are abundantly present in blood as well as in the commonly used cell culture medium that is supplemented with 10% fetal bovine serum (FBS). We studied the stability of HSA coated DNs in DMEM + 10% FBS and our findings showed almost 2 fold increase in half-life of Td and ~2.5 fold increase in case of DNO.

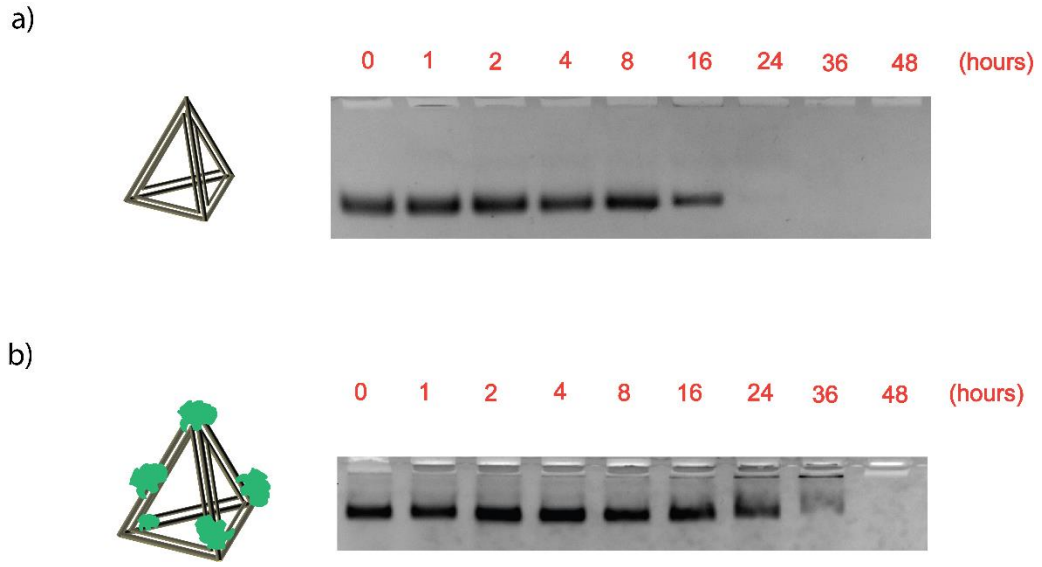

Figure 4.6: Time vs stability of a) bare Td b) HAS-coated Td.

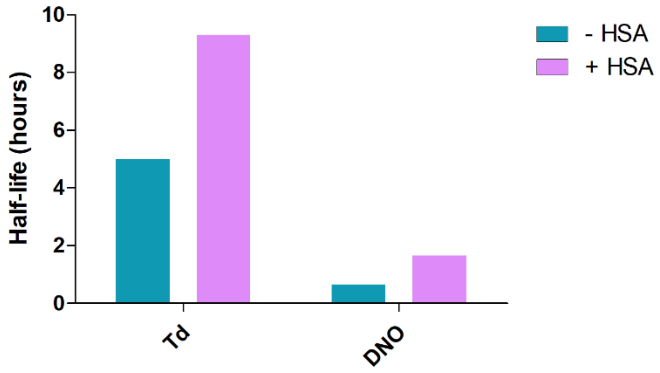

Figure 4.7: Half-lives of coated and uncoated DNs.

4.3.6 Confocal Microscopy

Before carrying out the flow cytometry studies to investigate the cellular uptake of albumin coated DNs, it was essential to be assured that the structures do not stick to the cell surface and thus do not contribute towards the fluorescence signal in cytometry leading to false positive results. So we incubated the structures with the RAW cells and recorded confocal microscopy images to confirm the cellular internalization of structures. We incubated dye-labeled S4, Td and DNO, and albumin coated Td and DNO with the RAW cells and imaged the living live. For all of them the internalization by the RAW cells was confirmed from the orthogonal section of the confocal microscopy images. In addition, we treated a batch of cells after incubation with the strands and the structures with DNase so that any strand or structure attached to the cell surface is degraded. The orthogonal sections of the confocal imaged recorded after DNase treatment also confirmed the presence of fluorescent particles inside the cells. Confocal microscopy images of Td, DNase treated Td, HSA coated Td, DNase treated HSA-coated Td are shown below.

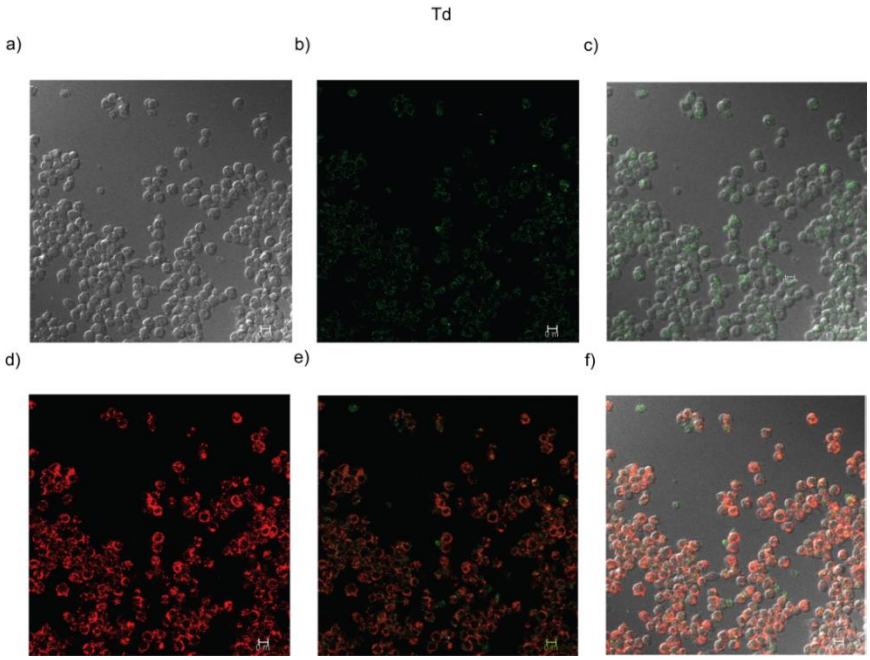

Figure 4.8*:* Confocal microscopy images of RAW cells incubated with Alexa fluor 488 labeled Td. The cell membranes were stained with CellTracker CM-Dil dye. a) Bright field image b) green fluorescence from internalized Td c) overlay of bright field and green fluorescence d) red fluorescence from CellTracker CM-Dil dye e) overlay of green and red fluorescence f) overlay of bright field, green and red fluorescence.

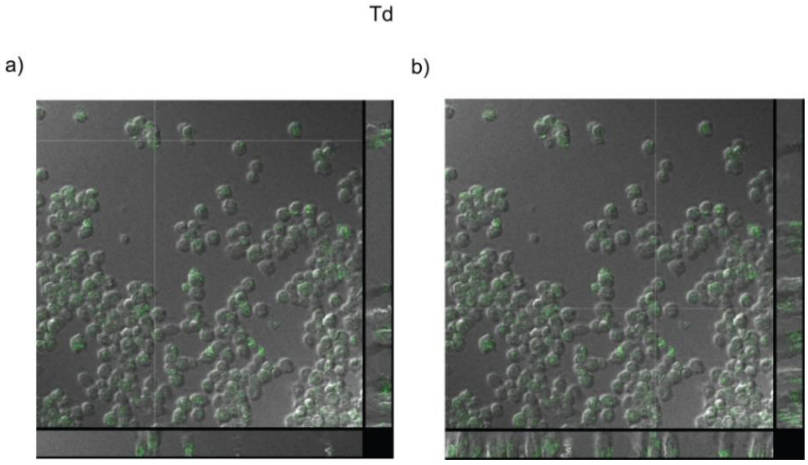

***Figure 4.9**:* Z-stacked confocal microscopy images of RAW cells incubated with Alexa fluor 488 labeled Td. The crosshairs indicate orthogonal sectioning. The bottom and right panels show the sectioned planes and confirm that fluorescent particles (green) are located inside the cells and not merely attached to the cell membrane.

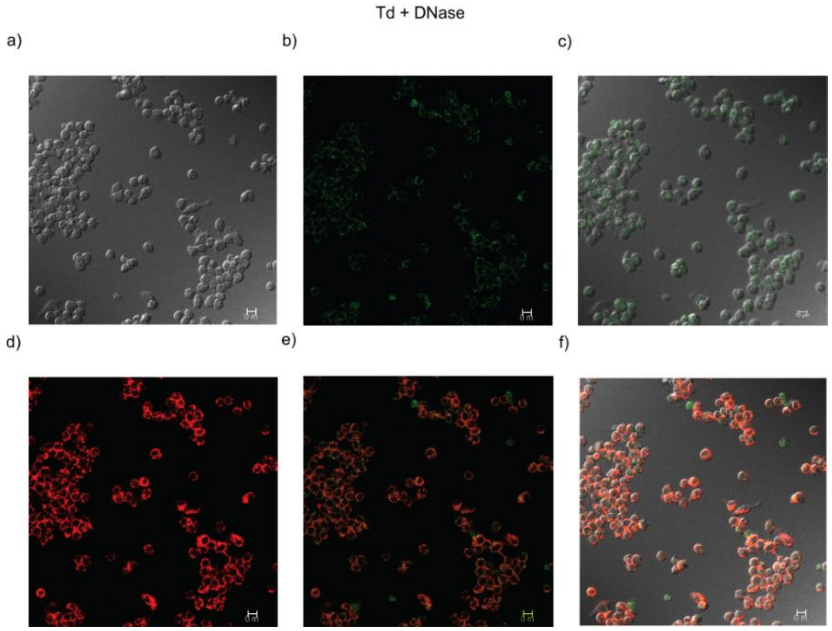

***Figure 4.10**:* Confocal microscopy images of RAW cells incubated with Alexa fluor 488 labeled Td and then treated with DNase. The cell membranes were stained with CellTracker CM-Dil dye. a) Bright field image b) green fluorescence from internalized Td c) overlay of bright field and green fluorescence d) red fluorescence from CellTracker CM-Dil dye e) overlay of green and red fluorescence f) overlay of bright field, green and red fluorescence.

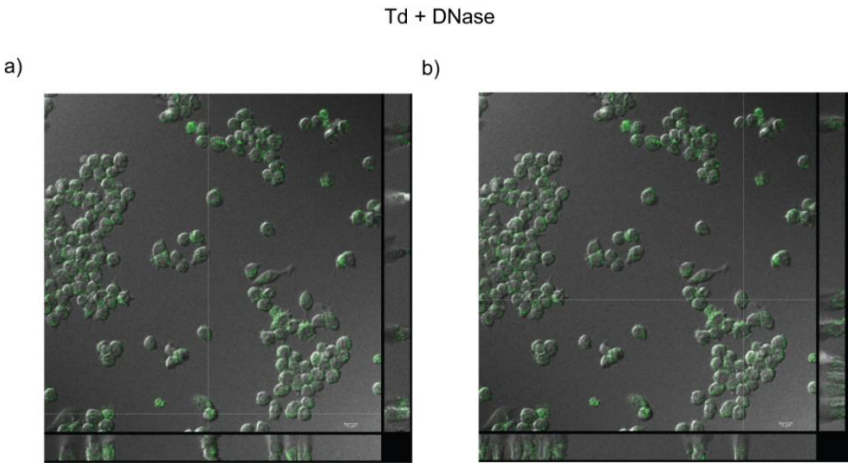

Figure 4.11: Z-stacked confocal microscopy images of RAW cells incubated with Alexa fluor 488 labeled Td and then treated with DNase.

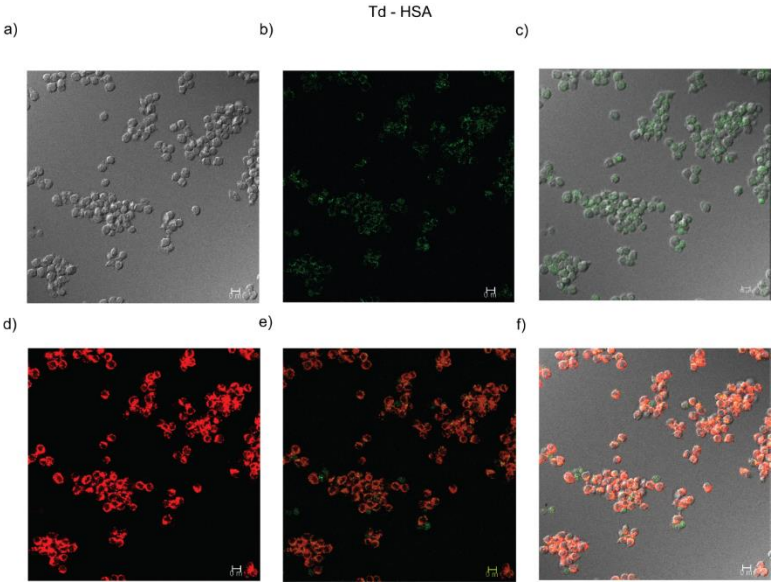

Figure 4.12: Confocal microscopy images of RAW cells incubated with Alexa fluor 488 labeled HSA-coated Td. The cell membranes were stained with CellTracker CM-Dil dye. a) Bright field image b) green fluorescence from internalized Td c) overlay of bright field and green fluorescence d) red fluorescence from CellTracker CM-Dil dye e) overlay of green and red fluorescence f) overlay of bright field, green and red fluorescence.

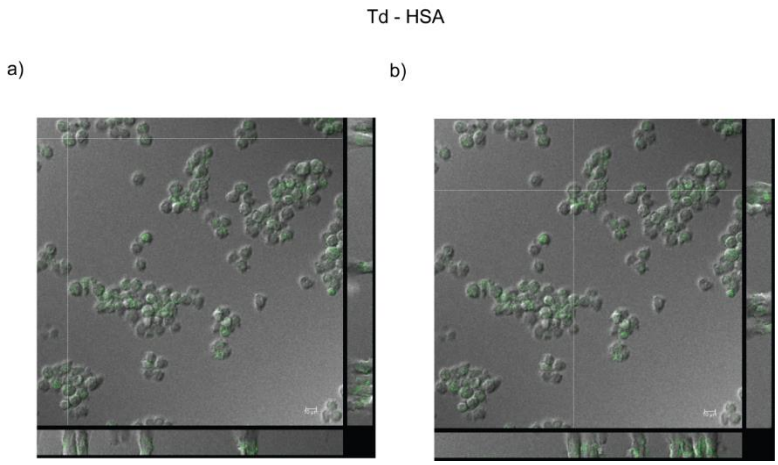

Figure 4.13*:* Z-stacked confocal microscopy images of RAW cells incubated with Alexa fluor 488 labeled HSA coated Td.

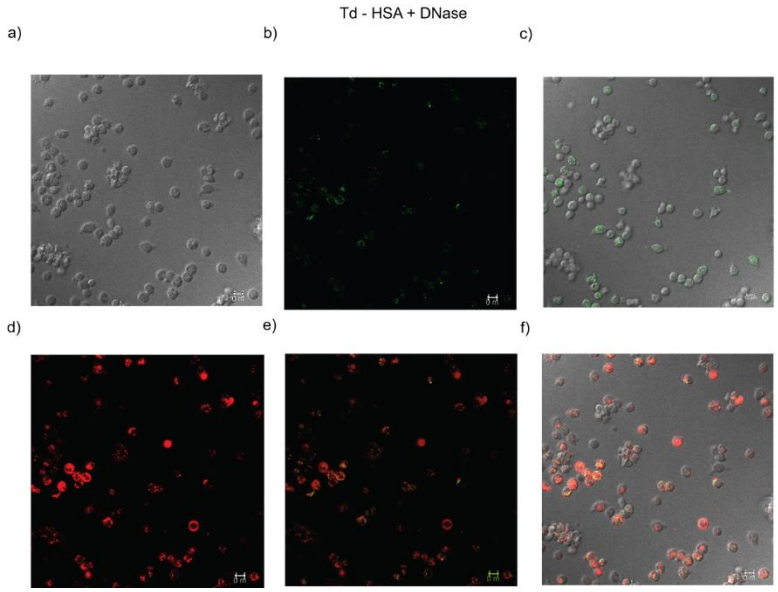

Figure 4.14*:* Confocal microscopy images of RAW cells incubated with Alexa fluor 488 labeled HSA-coated Td followed by DNase treatment. The cell membranes were stained with CellTracker CM-Dil dye. a) Bright field image b) green fluorescence from internalized Td c) overlay of bright field and green fluorescence d) red fluorescence from

CellTracker CM-Dil dye e) overlay of green and red fluorescence f) overlay of bright field, green and red fluorescence.

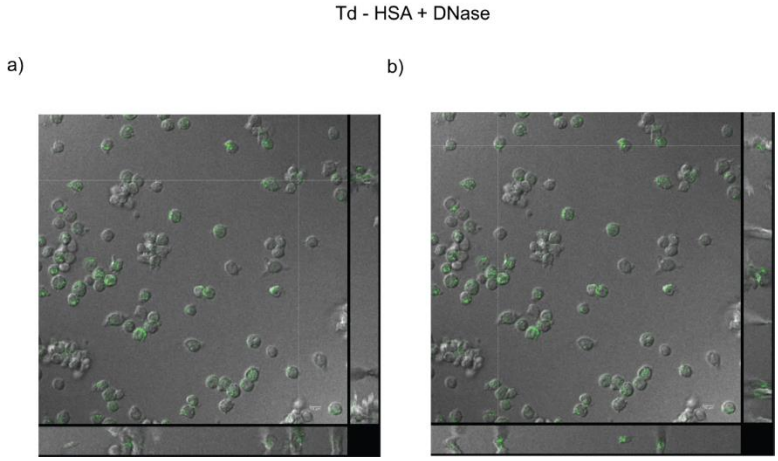

Figure 4.15*:* Z-stacked confocal microscopy images of RAW cells incubated with Alexa fluor 488 labeled HSA coated Td followed by DNase treatment.

4.3.6 Cellular Uptake of Albumin-coated DNs

Albumin being a ubiquitously occurring member in the blood, the albumin-coated structures would not be identified by the macrophages as potential candidates of phagocytosis. We used murine macrophage (RAW) cells to study how the albumin-coating influences uptake of DNs. The bare and HAS coated structures were incubated with the RAW cells in DMEM + 10% FBS medium at 37°C and in 5% carbon dioxide for 1 h. The dye labeled DNA was also incubated as a control. The membrane of the dead cells have higher permeability towards foreign particles and hence they can contribute largely to the fluorescence signals, thus leading to erroneous conclusions. Before subjecting to flow cytometry analysis, the cells were suspended in a propidium iodide solution in order to

detect and exclude the dead cells from analysis. As controls, we also treated separate batches of cells (pre-incubated with controls and structures) with DNase for ten minutes before flow cytometry analysis.

Comparing the fluorescence, it was found that there was almost no difference between the DNase treated and untreated controls. This confirmed that all the results obtained are from actually internalized structures and not mere DNs sticking to the cell surface.

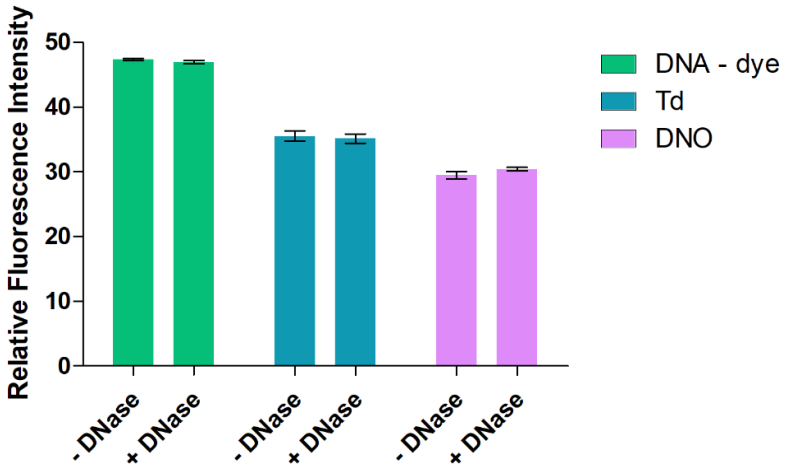

Figure 4.16*:* Comparing fluorescence intensity of DNase treated and untreated controls.

On comparing the RFI values of bare and coated Tds we see that the albumin coating had reduced the internalization by almost 50% while the same is around 40% in case of DNO.

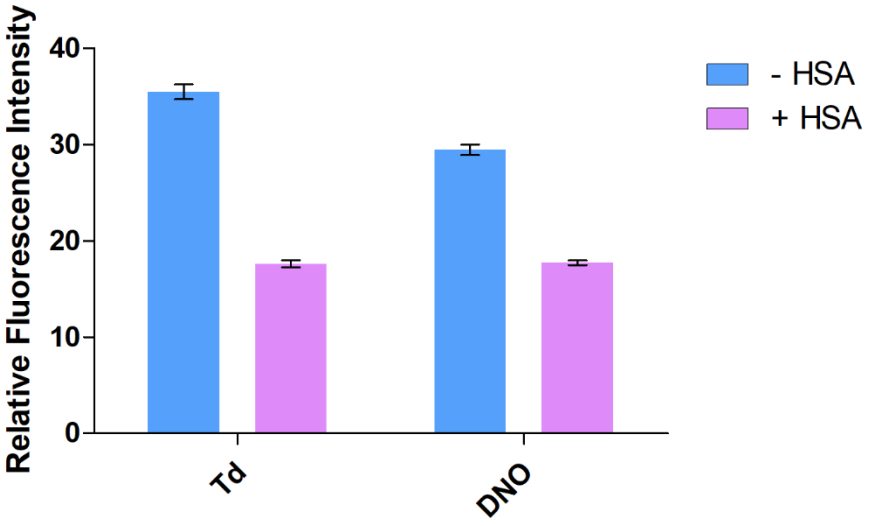

Figure 4.17*:* Cellular uptake of bare and albumin coated DNs.

4.4 Conclusion

We reported a successful synthesis of an albumin attracting molecule and coated two DNA nanostructures with that AAM. Those DNs when incubated with HSA developed an albumin coating around them. The coating was able to stabilize the DNs under physiological conditions and reduced their uptake by macrophages when incubated with murine RAW cells. The decrease in cellular uptake was lower in case of the larger DNO structure in comparison to Td. This might be due to the insufficient surface coverage of DNO by albumin molecules. Further studies can be done by varying the number and position of albumin attachment on larger DNs and this study would be able to reveal the optimal surface coverage that leads to minimum internalization of the coated DNs.

4.5 References

1. Dietz, H.; Douglas, S. M.; Shih, W. M. *Science* **2009**, *325*, 725.
2. Douglas, S. M.; Dietz, H.; Liedl, T.; Högberg, B.; Graf, F.; Shih, W. M. *Nature* **2009**, *459*, 414.
3. Rothemund, P. W. *Nature* **2006**, *440*, 297.
4. Han, D.; Pal, S.; Nangreave, J.; Deng, Z.; Liu, Y.; Yan, H. *Science* **2011**, *332*, 342.
5. Zheng, D.; Seferos, D. S.; Giljohann, D. A.; Patel, P. C.; Mirkin, C. A. *Nano letters* **2009**, *9*, 3258.
6. Pei, H.; Lu, N.; Wen, Y.; Song, S.; Liu, Y.; Yan, H.; Fan, C. *Advanced Materials* **2010**, *22*, 4754.
7. Li, J.; Pei, H.; Zhu, B.; Liang, L.; Wei, M.; He, Y.; Chen, N.; Li, D.; Huang, Q.; Fan, C. *ACS nano* **2011**, *5*, 8783.
8. Liu, X.; Xu, Y.; Yu, T.; Clifford, C.; Liu, Y.; Yan, H.; Chang, Y. *Nano letters* **2012**, *12*, 4254.
9. Lee, H.; Lytton-Jean, A. K.; Chen, Y.; Love, K. T.; Park, A. I.; Karagiannis, E. D.; Sehgal, A.; Querbes, W.; Zurenko, C. S.; Jayaraman, M. *Nature nanotechnology* **2012**, *7*, 389.
10. Zhao, Y.-X.; Shaw, A.; Zeng, X.; Benson, E.; Nyström, A. M.; Högberg, B. r. *ACS nano* **2012**, *6*, 8684.
11. Chang, M.; Yang, C.-S.; Huang, D.-M. *ACS nano* **2011**, *5*, 6156.
12. Hahn, J.; Wickham, S. F.; Shih, W. M.; Perrault, S. D. *ACS nano* **2014**, *8*, 8765.
13. Perrault, S. D.; Shih, W. M. *ACS nano* **2014**, *8*, 5132.
14. Ponnuswamy, N.; Bastings, M. M.; Nathwani, B.; Ryu, J. H.; Chou, L. Y.; Vinther, M.; Li, W. A.; Anastassacos, F. M.; Mooney, D. J.; Shih, W. M. *Nature communications* **2017**, *8*, 15654.
15. Lacroix, A.; Edwardson, T. G.; Hancock, M. A.; Dore, M. D.; Sleiman, H. F. *Journal of the American Chemical Society* **2017**, *139*, 7355.
16. Sleep, D.; Cameron, J.; Evans, L. R. *Biochimica et Biophysica Acta (BBA)-General Subjects* **2013**, *1830*, 5526.
17. Iyer, A. K.; Khaled, G.; Fang, J.; Maeda, H. *Drug discovery today* **2006**, *11*, 812.
18. Gradishar, W. J.; Tjulandin, S.; Davidson, N.; Shaw, H.; Desai, N.; Bhar, P.; Hawkins, M.; O'Shaughnessy, J. *J clin Oncol* **2005**, *23*, 7794.

19. Manoharan, M.; Inamati, G. B.; Lesnik, E. A.; Sioufi, N. B.; Freier, S. M. *ChemBioChem* **2002**, *3*, 1257.

20. Huang, Y.; Reis, E. S.; Knerr, P. J.; van der Donk, W. A.; Ricklin, D.; Lambris, J. D. *ChemMedChem* **2014**, *9*, 2223.

21. Sahu, A.; Kay, B. K.; Lambris, J. D. *The Journal of Immunology* **1996**, *157*, 884.

22. Ricklin, D.; Lambris, J. D. In *Current Topics in Complement II*; Springer: 2008, p 262.

23. C. Amedio Jr, J.; Bernard, P. J.; Fountain, M.; VanWagenen Jr, G. *Synthetic communications* **1998**, *28*, 3895.

24. Deleavey, G. F.; Damha, M. J. *Chemistry & biology* **2012**, *19*, 937.

CHAPTER 5

PROXIMITY LIGATION ASSAY TO ESTIMATE THE STABILITY OF DNA NANOSTRUCTURES

5.1 Abstract

DNA nanotechnology has emerged as a promising tool that can build 2D and 3D DNA nanostructures (DNs) with desired shape, size and complexity. The diverse scopes of modification of these structures along with their biocompatibility render them potential candidates for *in vivo* applications like biosensing and drug delivery. But for successful *in vivo* applications, DNs must be stable in circulation for at least a therapeutically relevant period of time. Currently, the most common method to estimate the time vs stability of DNs is to compare the electrophoretic gel mobility of the intact DNs and injected DNs. This method is not very sensitive and in many cases it is not able to differentiate between intact and partially degraded structures. We have developed a proximity based sensitive assay to estimate the time vs stability of DNs in realistic situations like cell culture medium and blood circulation. The concept of the assay, named the proximity ligation assay (PLA), is adopted from protein research and applied to the DNs. Two single stranded antennae on a wireframe DNA tetrahedron (Td), which, due to their proximity, were ligated during the PLA and the new sequence was amplified using PCR. The read out, when compared to a calibration curve, was able to estimate the number of intact Td present in the analyte after a certain time. In case of a degraded Td that is missing one or both of the antennae, or if they are far away from each other (due to partial degradation of the structure) ligation would not occur, thus differentiating between an intact and degraded structure with

excellent sensitivity. The PLA also works with antennae having phosphorothioate backbone (which is required to avoid nuclease degradation occurring *in vivo*.) We subjected the DNs to various degrading conditions (like low magnesium salt buffer, cell culture medium and human serum) and confirmed the validity of the newly developed assay results by comparison with electrophoretic gel results. We also injected the Td in mice models and established that the PLA can estimate the stay-time of the structures in circulation. In order to establish the generality of the assay we performed it on a larger tetrahedron and a DNA origami and confirmed its functionality.

5.2 Introduction

Over the past few decades DNA nanotechnology has become a promising area of research that exploits programmed self-assembly of single stranded DNA to build complex 3D structures with a variety of shapes and sizes in nanoscale, with high degree of responsiveness and controllable dynamic properties.[1-3] These DNs can be modified in diverse ways leading to site-specific functionalizations and owing to non-immunogenic and biodegradable nature, they are potential candidates for diagnostics and therapeutics. A nanorobot that can release Fab antibody fragments in the presence of target cells was built by Douglas and co-workers in 2012.[4] Anderson and co-workers employed a tetrahedron for *in vivo* delivery of small interfering RNA to target and suppress gene expression in a mouse model.[5] Fan, Huang and co-workers assembled a multivalent DNA tetrahedron for noninvasive delivery of immunostimulatory CpG oligonucleotides[6] and thus demonstrated that DNs can also serve as platforms for synthetic vaccines. Yan, Chang and co-workers have employed a DNA tetrahedron for coassembly of model antigens and CpG with precise

control over the valency and spatial arrangement of each constituent.[7] DNs have also been employed to carry drug molecules *in vivo* either by intercalation into the carrier DNA helix or by attachment through chemical conjugation. Huang and co-workers demonstrated the application of aptamer-conjugated DNA icosahedral NPs as carriers of doxorubicin for cancer therapy.[8] In 2012, Ding and co-workers constructed 2- and 3-D doxorubicin-loaded (through intercalation) DNs and showed that their construct demonstrated prominent cytotoxicity to regular human breast adenocarcinoma cancer cells (MCF 7) and also to doxorubicin-resistant cancer cells.[9] In the same year Högberg and co-workers developed DNA origami delivery systems for cancer therapy that have tunable release properties.[10]

In spite of these outstanding reports, there are several concerns regarding biomedical application of DNs, the major ones are about their stability of DNs in low salt conditions, vulnerability towards nucleases and opsonization when injected leading to rapid removal from the body.[11] Salt concentrations (~5–20 mM Mg^{2+}) required for the stability of DNs is not present in normal physiological fluids. Divalent ions screen the negative charges on the phosphate backbones and assist the folding of DNs with varying density of packing. In absence of required amount of salt the DNs denature, their lifetime being dependent on several factors like the density of packing, shape and size of the structures, etc. In addition to denaturation, nuclease activity and opsonization also limit the circulation time of DNs in blood.

To estimate the stability of DNs in physiological conditions, we need to administer them in a living animal, draw blood after regular intervals and subject the samples to an assay for obtaining a read-out. But after injection, DNs get highly diluted, and also develop

a corona of plasma proteins around them. Thus the structures exist in diverse states ranging from single intact entities to aggregates and deformed structures. This demands a very sensitive and accurate system of detection that can differentiate between the intact structures and everything else. The most common current method for stability detection is isolating structures from blood and running two dimensional electrophoretic gels, the band intensities being indicative of the stability of the injected DNs. This methods includes a high degree of approximation and lacks sensitivity and specificity. Electrophoresis could not be carried out with very low concentration of DNs, thus having a sensitivity limitation. In addition, the structures might be partially degraded and still show the same mobility as the intact structures. The intact structures might also aggregate with the mediation of plasma proteins and thus are collected in the gel wells, instead of running into the gel. The assay to be developed should be specific enough to differentiate based on the single criteria of the intactness of the DNs. Another issue is the time required to isolate the DNs from blood, as this lag period can lead to significant degradation. In 2013 Krishnan and coworkers demonstrated a method to estimate the *in vivo* stability of DNs.[12] Their protocol involves incorporation of an I-switch into the DN and can be used only under special conditions. So we need to develop a smart solution-based assay that can be executed quickly, must yield easily detectable signals, have low background noise, and must be able differentiate between intact and denatured DNs even from a very low concentration of the structures.

For development of the assay we direct our attention towards the arena of protein research. In 2002 Frederickson et al. proposed a method named Proximity Ligation for *in*

vitro detection and quantification of very small amounts of a specific protein.[13] In terms of sensitivity, **t**his method was far superior to existing methods like gel electrophoresis, mass spectrometry, and antibody-based ELISA. The researchers exploited the spatial proximity of two oligonucleotide extensions from two DNA aptamers that bind to the homodimer of the analyte protein. Once aptamer pair bind to the protein, the ends of the oligonucleotide extensions come into close vicinity and then they can be fixed by being hybridized to a connecter oligonucleotide. The free ends of the extensions are then ligated together by T4 DNA ligase and the resulting sequence can act as PCR template, thus leading to amplification and quantification with remarkable sensitivity. It was able to detect 24,000 molecules (4×10^{-20} moles) of the platelet-derived growth factor B-chain (PDGF-BB) protein, almost 10^3 fold lesser than that a standard sandwich ELISA assay can detect for the same target.

We translated this assay to DNs to estimate their stability under various conditions both *in vitro* and *in vivo*. We hypothesized that we can extend two constituent strands of a DN and the extensions can act as the antennae that can be connected by the 'connector' strand, ligated and the resulting sequence can be used as the template for PCR amplification. For testing our hypothesis, we modified the wireframe DNA tetrahedron (Td) synthesized by Tuberfield and coworkers in 2004[14] first with a single pair of antennae (single-pair experiment) and incubated them in different media like low magnesium buffer (containing 1.2 mM Mg^{2+}), cell culture medium (with and without FBS) and human serum. To study the dependence of sensitivity on the number of antennae we tested both single and double pairs of antennae (double-pair experiment). As the blood contains a number of

nucleases, there is always a chance that the nucleic acid antennae are chopped off by these enzymes. So we tested if the assay can be carried out with antennae having phosphorothioate backbone and the results turned out to be positive. After this, we injected two Tds with phosphodiester backbone (TdP) and phosphorothioate backbone (TdS) into mouse model to demonstrate the successful application of this assay. Finally we tested if this assay can be applied to estimate the stability of a more complex structure. When applied to a higher molecular weight Td (TD) made up of four symmetric units used by Yan, Chang and co-workers[7] and a DNA origami (DNC), appreciable sensitivity of the assay was demonstrated.

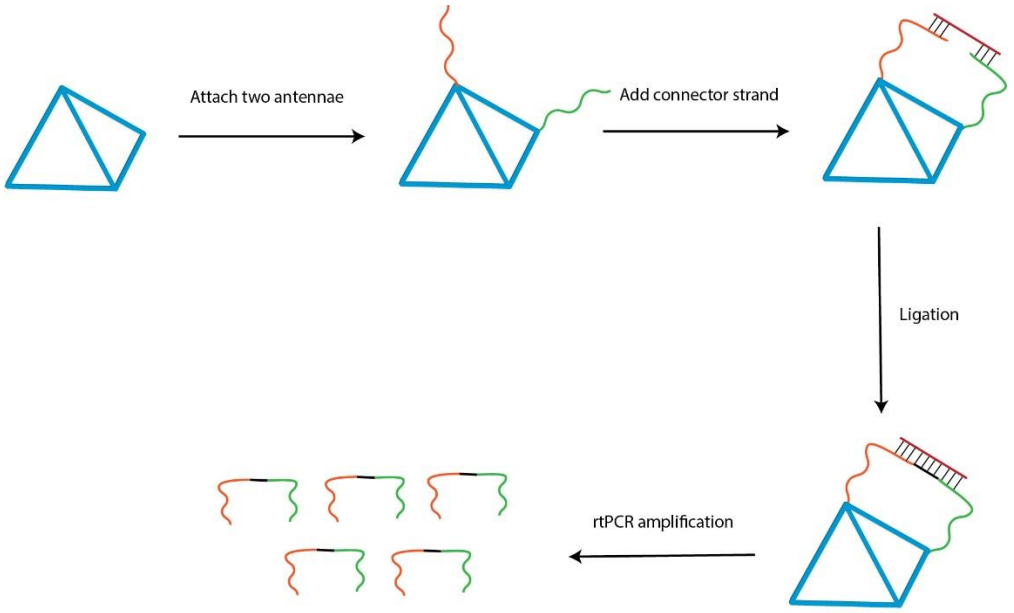

Figure 5.1: Proximity Ligation Assay design on a DNA tetrahedron.

5.3 Results and Discussion

The structural designs and characterization was performed by Saswata Banerjee in the Yan Lab, ASU. All the RT PCR experiments were done by Dr. Nenad Milosavic from the Stojanovic research group at Columbia University in New York.

5.3.1 PLA on Antennae with Phosphodiester Backbone

For the first trial we modified a very simple tetrahedron Td[14] comprising of four single stranded DNA with two antennae that are extensions of two constituent strands. The antennae pair had normal phosphodiester backbones (hence denoted as TdP2). After annealing the tetrahedron following a standard protocol, we ligated the antennae pair using T4 ligase. The resulting structure was subjected to PCR amplification following the protocol described in S5.6. A mixture of the free antennae, TdP with single antenna (TdP1) and a Td without any antenna were used as controls. When compared to the mixture of free antennae, PLA on TdP2 yielded ~$2x10^3$ fold greater sensitivity, while compared to a mixture of TdP1 and the other antenna free in solution, PLA was ~$5x10^3$ fold more sensitive in detecting TdP2.

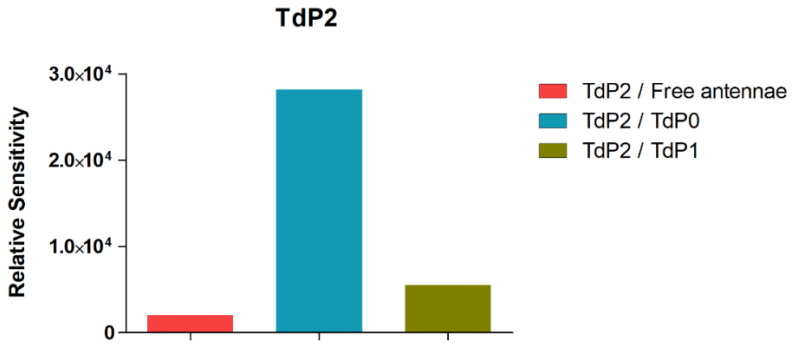

***Figure 5.2*:** PLA on TdP2.

After achieving positive results from the first trial, we wanted to estimate the effect of number of antennae on the sensitivity of PLA. On practical grounds, multiple pairs of antennae at different points on the structure can provide information about its overall integrity with time. We incorporated another antennae-pair (having same sequence as A1 and A2) into Td by extending the remaining two constituent single strands (resulting structure being denoted as TdP4). When compared with structures (TdP3) having three antennae (A1, A2, A1 or A1, A2, A2), the TdP4 showed ~3 times higher sensitivity.

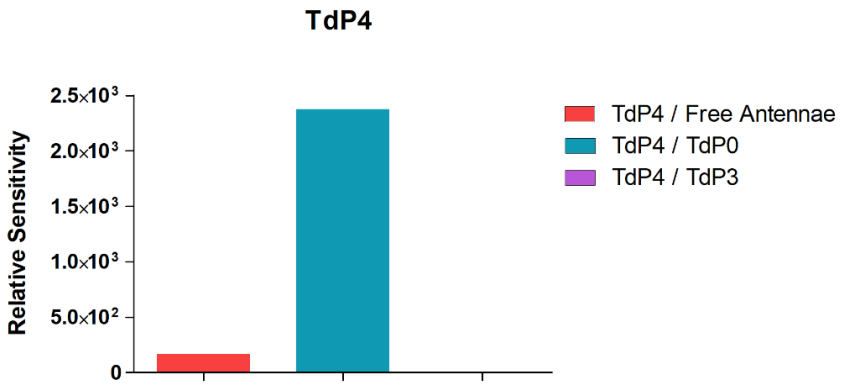

***Figure 5.3*:** PLA on TdP4.

The obvious next attempt was to test the generality of the designed assay by employing larger and more complex structures. With this goal in mind, we used the tetrahedron (TD) used by Chang, Yan and coworkers in 2012[7] and also designed a DNA origami cage (DNC) based on the square lattice motif of the caDNAno. The rationale behind designing this cuboid structure with a cavity inside, is to test whether PLA can work on a potential drug delivery vehicle. DNC can carry certain cargo in its cavity and the cavity being walled on all sides, chance of leakage is also reduced.

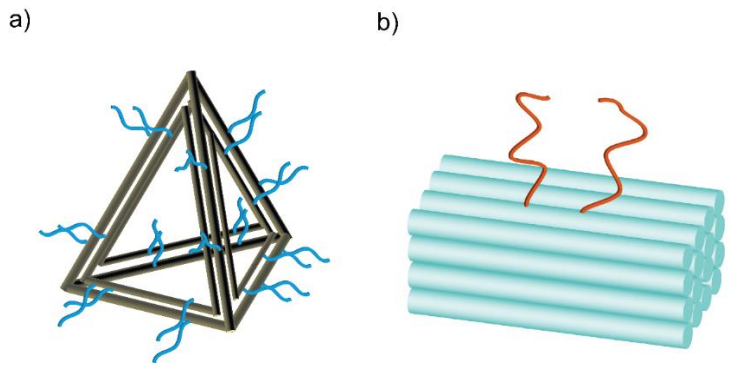

***Figure 5.4*:** a) TD b) DNC.

TD was comprised of four symmetric units, each of which is made up of ten single stranded DNA – one central strand hybridized to three sets of three single strands. We selected two strands from two of these three sets and attached the antenna sequences (A1 and A2) to each of them. Thus each constituent unit of TD has three antennae pairs and the complete structure consisted of 12 antennae pairs. When subjected to PLA, the TD showed ~$3x10^3$ fold higher sensitivity over the TD with no antennae. This increase is probably due to the higher number of antennae present on the structure. We placed a single pair of antenna at a distance of ~5 nm on its surface. When subjected to PLA, DNC with an antennae pair showed ~$2.6x10^5$ times more sensitivity over the control having no antenna.

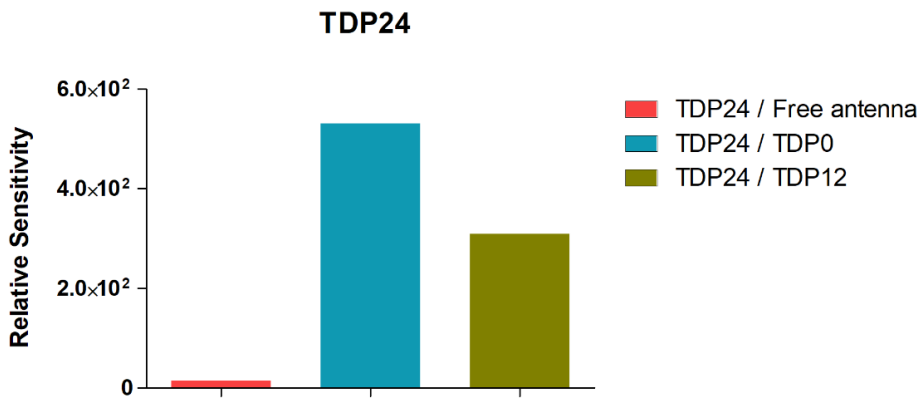

***Figure 5.5*:** PLA on TDP24.

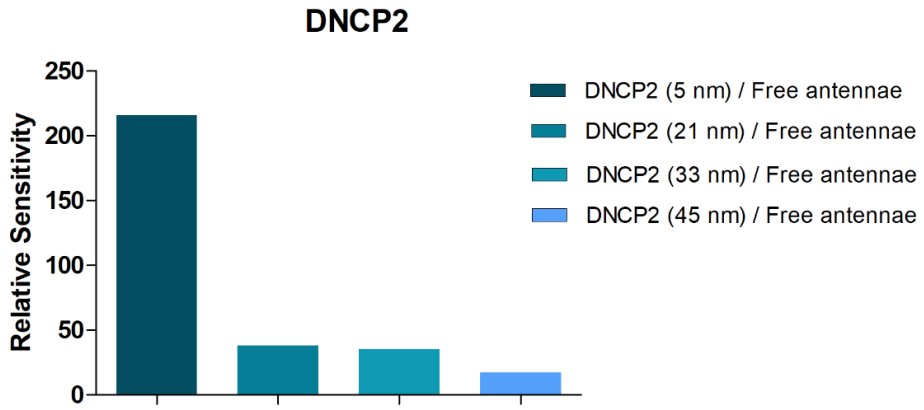

***Figure 5.6*:** PLA on DNC with a various inter-antennae distances.

5.3.2. PLA on antennae with Phosphorothioate Backbone

In realistic situations, when we inject the structures into blood stream, we need to consider the chance of degradation of antennae by nucleases abundant in blood. A common method to turn nucleic acids nuclease-resistant is backbone modification. So we replaced the backbone of the antenna pair on TdP2 with phosphorothioate backbone and constructed TdS2. PLA on this structure led to compromised sensitivity but it was ~2–3 fold higher

sensitivity over the free mixture of antennae. However, the sensitivity was higher when compared to the zero antenna and single antenna TDS controls. The backbone of DNC (5 nm) on phosphorothioation resulted in much higher sensitivities both over the free antennae and DNCS0 and DNCS1 controls.

a)

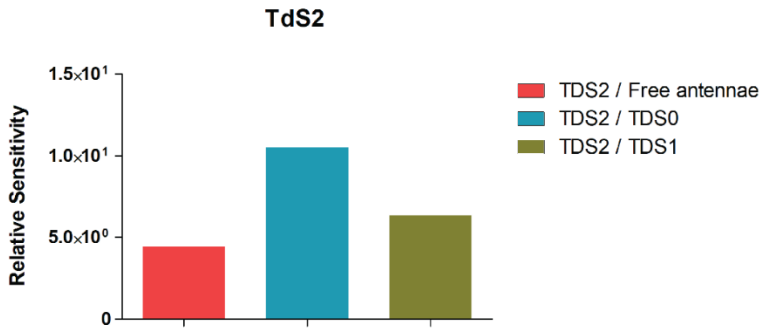

b)

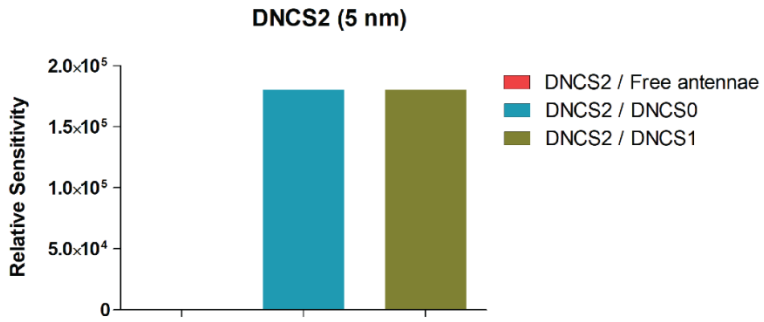

***Figure 5.7*:** Comparison of PLA results obtained from a) TdS2 and b) DNCS2.

5.3.3 Time vs Stability Studies *In Vitro*

We wanted to test if the PLA can be applied to realistic situations where the existing conditions are detrimental to the structural integrity of the DNs. For formation of DNs, the individual DNA strands have to come closer and form a somewhat dense packing

(depending on the structure design). But the phosphodiester backbones being negatively charged repel the single strands approaching towards each other. So, conventionally high concentrations of magnesium (~5–20 nM) are used to screen the negative charges on DNA backbone. This concentration of magnesium is not available in physiological conditions or tissue culture medium. Hence, when DNs are incubated with cells for any experimental purposes or injected in blood, they degrade rapidly. Another factor aggravating their denaturation is the presence of nucleases in the serum. Combined, they lead to fast degradation of DNs in physiological conditions. We decided to subject one of the DNs we used previously under these conditions and estimate their stability with time using both PLA and conventional gel electrophoretic techniques and compare the results from both. We chose the TdP2 for this purpose. The rationale behind choosing this particular structure is that among the three structures studied, this one being the simplest wireframe structure does not involve any dense packing of DNA and hence is the least demanding in terms of salt concentration in the medium to maintain structural integrity. This would allow us to study the time vs stability for a considerable length of time involving several data points. We subjected TdP2 to four different conditions – a) buffer containing 0.8 mM Mg^{2+}, b) DMEM medium, c) DMEM with 10% FBS, and d) human serum, and tested the time vs stability using PLA. It was found that in all the media the TdP2 showed exponential degradation. The results obtained from PLA closely matched with the ones obtained via gel electrophoresis.

a)

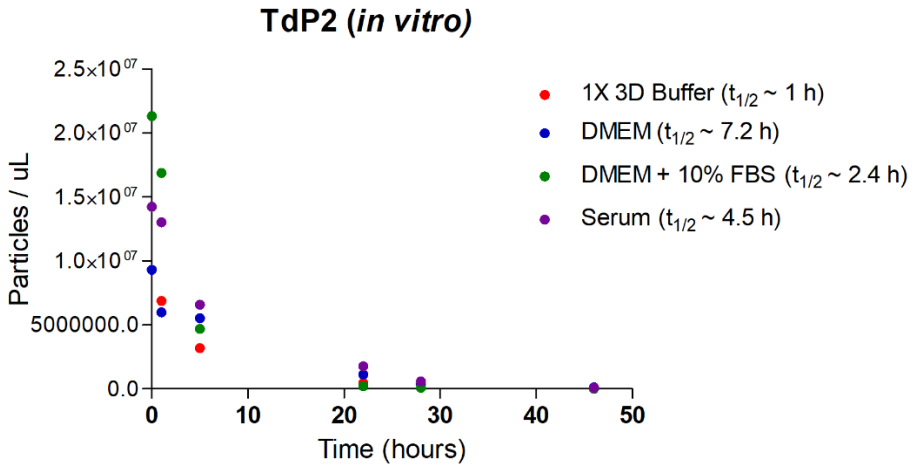

b)

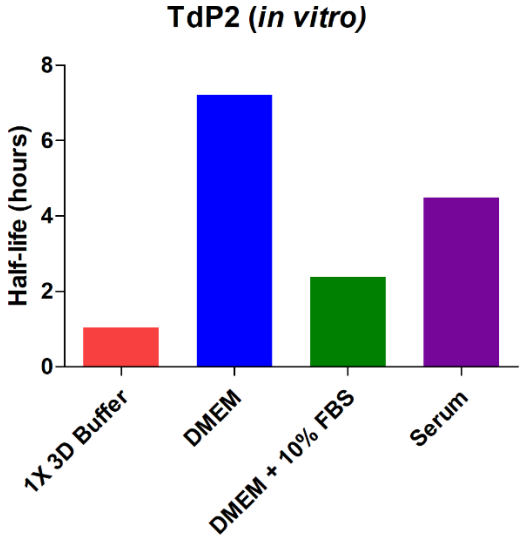

Figure 5.8: PLA results from in vitro TdP2 samples. a) Particles/uL plotted with time b) comparison of half-lives.

5.3.4 Time vs Stability Studies *In Vivo*

Finally, we attempted to test whether PLA can estimate the stability of DNA nanostructures from *in vivo* samples. So both TdP2 and TdS2 were injected into rats and

the time vs stability curves were constructed following similar PLA protocols as was done in *in vitro* experiments. It is found that the PLA results obtained from the *in vivo* samples are in good agreement with the ones obtained from *in vitro* experiments.

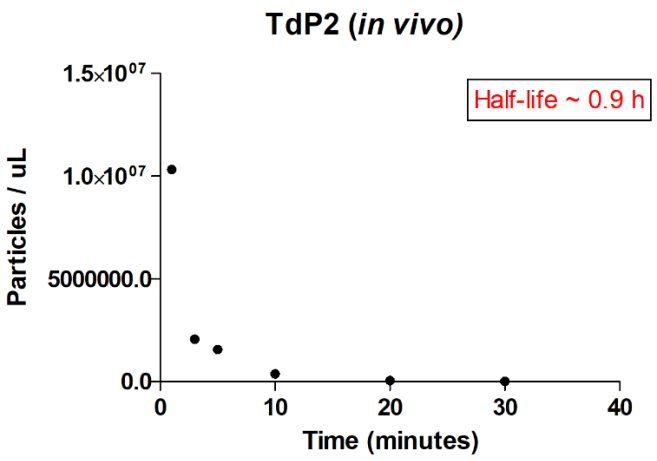

Figure 5.9: Time vs stability curve for TdP2 from *in vivo* sample.

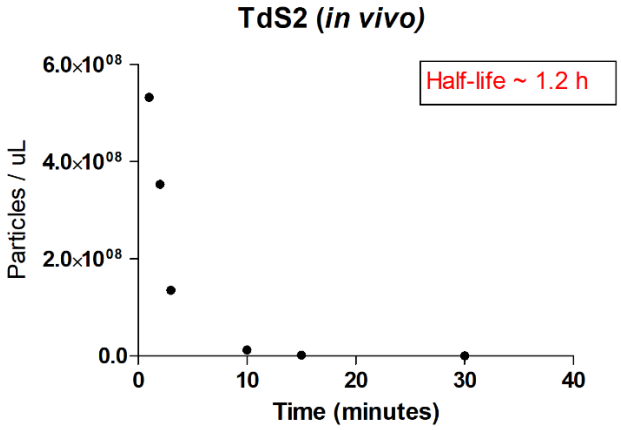

Figure 5.10: Time vs stability curve for TdS2 from *in vivo* sample.

5.4 Conclusion

Herein we reported a simple proximity based assay that can estimate the stability of DNA nanostructures with high sensitivity. However, three aspects still need further investigation. The first is the dependence of PLA sensitivity on antenna sequence. By optimizing the GC content of the antennae better results could be obtained. The second point of interest should be using higher number of antenna. We used a single pair of antenna in most of our studies. By incorporating more number of similar and dissimilar pairs of antenna estimates about DN stability on local and global scales can be obtained. The next step of this research is to plant multiple pairs on 3D origamis and use smarter combinations of antennae where one central antenna can act as the pair-member for several surrounding antennae. Then by judicious use of different connecting strands and PCR primers, we can determine which antenna is present and which one is missing with time when DNs are subjected to degrading conditions. Comparison of results from our *in vivo* experiments show that phosphorothioate backbone perform better. From our in vitro experiments we found when the backbone was shifter from phosphodiester to phosphorothioate, there was a reduction in sensitivity. This aspect needs further investigations so that the PLA sensitivity can be improved with phosphorothioate antennae.

5.5 References

1. Dietz, H.; Douglas, S. M.; Shih, W. M. *Science* **2009**, *325*, 725.
2. Douglas, S. M.; Dietz, H.; Liedl, T.; Högberg, B.; Graf, F.; Shih, W. M. *Nature* **2009**, *459*, 414.
3. Han, D.; Pal, S.; Nangreave, J.; Deng, Z.; Liu, Y.; Yan, H. *Science* **2011**, *332*, 342.
4. Douglas, S. M.; Bachelet, I.; Church, G. M. *Science* **2012**, *335*, 831.
5. Lee, H.; Lytton-Jean, A. K.; Chen, Y.; Love, K. T.; Park, A. I.; Karagiannis, E. D.; Sehgal, A.; Querbes, W.; Zurenko, C. S.; Jayaraman, M. *Nature nanotechnology* **2012**, *7*, 389.
6. Li, J.; Pei, H.; Zhu, B.; Liang, L.; Wei, M.; He, Y.; Chen, N.; Li, D.; Huang, Q.; Fan, C. *ACS nano* **2011**, *5*, 8783.
7. Liu, X.; Xu, Y.; Yu, T.; Clifford, C.; Liu, Y.; Yan, H.; Chang, Y. *Nano letters* **2012**, *12*, 4254.
8. Chang, M.; Yang, C.-S.; Huang, D.-M. *ACS nano* **2011**, *5*, 6156.
9. Jiang, Q.; Song, C.; Nangreave, J.; Liu, X.; Lin, L.; Qiu, D.; Wang, Z.-G.; Zou, G.; Liang, X.; Yan, H. *Journal of the American Chemical Society* **2012**, *134*, 13396.
10. Zhao, Y.-X.; Shaw, A.; Zeng, X.; Benson, E.; Nyström, A. M.; Högberg, B. r. *ACS nano* **2012**, *6*, 8684.
11. Hahn, J.; Wickham, S. F.; Shih, W. M.; Perrault, S. D. *ACS nano* **2014**, *8*, 8765.
12. Surana, S.; Bhatia, D.; Krishnan, Y. *Methods* **2013**, *64*, 94.
13. Famulok, M. *nature biotechnology* **2002**, *20*, 448.
14. Goodman, R. P.; Berry, R. M.; Turberfield, A. J. *Chemical Communications* **2004**, 1372.

CHAPTER 6

SUMMARY AND FUTURE DIRECTIONS

6.1 Summary

This thesis has mainly focused on enhancing the stability of 3D DNs under *in vivo* conditions. Three primary factors limiting the *in vivo* lifetime of the DNs are – a) low salt stability b) nuclease degradation, and c) opsonization. Coating the DNs with PEG have shown positive effects in terms of enhancing the DN lifetime *in vivo*. It can maintain the integrity of the DNs under low salt conditions for a higher length of time, prevent nuclease degradation to some extent and reduce the uptake of DNs by macrophages, thus increasing the circulation times. The various conformations and lengths of PEGs influence the uptake profiles of DNs and there are scopes of tuning these features (length, type and extent of branching, etc.) in order to achieve DNs with desirable *in vivo* lifetimes. The term 'desirable' is crucial as we don't want to have nanocarriers circulating forever in the living system and the ideal circulation time of a nanomedicine is also dependent on the type of disease and drug we want to cure.

Human serum albumin has demonstrated its potential to confer stability to in vivo drug carriers. We have synthesized an albumin attracting molecule and coated DNs with albumin with the mediation of that molecule. The protein coated structure had higher stability in physiological conditions and it can avoid recognition by the macrophages more than the uncoated structures.

We have screened and selected some stabling agents which when added to the annealing solution of DNs enhance their thermodynamic stability and help them to survive under low magnesium conditions for prolonged periods. In our study, we combined some of these stabilizing agents and achieved even higher DN lifetimes for certain combinations. This is a significant towards building inherently stable DNs that would no longer require any coating or stealth sheath in order to become long circulating in the living system.

We have also demonstrated that the proximity ligation assay, an assay well known to the protein researches, can also be applied to estimate the time vs stability of DNs with high sensitivity. The advantages of this assay lies in its very simple modification, extreme sensitivity and the very less amount of sample required for the investigations.

6.2 Future Directions

6.2.1 Further studies on PEG coated DNs

PEGs have been used for few decades to produce long-circulating liposomes and currently there are drugs available in the market that employ this strategy. Reports are abundant that study biodistribution and pharmacokinetics of PEGylated nanoparticles *in vivo*. However, most of the NPs studied to reveal the effect of PEGs are polystyrene NPs and metal NPs. As the *in vivo* behavior and fate of NPs is highly dependent on the material of the core, the results obtained so far would definitely vary when PEGylated DNs will be injected in blood. More detailed investigation is required to study the effect of grafting densities of PEGs on DN surface, lengths and conformations of PEGs and PEG derivatives on the biological stability of these new class of potential DDS. The grafting density has to

be optimized based on the dimension of the drug delivery vehicle and the length of time the vehicle is required to be stable in circulation.

Another important phenomenon to be studied is the drug release profile of the protected DNs. A dense bush of stealth polymer around a delivery vehicle can obviously reduce the leakage of drug molecules, but on the other hand it can also hamper the release of the same when required. This would require prolonged circulation times so that the desired concentration of the drug is attained.

Several DNs have been designed whose dynamics can be controlled by stimuli like small molecules, pH, temperature and a small external nucleic acid. But till date it has never been studied how is the dynamics influenced when the structure is coated for rendering it long circulating. Generally, controlled dynamics require recognition of stimuli quickly, and the component processes occur in a narrow timescale to render the overall process of structural reconfiguration effective and highly responsive. But, surface coating of polymers might hamper the recognition thus making the process sluggish.

6.2.2 New class of stealth polymers

The wide usage of PEG was possible primarily because of its biocompatibility and non-immunogenicity. But reports have started appearing where researchers have found repeated dosages of PEGylated nanomedicines lead to the production of anti-PEG IgM. So, search for a new polymer that can be used as a coating material is evident now. Polyphosphates have started emerging as a new class of biodegradable polymers that are

completely non-immunogenic. DNs are to be coated with these new materials and their stability, and cellular uptake profiles should be studied.

6.2.3 Self-coating structures

From the first project, we found that clusterin has crucial roles in reducing uptake of NPs by MPS. Hence, if we can precoat structures with clusterin, they would have very high chance to become long circulating. In another project we synthesized the albumin attracting molecule tag that helped the DNs to develop ann albumin coating around them. From this, we can envision to build structures that could be injected with the affinity tags on their surface, and as soon as they are injected, they would themselves bind to the stabilizing components from blood, preferably clusterin.

6.2.4 Improvement of the PLA Assay

The assay that we developed in this thesis for estimation of DN stability is an initial attempt towards more detailed and serious investigation into the issue. Unlike metal nanoparticles, the stability of DNs very much depends on their individual structure like size, shape, global and local morphologies density of packing. So any assay that works for one structure might not be applicable to another one. But PLA seems to be quite general and robust regarding structure with an appreciable degree of sensitivity over the free antennae and zero-antenna DN controls. But there remains a vast domain that can and must be explored to improve the overall efficiency and applicability of PLA on DNs.

The effect of multiple pairs of antennae on large structures demands a more meticulous investigation. And depending on the similarity or dissimilarity of the antennae

sequences, we can gain insights into the global and local stabilities of structures. We can build a structure where n pairs of antennae can be attached and then can construct a calibration curve with known amounts of the structure itself starting from 1 pair to n pairs. When the DN with n pairs of antennae is injected and stability of the *in vivo* samples tested, we can determine the percentage of degradation of each structure from the previously constructed calibration curve. This would lead us estimating the global stability of a DN (as antennae sequences being the same, we cannot differentiate between two pairs and their corresponding locations). But in another strategy, n pair of antennae having dissimilar sequences can be planted on a DN surface. Hence the connector strand and the primers for PCR amplification would be different. After collecting *in vivo* samples at a particular time point, we can separately carry out PCR reactions on sample aliquots using the corresponding primers. Comparing these results, we can determine which antenna/antennae are missing and thus obtain insights on structural integrity at a local level. Even, we can try to correlate the results with degradation patterns and eventually find out areas on a structure that are more liable to *in vivo* degradation.

We can make this PLA even smarter by removing the concept of individual antennae pairs. For example, on a cuboid DN, we can have one antenna on a particular face acting as the central antenna and plant one antenna on each of the remaining five faces. Now, by judicious use of connector strands, we can ligate the central antenna with each of the other five antennae in separate sample aliquots and carry out the PLA assay. The results would enable us finding out the missing antennae as a result of structural degradation. In

addition to the number of antenna pair, we can play with the distance between the members of each pair and also with their sequence.

REFERENCES

Chapter 1 References

1. Langer, R. In *Nature* 1998; Vol. 392, p 5.
2. McNamara, K.; Tofail, S. A. *Advances in Physics: X* **2017**, *2*, 54.
3. Nicolas, J.; Mura, S.; Brambilla, D.; Mackiewicz, N.; Couvreur, P. *Chemical Society Reviews* **2013**, *42*, 1147.
4. Peer, D.; Karp, J. M.; Hong, S.; Farokhzad, O. C.; Margalit, R.; Langer, R. *Nature nanotechnology* **2007**, *2*, 751.
5. Adams, M. L.; Lavasanifar, A.; Kwon, G. S. *Journal of pharmaceutical sciences* **2003**, *92*, 1343.
6. Oerlemans, C.; Bult, W.; Bos, M.; Storm, G.; Nijsen, J. F. W.; Hennink, W. E. *Pharmaceutical research* **2010**, *27*, 2569.
7. Kedar, U.; Phutane, P.; Shidhaye, S.; Kadam, V. *Nanomedicine: Nanotechnology, Biology and Medicine* **2010**, *6*, 714.
8. Hillaireau, H.; Couvreur, P. *Cellular and Molecular Life Sciences* **2009**, *66*, 2873.
9. Battaglia, G.; Ryan, A. J. *Journal of the American Chemical Society* **2005**, *127*, 8757.
10. Bangham, A. D. *BioEssays* **1995**, *17*, 1081.
11. Allen, T. M.; Cullis, P. R. *Science* **2004**, *303*, 1818.
12. Barenholz, Y. C. *Journal of controlled release* **2012**, *160*, 117.
13. Minisini, A. M.; Andreetta, C.; Fasola, G.; Puglisi, F. *Expert review of anticancer therapy* **2008**, *8*, 331.
14. Verma, S.; Dent, S.; Chow, B. J.; Rayson, D.; Safra, T. *Cancer treatment reviews* **2008**, *34*, 391.
15. Greineder, C. F.; Howard, M. D.; Carnemolla, R.; Cines, D. B.; Muzykantov, V. R. *Blood* **2013**, *122*, 1565.
16. Strebhardt, K.; Ullrich, A. *Nature Reviews Cancer* **2008**, *8*, 473.
17. Dreher, M. R.; Liu, W.; Michelich, C. R.; Dewhirst, M. W.; Yuan, F.; Chilkoti, A. *Journal of the National Cancer Institute* **2006**, *98*, 335.

18. Senter, P. D.; Springer, C. J. *Advanced drug delivery reviews* **2001**, *53*, 247.
19. Vrouenraets, M. B.; Visser, G.; Snow, G.; Van Dongen, G. *Anticancer research* **2003**, *23*, 505.
20. Allen, T. M. *Nature Reviews Cancer* **2002**, *2*, 750.
21. Kopeček, J.; Kopečková, P.; Minko, T.; Lu, Z.-R. *European Journal of Pharmaceutics and Biopharmaceutics* **2000**, *50*, 61.
22. Duncan, R. *Nature reviews Drug discovery* **2003**, *2*, 347.
23. Lewis, W. H. *Bull Johns Hopkins Hosp* **1927**, *41*, 156.
24. Sandison, J. *Developmental Dynamics* **1928**, *41*, 475.
25. 窶; deAG, B. *AJR Am J Roentgenol1939*, *42*, 891.
26. Algire, G. H.; Chalkley, H. W.; Earle, W. R.; Legallais, F. Y.; Park, H. D.; Shelton, E.; Schilling, E. L. **1950**.
27. Duran-Reynals, F. *The American Journal of Cancer* **1939**, *35*, 98.
28. Babson, A. L.; Winnick, T. *Cancer Research* **1954**, *14*, 606.
29. Busch, H.; Greene, H. S. *The Yale journal of biology and medicine* **1955**, *27*, 339.
30. Dewey, W. C. *American Journal of Physiology--Legacy Content* **1959**, *197*, 423.
31. Song, C. W.; Levitt, S. H. *Cancer research* **1971**, *31*, 587.
32. Underwoodand, J.; Carr, I. *The Journal of pathology* **1972**, *107*, 157.
33. Peterson, H.-I.; Appelgren, K. *European Journal of Cancer (1965)* **1973**, *9*, 543.
34. Heuser, L. S.; Miller, F. N. *Cancer* **1986**, *57*, 461.
35. Gerlowski, L. E.; Jain, R. K. *Microvascular research* **1986**, *31*, 288.
36. Dvorak, H. F.; Nagy, J. A.; Dvorak, J.; Dvorak, A. *The American journal of pathology* **1988**, *133*, 95.
37. Matsumura, Y.; Maeda, H. *Cancer research* **1986**, *46*, 6387.
38. Maeda, H.; Matsumura, Y. *Critical reviews in therapeutic drug carrier systems* **1989**, *6*, 193.
39. Maeda, H.; Seymour, L. W.; Miyamoto, Y. *Bioconjugate chemistry* **1992**, *3*, 351.
40. Ishida, T.; Kiwada, H. *International journal of pharmaceutics* **2008**, *354*, 56.

41. Elsabahy, M.; Wooley, K. L. *Chemical Society Reviews* **2012**, *41*, 2545.

42. Chono, S.; Tanino, T.; Seki, T.; Morimoto, K. *Journal of pharmacy and pharmacology* **2007**, *59*, 75.

43. Win, K. Y.; Feng, S.-S. *Biomaterials* **2005**, *26*, 2713.

44. Foged, C.; Brodin, B.; Frokjaer, S.; Sundblad, A. *International journal of pharmaceutics* **2005**, *298*, 315.

45. Chithrani, B. D.; Ghazani, A. A.; Chan, W. C. *Nano lett* **2006**, *6*, 662.

46. Lu, F.; Wu, S. H.; Hung, Y.; Mou, C. Y. *Small* **2009**, *5*, 1408.

47. Lee, K. D.; Nir, S.; Papahadjopoulos, D. *Biochemistry* **1993**, *32*, 889.

48. He, C.; Hu, Y.; Yin, L.; Tang, C.; Yin, C. *Biomaterials* **2010**, *31*, 3657.

49. Zorko, M.; Langel, Ü. *Advanced drug delivery reviews* **2005**, *57*, 529.

50. Abuchowski, A.; Van Es, T.; Palczuk, N.; Davis, F. *Journal of Biological Chemistry* **1977**, *252*, 3578.

51. Allen, T.; Redemann, C.; Yau-Young, A.; Hansen, C. In *Proceedings, 10th International Biophysics Congress, International Union of Pure and Applied Biophysics* 1990, p 312.

52. Woodle, M.; Newman, M.; Collins, L.; Martin, F. In *Biophysical Journal*; BIOPHYSICAL SOCIETY 9650 ROCKVILLE PIKE, BETHESDA, MD 20814-3998: 1990; Vol. 57, p A261.

53. Klibanov, A. L.; Maruyama, K.; Torchilin, V. P.; Huang, L. *FEBS letters* **1990**, *268*, 235.

54. Blume, G.; Cevc, G. *Biochimica et Biophysica Acta (BBA)-Biomembranes* **1990**, *1029*, 91.

55. Ilium, L.; Hunneyball, I.; Davis, S. *International journal of pharmaceutics* **1986**, *29*, 53.

56. Woodle, M. C.; Lasic, D. D. *Biochimica et Biophysica Acta (BBA)-Reviews on Biomembranes* **1992**, *1113*, 171.

57. Needham, D.; Hristova, K.; McIntosh, T.; Dewhirst, M.; Wu, N.; Lasic, D. *Journal of Liposome Research* **1992**, *2*, 411.

58. Needham, D.; McIntosh, T.; Lasic, D. *Biochimica et Biophysica Acta (BBA)-Biomembranes* **1992**, *1108*, 40.

59. Woodle, M.; Collins, L.; Sponsler, E.; Kossovsky, N.; Papahadjopoulos, D.; Martin, F. *Biophysical journal* **1992**, *61*, 902.

60. Lasic, D. D.; Woodle, M. C.; Papahadjopoulos, D. *Journal of Liposome Research* **1992**, *2*, 335.

61. Lasic, D.; Martin, F.; Gabizon, A.; Huang, S.; Papahadjopoulos, D. *Biochimica et Biophysica Acta (BBA)-Biomembranes* **1991**, *1070*, 187.

62. Douglas, S. M.; Dietz, H.; Liedl, T.; Högberg, B.; Graf, F.; Shih, W. M. *Nature* **2009**, *459*, 414.

63. Dietz, H.; Douglas, S. M.; Shih, W. M. *Science* **2009**, *325*, 725.

64. Han, D.; Pal, S.; Nangreave, J.; Deng, Z.; Liu, Y.; Yan, H. *Science* **2011**, *332*, 342.

65. Liedl, T.; Högberg, B.; Tytell, J.; Ingber, D. E.; Shih, W. M. *Nature nanotechnology* **2010**, *5*, 520.

66. Seeman, N. C. *Annual review of biochemistry* **2010**, *79*, 65.

67. Mao, C.; Sun, W.; Shen, Z.; Seeman, N. C. *Nature* **1999**, *397*, 144.

68. Seelig, G.; Soloveichik, D.; Zhang, D. Y.; Winfree, E. *science* **2006**, *314*, 1585.

69. Rothemund, P. W. *Nature* **2006**, *440*, 297.

70. Liu, Y.; Lin, C.; Li, H.; Yan, H. *Angewandte Chemie* **2005**, *117*, 4407.

71. He, Y.; Tian, Y.; Ribbe, A. E.; Mao, C. *Journal of the American Chemical Society* **2006**, *128*, 12664.

72. Dutta, P. K.; Varghese, R.; Nangreave, J.; Lin, S.; Yan, H.; Liu, Y. *Journal of the American Chemical Society* **2011**, *133*, 11985.

73. Schreiber, R.; Do, J.; Roller, E.-M.; Zhang, T.; Schüller, V. J.; Nickels, P. C.; Feldmann, J.; Liedl, T. *Nature nanotechnology* **2014**, *9*, 74.

74. Langer, R. *Nature* **1998**, *392*, 5.

75. Pozzi, D.; Colapicchioni, V.; Caracciolo, G.; Piovesana, S.; Capriotti, A. L.; Palchetti, S.; De Grossi, S.; Riccioli, A.; Amenitsch, H.; Laganà, A. *Nanoscale* **2014**, *6*, 2782.

76. Douglas, S. M.; Bachelet, I.; Church, G. M. *Science* **2012**, *335*, 831.

77. Lee, H.; Lytton-Jean, A. K.; Chen, Y.; Love, K. T.; Park, A. I.; Karagiannis, E. D.; Sehgal, A.; Querbes, W.; Zurenko, C. S.; Jayaraman, M. *Nature nanotechnology* **2012**, *7*, 389.

78. Li, J.; Pei, H.; Zhu, B.; Liang, L.; Wei, M.; He, Y.; Chen, N.; Li, D.; Huang, Q.; Fan, C. *ACS nano* **2011**, *5*, 8783.

79. Liu, X.; Xu, Y.; Yu, T.; Clifford, C.; Liu, Y.; Yan, H.; Chang, Y. *Nano letters* **2012**, *12*, 4254.

80. Chang, M.; Yang, C.-S.; Huang, D.-M. *ACS nano* **2011**, *5*, 6156.

81. Jiang, Q.; Song, C.; Nangreave, J.; Liu, X.; Lin, L.; Qiu, D.; Wang, Z.-G.; Zou, G.; Liang, X.; Yan, H. *Journal of the American Chemical Society* **2012**, *134*, 13396.

82. Zhao, Y.-X.; Shaw, A.; Zeng, X.; Benson, E.; Nyström, A. M.; Högberg, B. r. *ACS nano* **2012**, *6*, 8684.

83. Aggarwal, P.; Hall, J. B.; McLeland, C. B.; Dobrovolskaia, M. A.; McNeil, S. E. *Advanced drug delivery reviews* **2009**, *61*, 428.

84. Du, H.; Chandaroy, P.; Hui, S. W. *Biochimica et Biophysica Acta (BBA)-Biomembranes* **1997**, *1326*, 236.

85. Schöttler, S.; Becker, G.; Winzen, S.; Steinbach, T.; Mohr, K.; Landfester, K.; Mailänder, V.; Wurm, F. R. *Nature nanotechnology* **2016**, *11*, 372.

Chapter 2 References

1. Riehemann, K.; Schneider, S. W.; Luger, T. A.; Godin, B.; Ferrari, M.; Fuchs, H. *Angewandte Chemie International Edition* **2009**, *48*, 872.

2. Rothemund, P. W. *Nature* **2006**, *440*, 297.

3. Douglas, S. M.; Dietz, H.; Liedl, T.; Högberg, B.; Graf, F.; Shih, W. M. *Nature* **2009**, *459*, 414.

4. Dietz, H.; Douglas, S. M.; Shih, W. M. *Science* **2009**, *325*, 725.

5. Han, D.; Pal, S.; Nangreave, J.; Deng, Z.; Liu, Y.; Yan, H. *Science* **2011**, *332*, 342.

6. Wei, B.; Dai, M.; Yin, P. *Nature* **2012**, *485*, 623.

7. Ke, Y.; Ong, L. L.; Shih, W. M.; Yin, P. *science* **2012**, *338*, 1177.

8. Andersen, E. S.; Dong, M.; Nielsen, M. M.; Jahn, K.; Subramani, R.; Mamdouh, W.; Golas, M. M.; Sander, B.; Stark, H.; Oliveira, C. L. *Nature* **2009**, *459*, 73.

9. Goodman, R. P.; Heilemann, M.; Doose, S.; Erben, C. M.; Kapanidis, A. N.; Turberfield, A. J. *Nature nanotechnology* **2008**, *3*, 93.

10. Liu, M.; Fu, J.; Hejesen, C.; Yang, Y.; Woodbury, N. W.; Gothelf, K.; Liu, Y.; Yan, H. *Nature communications* **2013**, *4*, 2127.

11. Modi, S.; Swetha, M.; Goswami, D.; Gupta, G. D.; Mayor, S.; Krishnan, Y. *Nature nanotechnology* **2009**, *4*, 325.

12. Liu, D.; Balasubramanian, S. *Angewandte Chemie International Edition* **2003**, *42*, 5734.

13. Lee, H.; Lytton-Jean, A. K.; Chen, Y.; Love, K. T.; Park, A. I.; Karagiannis, E. D.; Sehgal, A.; Querbes, W.; Zurenko, C. S.; Jayaraman, M. *Nature nanotechnology* **2012**, *7*, 389.

14. Liu, X.; Xu, Y.; Yu, T.; Clifford, C.; Liu, Y.; Yan, H.; Chang, Y. *Nano letters* **2012**, *12*, 4254.

15. Douglas, S. M.; Bachelet, I.; Church, G. M. *Science* **2012**, *335*, 831.

16. Lu, C.-H.; Willner, B.; Willner, I. *ACS nano* **2013**, *7*, 8320.

17. Campolongo, M. J.; Tan, S. J.; Xu, J.; Luo, D. *Advanced drug delivery reviews* **2010**, *62*, 606.

18. Zhao, Y.-X.; Shaw, A.; Zeng, X.; Benson, E.; Nyström, A. M.; Högberg, B. r. *ACS nano* **2012**, *6*, 8684.

19. Jahnen-Dechent, W.; Ketteler, M. *Clinical kidney journal* **2012**, *5*, i3.

20. Mei, Q.; Wei, X.; Su, F.; Liu, Y.; Youngbull, C.; Johnson, R.; Lindsay, S.; Yan, H.; Meldrum, D. *Nano letters* **2011**, *11*, 1477.

21. Conway, J. W.; McLaughlin, C. K.; Castor, K. J.; Sleiman, H. *Chemical Communications* **2013**, *49*, 1172.

22. Hahn, J.; Wickham, S. F.; Shih, W. M.; Perrault, S. D. *ACS nano* **2014**, *8*, 8765.

23. Surana, S.; Bhatia, D.; Krishnan, Y. *Methods* **2013**, *64*, 94.

24. Johnson, R. J. In *Biomaterials Science (Third Edition)*; Elsevier: 2013, p 533.

25. Frank, M. M.; Fries, L. F. *Immunology today* **1991**, *12*, 322.

26. Dunn, S. E.; Brindley, A.; Davis, S. S.; Davies, M. C.; Illum, L. *Pharmaceutical research* **1994**, *11*, 1016.

27. Tenzer, S.; Docter, D.; Kuharev, J.; Musyanovych, A.; Fetz, V.; Hecht, R.; Schlenk, F.; Fischer, D.; Kiouptsi, K.; Reinhardt, C. *Nature nanotechnology* **2013**, *8*, 772.

28. Aggarwal, P.; Hall, J. B.; McLeland, C. B.; Dobrovolskaia, M. A.; McNeil, S. E. *Advanced drug delivery reviews* **2009**, *61*, 428.

29. Monopoli, M. P.; Åberg, C.; Salvati, A.; Dawson, K. A. *Nature nanotechnology* **2012**, *7*, 779.

30. Sacchetti, C.; Motamedchaboki, K.; Magrini, A.; Palmieri, G.; Mattei, M.; Bernardini, S.; Rosato, N.; Bottini, N.; Bottini, M. *ACS nano* **2013**, *7*, 1974.

31. Owens III, D. E.; Peppas, N. A. *International journal of pharmaceutics* **2006**, *307*, 93.

32. Klibanov, A. L.; Maruyama, K.; Torchilin, V. P.; Huang, L. *FEBS letters* **1990**, *268*, 235.

33. Woodle, M. C.; Lasic, D. D. *Biochimica et Biophysica Acta (BBA)-Reviews on Biomembranes* **1992**, *1113*, 171.

34. Needham, D.; McIntosh, T.; Lasic, D. *Biochimica et Biophysica Acta (BBA)-Biomembranes* **1992**, *1108*, 40.

35. Du, H.; Chandaroy, P.; Hui, S. W. *Biochimica et Biophysica Acta (BBA)-Biomembranes* **1997**, *1326*, 236.

36. Price, M.; Cornelius, R.; Brash, J. *Biochimica et Biophysica Acta (BBA)-Biomembranes* **2001**, *1512*, 191.

37. Schöttler, S.; Becker, G.; Winzen, S.; Steinbach, T.; Mohr, K.; Landfester, K.; Mailänder, V.; Wurm, F. R. *Nature nanotechnology* **2016**, *11*, 372.

38. Perrault, S. D.; Shih, W. M. *ACS nano* **2014**, *8*, 5132.

39. Ponnuswamy, N.; Bastings, M. M.; Nathwani, B.; Ryu, J. H.; Chou, L. Y.; Vinther, M.; Li, W. A.; Anastassacos, F. M.; Mooney, D. J.; Shih, W. M. *Nature communications* **2017**, *8*, 15654.

Chapter 3 References

1. Seeman, N. C. *Annual review of biochemistry* **2010**, *79*, 65.

2. Douglas, S. M.; Dietz, H.; Liedl, T.; Högberg, B.; Graf, F.; Shih, W. M. *Nature* **2009**, *459*, 414.

3. Dietz, H.; Douglas, S. M.; Shih, W. M. *Science* **2009**, *325*, 725.

4. Han, D.; Pal, S.; Nangreave, J.; Deng, Z.; Liu, Y.; Yan, H. *Science* **2011**, *332*, 342.

5. Rothemund, P. W. *Nature* **2006**, *440*, 297.

6. Dutta, P. K.; Varghese, R.; Nangreave, J.; Lin, S.; Yan, H.; Liu, Y. *Journal of the American Chemical Society* **2011**, *133*, 11985.

7. Schreiber, R.; Do, J.; Roller, E.-M.; Zhang, T.; Schüller, V. J.; Nickels, P. C.; Feldmann, J.; Liedl, T. *Nature nanotechnology* **2014**, *9*, 74.

8. Liu, Y.; Lin, C.; Li, H.; Yan, H. *Angewandte Chemie* **2005**, *117*, 4407.

9. He, Y.; Tian, Y.; Ribbe, A. E.; Mao, C. *Journal of the American Chemical Society* **2006**, *128*, 12664.

10. Zhang, F.; Nangreave, J.; Liu, Y.; Yan, H. *Journal of the American Chemical Society* **2014**, *136*, 11198.

11. Chhabra, R.; Sharma, J.; Liu, Y.; Rinker, S.; Yan, H. *Advanced drug delivery reviews* **2010**, *62*, 617.

12. Lu, C.-H.; Willner, B.; Willner, I. *ACS nano* **2013**, *7*, 8320.

13. Campolongo, M. J.; Tan, S. J.; Xu, J.; Luo, D. *Advanced drug delivery reviews* **2010**, *62*, 606.

14. Douglas, S. M.; Bachelet, I.; Church, G. M. *Science* **2012**, *335*, 831.

15. Lee, H.; Lytton-Jean, A. K.; Chen, Y.; Love, K. T.; Park, A. I.; Karagiannis, E. D.; Sehgal, A.; Querbes, W.; Zurenko, C. S.; Jayaraman, M. *Nature nanotechnology* **2012**, *7*, 389.

16. Li, J.; Pei, H.; Zhu, B.; Liang, L.; Wei, M.; He, Y.; Chen, N.; Li, D.; Huang, Q.; Fan, C. *ACS nano* **2011**, *5*, 8783.

17. Liu, X.; Xu, Y.; Yu, T.; Clifford, C.; Liu, Y.; Yan, H.; Chang, Y. *Nano letters* **2012**, *12*, 4254.

18. Chang, M.; Yang, C.-S.; Huang, D.-M. *ACS nano* **2011**, *5*, 6156.

19. Jiang, Q.; Song, C.; Nangreave, J.; Liu, X.; Lin, L.; Qiu, D.; Wang, Z.-G.; Zou, G.; Liang, X.; Yan, H. *Journal of the American Chemical Society* **2012**, *134*, 13396.

20. Zhao, Y.-X.; Shaw, A.; Zeng, X.; Benson, E.; Nyström, A. M.; Högberg, B. r. *ACS nano* **2012**, *6*, 8684.

21. Perrault, S. D.; Shih, W. M. *ACS nano* **2014**, *8*, 5132.

22. Hahn, J.; Wickham, S. F.; Shih, W. M.; Perrault, S. D. *ACS nano* **2014**, *8*, 8765.

23. Ponnuswamy, N.; Bastings, M. M.; Nathwani, B.; Ryu, J. H.; Chou, L. Y.; Vinther, M.; Li, W. A.; Anastassacos, F. M.; Mooney, D. J.; Shih, W. M. *Nature Communications* **2017**, *8*.

24. Albanese, A.; Tang, P. S.; Chan, W. C. *Annual review of biomedical engineering* **2012**, *14*, 1.

25. Chithrani, B. D.; Chan, W. C. *Nano lett* **2007**, *7*, 1542.

26. Lu, F.; Wu, S. H.; Hung, Y.; Mou, C. Y. *Small* **2009**, *5*, 1408.

27. Jin, H.; Heller, D. A.; Sharma, R.; Strano, M. S. *Acs Nano* **2009**, *3*, 149.

Chapter 4 References

25. Dietz, H.; Douglas, S. M.; Shih, W. M. *Science* **2009**, *325*, 725.

26. Douglas, S. M.; Dietz, H.; Liedl, T.; Högberg, B.; Graf, F.; Shih, W. M. *Nature* **2009**, *459*, 414.

27. Rothemund, P. W. *Nature* **2006**, *440*, 297.

28. Han, D.; Pal, S.; Nangreave, J.; Deng, Z.; Liu, Y.; Yan, H. *Science* **2011**, *332*, 342.

29. Zheng, D.; Seferos, D. S.; Giljohann, D. A.; Patel, P. C.; Mirkin, C. A. *Nano letters* **2009**, *9*, 3258.

30. Pei, H.; Lu, N.; Wen, Y.; Song, S.; Liu, Y.; Yan, H.; Fan, C. *Advanced Materials* **2010**, *22*, 4754.

31. Li, J.; Pei, H.; Zhu, B.; Liang, L.; Wei, M.; He, Y.; Chen, N.; Li, D.; Huang, Q.; Fan, C. *ACS nano* **2011**, *5*, 8783.

32. Liu, X.; Xu, Y.; Yu, T.; Clifford, C.; Liu, Y.; Yan, H.; Chang, Y. *Nano letters* **2012**, *12*, 4254.

33. Lee, H.; Lytton-Jean, A. K.; Chen, Y.; Love, K. T.; Park, A. I.; Karagiannis, E. D.; Sehgal, A.; Querbes, W.; Zurenko, C. S.; Jayaraman, M. *Nature nanotechnology* **2012**, *7*, 389.

34. Zhao, Y.-X.; Shaw, A.; Zeng, X.; Benson, E.; Nyström, A. M.; Högberg, B. r. *ACS nano* **2012**, *6*, 8684.

35. Chang, M.; Yang, C.-S.; Huang, D.-M. *ACS nano* **2011**, *5*, 6156.

36. Hahn, J.; Wickham, S. F.; Shih, W. M.; Perrault, S. D. *ACS nano* **2014**, *8*, 8765.

37. Perrault, S. D.; Shih, W. M. *ACS nano* **2014**, *8*, 5132.

38. Ponnuswamy, N.; Bastings, M. M.; Nathwani, B.; Ryu, J. H.; Chou, L. Y.; Vinther, M.; Li, W. A.; Anastassacos, F. M.; Mooney, D. J.; Shih, W. M. *Nature communications* **2017**, *8*, 15654.

39. Lacroix, A.; Edwardson, T. G.; Hancock, M. A.; Dore, M. D.; Sleiman, H. F. *Journal of the American Chemical Society* **2017**, *139*, 7355.

40. Sleep, D.; Cameron, J.; Evans, L. R. *Biochimica et Biophysica Acta (BBA)-General Subjects* **2013**, *1830*, 5526.

41. Iyer, A. K.; Khaled, G.; Fang, J.; Maeda, H. *Drug discovery today* **2006**, *11*, 812.

42. Gradishar, W. J.; Tjulandin, S.; Davidson, N.; Shaw, H.; Desai, N.; Bhar, P.; Hawkins, M.; O'Shaughnessy, J. *J clin Oncol* **2005**, *23*, 7794.

43. Manoharan, M.; Inamati, G. B.; Lesnik, E. A.; Sioufi, N. B.; Freier, S. M. *ChemBioChem* **2002**, *3*, 1257.

44. Huang, Y.; Reis, E. S.; Knerr, P. J.; van der Donk, W. A.; Ricklin, D.; Lambris, J. D. *ChemMedChem* **2014**, *9*, 2223.

45. Sahu, A.; Kay, B. K.; Lambris, J. D. *The Journal of Immunology* **1996**, *157*, 884.

46. Ricklin, D.; Lambris, J. D. In *Current Topics in Complement II*; Springer: 2008, p 262.

47. C. Amedio Jr, J.; Bernard, P. J.; Fountain, M.; VanWagenen Jr, G. *Synthetic communications* **1998**, *28*, 3895.

48. Deleavey, G. F.; Damha, M. J. *Chemistry & biology* **2012**, *19*, 937.

Chapter 5 References

1. Dietz, H.; Douglas, S. M.; Shih, W. M. *Science* **2009**, *325*, 725.

2. Douglas, S. M.; Dietz, H.; Liedl, T.; Högberg, B.; Graf, F.; Shih, W. M. *Nature* **2009**, *459*, 414.

3. Han, D.; Pal, S.; Nangreave, J.; Deng, Z.; Liu, Y.; Yan, H. *Science* **2011**, *332*, 342.

4. Douglas, S. M.; Bachelet, I.; Church, G. M. *Science* **2012**, *335*, 831.

5. Lee, H.; Lytton-Jean, A. K.; Chen, Y.; Love, K. T.; Park, A. I.; Karagiannis, E. D.; Sehgal, A.; Querbes, W.; Zurenko, C. S.; Jayaraman, M. *Nature nanotechnology* **2012**, *7*, 389.

6. Li, J.; Pei, H.; Zhu, B.; Liang, L.; Wei, M.; He, Y.; Chen, N.; Li, D.; Huang, Q.; Fan, C. *ACS nano* **2011**, *5*, 8783.

7. Liu, X.; Xu, Y.; Yu, T.; Clifford, C.; Liu, Y.; Yan, H.; Chang, Y. *Nano letters* **2012**, *12*, 4254.

8. Chang, M.; Yang, C.-S.; Huang, D.-M. *ACS nano* **2011**, *5*, 6156.

9. Jiang, Q.; Song, C.; Nangreave, J.; Liu, X.; Lin, L.; Qiu, D.; Wang, Z.-G.; Zou, G.; Liang, X.; Yan, H. *Journal of the American Chemical Society* **2012**, *134*, 13396.

10. Zhao, Y.-X.; Shaw, A.; Zeng, X.; Benson, E.; Nyström, A. M.; Högberg, B. r. *ACS nano* **2012**, *6*, 8684.

11. Hahn, J.; Wickham, S. F.; Shih, W. M.; Perrault, S. D. *ACS nano* **2014**, *8*, 8765.

12. Surana, S.; Bhatia, D.; Krishnan, Y. *Methods* **2013**, *64*, 94.

13. Famulok, M. *nature biotechnology* **2002**, *20*, 448.

14. Goodman, R. P.; Berry, R. M.; Turberfield, A. J. *Chemical Communications* **2004**, 1372.

15. Jiang, Q.; Song, C.; Nangreave, J.; Liu, X.; Lin, L.; Qiu, D.; Wang, Z.-G.; Zou, G.; Liang, X.; Yan, H. *Journal of the American Chemical Society* **2012**, *134*, 13396.

16. Zhao, Y.-X.; Shaw, A.; Zeng, X.; Benson, E.; Nyström, A. M.; Högberg, B. r.

    ACS nano **2012**, *6*, 8684.

17. Hahn, J.; Wickham, S. F.; Shih, W. M.; Perrault, S. D. *ACS nano* **2014**, *8*, 8765.

18. Surana, S.; Bhatia, D.; Krishnan, Y. *Methods* **2013**, *64*, 94.

19. Famulok, M. *nature biotechnology* **2002**, *20*, 448.

20. Goodman, R. P.; Berry, R. M.; Turberfield, A. J. *Chemical Communications* **2004**, 1372.

APPENDIX A

SUPPLEMENTAL NFORMATION FOR CHAPTER 2

EFFECT OF PEG LENGTH AND CONFORMATION AND PEG-LIPID COATING ON STABILITY AND CELLULAR UPTAKE OF DNA NANOSTRUCTURES

S2.1 PEG-azides and Lipid-PEG-azide and their abbreviations

	Chemical	Molecular Weight	Abbreviation	Structure
1.	Linear PEG-azide	2 kD	2L	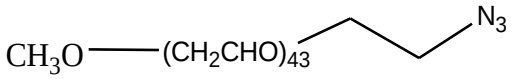
2.	Linear PEG-azide	5 kD	5L	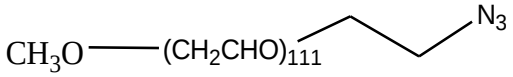
3.	Linear PEG-azide	10 kD	10L	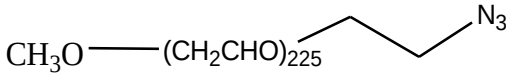
4.	Branched PEG-azide having 4 arms	2 kD	2 – 4 arm	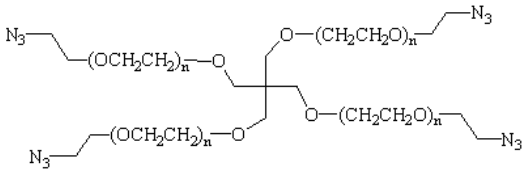
5.	Branched PEG-azide having 4 arms	10 kD	10 – 4 arm	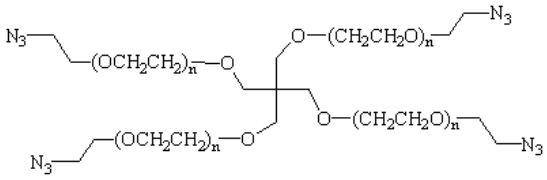
6.	Branched PEG-azide having 8 arms	10 kD	10 – 8 arm	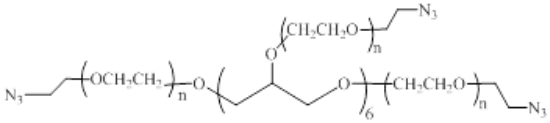
7.	DSPE-PEG azide*	2 kD	2 - Lip	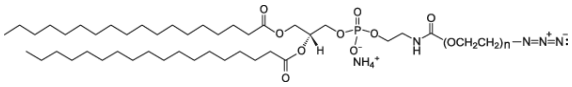

Table S2.1: PEG-azides and Lipid-PEG-azide and their abbreviations.

*1,2-distearoyl-sn-glycero-3-phosphoethanolamine-N-[azido(polyethylene glycol)-2000] (ammonium salt)

S2.2 Materials and Instruments

All DNA strands were purchased from Integrated DNA technologies. The strands for DNO were bought in 96 well plates and used without any further purification. Rest of the strands were purified using 10% denaturing polyacrylamide gels prior to annealing structures. DBCO-NHS ester was bought from Click Chemistry Tools. Anhydrous DMSO was purchased from Life Technologies. All the linear and branched PEG-azides were bought from Creative PEGWorks. DSPE-PEG (2000) Azide was bought from Avanti Polar Lipids. Propidium iodide and CellTracker CM-Dil dye were bought from ThermoFisher Scientific. RAW264.7 cells used in the cellular uptake study were bought from ATCC. FBS that was used to supplement DMEM cell culture medium was purchased from Gibco Life Technologies. Mouse serum was purchased from Sigma Aldrich. DNase I, Bovine Pancreas was purchased from Gold Biotechnology. Recombinant Human Clusterin alpha chain protein was purchased from Abcam. All the other chemicals that are not mentioned here were bought from Sigma-Aldrich.

Live cell confocal microscopy was done using the Confocal laser scanning microscope Leica TCS SP8. Flow cytometry studies were conducted using the S1000EXi flow cytometer coupled with the CellCapTure software from Stratedigm. The cytometry data were analyzed using the Flowjo v10 software from Flowjo, LLC and plotted using the Prism 5 software from Graphpad. For the time vs stability experiments, the band intensities of gels were measured using the ImageJ software.

S2.3 Details of Td and DNO Structures

S.2.3.1 Td

S2.3.1.1 Strands for Td

Strand 1: AGG CAC CAT CGT AGG TTT C TTG CCA GGC ACC ATC GTA GGT TTCT TGC CAG GCA CCA TCG TAG GTT T CTT GCC

Strand 2: CAG AGG CGC TGC AAG CCT ACG ATG GAC ACG GTA ACG ACT

Strand 3: AGC AAC CTG CCT GTT AGC GCC TCT GTT TTT TCG ATC ACG TAG CAC AGC AT

Strand 4: /5Alex488N/TTA CCG TGT GGT TGC TAG TCG TT

The complementary of the single stranded handle (labeled in red) with strand 3 was named strand 5 and it had an amine modification at the 5' end.

Strand 5: /5AmMC12/AT GCT GTG CTA CGT GAT CGA

The Alexa fluor 488 dye was attached to strand 4 for flow cytometry studies. For all other experiments the unlabeled strand was used.

S2.3.1.2 Schematic for Td

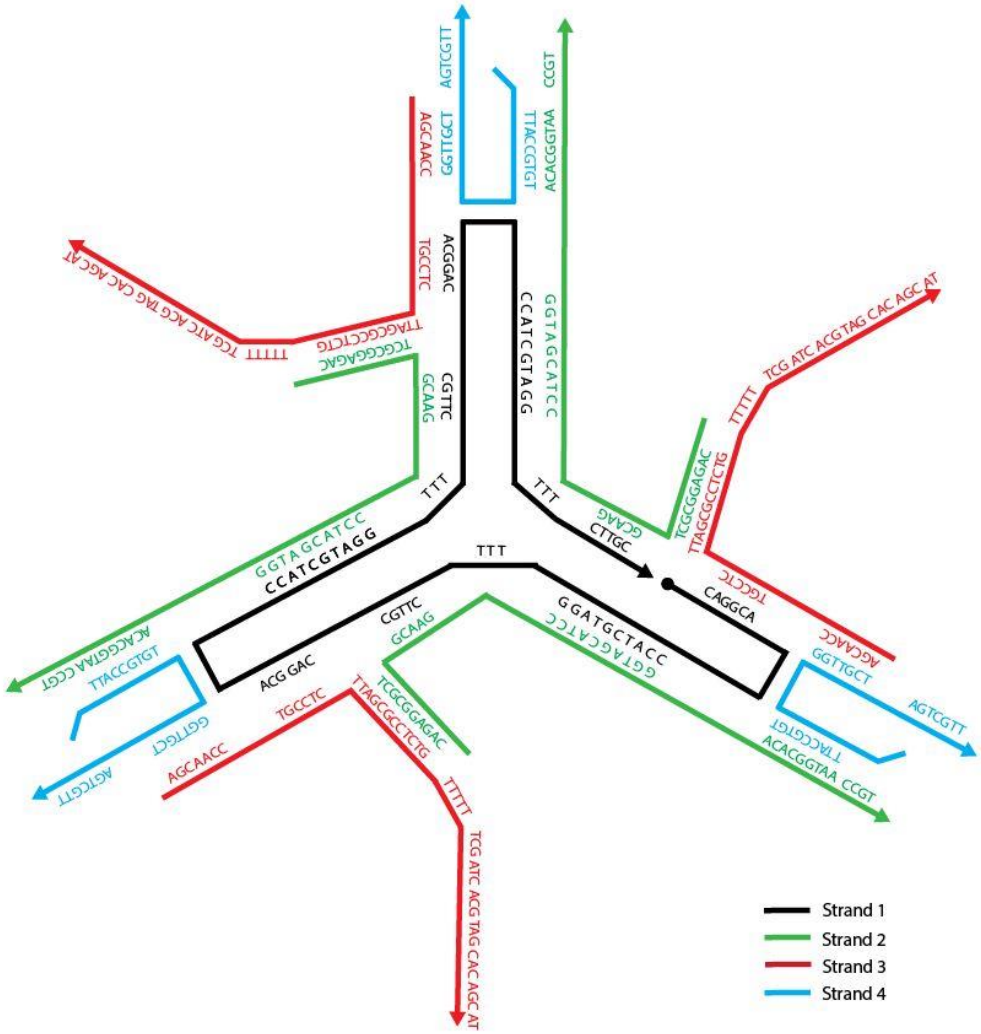

Figure S2.1: Schematic showing one unit of Td. 4 similar units assemble together through sticky end hybridization to build up the complete Td.

S.2.3.2 DNO

S2.3.2.1 Schematic for DNO

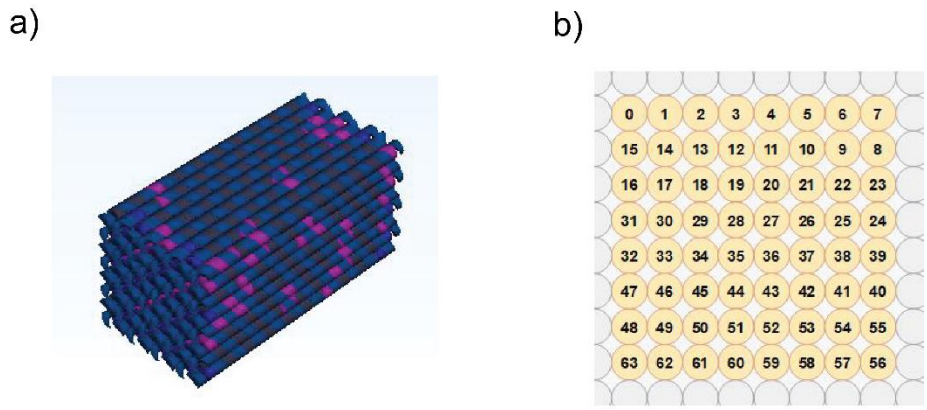

Figure S2.2: caDNAno image of DNO. a) DNO b) caDNAno image showing the arrangement of double helices constituting DNO.

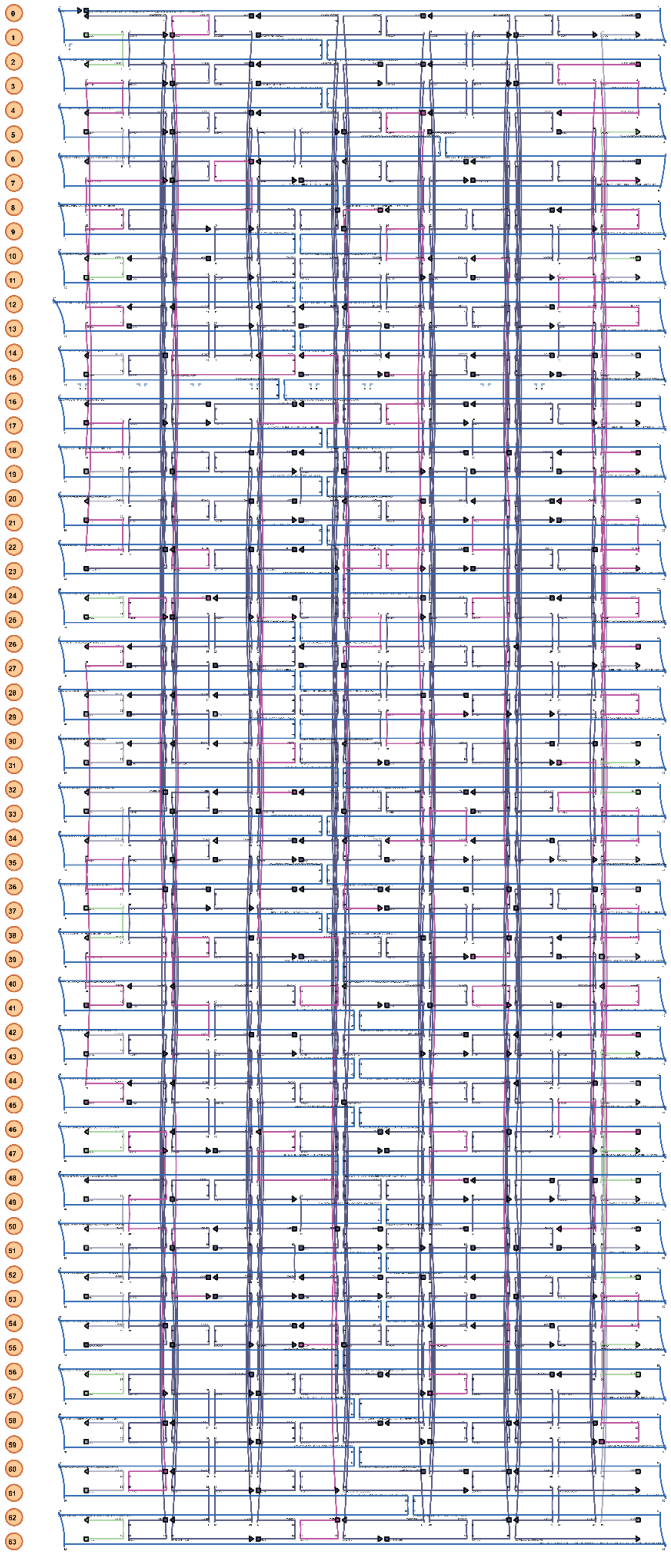

Figure S2.3: caDNAno design of DNO.

S2.3.2.2 Sequences for DNO

Start	End	Sequence
16[111]	15[111]	CATATGTATTTTAACC
20[111]	11[111]	TAAAAATTAGCGCCAT
13[16]	1[23]	AGAGATAGTAGAGCTTATCAAGTT
38[39]	40[24]	GACCGTGTTGTTTAGTAAAGCCAACGCTCAAC
50[63]	61[79]	GAGCGTCTGCAAGGCCGGAAACTCAGAGCCGC
11[16]	3[23]	ATTTTGACGCGCGTAAGAGAAAGG
58[63]	52[48]	TGCCTAACGCAAAGACGAGGGAGGCATAAAAA
44[103]	53[103]	AGCATCGGAAAATACGAACCCATGACCCTCAT
50[79]	35[79]	ATTTTCTGGCTTGCAGGCTACAGAGCTCATTA
59[8]	58[8]	TTACCAGCTAGAAAAT
29[16]	17[23]	TTACAAAAACCTCAAACCGCCTGC
60[87]	49[87]	CCTTGATACACCAGAAGTAAATGACAACAGTT
3[88]	13[95]	GGGTGGTTCACCGCCTGATTGACC
29[8]	28[8]	ATACCAAGTCGCCTGA
35[64]	51[63]	AAGAACTGGGCTTTGAGGACTTCCTTTACAGA
60[79]	43[79]	TTCACAAAGCCTGTAGTTCGTCACTGAGGAAG
60[71]	61[55]	CAAATAAATCCTCGGTAAATATTGTACCATTA
28[71]	36[64]	GAGCTTCAGTCAGGATTAATCATT
62[111]	49[111]	CAGAGCCGAGAAAGGA
51[8]	52[8]	AAATAAGAAACACCCT
20[39]	25[39]	ATCTTTAGAAGTATTACAAAATTATGGAAGGG
48[103]	61[111]	GAATAATAGTGAGAATCCACCCTCAGAGCCGCCGCCAGCA

15[80]	0[72]	AAATTTTTAGTGTTGTTCCAGTTT
2[71]	11[71]	CAGCAAGCAGGCGGTTGACGACGACAGCTTTC
53[8]	54[8]	CAGAGGGTAAGCCCTT
46[63]	63[63]	ATATACACACGCTAACGCTCCAAAAGCGTTTG
50[111]	45[111]	GTTTTGTCATCGTCAC
32[23]	32[8]	ACCTTGCTTCTGTAAA
33[40]	16[48]	ATAGCGATAGCTTTACGAGAATGATAATGGAACAAATATT
7[48]	6[56]	CTGTCCATAGCTCGAAGCGGGAGC
32[79]	17[79]	ACCAAAATGAGGGGGTAATGCTTTAGCAAACA
56[39]	57[23]	CCCAAAAGAACTGGCATGATTAAGAAACGTAG
22[23]	10[16]	CGAACGTTACATTTGATGCAACAG
42[47]	26[48]	TAAAGTACACCTAAATTTAATTACCAACTAAA
51[80]	34[80]	CATTCCACTAGCAACGGGAGTTAAACAGGTAG
19[80]	1[87]	GACAGTCATCTGCCAGAAACGGCGGGCCCTGATTGATGGT
3[24]	17[31]	AAGGGAAGCCCCGATTAACCCTTCCAATATTTAACAGTGC
55[24]	58[24]	AACAAAGTAATAGCTAAAAATACAATTTTGTC
42[39]	55[39]	CGACAAAATTAGGCAGGAAATAGCTACCAGAA
30[111]	17[111]	AATCGTCAAAAACTAG
41[64]	56[64]	AGCGATTACAGAACCGTCAGTACCGGATTAGG
36[103]	42[96]	AAATTGGGCTTGCCCTTAAAACGA
5[8]	6[8]	CTTAATGCTACGCCAG
19[56]	30[56]	TTCAAAAGAGGCTATCCAAAAATCCAGAAAAC
43[8]	42[8]	ACAACATGCCAGACGA
15[8]	14[8]	GCGAACTGCTATTAGT

62[23]	48[8]	CAGAATCAGCGCGTTTGAGGTTTTGAAGCCTT
30[103]	35[103]	TAAATATTAAAGCGGAACGGAACAGGGAAGAA
16[79]	2[72]	CCAAAAACTTCGCATTGTAGCCAGAATCCTGTGAGAGTTG
22[103]	24[96]	GCAAAGAATAGCATTAACATTTCG
38[71]	40[56]	ACAAGAACCATAAGGGCGGAACGAGGCGCAGA
		GGTCCACGACCCGTCGAACATTAATTGCCTGATGTATAAGAA
2[63]	31[63]	AAGAAG
18[47]	12[40]	AAATCTAAAAGCGTAATTACATTG
23[80]	6[80]	ATTCTACTGCAGGTCGGTAACGCCAAAGTGTA
27[32]	37[39]	GAATATACATGCAAATATCTTCTG
36[23]	28[16]	AAGACAAACTTTTTAATAACGGAT
36[31]	44[24]	CCAATCGCATGCAGAACCTAATTT
21[48]	4[40]	AAACACGGGCTGGCGAAAGATCGCCAAAGGGCGCTGGCAA
52[31]	60[24]	ACGGGAGACAAAAGGGAAAGGTGA
50[55]	32[48]	TTCCAGAGTCTTACCATCATCGAGTAAGAACGACAGTACA
31[8]	30[8]	AATTAATTAAACATCA
1[88]	15[95]	GGTTCCGATAGGGTTGGTTAAATC
55[8]	40[16]	AGTAAGCAGATAGCCGAGTAGGGC
51[32]	59[39]	ACGTCAAATATTCATTCGACATTC
35[48]	18[48]	AACTATATCAGACCGGCCATAAATAGGATGAA
36[87]	29[87]	GGTTTAATTACCAGTCTATCGCGTTATTATAG
50[47]	35[47]	CCTAATTTGGTATTAAAAAAATAAGGTTATAT
59[40]	53[47]	AACCGATTACCACGGATAACCCAC
5[96]	9[103]	TAACTCACCAACTGTTCCCAGTCA

41[16]	26[16]	AACGCCAAAGGCGTTATATTTTAGTAAAACAG
22[79]	7[79]	ATAAAGCCTAAGTTGGACTCTAGACATGGTCA
36[79]	21[79]	TTCAACTTTAGAGAGTGTAGCTCAATGACCCT
61[8]	60[8]	ATTTGGGACGTCACCG
18[39]	28[32]	AGCATCACCAGTTGAAACATCGGG
		GAGTAACATTATCATTTGATTAGTGAACTCAAAGGAACG
23[8]	5[23]	GGCCGCTAC
28[79]	10[72]	TTTAATTCAGGCCGGATGCAATGCCGGCACCGGCGGGCCT
5[24]	12[24]	AGGGCGCGGTCACGCTGCTCAATCACCAGTCA
8[55]	5[55]	CACGCAAAAAGGGGGATAAACAGGACGAGCAC
18[79]	4[72]	TTTGAGAGGTGGGAACTTTGAGGGTGCGTATTTGCCAGCT
24[47]	23[55]	TCATATTCCCACCAGAAGGAGCGG
57[40]	55[47]	GGTGGCAAACGGAATAGGAAACCG
53[88]	60[88]	GAGCCACCTACCGTAATGAATTTAACGATTGG
6[111]	8[96]	ACACAACATACGAGCCGAAATTGTCCAAGCTT
46[87]	32[80]	ACAACCATATCAGCTTCGATAAAA
15[96]	17[103]	AGCTCATTCCCCGGTTGTAATCGT
27[56]	34[56]	TCCAACAGAAGCGAACGCGATTTTAGATTTAG
3[40]	3[63]	AGGAGCGGGCGCTCGCGCGGGGAG
53[80]	43[87]	CACCCTCAAAAGAATATTTCCATT
20[71]	25[71]	CTGAGTAAAAAACATTACATGTTTTTTCATTC
7[24]	9[31]	AGTGAGGCTTTTAGACACTATCGG
47[32]	61[39]	GGCTTATCACCTCCCGACAATTTTCCGTAATCTCACCAGT
30[95]	47[103]	CATTGAATAAGGAATTCCAGACGAGCTTTCGAGGTGAATT

49[24]	63[39]	ACCCAGCTACTTGCGGTCATCGGCATTTTCGG
54[95]	58[88]	CAGGAGGTTGCCCCCTAGTGTACT
0[39]	13[39]	TCCAACGTTCGAGGTGGGCACAGATGACCTGA
55[56]	57[71]	GGTTTTGCCCAATAATAGATGAGTAACAGTGC
33[8]	34[8]	TTAATTAACAAAATCA
0[111]	1[103]	AAAGAATAGCCCGAGAAATCGGCA
		TAGCTGTTTCCTGTGTGGAAGCATAGGGTTTTGGGAAG
7[80]	21[95]	GGTTTGCGGG
44[111]	35[111]	CGAAAGACAAATCTAC
27[16]	12[16]	AGGTTTAAACAACTAATCAGTTGGCACGACCA
41[72]	39[79]	TACCAAGCTACTTAGCAACCGAAC
6[79]	8[64]	AAGCCTTAGAATCAGATTCGTAATGGATCCCC
45[56]	51[71]	CCGTTCGGTCGCTGAGTATGGGATACTACAAC
51[48]	34[48]	TAGCAGCCTGAACAAGACCAAGTAGAAAGATT
37[64]	53[63]	ACGTAACACACTCATCTTTGAATAAGTTAAGC
14[95]	31[95]	CGCGTCTGGATGAACGGATAATCAAATGTTTA
58[87]	52[80]	GGTAATAAGCAGTCTCCACTGAGT
27[48]	12[48]	AAGCAAACTAAGGTTAAGGAAAGAGCCTCAGG
34[95]	49[95]	ACATTATTAGGCCGCTCAATGACATCAGCGGA
36[47]	21[47]	AAATGCTGAGTAACAGTACCATATGACTTTAC
54[23]	43[23]	TCTTACCGAATTGAGCAATTCTGTTTCAGCTA
9[56]	20[56]	TGTGCTGCTTACGCCATTGTACCATGTGTAGG
51[96]	59[103]	CTCATAGTCAGGTCAGCCGTTCCA
39[48]	22[48]	CGTTATACAATTATCAGTACGGTGAATATTCG

13[64]	19[71]	GATTCTCCATCTACAAGGTGAGAA
33[32]	50[32]	TTGAAAACAGCCGTTTCAAGAACGGCCAGTTA
60[111]	51[111]	GGTTGAGGTAGCGTAA
36[63]	43[71]	GTGAATTAAAGAAAGACTTTTTCA
22[39]	24[32]	TATTAAATCAAAGAAACTGATTAT
		CACTAAAAAAGCTGCTTAATCTTGCATATAACTGTTTAGC
42[79]	23[79]	TGGCATCA
35[32]	52[32]	TTAGGTTGTATCCCATCGCGCCTGCGCATTAG
14[103]	18[96]	AAATAATTGTAATGGGTTAATGCC
12[95]	29[95]	ACCGTGCAAATCACCAGGAGAGGGTCAGAAGC
8[95]	26[88]	GCATGCCTAATAGTAGTTAGCAAACCCAATTCTGCTGAAT
10[31]	28[24]	CCAGCCATGGATTTAGGAGCACTACGTCAGATAGAAACAA
24[95]	42[88]	CAAATGGTTTTGAAAGTGACCTTCAAGTACAAAAGAGGCA
15[48]	0[40]	GTAAACGTATTAAAGAACGTGGAC
24[71]	41[63]	TATATTTTCATTTGGGCGGTCAATCGGATATTGTACCCCC
29[32]	34[32]	AGGCGAATGAGAAGAG
37[88]	44[88]	GAATAAGGCTTGAGATAAACGGGTAACGAGGG
2[39]	11[39]	AAGGGAGCAAAGCGAAGCAGATTCGTCTGAAA
53[48]	36[48]	AAGAATTGAGAGAATACAATAGATCCTTATGT
4[39]	9[39]	GTGTAGCGTACTATGGTATTACCGCCTTGCTG
39[104]	39[111]	TGAACGGT
63[40]	49[47]	TCATAGCCTAGCAGCAATCCTGAA
54[47]	39[47]	GAAACAATAGGCATTTACCAGTATATCATATG
48[95]	63[111]	ATTTTTTCCGGAACCAGAGCCACCACCGGAAC

19[24]	30[24]	CAAATCAACTTGCTGATCGCGCAGAAGAAGAT
1[40]	15[63]	CCGTAAAGCACTAGTTTGCCCCAGAGTCCACTTAATATTT
13[48]	2[40]	GAGTAACACTGAATCGGAACCCTA
51[24]	62[24]	TTTGTTTACAAAATAACAGCAAAAAGTAGCGA
56[63]	54[48]	ATTAGCGGCAATAATACATATAAAAAGAGCAA
20[47]	6[40]	TCTAAAATTGGATTATCAGAACAATTGCTTTGAGGCCGAT
59[72]	54[72]	TGGAAAGCGTTTTAACAGAACCGCGCCACCCT
0[71]	14[64]	GGAACAAGCAGGCGAACTTTCATC
31[64]	46[64]	TTTTGCCAAGCGAGAGACTAATGCCATAACCG
20[95]	35[95]	CCTCATATTTGCTCCTACTTCAAAAGGACGTT
39[96]	55[95]	AGGACAGACGAAATCCGCGACCTGTCGAGAGG
19[96]	27[103]	TCAATATGCCCGAAAGTTTGATAA
41[96]	56[96]	CGGAGATTACCGTACTGTTGATATAAGTATTA
22[47]	7[47]	ACAACTCGGTAATATCTTAACCGTAAAAGAGT
33[24]	47[31]	TAGAATCCAGTGAATAATATAGAA
51[88]	62[88]	AGACAGCCAGACGTTACCACCACCAGAACCGC
16[31]	32[32]	CAGCAGAACAATTTCATTTGAATTTATATGTG
25[24]	37[31]	CTGAATAATTTGCACGTTAATTTC
45[16]	30[16]	TCTTTCCTGAATTTATTTTTCCCTGATGAAAC
19[8]	20[8]	ATATCTGGTAGATTAG
36[111]	27[111]	CGAGTAGTGAGGTCAT
35[24]	46[24]	CCTCCGGCTCAATAGTTATCATTCTTATTTTC
47[64]	62[56]	TTAATTGTAAAAAAAGTTTGCTAAACCCGTCACCAATGAA
5[72]	11[95]	TCGTGGGGTGCCTAATGAGTGAGCGTCGGGAAGCCGGAAA

21[96]	38[96]	AGAAGCCTAGCTTAATTGCGAACGAGGCTGGC
16[47]	30[32]	TAACCGAACGAACCACCACGCTGACTGAGCAA
11[80]	3[87]	CTTCTGGTACCTGTCGGGGCGCCA
58[23]	44[16]	ACAATCAAGCCAAAGAATTAACTGAACGATTTACGAGCAT
56[95]	54[80]	AGAGGCTGAGACTCCTACAGTTAATTAGTACC
34[47]	19[47]	AAGACGCTTATTCATTTACCTTTTAGGAATTG
63[64]	49[79]	CCATCTTTTCATAATCGAGCCACCACAACTTT
33[56]	47[63]	CACATTCAGCTTTTGCAGGAGCCT
58[103]	57[111]	GATACAGGGCCTATTTCGGAACCT
62[87]	48[80]	CACCCTCAAAAATCACACGTTGAA
49[8]	50[8]	TTAGTTGCATTATTTA
38[87]	20[80]	ATCAAGAGCATTCAGTATAATGCTACCTTTAAATTTTAAA
33[80]	16[80]	AACGCCAACCCCCTCAAATAGTAAGAAAAGCC
61[40]	43[47]	AGCACCATACGGAAATAATGAAAACAGGGAAGTTTATCAA
14[111]	1[111]	GCCATCAAAAATCCCT
14[23]	0[8]	TTGAATGGATAGCCCTGAAAAACCGTCTATCA
31[16]	16[8]	ACATTTAAGATAAAACAGAGGTGA
5[56]	12[56]	GTATAACGGAATCGGCACTCCAGCCAGTATCG
53[32]	57[39]	CAGAGAGAATAAGTTTTACATAAA
52[71]	58[64]	CAGTACAACCACCCTCGGGGTCAG
18[87]	14[80]	TAGCTATTAGAGAATCGCCTTCCT
52[63]	59[71]	GAGAATAAGAAATTAAAGCCAGAA
63[8]	62[8]	AGACTGTAAGTTTGCC
56[111]	55[111]	AAACATGAAAGTATAG

37[8]	38[8]	TTCAAATAAATAAGAA
48[111]	47[111]	GGAATTGCTCTTAAAC
57[8]	56[8]	ATGTTAGCACTCCTTA
10[111]	5[111]	AGGCTGCGATTAATTG
25[8]	24[8]	TGTTTGGAATCAATAT
32[111]	31[111]	TCATAACCAGCGTCCA
11[8]	10[8]	ATACCTACGAAAAACG
47[8]	46[8]	ATAGCAAGAATCATTA
1[8]	2[8]	TCACCCAAGACGGGGA
52[111]	43[111]	CCAATAGGTAATGCCA
4[71]	23[71]	GCATTAATTGCTTTCCCTTCGCTAAAGGCGATTCAGAGCATGAAAAGG
2[111]	20[96]	ACAGCTGATTGCCCTTTTTCTTTTGCATCGTACCAGGCAATTTAGAAC
57[72]	41[87]	CCGTATAACAAGAGAAAGGCGGATAAGTGCCGCTCCATGTGCGAAACA
42[111]	23[111]	CACCAACCGACGAGAAAGGCGCATAGTAGATTCATTAGATACATCCAA
39[80]	10[80]	TGACCAACCAATAACCAGTTGATTATTAAGCAGTAATACTCGATCGGT
48[79]	29[79]	AATCTCCAATCGGTTTCGCCCACGAGATACATAAAGATTCACCCTGAC
31[96]	50[96]	GACTGGATCTCGTTTAACGAGGCATGCGCCGATTTGCGGGGTCTTTCC
21[8]	7[23]	TAGATAATATTAATTTGAGTAGAAAATAACATAAGTGTTTTTATAATC
41[8]	25[23]	TATTTAACTTAATTGAGAATCATAATTACTAGGGCAATTCTTATACTT
60[23]	47[23]	ATTATCACATTAGAGCACAGCCATTATTTTGCATCGTAGGCAAATCAG
1[24]	14[40]	TTTTGGGGCAAAGGGCAAAACATCGCCATTAAAAATAATTGAATACGT

The green strands are modified with a handle at their five prime end for hybridization with a strand containing alexafluor488 dye at its 5’ end. The modified sequences are:

Start	End	Sequence
63[8]	62[8]	**AAT GGC ACA CCA ACG ATC AGC**
		AAAGACTGTAAGTTTGCC

56[111]	55[111]	**AAT GGC ACA CCA ACG ATC AGC**
		AAAAACATGAAAGTATAG
37[8]	38[8]	**AAT GGC ACA CCA ACG ATC AGC**
		AATTCAAATAAATAAGAA
48[111]	47[111]	**AAT GGC ACA CCA ACG ATC AGC**
		AAGGAATTGCTCTTAAAC
57[8]	56[8]	**AAT GGC ACA CCA ACG ATC AGC**
		AAATGTTAGCACTCCTTA
10[111]	5[111]	**AAT GGC ACA CCA ACG ATC AGC**
		AAAGGCTGCGATTAATTG
25[8]	24[8]	**AAT GGC ACA CCA ACG ATC AGC**
		AATGTTTGGAATCAATAT
32[111]	31[111]	**AAT GGC ACA CCA ACG ATC AGC**
		AATCATAACCAGCGTCCA
11[8]	10[8]	**AAT GGC ACA CCA ACG ATC AGC**
		AAATACCTACGAAAAACG
47[8]	46[8]	**AAT GGC ACA CCA ACG ATC AGC**
		AAATAGCAAGAATCATTA
1[8]	2[8]	**AAT GGC ACA CCA ACG ATC AGC**
		AATCACCCAAGACGGGGA
52[111]	43[111]	**AAT GGC ACA CCA ACG ATC AGC**
		AACCAATAGGTAATGCCA

The pink strands are modified with a handle at their five prime end for further attachment of PEGs and DSPE-PEG. The modified sequences are:

Start	End	Sequence
4[71]	23[71]	**TCG ATC ACG TAG CAC AGC**
		ATGCATTAATTGCTTTCCCTTCGCTAAAGGCGATTCAGAGCATGAAAAGG
2[111]	20[96]	**TCG ATC ACG TAG CAC AGC**
		ATACAGCTGATTGCCCTTTTTCTTTTGCATCGTACCAGGCAATTTAGAAC
57[72]	41[87]	**TCG ATC ACG TAG CAC AGC**
		ATCCGTATAACAAGAGAAAGGCGGATAAGTGCCGCTCCATGTGCGAAACA
42[111]	23[111]	**TCG ATC ACG TAG CAC AGC**
		ATCACCAACCGACGAGAAAGGCGCATAGTAGATTCATTAGATACATCCAA
39[80]	10[80]	**TCG ATC ACG TAG CAC AGC**
		ATTGACCAACCAATAACCAGTTGATTATTAAGCAGTAATACTCGATCGGT
48[79]	29[79]	**TCG ATC ACG TAG CAC AGC**
		ATAATCTCCAATCGGTTTCGCCCACGAGATACATAAAGATTCACCCTGAC
31[96]	50[96]	**TCG ATC ACG TAG CAC AGC**
		ATGACTGGATCTCGTTTAACGAGGCATGCGCCGATTTGCGGGGTCTTTCC
21[8]	7[23]	**TCG ATC ACG TAG CAC AGC**
		ATTAGATAATATTAATTTGAGTAGAAAATAACATAAGTGTTTTTATAATC
41[8]	25[23]	**TCG ATC ACG TAG CAC AGC**
		ATTATTTAACTTAATTGAGAATCATAATTACTAGGGCAATTCTTATACTT
60[23]	47[23]	**TCG ATC ACG TAG CAC AGC**
		ATATTATCACATTAGAGCACAGCCATTATTTTGCATCGTAGGCAAATCAG
1[24]	14[40]	**TCG ATC ACG TAG CAC AGC**
		ATTTTTGGGGCAAAGGGCAAAACATCGCCATTAAAAATAATTGAATACGT
55[48]	25[47]	**TCG ATC ACG TAG CAC AGC**
		ATAGGAAACGAAATTCTTTCGAGCCACATGGTTTGAAATACCTTAGAACC
59[104]	40[104]	**TCG ATC ACG TAG CAC AGC**
		ATGTAAGCGTCTTTTGATTTTCAGGGGGTGTATCTGTATCATAATTGTGT
46[111]	19[111]	**TCG ATC ACG TAG CAC AGC**
		ATCCGATAGTTAGTAAGAACGAACTATTGCATCAAGAGGAAGATATTCAA

26[111]	7[111]	**TCG ATC ACG TAG CAC AGC**
		ATTGGCTTAGTTATTTCACAGGCAAGCGACGTTGGGCCAGTGTATCCGCT
18[111]	4[96]	**TCG ATC ACG TAG CAC AGC**
		ATCTGATAAAATAGGTCAAGATGGGCCACCAGTGCACTGCCCGCTTTCCA
17[8]	4[8]	**TCG ATC ACG TAG CAC AGC**
		ATTATTAACATATCAAACTGGCCAACGTAATAAAAACGTGGCCCACCACA
62[55]	46[40]	**TCG ATC ACG TAG CAC AGC**
		ATACCATCGACCCTTATTCGAGGCGTTTTAGCGACGGTATTCAACAAGCA
45[8]	26[8]	**TCG ATC ACG TAG CAC AGC**
		ATATCGGCTGGTAGAAACGAGACTACGAACGCGAAGATTTTCAAATAAAG
8[63]	37[63]	**TCG ATC ACG TAG CAC AGC**
		ATGGGTACCGGCGCGAGCTAAAGCTATCTGGAAGTAAATATGCCAAATCA
24[31]	53[31]	**TCG ATC ACG TAG CAC AGC**
		ATCAGATGATAAAAAGCCGATAAATACATGTAATGGTAAAGTGCTAATAT
15[64]	34[64]	**TCG ATC ACG TAG CAC AGC**
		ATTGTTAAAAAGGAAGATGAGTCTGGAAACAGTTAGGTCTTTATCAGTTG
6[39]	22[24]	**TCG ATC ACG TAG CAC AGC**
		ATTAAAGGGACACCGAGTTGTAGCAATACTTCTTTTGCGGAACCTTTGCC
32[47]	14[48]	**TCG ATC ACG TAG CAC AGC**
		ATTAAATCAAACCTTTTTTCAATTACGAGCCAGCAGCAATCAATGTGAGC

S2.4 Annealing the DNs

S.2.4.1 Td

Strand 5 was reacted with DBCO-NHS ester separately and converted to DNA-DBCO. The five strands (1:2:3:4:5) were mixed in the molar ratio of 1:3:3:3:3 in 1X TAE buffer (containing 12.5 mM Mg^{2+}) and was subjected to a 12 hour thermal annealing

program starting from 80°C and ending at 4°C with a regular decrease in the temperature by 1°C. The structure was characterized and purified using 1% agarose gel electrophoresis.

S.2.4.2 DNO

DNO was annealed in 5 nM concentration by mixing 5 nM m13 scaffold and 10X staples in 1X 3D buffer. The annealing program used heated the mixture of strands to 95°C and cooled them to 4°C over a period of 37 hours.

S2.5 Conjugation of DBCO to S5-amine

100 mM stock solution of DBCO-NHS ester was prepared in anhydrous DMSO. 20 uL of DBSO-NHS stock was diluted using the same solvent and reacted with 100 uM aqueous solution of S5-amine in 50 mM phosphate buffer (pH = 8.5). The volume ratio of S5-amine: DBSO-NHS (diluted with anhydrous DMSO): phosphate buffer was 1:8:3. The reaction mixture was stirred at room temperature for 30 minutes and then lyophilized overnight. The lyophilized powder was dissolved in water and purified using HPLC to obtain pure S5-DBCO.

S2.6 Conjugation of different PEGs and DSPE-PEG with S5 – DBCO

The linear and branched PEGs being water soluble, their stock solutions were made in water. Only the stock solution of DSPE–PEG was made in chloroform. 1, 2.5, 5 and 10 equivalents of different PEG azides and DSPE–PEG were reacted with 100 uM S5-DBCO in 50 mM phosphate buffer (pH = 7.0) at room temperature for 4 hours. All the reaction mixtures were separately run on 10% denaturing polyacrylamide gels using 1X TBE as the

running buffer for 1 hour at 45°C under 45 mA/gel. In each gel, S5-DBCO (named as 'No PEG) was used as a control. In case of branched PEG conjugation, the conjugation product of the corresponding linear isomer with S5-DBCO was used as an additional control.

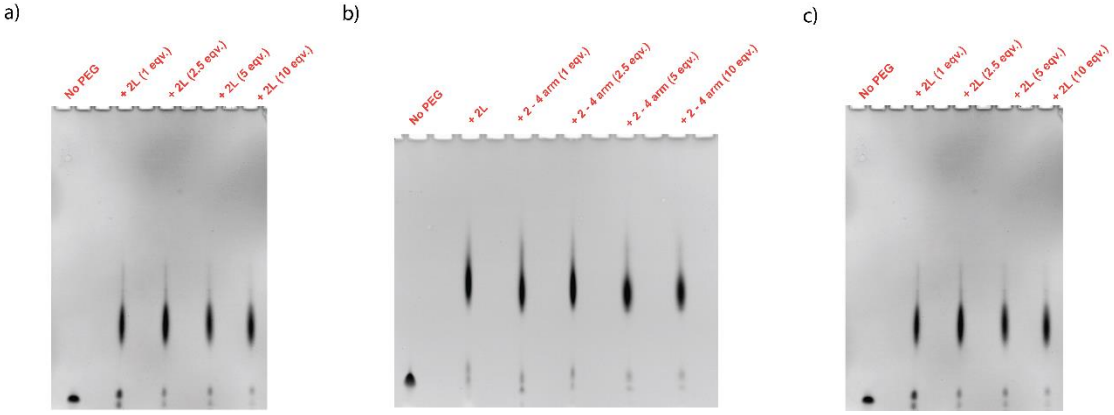

Figure S2.4: Conjugation of 2 kD linear and branched PEGs with S5.

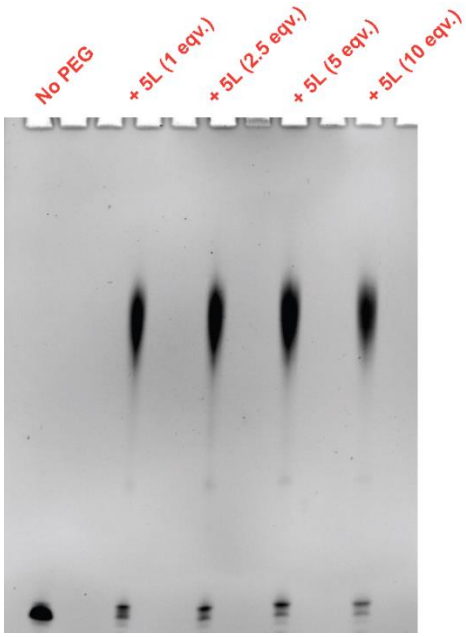

Figure S2.5: Conjugation of 5 kD linear PEG with S5.

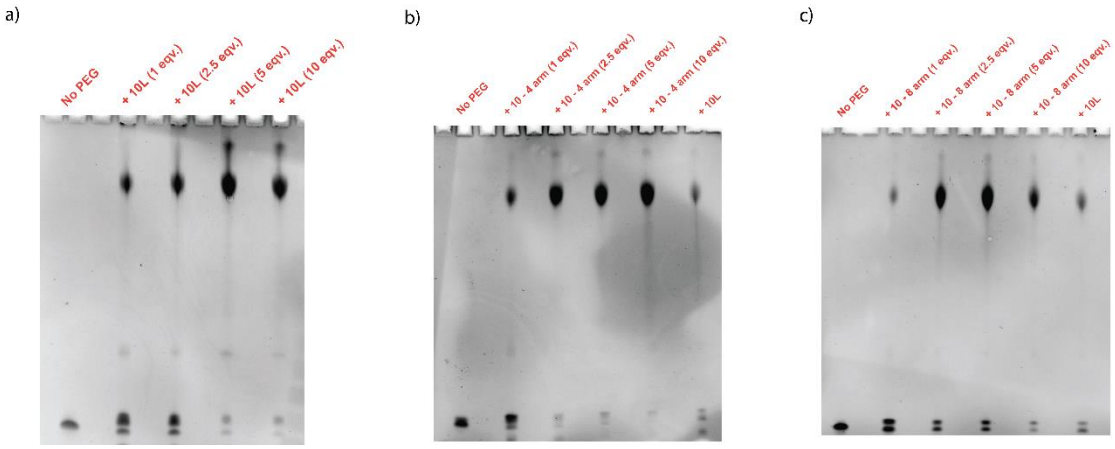

Figure S2.6: Conjugation of 10 kD linear and branched PEGs with S5.

S2.8 Conjugation of Different PEGs and DEPE-PEG to Td and DNO

We used 250 nM Td and 10 nM DNO to run the agarose gels. The Td samples were run on a 1.5 % gel for 45 minutes while the DNO samples were run on a 1% gel for an hour under 100V. Both the gels were run in 1X TAE/Mg^{2+} buffer at 4°C and stained with SYBR green to visualize the bands.

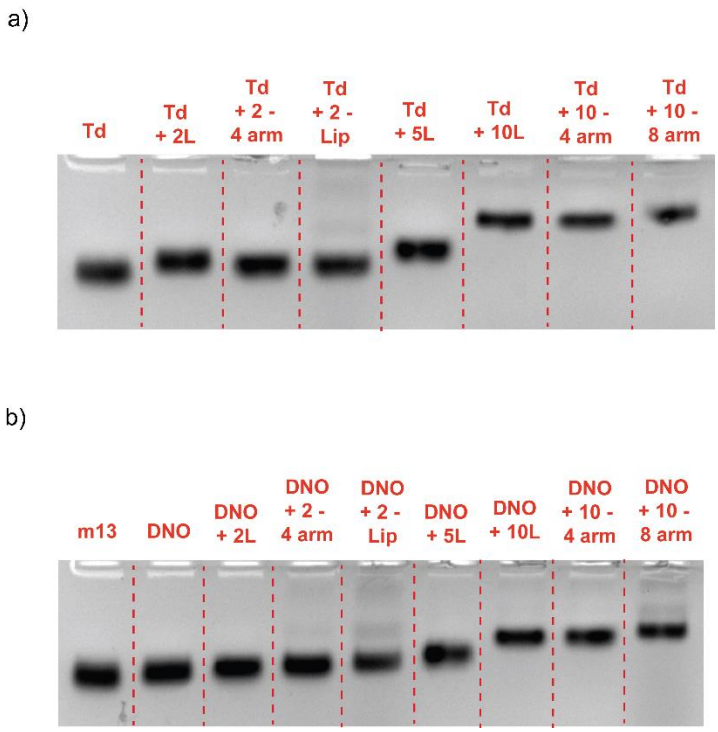

Figure S2.7: Conjugation of different PEGs and DSPE-PEG to a) Td b) DNO.

S2.9 Time vs stability studies

For the time vs stability studies the Td and DNO samples were concentrated 20 fold and then diluted to DMEM + 10% FBS medium, the final concentrations being 1 uM and 10 nM for Td and DNO respectively. The Td samples were studied for 48 hours while the DNO samples were studied for 5 hours. 30 uL aliquots were taken out from each sample at different time points and were run on three separate gels (triplicate). The Td samples were run on 1.5 % agarose gel and the DNO samples on 1% agarose gel, both in 1X 3D buffer, at 4°C. After the completion of run, the gels were stained with SYBR green for band visualization.

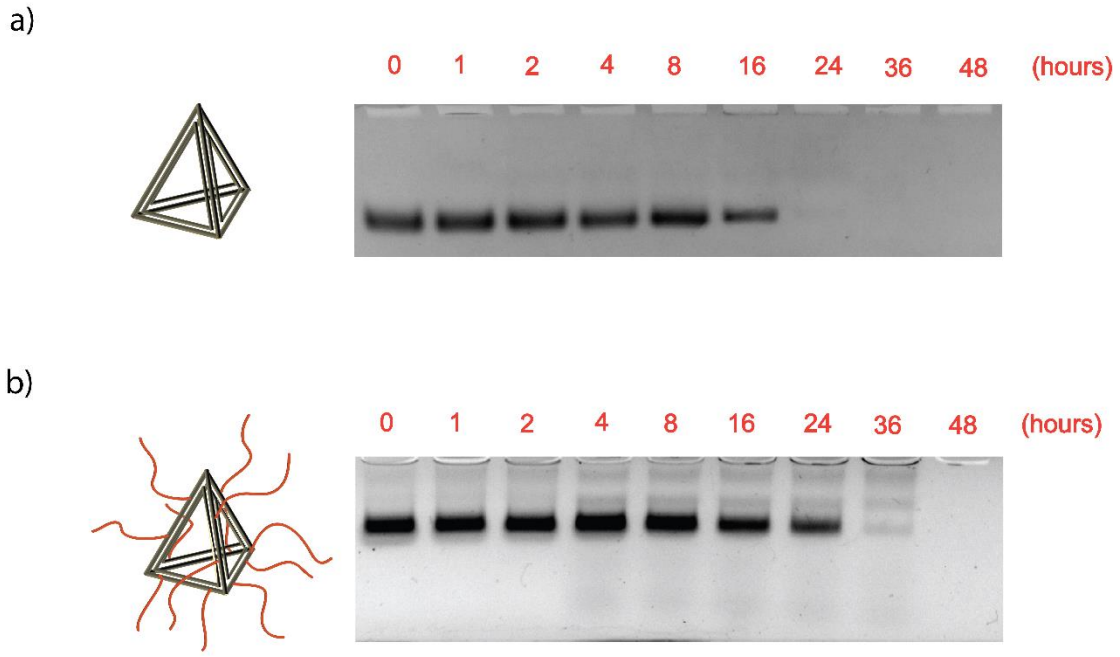

Figure S2.8: Agarose gels showing time vs stability of a) bare Td, b) Td coated with 10 kD linear PEG.

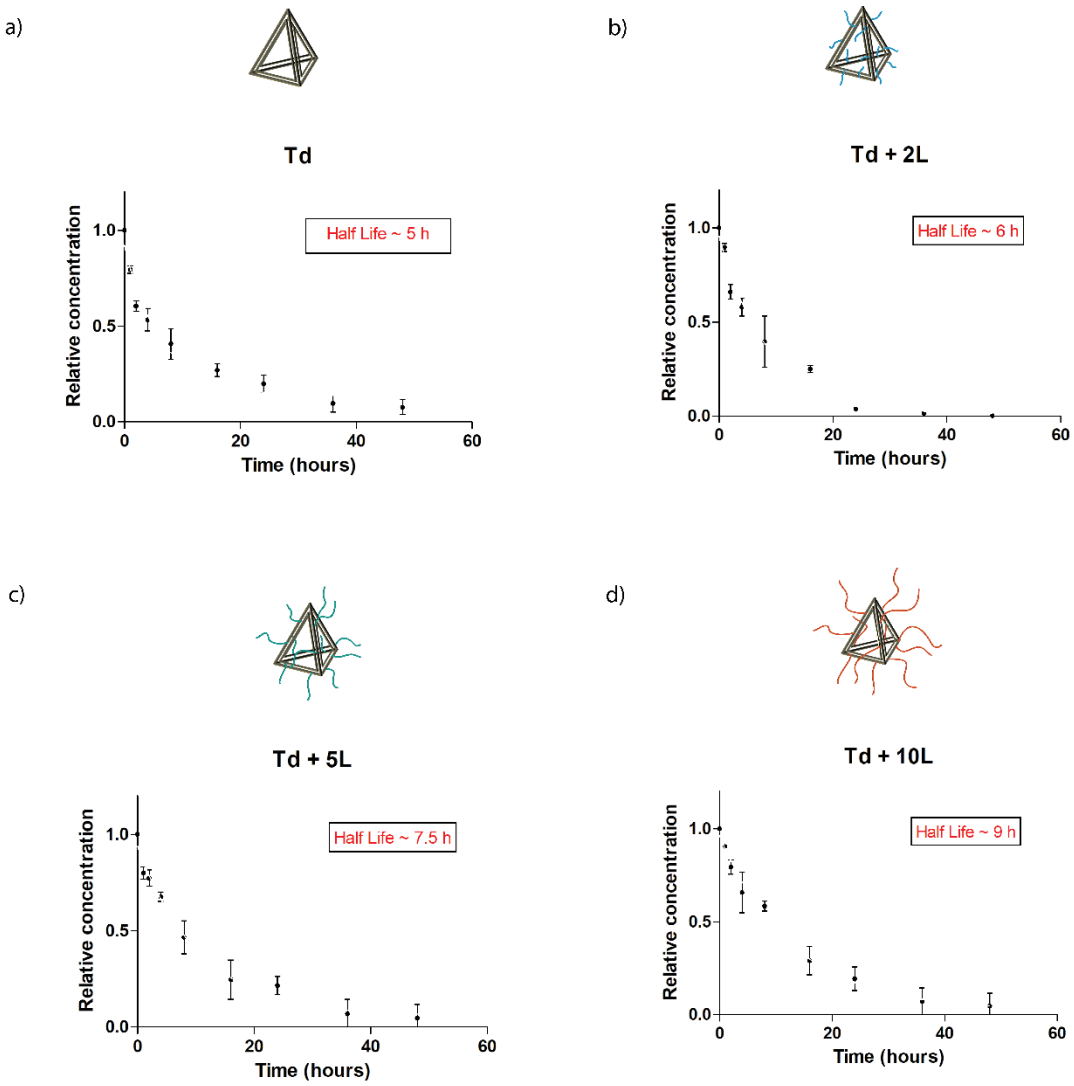

Figure S2.9: Time vs stability plots for a) bare Td, b) 2L coated Td, c) 5L coated Td, and d) 10L coated Td.

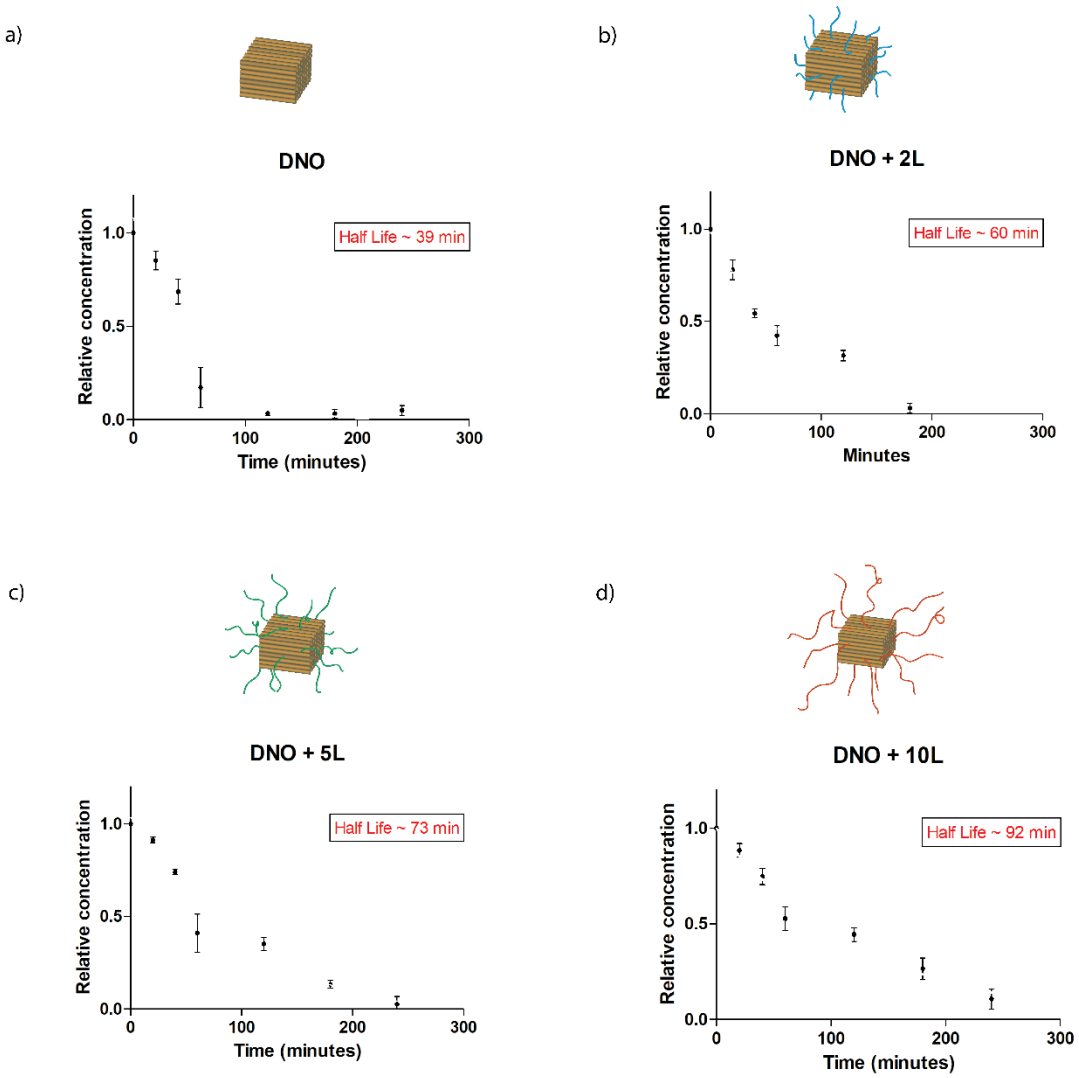

Figure S2.10: Time vs stability plots for a) bare DNO, b) 2L coated DNO, c) 5L coated DNO, and d) 10L coated DNO.

S2.10 Cell Culture

The RAW cells were cultured in DMEM medium supplemented with 10% FBS under conditions of 37°C and 5% CO_2. The cells were seeded in 12 well plates at a density of 20,000 cells/well and cultured for 24 h.

S2.11 Flow Cytometry

S.2.11.1 Incubation with DNs

Before incubation the existing medium was replaced with fresh medium. The cells in each well were incubated with 10 uL of each sample (S5-dye or DN), the concentration of the sample was such adjusted that the concentration of Alexa fluor 488 was always 120 nM. Td was annealed in 250 nM concentration and as each Td contained 12 fluorophore, hence the concentration of the fluorophore became 3 uM. The sample was diluted 25 fold and 10 uL of the diluted sample was added to each well when required. DNO was annealed in 5 nM and then concentrated to 10 nM. As each structure contained 12 fluorophores, hence concentration of fluorophore became 120 nM.

An issue that we had to face during incubation of the cells with DNs was the instability of the structures in cell culture medium. Our previous experiments showed that Td had a half-life of about 5 h in DMEM + 10% FBS medium whereas the same was only ~ 39 minutes for DNO. So, if we incubate the cells with only one aliquot of the structure, there was obvious chances of the macrophages internalizing free dye labeled DNA that resulted from the degradation of DNs. Hence, we replaced the medium every 30 minutes for Td incubation and added fresh aliquot of Td (10 nM, 10 uL) and for incubation with DNO the process was repeated every 10 minutes. This minimized the chance of dye labeled DNA internalization.

S.2.9.2 Dead cell staining

Propidium iodide stock was prepared by dissolving solid propidium iodide in deionized water and the stock concentration was 1 mg/mL. While staining the cells, the stock was diluted to 3 uM by using 1X PBS buffer. 1 mL of the 3 uM dye was added to each well.

S.2.9.3 DNase treatment

DNase powder was dissolved at a concentration of 1 mg/mL in 50% Glycerol with 20 mM Tris-HCl, pH 7.5, and 1 mM $MgCl_2$. After the cells have been incubated with the DN, we replaced the medium and added 10 uL of the DNase stock per mL of the medium, incubated at 37°C for 10 minutes and again changed the medium with 1X PBS in case of confocal microscopy or with 3 uM propidium iodide solution (in 1X PBS) in case of flow cytometry studies.

S.2.9.4 Analysis of FACS data

The RFI value from RAW cells incubated 10 uL of the blank was collected each time the experiment was done and this value was subtracted from the RFI values of samples. 40,000 events were collected for each sample and each sample was studied in triplicates. A separate sample was prepared for dead cells and they were incubated with propidium iodide (PI) for 15 minutes prior to the flow cytometry experiment. RFI value from this control sample show that most of the dead cells has an RFI (form PI) higher than 10^2. This value for PI RFI was used as a gating. All the samples were incubated with PI solution prior to flow analysis and the gating was applied so that while analysis we could

collect the RFI values only from living cells. This minimized the chance of false positives as dead cells have a much higher permeability in comparison to the living ones.

S2.12 Confocal Microscopy

The confocal microscopy was performed on living cells in 1X PBS buffer. Cells were seeded at 3000 cells/well and grown for 24 h in a special 8 well transparent bottomed in DMEM + 10% FBS medium. Then each well was incubated with 2 uL of the sample (dye labeled DNA or structure, their concentrations modified in a way that alexa fluor 488 concentration in each sample was always 120 nM). Incubation procedure similar to the one followed during flow cytometry studies was followed. After incubation for 1h, the cells were washed once with 1X PBS and 1 uM solution of the CellTracker CM-Dil dye in 1X PBS was added. The cells were incubated at 37°C for 5 minutes and then at 4°C for 15 more minutes. The medium was again replaced with fresh 1X PBS. In addition to imaging cells directly after incubation, we also studied batches treated with DNase after incubation, such that any DNA or DN sticking to the surface was degraded by the nuclease.

Conditions similar to cell growth were maintained during imaging. We used a 40X immersion objective and a white light laser for imaging.

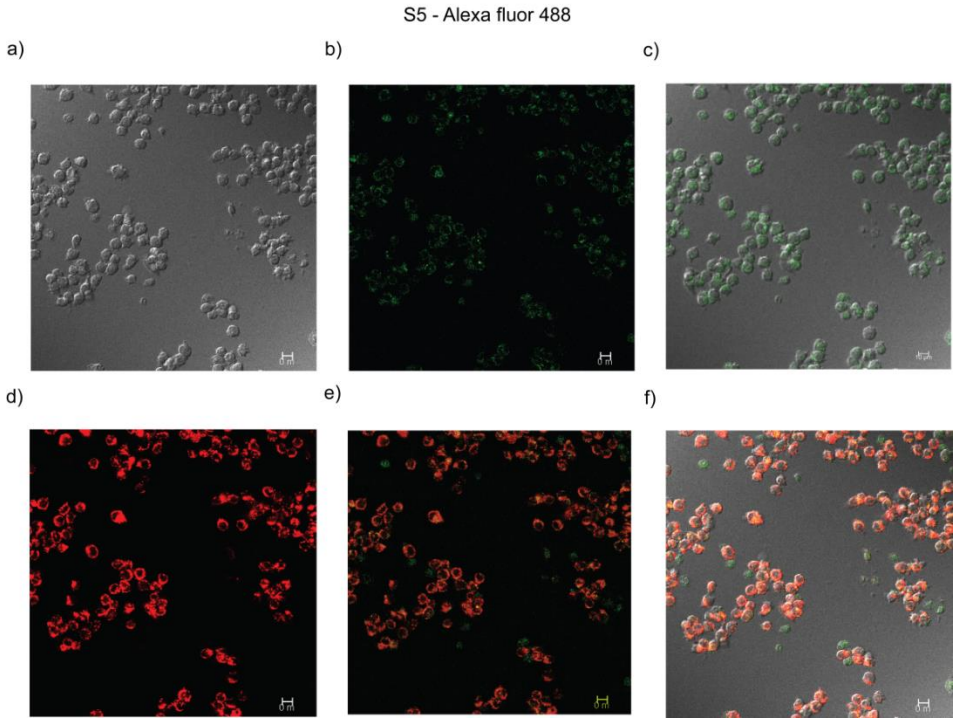

Figure S2.11*:* Confocal microscopy images of RAW cells incubated with Alexa fluor 488 labeled S5. The cell membranes were stained with CellTracker CM-Dil dye. a) Bright field image b) green fluorescence from internalized S5 c) overlay of bright field and green fluorescence d) red fluorescence from CellTracker CM-Dil dye e) overlay of green and red fluorescence f) overlay of bright field, green and red fluorescence.

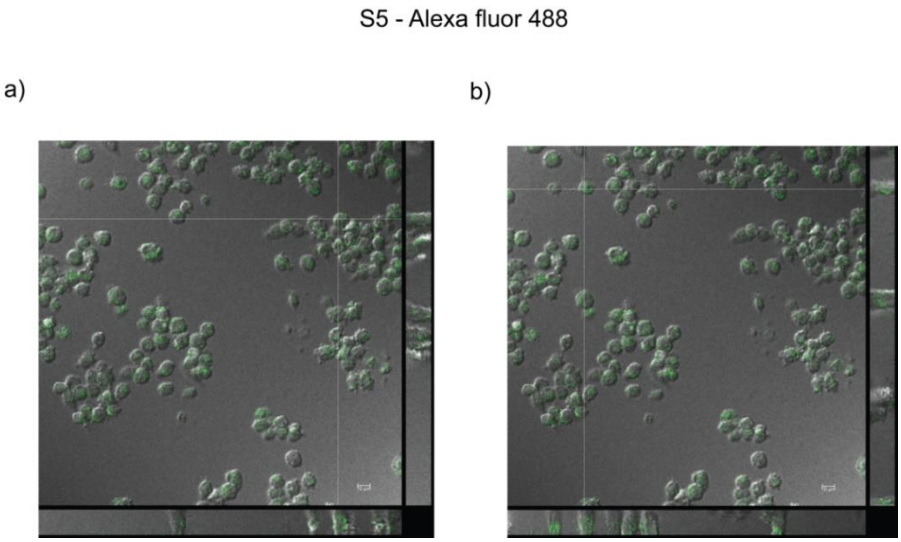

Figure S2.12*:* Z-stacked confocal microscopy images of RAW cells incubated with Alexa fluor488 labeled S5. The crosshairs indicate orthogonal sectioning. The bottom and right panels show the sectioned planes and confirm that fluorescent particles (green) are located inside the cells and not merely attached to the cell membrane.

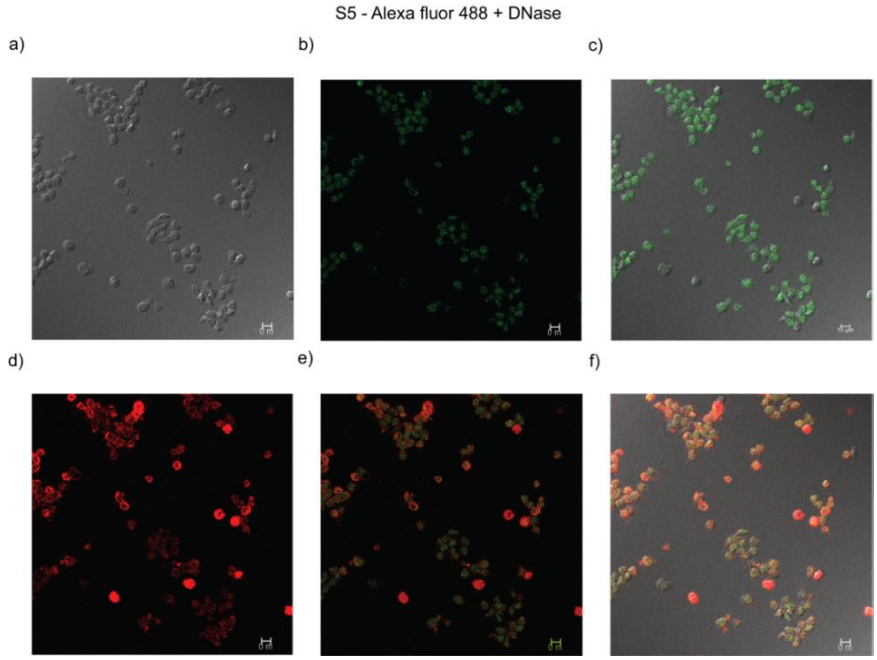

Figure S2.13*:* Confocal microscopy images of RAW cells incubated with Alexa fluor 488 labeled S5 followed by DNase treatment. The cell membranes were stained with CellTracker CM-Dil dye. a) Bright field image b) green fluorescence from internalized S5 c) overlay of bright field and green fluorescence d) red fluorescence from CellTracker CM-Dil dye e) overlay of green and red fluorescence f) overlay of bright field, green and red fluorescence.

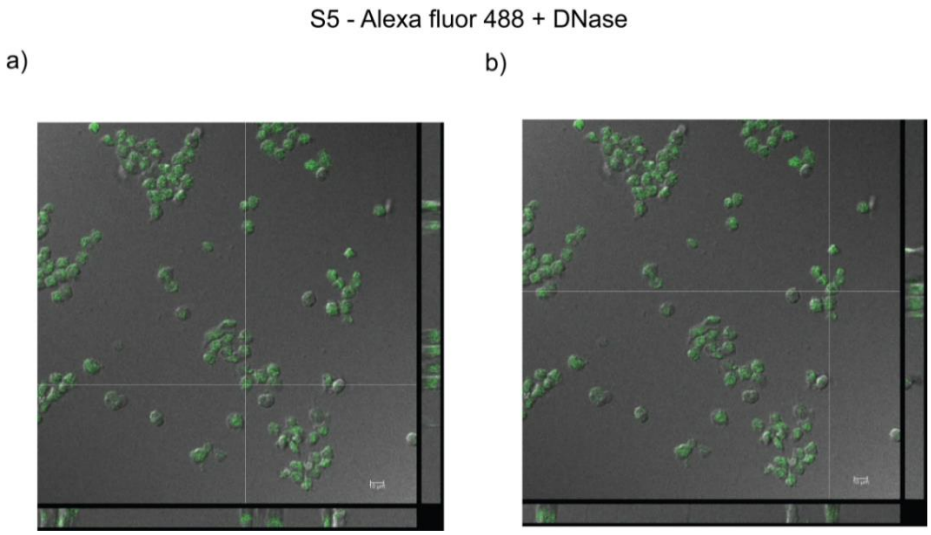

Figure S2.14*:* Z-stacked confocal microscopy images of RAW cells incubated with Alexa fluor 488 labeled S5 and then treated with DNase.

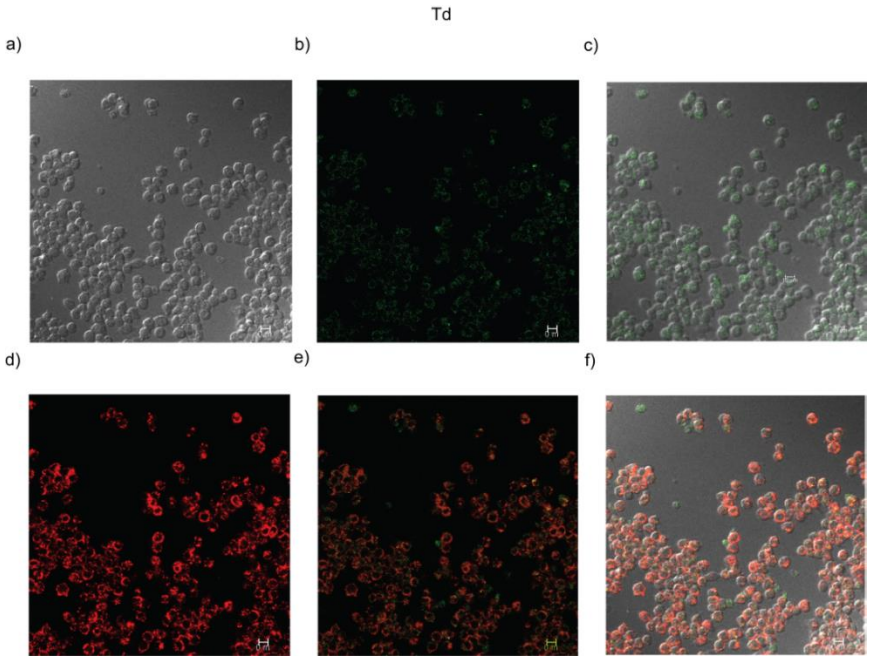

Figure S2.15*:* Confocal microscopy images of RAW cells incubated with Alexa fluor 488 labeled Td. The cell membranes were stained with CellTracker CM-Dil dye. A) Bright field image b) green fluorescence from internalized Td c) overlay of bright field and green fluorescence d) red fluorescence from CellTracker CM-Dil dye e) overlay of green and red fluorescence f) overlay of bright field, green and red fluorescence.

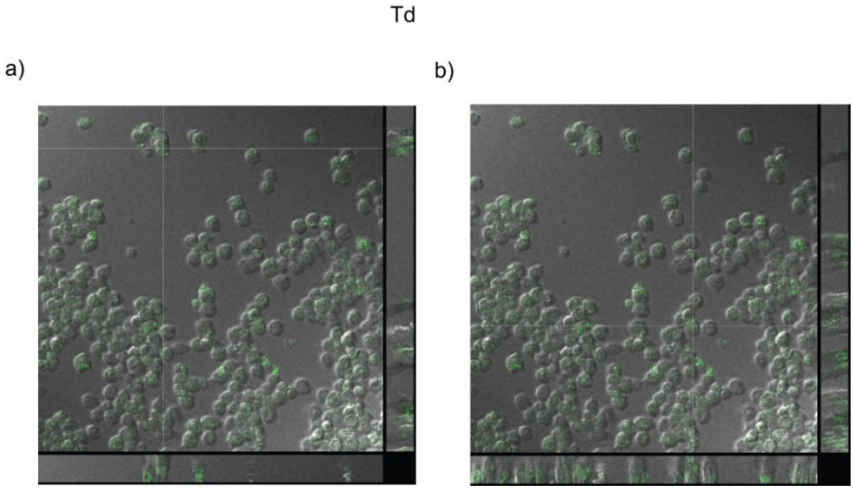

Figure S2.16*:* Z-stacked confocal microscopy images of RAW cells incubated with Alexa fluor488 labeled Td.

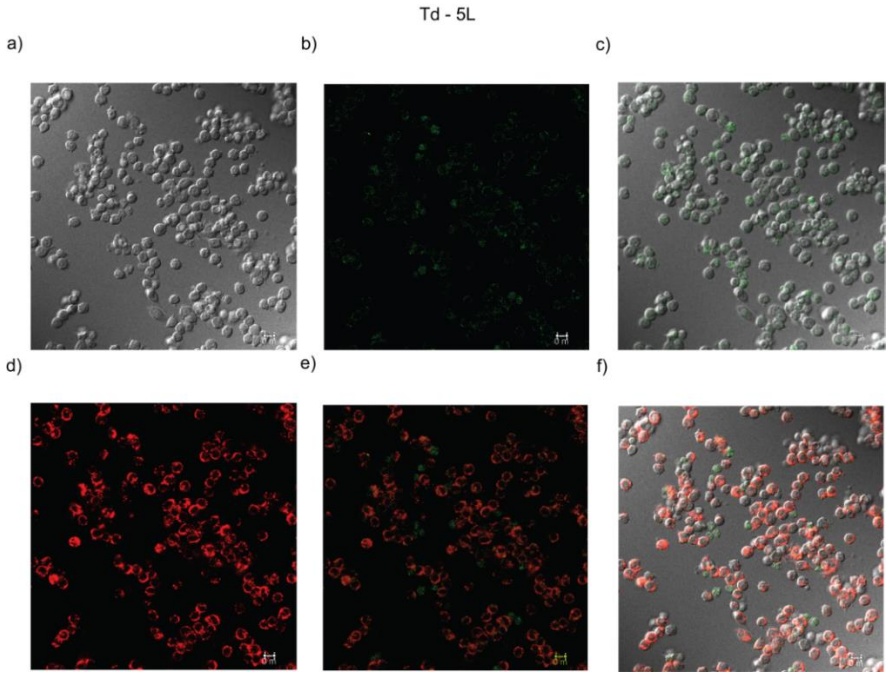

Figure S2.17*:* Confocal microscopy images of RAW cells incubated with Alexa fluor 488 labeled Td–5L. The cell membranes were stained with CellTracker CM-Dil dye. a) Bright field image b) green fluorescence from internalized Td–5L c) overlay of bright field and green fluorescence d) red fluorescence from CellTracker CM-Dil dye e) overlay of green and red fluorescence f) overlay of bright field, green and red fluorescence.

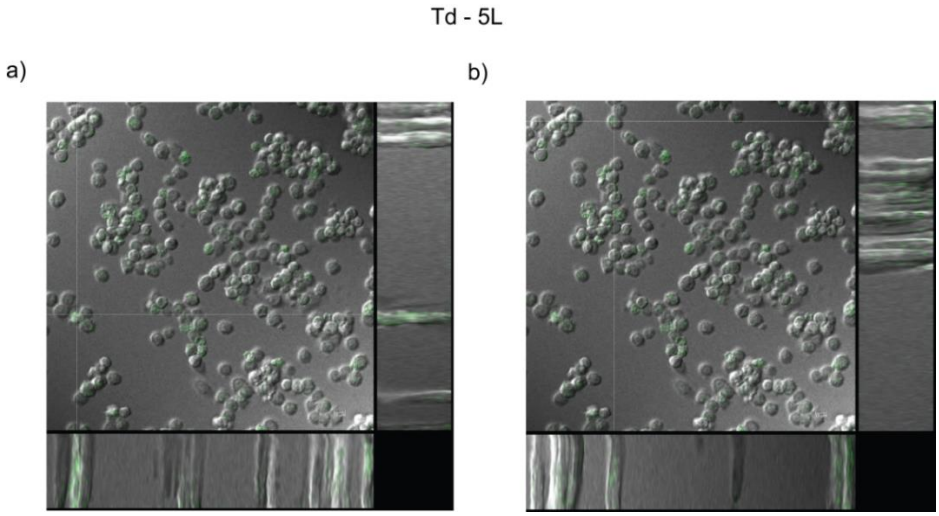

Figure S2.18*:* Z-stacked confocal microscopy images of RAW cells incubated with Alexa fluor488 labeled Td-5L.

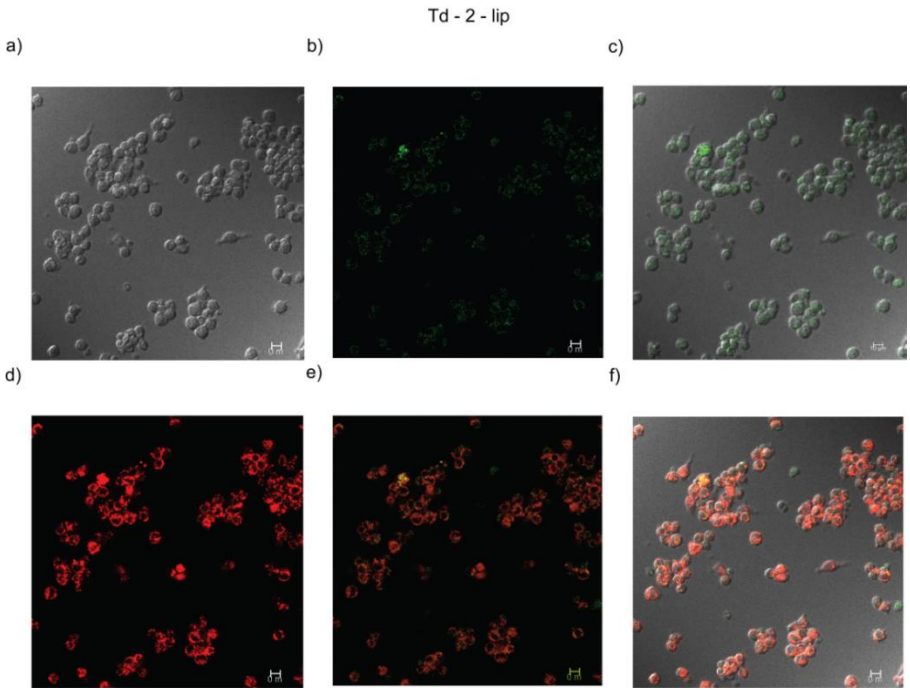

Figure 2.19*:* Confocal microscopy images of RAW cells incubated with Alexa fluor 488 labeled Td-2-lip. The cell membranes were stained with CellTracker CM-Dil dye. A) Bright field image b) green fluorescence from internalized Td-2-lip c) overlay of bright

field and green fluorescence d) red fluorescence from CellTracker CM-Dil dye e) overlay of green and red fluorescence f) overlay of bright field, green and red fluorescence.

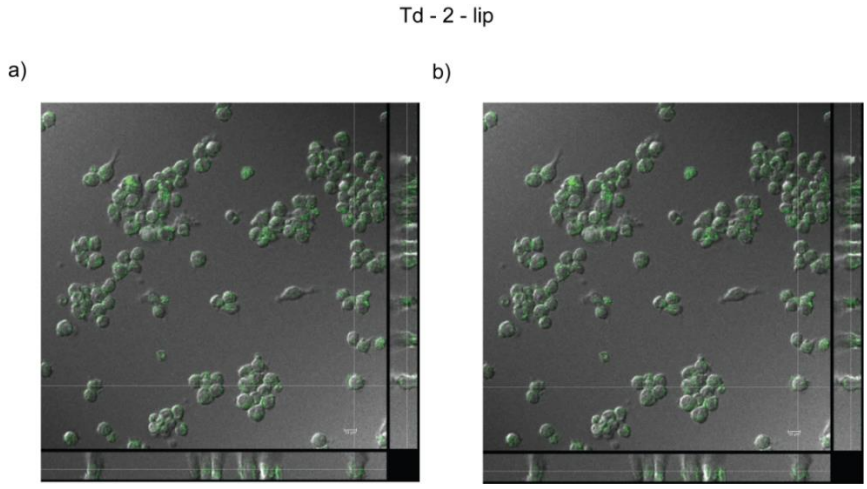

Figure S2.20*:* Z-stacked confocal microscopy images of RAW cells incubated with Alexa fluor 488 labeled Td-2-lip.

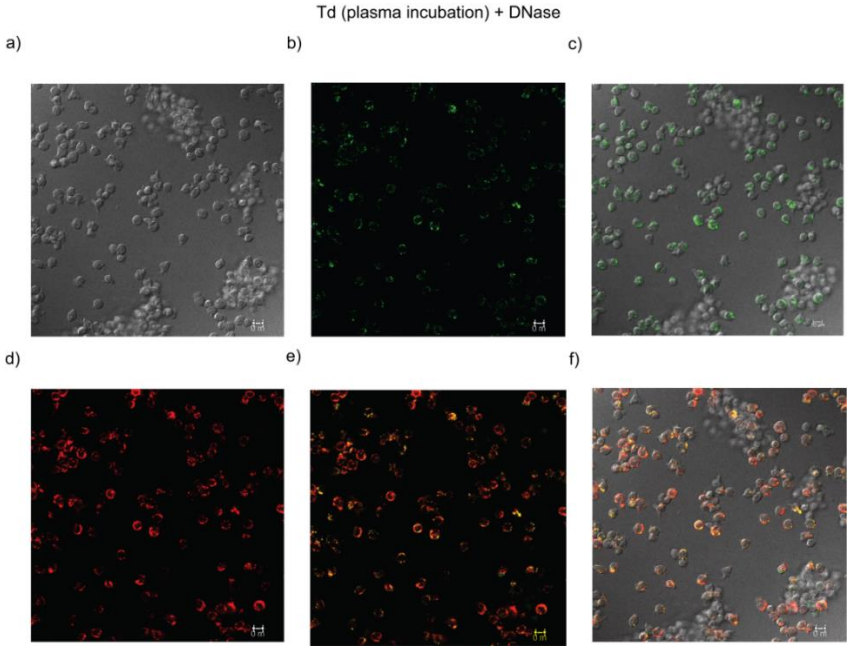

Figure S2.21*:* Confocal microscopy images of RAW cells incubated with Alexa fluor 488 labeled Td that were pre-incubated with mouse plasma followed by DNase treatment. The cell membranes were stained with CellTracker CM-Dil dye. a) Bright field image b) green fluorescence from internalized Td c) overlay of bright field and green fluorescence d) red fluorescence from CellTracker CM-Dil dye e) overlay of green and red fluorescence f) overlay of bright field, green and red fluorescence.

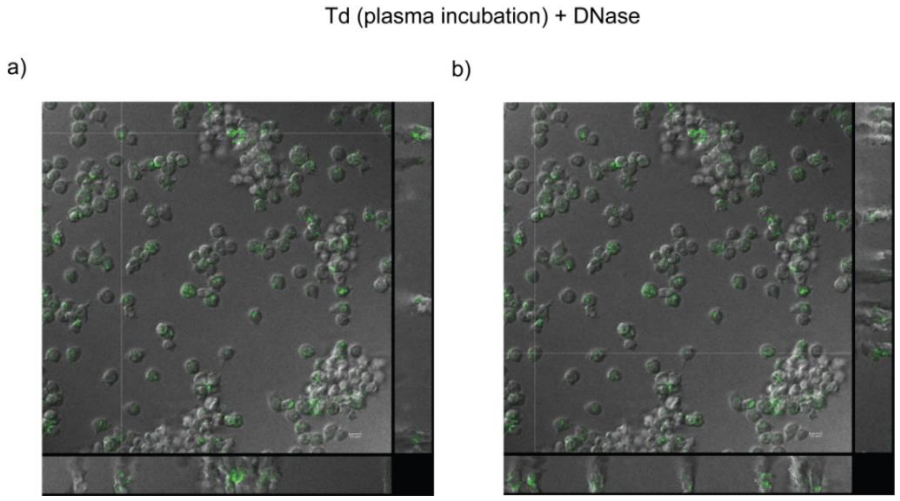

Figure S2.22*:* Z-stacked confocal microscopy images of RAW cells incubated with Alexa fluor 488 labeled Td that were pre-incubated with mouse plasma. The incubated cells were treated with DNase.

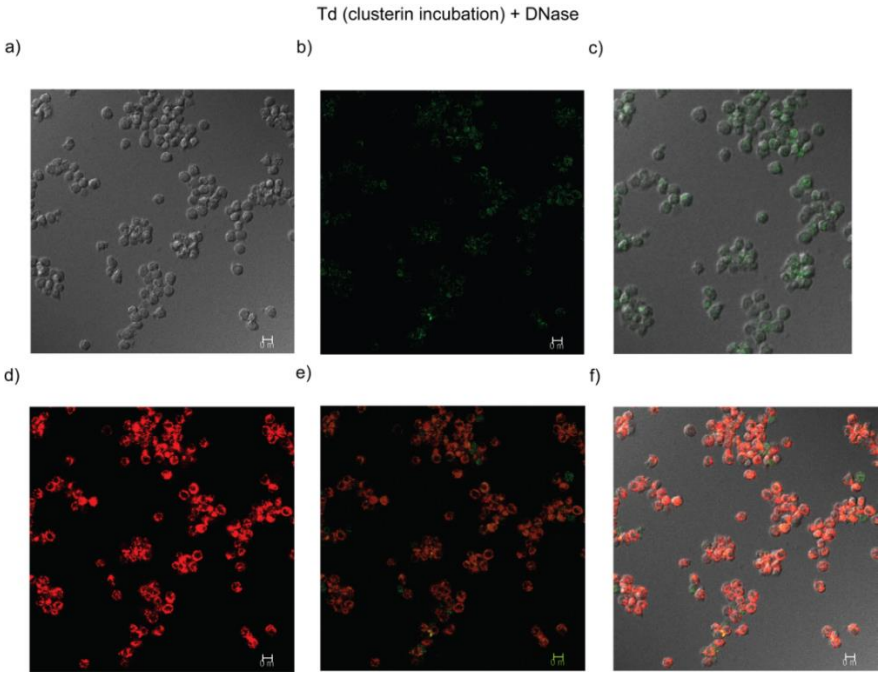

Figure S2.23*:* Confocal microscopy images of RAW cells incubated with Alexa fluor 488 labeled Td that were pre-incubated with clusterin. The incubated cells were treated with DNase. The cell membranes were stained with CellTracker CM-Dil dye. a) Bright field image b) green fluorescence from internalized Td c) overlay of bright field and green fluorescence d) red fluorescence from CellTracker CM-Dil dye e) overlay of green and red fluorescence f) overlay of bright field, green and red fluorescence.

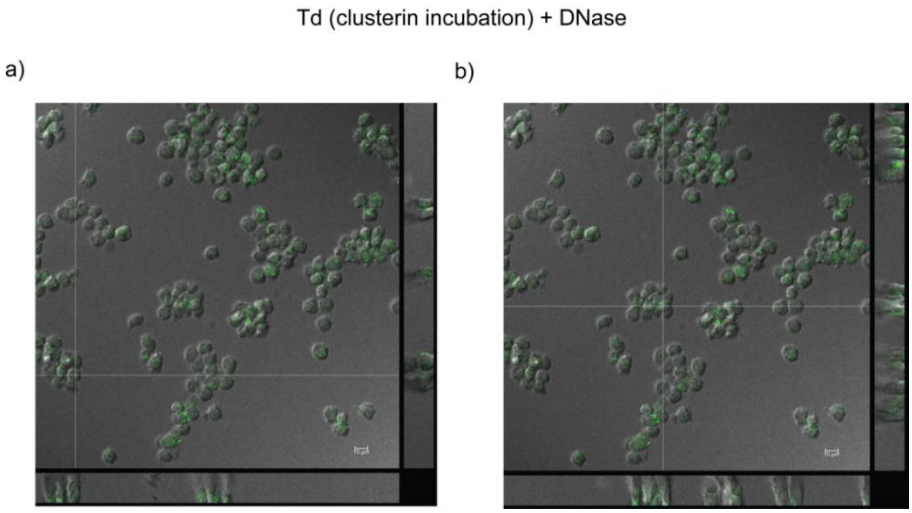

Figure S2.24*:* Z-stacked confocal microscopy images of RAW cells incubated with Alexa fluor 488 labeled Td that were pre-incubated with clusterin. The incubated cells were treated with DNase.

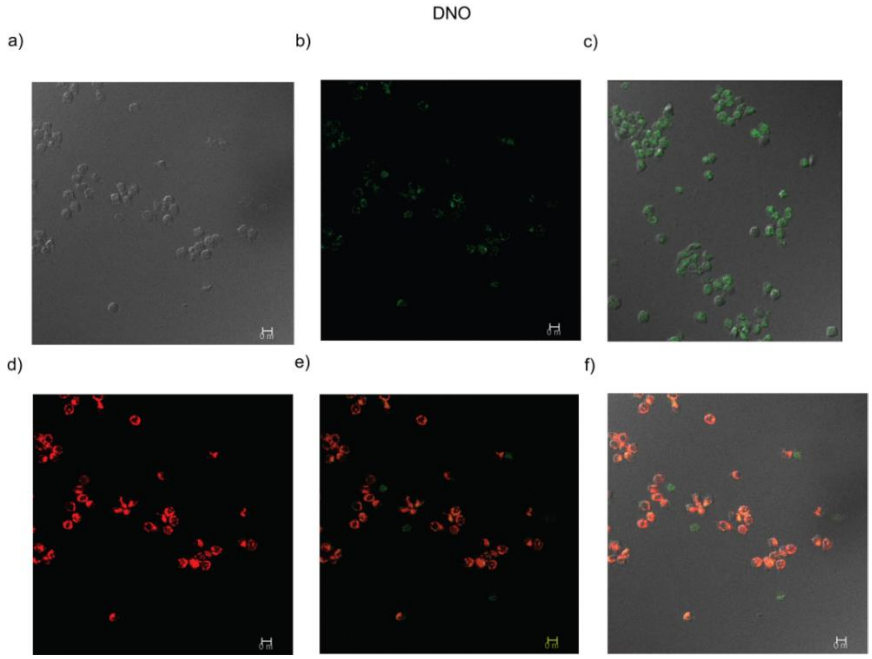

Figure S2.25*:* Confocal microscopy images of RAW cells incubated with Alexa fluor 488 labeled DNO. The cell membranes were stained with CellTracker CM-Dil dye. A) Bright

field image b) green fluorescence from internalized DNO c) overlay of bright field and green fluorescence d) red fluorescence from CellTracker CM-Dil dye e) overlay of green and red fluorescence f) overlay of bright field, green and red fluorescence.

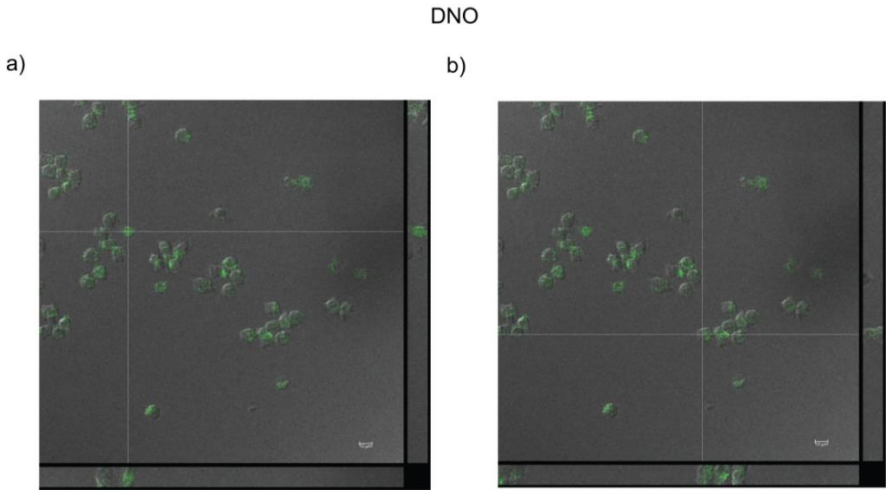

Figure S2.26*:* Z-stacked confocal microscopy images of RAW cells incubated with Alexa fluor 488 labeled DNO.

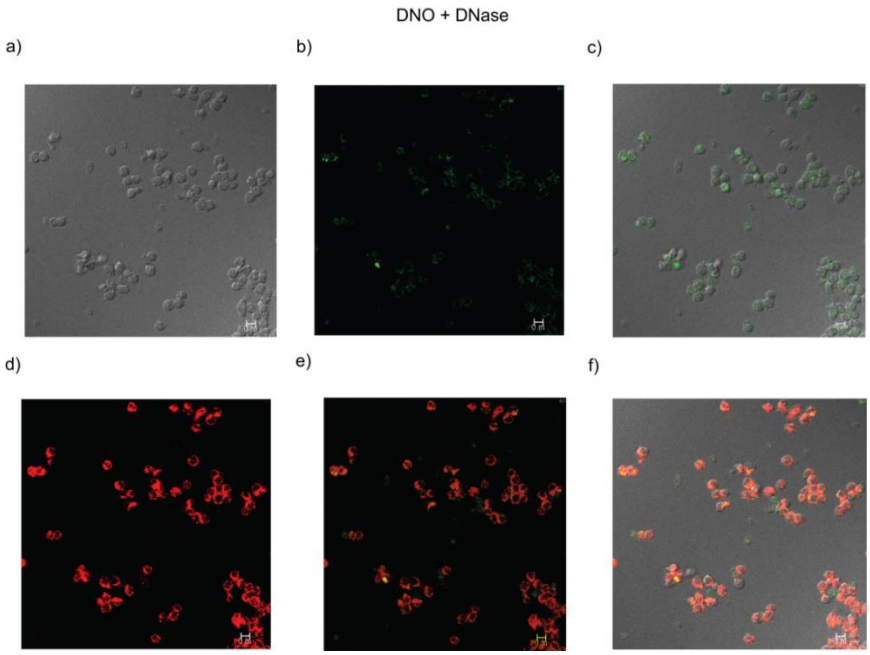

Figure S2.27*:* Confocal microscopy images of RAW cells incubated with Alexa fluor 488 labeled DNO and then treated with DNase. The cell membranes were stained with CellTracker CM-Dil dye. a) Bright field image b) green fluorescence from internalized DNO c) overlay of bright field and green fluorescence d) red fluorescence from CellTracker CM-Dil dye e) overlay of green and red fluorescence f) overlay of bright field, green and red fluorescence.

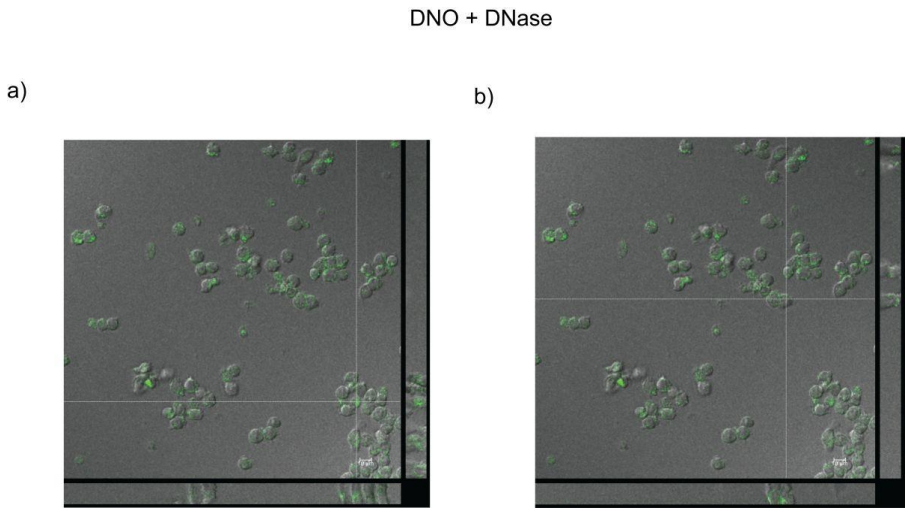

Figure S2.28*:* Z-stacked confocal microscopy images of RAW cells incubated with Alexa fluor488 labeled DNO and then treated with DNase.

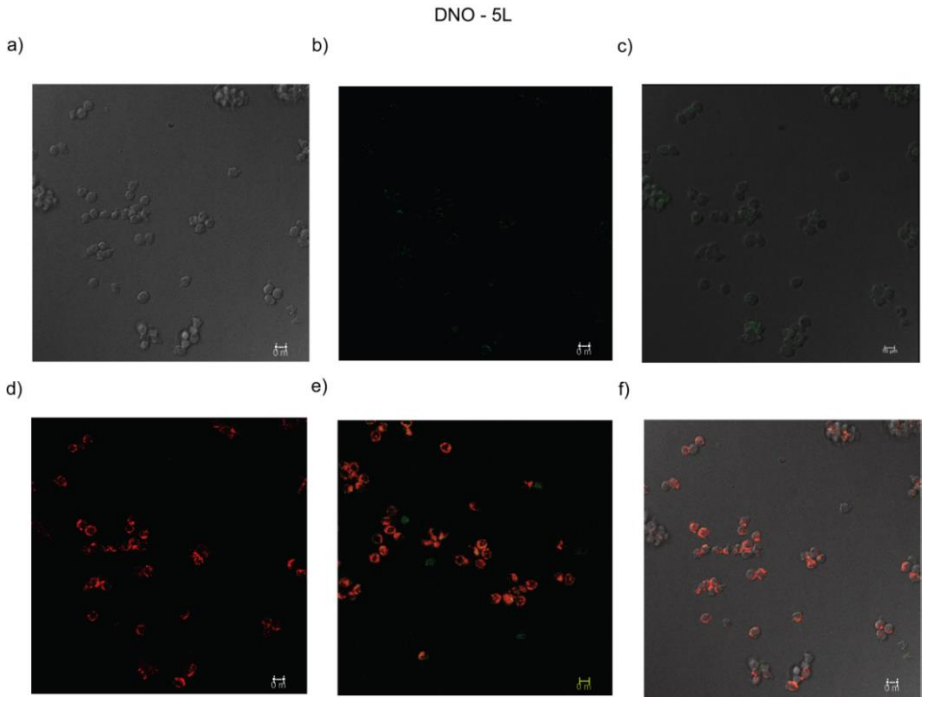

Figure S2.29*:* Confocal microscopy images of RAW cells incubated with Alexa fluor 488 labeled DNO–5L. The cell membranes were stained with CellTracker CM-Dil dye. a) Bright field image b) green fluorescence from internalized DNO–5L c) overlay of bright field and green fluorescence d) red fluorescence from CellTracker CM-Dil dye e) overlay of green and red fluorescence f) overlay of bright field, green and red fluorescence.

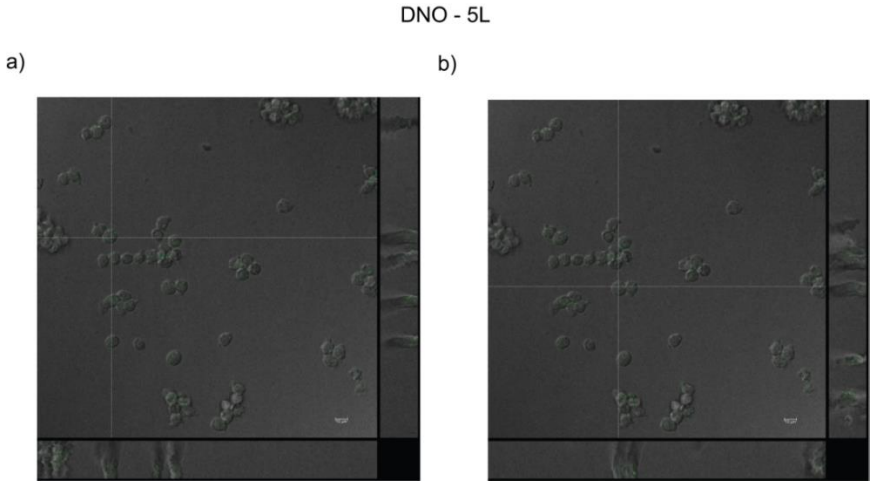

***Figure S2.30**:* Z-stacked confocal microscopy images of RAW cells incubated with Alexa fluor488 labeled DNO-5L and then treated with DNase.

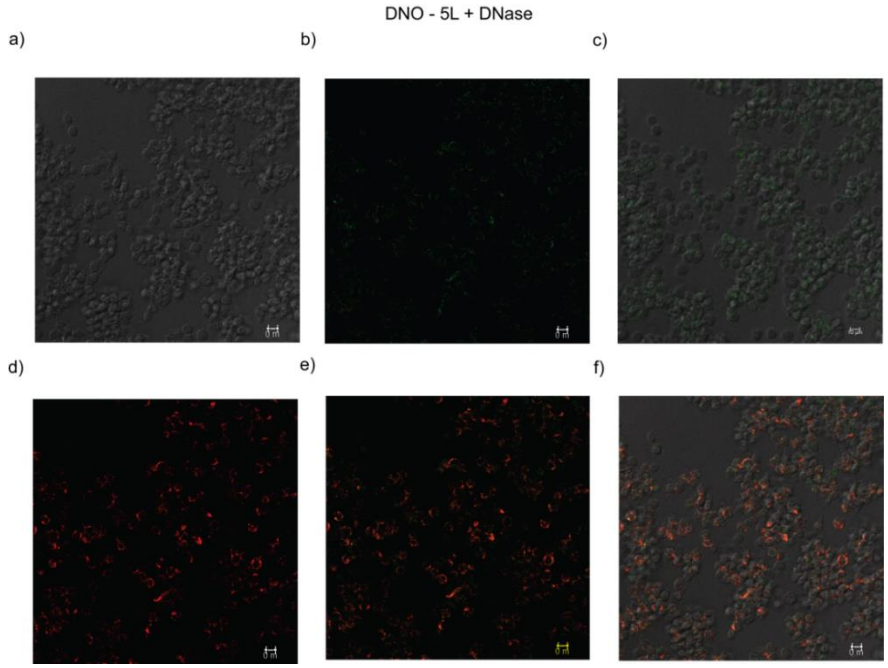

***Figure S2.31**:* Confocal microscopy images of RAW cells incubated with Alexa fluor 488 labeled DNO–5L and then treated with DNase. The cell membranes were stained with CellTracker CM-Dil dye. a) Bright field image b) green fluorescence from internalized DNO–5L c) overlay of bright field and green fluorescence d) red fluorescence from CellTracker CM-Dil dye e) overlay of green and red fluorescence f) overlay of bright field, green and red fluorescence.

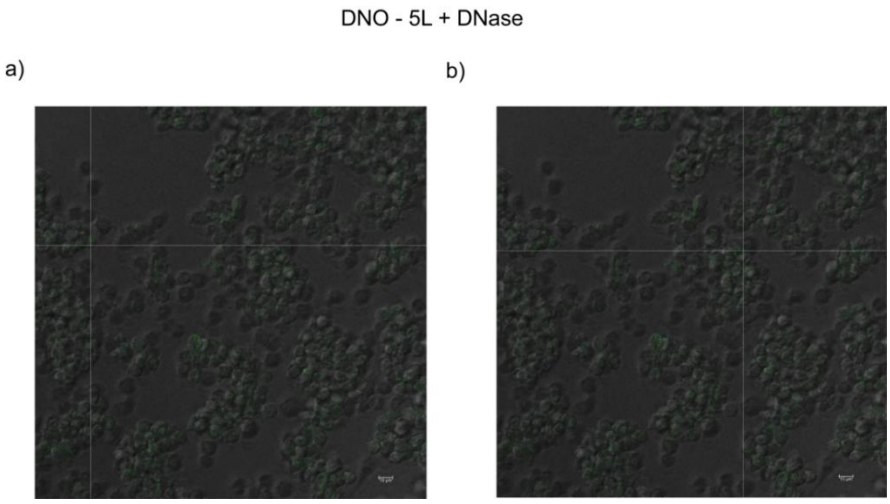

Figure S2.32*:* Z-stacked confocal microscopy images of RAW cells incubated with Alexa fluor488 labeled DNO–5L and then treated with DNase.

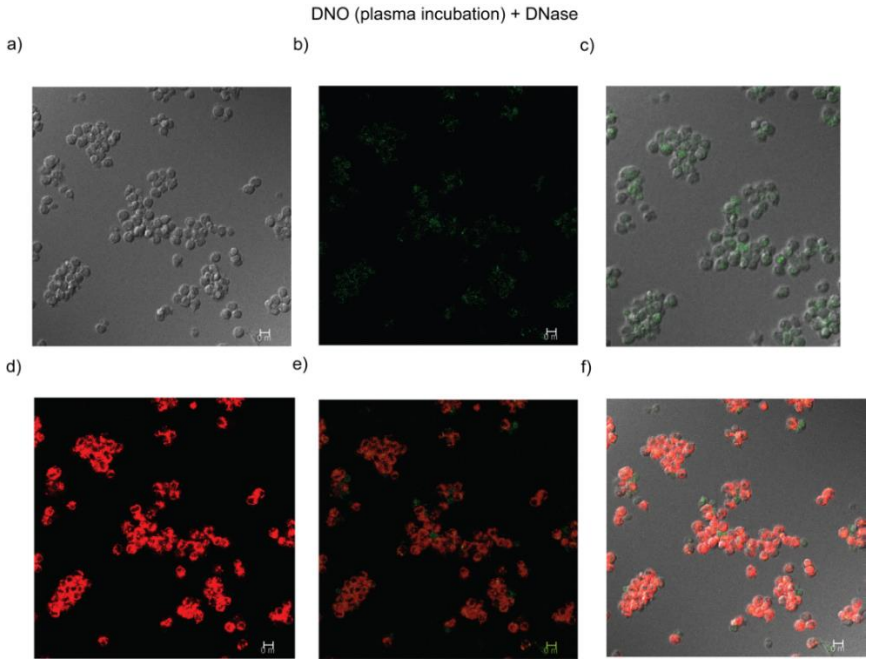

Confocal microscopy images of RAW cells incubated with Alexa fluor 488 labeled DNO that were pre-incubated with mouse plasma. The incubated cells were treated with DNase. The cell membranes were stained with CellTracker CM-Dil dye. a) Bright field image b)

green fluorescence from internalized DNO c) overlay of bright field and green fluorescence d) red fluorescence from CellTracker CM-Dil dye e) overlay of green and red fluorescence f) overlay of bright field, green and red fluorescence.

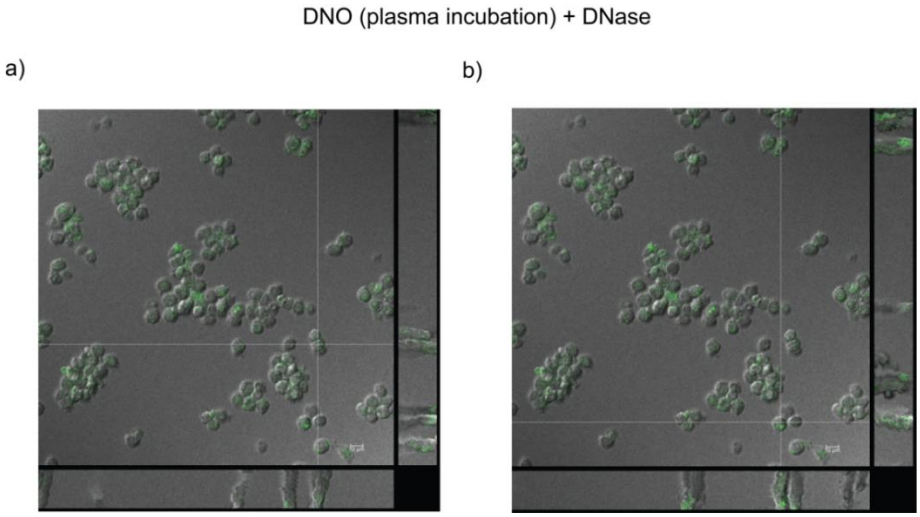

Figure S2.33*:* Z-stacked confocal microscopy images of RAW cells incubated with Alexa fluor488 labeled DNO that were pre-incubated with mouse plasma. The incubated cells were treated with DNase.

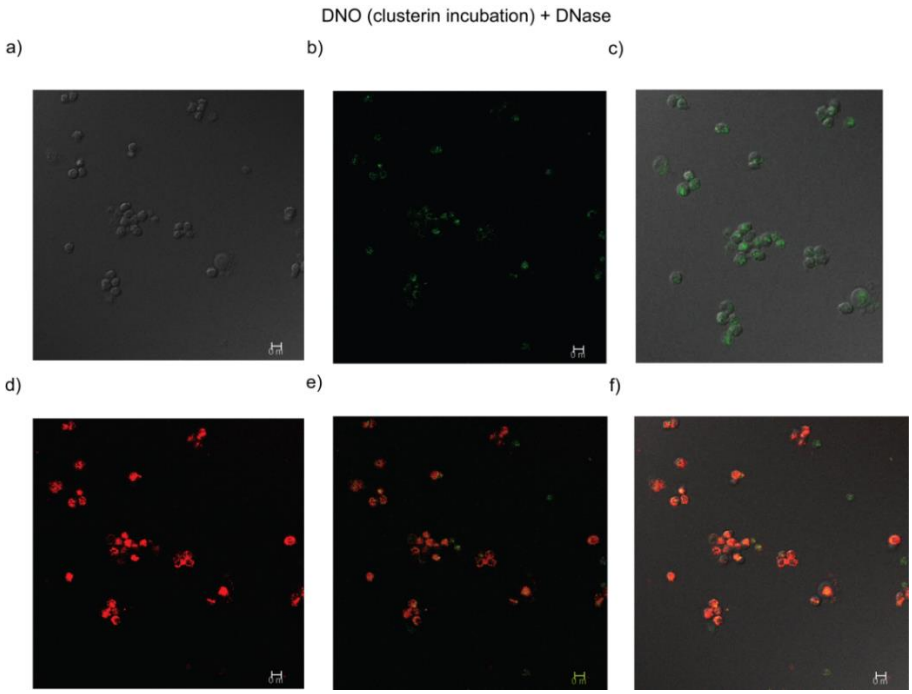

Figure S2.34*:* Confocal microscopy images of RAW cells incubated with Alexa fluor 488 labeled DNO that were pre-incubated with clusterin. The incubated cells were treated with DNase. The cell membranes were stained with CellTracker CM-Dil dye. a) Bright field image b) green fluorescence from internalized DNO c) overlay of bright field and green fluorescence d) red fluorescence from CellTracker CM-Dil dye e) overlay of green and red fluorescence f) overlay of bright field, green and red fluorescence.

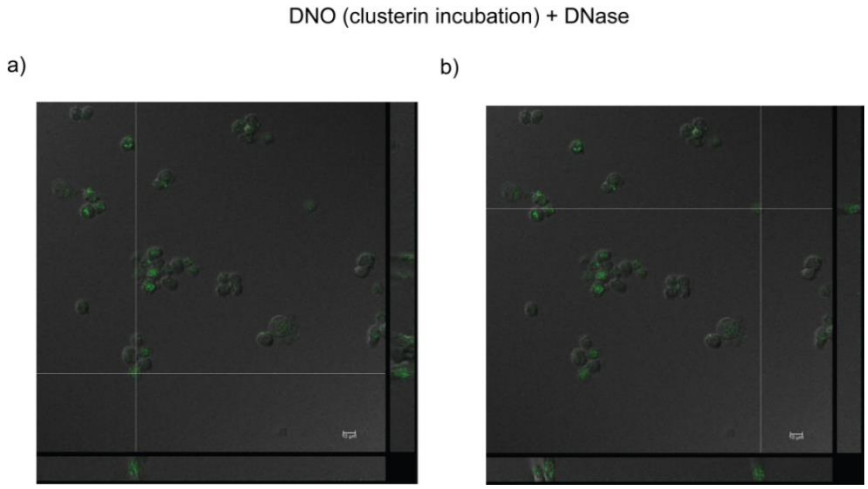

Figure S2.35*:* Z-stacked confocal microscopy images of RAW cells incubated with Alexa fluor488 labeled DNO that were pre-incubated with clusterin. The incubated cells were treated with DNase.

APPENDIX B

SUPPLEMENTAL INFORMATION FOR CHAPTER 3

ENHANCING LOW SALT STABILITY OF DNA NANOSTRUCTURES USING FREE STABILIZING AGENTS

S3.1 Materials and Instruments

L-arginine, L-lysine, poly-arginine, poly-lysine, spremine, netropsin, Hoechst dye and thiazole orange were purchased from Sigma-Aldrich and used without further purification. DAPI, YOYO, SYBR Green were purchased from Invitrogen. Glyoxyl-derived lysine dimer trifluoroacetate salt was purchased from Iris Biotech GmbH. 30 nm AuNPs were purchased from Ted Pella, Inc. and used without any further treatment. M13mp18 single stranded DNA was purchased from New England Biolabs and was used without any further purification. All DNA strands except the m13 scaffold were purchased from Integrated DNA Technologies, Inc. (IDT, www.idtdna.com) in 96-well plate format, suspended in nanopure water (H2O, with resistivity up to 18.2 MΩ·cm) and used without further purification. All solutions were prepared with nanopure water as the solvent.

Buffers: The buffers used in this study are described below –

1. 1X 3D Buffer: 5mM Tris + 1mM EDTA (pH 7.9 at 20 °C) + 16mM $MgCl_2$
2. Physiological buffer: 1.2 mM $MgCl_2$ + 13.6 mM KCl + 136 mM NaCl

Transmission electron microscopy was performed using Philips CM12 instrument. The melting points of DNs were measured using the PCR instrument from Qiagen. Prism 5 software from Graphpad was used for plotting and analyzing the data.

S3.2 DN designs

S3.2.1 DN1

S3.2.1.1 Schematic for DN1

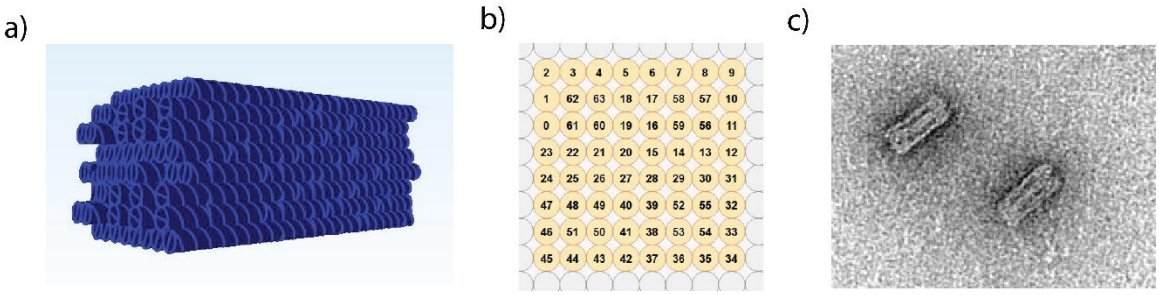

Figure S3.1: DN1. a) Cartoon b) arrangement of double helices constituting DN1 c) TEM image (scale bar = 100 nm).

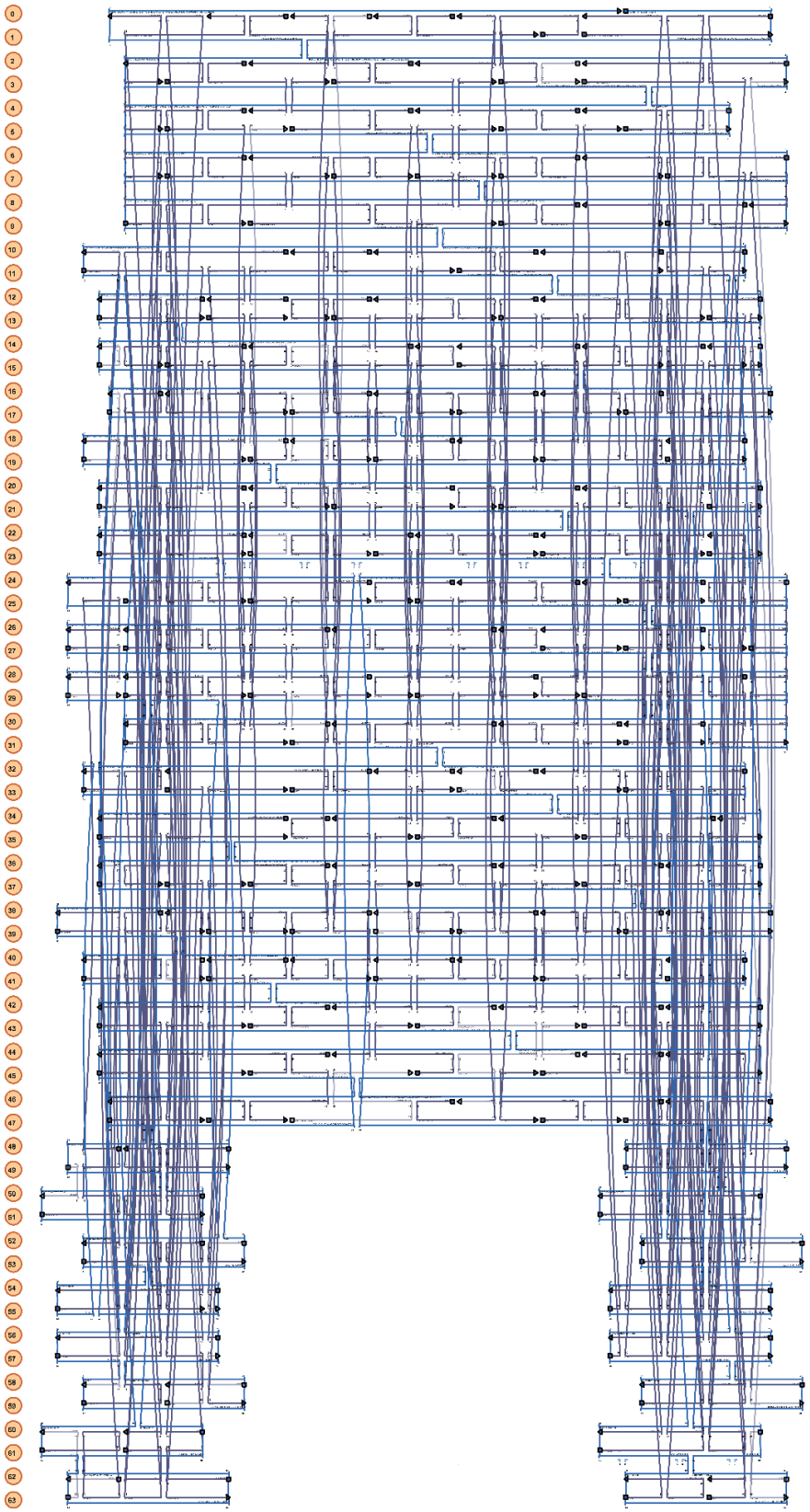

Figure S3.2: caDNAno schematic showing individual strands and scaffold for DN1.

S3.2.1.2 Sequences for DN1

Start	End	Sequence
0[79]	2[72]	TCGAGGTGTAGCCCGAGATAGGGTGAAAATCCTGTTTGAT
33[80]	32[80]	GAAACGCAAGTTTTGC
35[104]	33[111]	TAGAAAGACAAAAGGAATAGTAAG
7[72]	10[64]	TACATTTTCGTCTGAAATGGATTACGTGGCACTTTGAATG
45[40]	43[39]	TTAAAGCCGCATTGACAGGAGGTTCCACCGGA
10[63]	12[64]	GCTATTAGAGGAATTGAGGAAGGTATAATACA
4[39]	19[39]	AGTGTTTTTGTCCATCTCGCCTGATTGCTTTGTTATTCATTTCAATTA
36[55]	40[48]	AAGAACTGGGCGACATCATTACCACACTACGAGAACGAGG
24[127]	47[140]	ATATGCAATACAACGCTGAGAATAGAAAG
23[64]	25[71]	GTATCACCCATTTTCAAAAAAGCC
42[87]	46[80]	CTTTTTCATCAGAGCCACCGGAGTTGCAGACCCTCAGAGCGCTTTCGAAAAAAGGC
44[119]	45[138]	CCGATATAACCGATAGTTGCGCCGACAATGACAAC
36[119]	42[120]	GTAAATTGATTCAGTGAATAAGGCCGAGGGTA
16[119]	5[111]	CCGGTTGAGCCGGAGAGTTCTAGCTGATAAATGGTTTGCG
28[95]	41[95]	AAACCAATCTGGCTGATTGTGTCGATACACTA
34[129]	54[109]	AATGCAGATACATAACGCTTCATCAGAAATCAGGTCT
32[95]	34[88]	GCAAAAGAATAATAACGGAGAGGCATTACATACCCAAAAG
35[72]	33[79]	AAAACGAATGATTAAGAAACCGAG
45[96]	44[104]	TCTTAAACAGCTTGATTTCGGTCG
10[95]	11[119]	CCAGTCACAGGAGCACTAACGACAGTATCGGCCTCAGGAA
2[71]	4[72]	GGTGGTTCACAGGGCGCGTACTATAAGGGATT
12[47]	10[48]	TATTAGACCAAATCAACAGTTGAATCTTTAAT

6[39]	9[39]	AAACTATCCGCCAGCCATTGCAACCACCAGTCACACGACCTAGAACCC
5[48]	3[55]	TAACCGTTGTAGCAATGAACGGTACGCCAGAACGCTTAAT
9[120]	57[140]	GAGGATCCCATAGCTGAGGCAAAGCGCCACAGCTGGC
3[56]	0[64]	GCGCCGCTCGAAATCGTTATAAATCAAAAGAACCGTAAAG
47[48]	45[71]	GGTTTTGCTCAGTATAGCAAGCCCGAGCCTTTAATCAGTCAAGCGTGTATCGGTTT
42[55]	44[56]	AAAATACGCCTCAGAGCCGCCACCACCAGAGC
20[79]	17[79]	AGCCTTTACTGAGTAATATACTTCAAGGCTAT
61[16]	0[32]	ATTAATTAACCTTGCTCGGCGAACGTGGCGAGAAAGGAAGGCCCCCGA
12[63]	30[56]	TTTGAGGATATCCGGTAGACGGGA
52[31]	38[24]	AGAGAGATCTAACGAGCGTCACCA
54[34]	33[47]	CCTAAGAAAAGTAAGCAGA
33[48]	32[24]	TAGCCGAACGACTTGCGGGAGGTTTTGAAGCCTTAAATCA
37[40]	37[23]	GACAAAAGGCTCATTATACATAAGTTTATTTTGTCACAATTTCATATG
50[138]	41[135]	GGATTTTGTAACAAGCGCG
23[40]	22[40]	ATATAAGTATCCAATC
20[39]	29[39]	AGAAGATGGCGGAACAAAGTACCGAATCCTAA
45[72]	43[71]	ATCAGCTTCGCCACCAGAACCACCCTCAGAAC
24[63]	25[39]	GGGACCAGGCGGATAAGTGCCGTCGAGAGCTTATAAGAAT
59[24]	16[24]	TGCAACAGTTGCACGT
52[146]	13[138]	AAGACTTCAAACAGACCGGTGAATCCCATG
42[119]	50[107]	GCAACGGCGGGATCGTAGTTTTGTCGTCT
47[112]	24[104]	GTACAAACCTAAAGTACGGCCACC
1[96]	23[95]	GTTCCAGTTCACCCAAATCAAGTTGTACCGCC
43[104]	39[111]	GCTTTTGCTACAGAGGATCTTTGAACCGTCACAAGAGTAA
32[135]	36[120]	TACCAGACGACGATAATATCATAATAAATCAATTGAGATTAACGAGTA
11[80]	9[87]	ATATCTTTGACGTTGTAAAATATTAGACAACGACGGCCAG
55[109]	31[111]	TTAATAGCGAGGGATAGCG

21[128]	27[135]	AAGCCTCAATTTTTGCAATTGCTC
4[103]	16[96]	GGGAGCTAGGAGAGGCTAATGCCGAGTCTGGACAATATAA
12[95]	30[88]	CTAATAGAGTAAAATGGAGAGAAT
7[56]	19[63]	CGCTCATGTCACTTGCACAGTAACACATCGGGATTTTAAA
37[104]	35[103]	AAAGGTGAGGCTTGAGATGGTTTAATTACAGG
5[112]	62[112]	TATTGGGCGCCAGGGTTTCACCAGTCTACTAAAGGAGCTGAAAAGGTG
31[112]	56[109]	TCCAATACTCTGCCAGATGGGATAACCGCTTCTGG
9[40]	7[55]	TTCTGACCTGAAAGCGTAAGAATATTTACATTGGCAGATTAGGAAAAA
0[47]	2[40]	TAAAGGGAGGAAGAAAGCGATCCCGCAAAAAAGGAGCGGG
58[146]	8[136]	CTTCGCTATTAAGTGAGCTAATTCGTA
7[24]	59[39]	AATATTACGGCCTTGCGTAGATTTTCAGGTTTAAAATTATTGCCACGC
36[138]	53[146]	AGAAGGAAGCCCGA
46[79]	24[80]	TCCAAAAGAATAGGAACCCATGTATCAGAGCC
17[48]	6[40]	ATGAATATCTGAGTAGAAGAACTC
42[138]	37[138]	CAGCATCGGAATTGCCCTGACG
24[103]	25[111]	CTCAGAACAAATTCTTACCAGTAT
31[48]	13[55]	AGAAGGCTTTTAGAAGATTAAATG
24[79]	22[72]	ACCACCCTGTACTCAGGGTTATAT
9[88]	7[87]	TGCCAAGCCTCACAATTCCTCAATGACGCACA
46[119]	47[111]	ATAATAATTTTTTCACCGTCACCA
2[39]	4[40]	CGCTAGGGACCACCACACCCGCCGTCCTGAGA
54[140]	34[130]	GATTGCATCAAAACCCTCGTTTCAACT
7[88]	19[95]	CAACATACACCTGTCGTGCCTGAGGAGAGGGTTAAAGATT
33[112]	30[112]	AGCAACACAAACCAAACCCTGACTCAGATGAA
32[79]	13[87]	CAGGAGGCAACGCAGGGGGTAATATTAGAGCCTCTCCGTG
56[34]	12[32]	GAATCAGTTGGTTTACAAA
43[40]	39[47]	ACCGCCTCTAACCCCTATAGCTGCTTAGCAAGCAACTTTG

3[88]	1[95]	TGACGAGCCAGCAGGCTGAGTGTT
20[103]	29[103]	ACCCTGTACAATTCATGCATGTAGATTTTTTG
10[47]	13[31]	GCGCGAACTGATAGCCCTAAAACAATATCTGGCCTCAAATACGCTGTA
28[63]	41[63]	CATTCCAACAGATGAACTTAGCCGAGGCACCA
16[23]	3[23]	AAAACAGAGAGGCGAAAATACCAAAAACAGTAGTGAGGCCGGTCACGC
32[63]	34[56]	GAACCTCCCAAAGTTACCAGAAGGACTCCTTATTACGCAG
27[96]	38[96]	AACAAGAACTGATAAACCTTCATCCGACTTGA
8[103]	9[119]	GTTATCCGTTGCATGCCTGCAGGTCGACTCTA
44[55]	47[47]	CGCCGCCAAGAATGGATCTGAATTTACCGTTCATTAGCGG
34[55]	36[56]	TATGTTAGTTGGGAAGAAAAATCTGCGATTTT
44[103]	43[103]	CTGAGGCTTAAAGGCC
47[96]	45[95]	CTGAGTTTGTTGAAAATCTCCAAAGGTGAATT
2[103]	3[103]	GTTTGCCCACGTATAA
27[112]	60[107]	TCCCAAGATACCAAAATTCGCAAACCTGTTTAGCTAT
36[87]	40[80]	TTTAATCAAAATATTGGGAATTAGGCAAAAGAAAATCCGC
33[24]	35[47]	CCCTTTTTGAATCTTAAAGACACCACGGACAGTCAGGACG
34[87]	36[88]	AACTGGCACTAACGGAACAACATTATTTCAAC
18[47]	5[47]	TAACGGATACGCAAAT
0[63]	23[63]	CACTAAATGAATAGGT
23[96]	22[96]	ACCCTCAGAACCGTGTTTAGTTTGACCTTTAA
6[143]	58[115]	AACTCACATTAATTGCGCCTAATGCGCTTCGCCATTCAGGCTGCG
4[71]	16[64]	TTAGACAGACTTCTTTTCTCTTTTAGTACACATGAATAAT
23[128]	49[143]	ATATAACATGTTTTAATGAATATACAGCGGAGGCGCTAAACAACTTTC
5[24]	63[36]	AAAGAGTCTATAATCACATAAATCAATAT
37[72]	35[71]	GGGAAGGTTTGTGAATTACCTTATACGTTAAT
28[135]	55[140]	TCCAACAGAAGCGAACTATCGCGTCAGAAGCAAAGCG
12[31]	55[31]	CAATTCGACCCAATAGAGTCAGAGTACAATTT

3[104]	2[104]	CGTGCTTTCCTCGGACGGGCAACAAGTTGCAGCAAGCGGTCCACGCTG
43[72]	39[79]	CGCCACCCTGAGGAAGCGAAAGAGAGCCAGCAAGACCAGG
5[88]	3[87]	ACGCGCGGAACAGGAGGCCGATTAGGTTGCTT
6[103]	7[119]	GTCGGGAAGAGCCGGAAGCATAAAGTGTAAAG
1[104]	1[140]	TTGGAACAAGAGTCCACTATTAAAGAACGTGGACTCC
27[136]	15[138]	CTTTTGATAAGCAAACAAT
25[16]	22[11]	ATAAATAAGAGAAAACTTTTT
48[15]	26[5]	ACTGGTAAACCGTGTGAGTACCGACAA
37[24]	42[11]	GTTTACCATTTGCCATCTTTTCATAATCA
62[15]	62[5]	TCTGTAAAACC
27[16]	20[11]	ATTCTGTCAACATCAAGAAAA
3[24]	2[16]	TGCGCGTACGCTGGCAAGTGTAGC
50[31]	44[11]	TTATTCTGCAGAGCCAGAGGCAGGTCAGACGATTGGC
63[128]	19[135]	TAGTAGTAAAAATTAATCACCATC
46[140]	43[138]	GAACAACTAAAGGTTTTCTGTCATCGCCCGCAGCGAAAGA
37[11]	36[11]	GAAAACAATA
9[16]	58[24]	TTCTGGCCAACAGAGAAGTAATAAATCACCTTAGCAGCAA
12[138]	31[127]	GGCGCATCGTAACCGTGCATGCGGAAT
43[11]	48[16]	AAATCACCGGAACCTTGAGTACCTATTTCACTAGTGT
31[16]	12[11]	TTACCGCGCAACTCGTATTAA
2[143]	62[128]	CGCCTGGCCCTGAGAGGCTGATTGAATCATAC
7[120]	18[120]	CCTGGGGTGTTGCGCTATGAACGGATTCAACC
10[119]	8[104]	AAGTTGGGCGGAAACCTTTCCTGTGTGAAATT
57[3]	10[8]	ATAAAACAGAGGTAAAAATAC
27[5]	28[5]	AAGGTAAAGTAGCAAGCCGTTT
24[143]	23[138]	GCTCAACAGTT
51[0]	40[8]	CAGTTAATGCCCCCTGACAGTGCCTTAACGGGAGCGTCAG

14[138]	59[146]	ATTGGTGCGGGCCT
61[0]	18[8]	TTTGAATTTCGTCGCTACATTTAATTTAATGGGTTACAAA
41[8]	38[3]	ACTGTAGCATCGATAGCAGCA
19[8]	16[13]	ATCGCGCAAAT
56[140]	11[135]	GAAAGGGGCCAGCTCCAGGAT
35[11]	54[3]	TAAAAGAAACGCACCAATAAGAGCAAGAAACAAT
17[13]	58[8]	AAAGAGGCGGT
4[132]	5[132]	TTCTTGGTTT
13[11]	56[3]	ATCCTTTGCCCGAATCAAACCCCACCAGCAGAAG
47[13]	24[5]	GATACAGGCCTAATTTAATGGTTTGAAATA
62[143]	3[143]	ATCCAATACCCTTCAC
55[3]	32[8]	GAAATAGCTTTTGTGCTAAAT
40[135]	39[140]	AAACAAAGATATTCATTACCC
48[143]	21[138]	AACAGTTTATGCTGTAAAGAGGTCGAG
18[135]	17[140]	AATATGATTAATCGTAAAACT
60[138]	63[143]	AGCGCATTAAC
49[5]	50[0]	GTTCGTATAAA
15[11]	14[11]	TTTGAAAAAG
38[140]	35[138]	AAATCAACGTAACAGATTAAGAACACCAGTAGGAATACCA
39[3]	52[8]	CCGTAATCAGTAGAGAATTGA
63[5]	60[0]	TTTCAATTTCA
23[11]	0[13]	CAAATATATTTTATTGACGGGGAA
38[95]	42[88]	GCCATTTGACGGAAATACTAAAGA
15[24]	49[36]	ATCATTTTATGAAACACAGACGACTAATAAGAAAACATGAAAGTA
38[23]	26[16]	ATGAAACCGCGTTTTCTTGCCTTTGTCAGTGCGAATATAA
38[63]	42[56]	AGTAGCACTCAACCGAAAACGGGT
19[40]	17[47]	CCTGAAACACCATATCAACGTCAG

41[120]	44[120]	GATTATACCGATCTAACACCCTCAACGCATAA
22[95]	47[95]	CCTCCGGCCGTTATACCGCCACCCCCGTAACA
19[96]	17[111]	CAAAAGGGTGAGAAAGTAATCAGAGCAAACAA
16[95]	26[88]	TCCTGATTGATGATGGATACTTTTAAGTCCTGAATTGAGA
51[107]	48[112]	TTCCAGACGTTAGTTCCACAG
29[104]	15[119]	TTTAACGTCAAAATTCATATTTTGAAAAACAG
17[112]	6[104]	GAGAATCGCACTGCCCGCTTTCCA
21[56]	25[63]	GTCAATAGGTAAATGCATTACTAG
16[63]	26[56]	GGAAGGGTGAGCGGAACAAGGATAATGCAGAAATGTAATT
30[55]	14[48]	GAATTAACTTACAAAACCATCAAA
14[71]	32[64]	TTAACCAATAACAACCAGCGCATTATTCTAAGGTTTTAGC
40[31]	41[31]	TAAGGAGTATCGGCAT
13[56]	29[63]	TGAGCGAGTAGGAACGTAAACAGC
39[32]	53[39]	GAACTGACGCCGGAAACGTCTTTC
57[109]	10[96]	TGCTAACGCCAGGGTTTTC
25[112]	0[104]	AAAGCAGCGAGTAGATCTGGAAGTGTCTATCAGTGAACCA
18[79]	7[71]	TTGAGAGAGATAATGAGCATTTAGTAATAACAGAAATACC
26[55]	0[48]	TAGGCAGAGAATCATATGATGCAAATAGCCCGCGGAACCC
59[115]	27[127]	CAACTGTTGGGAATATGTACCGAAGATTGATCGGTTGGTACCTTT
39[80]	21[87]	CGCATAGGCAATAATCCAATAGATGCGGGAGAATAGGTCT
19[120]	25[127]	CAGTCAAAGCAAATAATGGTCATACTGCGAACTTAATTGC
13[88]	29[95]	GGAACAAAATTTTTGTAAGAAACG
29[40]	13[47]	TTTGCCAGTGAACACCTCATCAAC
39[48]	21[55]	AAAGAGGAGAACGGGTTTCAGCTAAAAATTTTTGAGAAGA
41[32]	37[39]	TTTCGGTCTATTAGCGGCGCCAAA
53[115]	38[120]	ACGAGAATGACCAAAAGCTGC
48[36]	51[31]	TTAAGAGGCTGAGGGAACCTA

41[96]	37[103]	AAACACTCCTTTGAGGTATTCATT
15[80]	18[80]	GATTATCAGTTTGGATTGTGTAGGAGCTATTT
49[112]	20[104]	ACAGCCCTTAGCAACGCTCAACAGAGATACATACATTATG
58[39]	57[34]	TGAGAGCCGCT
39[112]	14[104]	TCTTGACATAGTCCTAATTTACGAAAAGCCCCTTAAAATT
40[79]	14[72]	GACCTGCTTTTATCAAGGCTGTCTATATTCCTCTCATTTT
13[32]	31[47]	GCCAGCTTCTGAACAACAAGCAAATCAGATAT
26[127]	46[120]	GGATGGCTCATAGTTACTGTAGCATAAATGAAAATTGCGA
60[31]	40[32]	TTAGAATCTAGCGATAGCTTAGATCGAGCCAGGACAATAAGTCAATCA
30[111]	12[96]	AATAGCAGTGACCGTATTTGAGGGGACGACAA
14[103]	32[96]	CGCATTAACGGCGGATCCTTTACATTTAGACTAGGCTTTT
40[47]	14[40]	CGCAGACGACAACATGATTAAACCAAGAAACCAATAATTC
13[128]	31[143]	TGGTGTAGCCTCAAATCGTCATAAATATTCAT
25[40]	20[40]	AAACACCGGGCATTTTTAAGACGCTAGGCAAA
41[64]	37[71]	ACCTAAAATTTCCATTTTGAGGGA
52[39]	55[34]	CAGAGATCTAT
62[36]	23[39]	ATGTGAGTGAATAATTTTCCCTTTAGAGCGTTAATTTCATGGTTG
29[16]	15[23]	GTAGGAATTTAATTTTGTAACATT
61[107]	23[127]	ATTTTCATTTGGGGCGCGCAAGAAAAACCTTCATTCC
21[88]	26[96]	GAGAGACTACCTTATTTAGGGCTT
22[71]	40[64]	AACTATATTGAATTTAACGCCAACCGCGCCTGCCATGTTA
30[127]	52[115]	GCTTTAAAATTATAGTTTTAATTCAGAAA
14[39]	39[31]	GCGTCTGGCCTTCTTATGAGCGCTCACTCATCTCAGAACC
19[64]	29[71]	TGCAATGCTTTCAACGTTATCATCTTCCTTATCATATTAT
38[119]	27[111]	TCATTATCCCCCCAGCAGATTTGTATCATCGCAAATAATA
26[87]	0[80]	ATCGCCATATCATATGTTAGGTTGGAGGTTTATTTTGGGG
29[72]	11[79]	TTATCCCAAACAGGGACGTCGGATGTCAATAGTATCTAAA

15[48]	18[48]	ACCAGAAGTAGAACCTCCTCATATAGAAACAA
17[80]	5[87]	CAGGTCATTGCCAGCTATCGGCCA
30[87]	14[80]	AACATAAAATCCAAATTAAATCAG
25[72]	21[79]	TGTTTAGTATTTAACATCAAAATC
39[64]	38[64]	CGGTGTACAAATCACC
22[39]	47[31]	GCAAGACAAAGAACGCGGCGTTAACTGACCTACAAGAGAA
14[127]	40[120]	AAACGTTAGAGCTTCAGTCAGGATAGAACCGGTACAACGG
63[112]	4[104]	GCATCAATTGATTAGAATCAGAGC
0[140]	22[128]	AACGTCAAAGGGCGGCAAAGATCCCAATT
29[5]	29[15]	TTATTTTCATC
33[8]	30[16]	AGCTATCTTACCGAAGAGATTAGTCACCCAGCGGTAATCA
10[135]	13[127]	GTGCTGCAAGGCGATTGATCGCACTTTCCGGCGGTCACGT
21[11]	60[16]	CAAAATTAAAACACTTGAATT
53[8]	28[16]	GTTAAGCCCAATAACGAACCCACACGACAGAAGAGAACAA
16[140]	14[128]	AGCATGTCAATCAGGGCGATCTAAATTGT
11[8]	7[23]	CGAACGAACTCAATCATCGCCATTTCTAAAGCAAGGGACATCCAGAAC
45[11]	45[39]	CTTGATATTCACAAACAAATAAATCCTCA
59[8]	5[23]	CAGTATTAACACCGCCATGAAAAAGAAATTGCTGGTAATAACCGAGTA
20[138]	15[135]	CATAAAGCTAATATAAGCA
47[32]	46[13]	GGATTAGGCAGTAAGCGTCATACATGGCTTTTGAT
8[135]	9[143]	ATCATGGTCCGGGTACCGAGCTCG
34[47]	34[11]	CAAACGTAGAAAATACATACATAAAGGTGGCAACATA

4 spacer Ts were added to all the strand termini (5’ or 3’ or both) that end at the edges of DN1.

S3.2.2 DN2

S3.2.2.1 Schematic for DN2

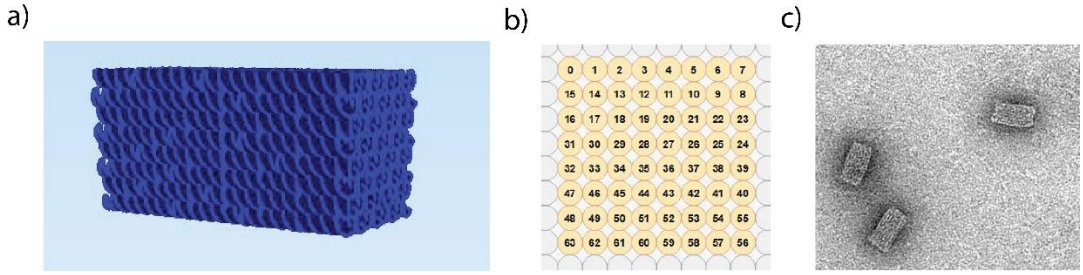

Figure S3.3: DN2. a) Cartoon b) arrangement of double helices constituting DNO c) TEM image (scale bar = 50 nm).

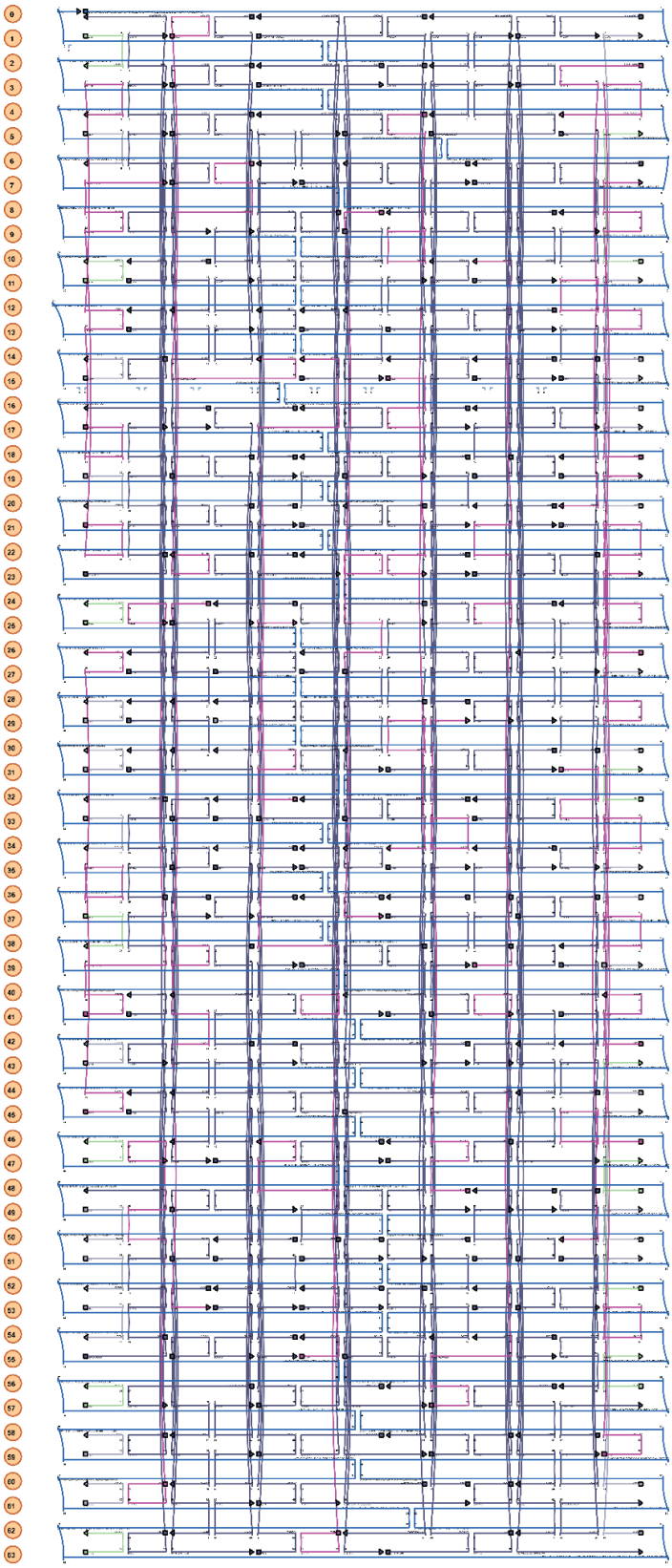

Figure S3.4: caDNAno schematic showing individual strands and scaffold for DN2.

S3.2.2.2 Sequences for DN2

Start	End	Sequence
16[111]	15[111]	CATATGTATTTTAACC
20[111]	11[111]	TAAAAATTAGCGCCAT
13[16]	1[23]	AGAGATAGTAGAGCTTATCAAGTT
38[39]	40[24]	GACCGTGTTGTTTAGTAAAGCCAACGCTCAAC
50[63]	61[79]	GAGCGTCTGCAAGGCCGGAAACTCAGAGCCGC
11[16]	3[23]	ATTTTGACGCGCGTAAGAGAAAGG
58[63]	52[48]	TGCCTAACGCAAAGACGAGGGAGGCATAAAAA
44[103]	53[103]	AGCATCGGAAAATACGAACCCATGACCCTCAT
50[79]	35[79]	ATTTTCTGGCTTGCAGGCTACAGAGCTCATTA
59[8]	58[8]	TTACCAGCTAGAAAAT
29[16]	17[23]	TTACAAAAACCTCAAACCGCCTGC
60[87]	49[87]	CCTTGATACACCAGAAGTAAATGACAACAGTT
3[88]	13[95]	GGGTGGTTCACCGCCTGATTGACC
29[8]	28[8]	ATACCAAGTCGCCTGA
35[64]	51[63]	AAGAACTGGGCTTTGAGGACTTCCTTTACAGA
60[79]	43[79]	TTCACAAAGCCTGTAGTTCGTCACTGAGGAAG
60[71]	61[55]	CAAATAAATCCTCGGTAAATATTGTACCATTA
28[71]	36[64]	GAGCTTCAGTCAGGATTAATCATT
62[111]	49[111]	CAGAGCCGAGAAAGGA
51[8]	52[8]	AAATAAGAAACACCCT
20[39]	25[39]	ATCTTTAGAAGTATTACAAAATTATGGAAGGG
48[103]	61[111]	GAATAATAGTGAGAATCCACCCTCAGAGCCGCCGCCAGCA

15[80]	0[72]	AAATTTTTAGTGTTGTTCCAGTTT
2[71]	11[71]	CAGCAAGCAGGCGGTTGACGACGACAGCTTTC
53[8]	54[8]	CAGAGGGTAAGCCCTT
46[63]	63[63]	ATATACACACGCTAACGCTCCAAAAGCGTTTG
50[111]	45[111]	GTTTTGTCATCGTCAC
32[23]	32[8]	ACCTTGCTTCTGTAAA
33[40]	16[48]	ATAGCGATAGCTTTACGAGAATGATAATGGAACAAATATT
7[48]	6[56]	CTGTCCATAGCTCGAAGCGGGAGC
32[79]	17[79]	ACCAAAATGAGGGGGTAATGCTTTAGCAAACA
56[39]	57[23]	CCCAAAAGAACTGGCATGATTAAGAAACGTAG
22[23]	10[16]	CGAACGTTACATTTGATGCAACAG
42[47]	26[48]	TAAAGTACACCTAAATTTAATTACCAACTAAA
51[80]	34[80]	CATTCCACTAGCAACGGGAGTTAAACAGGTAG
19[80]	1[87]	GACAGTCATCTGCCAGAAACGGCGGGCCCTGATTGATGGT
3[24]	17[31]	AAGGGAAGCCCCGATTAACCCTTCCAATATTTAACAGTGC
55[24]	58[24]	AACAAAGTAATAGCTAAAAATACAATTTTGTC
42[39]	55[39]	CGACAAAATTAGGCAGGAAATAGCTACCAGAA
30[111]	17[111]	AATCGTCAAAAACTAG
41[64]	56[64]	AGCGATTACAGAACCGTCAGTACCGGATTAGG
36[103]	42[96]	AAATTGGGCTTGCCCTTAAAACGA
5[8]	6[8]	CTTAATGCTACGCCAG
19[56]	30[56]	TTCAAAAGAGGCTATCCAAAAATCCAGAAAAC
43[8]	42[8]	ACAACATGCCAGACGA
15[8]	14[8]	GCGAACTGCTATTAGT
62[23]	48[8]	CAGAATCAGCGCGTTTGAGGTTTTGAAGCCTT
30[103]	35[103]	TAAATATTAAAGCGGAACGGAACAGGGAAGAA
16[79]	2[72]	CCAAAAACTTCGCATTGTAGCCAGAATCCTGTGAGAGTTG

22[103]	24[96]	GCAAAGAATAGCATTAACATTTCG
38[71]	40[56]	ACAAGAACCATAAGGGCGGAACGAGGCGCAGA
		GGTCCACGACCCGTCGAACATTAATTGCCTGATGTA
2[63]	31[63]	TAAGAAAAGAAG
18[47]	12[40]	AAATCTAAAAGCGTAATTACATTG
23[80]	6[80]	ATTCTACTGCAGGTCGGTAACGCCAAAGTGTA
27[32]	37[39]	GAATATACATGCAAATATCTTCTG
36[23]	28[16]	AAGACAAACTTTTTAATAACGGAT
36[31]	44[24]	CCAATCGCATGCAGAACCTAATTT
21[48]	4[40]	AAACACGGGCTGGCGAAAGATCGCCAAAGGGCGCTGGCAA
52[31]	60[24]	ACGGGAGACAAAAGGGAAAGGTGA
50[55]	32[48]	TTCCAGAGTCTTACCATCATCGAGTAAGAACGACAGTACA
31[8]	30[8]	AATTAATTAAACATCA
1[88]	15[95]	GGTTCCGATAGGGTTGGTTAAATC
55[8]	40[16]	AGTAAGCAGATAGCCGAGTAGGGC
51[32]	59[39]	ACGTCAAATATTCATTCGACATTC
35[48]	18[48]	AACTATATCAGACCGGCCATAAATAGGATGAA
36[87]	29[87]	GGTTTAATTACCAGTCTATCGCGTTATTATAG
50[47]	35[47]	CCTAATTTGGTATTAAAAAAATAAGGTTATAT
59[40]	53[47]	AACCGATTACCACGGATAACCCAC
5[96]	9[103]	TAACTCACCAACTGTTCCCAGTCA
41[16]	26[16]	AACGCCAAAGGCGTTATATTTTAGTAAAACAG
22[79]	7[79]	ATAAAGCCTAAGTTGGACTCTAGACATGGTCA
36[79]	21[79]	TTCAACTTTAGAGAGTGTAGCTCAATGACCCT
61[8]	60[8]	ATTTGGGACGTCACCG
18[39]	28[32]	AGCATCACCAGTTGAAACATCGGG
23[8]	5[23]	GAGTAACATTATCATTTGATTAGTGAACTCAAAGGAA

		CGGGCCGCTAC
28[79]	10[72]	TTTAATTCAGGCCGGATGCAATGCCGGCACCGGCGGGCCT
5[24]	12[24]	AGGGCGCGGTCACGCTGCTCAATCACCAGTCA
8[55]	5[55]	CACGCAAAAAGGGGGATAAACAGGACGAGCAC
18[79]	4[72]	TTTGAGAGGTGGGAACTTTGAGGGTGCGTATTTGCCAGCT
24[47]	23[55]	TCATATTCCCACCAGAAGGAGCGG
57[40]	55[47]	GGTGGCAAACGGAATAGGAAACCG
53[88]	60[88]	GAGCCACCTACCGTAATGAATTTAACGATTGG
6[111]	8[96]	ACACAACATACGAGCCGAAATTGTCCAAGCTT
46[87]	32[80]	ACAACCATATCAGCTTCGATAAAA
15[96]	17[103]	AGCTCATTCCCCGGTTGTAATCGT
27[56]	34[56]	TCCAACAGAAGCGAACGCGATTTTAGATTTAG
3[40]	3[63]	AGGAGCGGGCGCTCGCGCGGGGAG
53[80]	43[87]	CACCCTCAAAAGAATATTTCCATT
20[71]	25[71]	CTGAGTAAAAAACATTACATGTTTTTTCATTC
7[24]	9[31]	AGTGAGGCTTTTAGACACTATCGG
47[32]	61[39]	GGCTTATCACCTCCCGACAATTTTCCGTAATCTCACCAGT
30[95]	47[103]	CATTGAATAAGGAATTCCAGACGAGCTTTCGAGGTGAATT
49[24]	63[39]	ACCCAGCTACTTGCGGTCATCGGCATTTTCGG
54[95]	58[88]	CAGGAGGTTGCCCCCTAGTGTACT
0[39]	13[39]	TCCAACGTTCGAGGTGGGCACAGATGACCTGA
55[56]	57[71]	GGTTTTGCCCAATAATAGATGAGTAACAGTGC
33[8]	34[8]	TTAATTAACAAAATCA
0[111]	1[103]	AAAGAATAGCCCGAGAAATCGGCA
		TAGCTGTTTCCTGTGTGGAAGCATAGGGTTTTGGGAAGG
7[80]	21[95]	GTTTGCGGG
44[111]	35[111]	CGAAAGACAAATCTAC

27[16]	12[16]	AGGTTTAAACAACTAATCAGTTGGCACGACCA
41[72]	39[79]	TACCAAGCTACTTAGCAACCGAAC
6[79]	8[64]	AAGCCTTAGAATCAGATTCGTAATGGATCCCC
45[56]	51[71]	CCGTTCGGTCGCTGAGTATGGGATACTACAAC
51[48]	34[48]	TAGCAGCCTGAACAAGACCAAGTAGAAAGATT
37[64]	53[63]	ACGTAACACACTCATCTTTGAATAAGTTAAGC
14[95]	31[95]	CGCGTCTGGATGAACGGATAATCAAATGTTTA
58[87]	52[80]	GGTAATAAGCAGTCTCCACTGAGT
27[48]	12[48]	AAGCAAACTAAGGTTAAGGAAAGAGCCTCAGG
34[95]	49[95]	ACATTATTAGGCCGCTCAATGACATCAGCGGA
36[47]	21[47]	AAATGCTGAGTAACAGTACCATATGACTTTAC
54[23]	43[23]	TCTTACCGAATTGAGCAATTCTGTTTCAGCTA
9[56]	20[56]	TGTGCTGCTTACGCCATTGTACCATGTGTAGG
51[96]	59[103]	CTCATAGTCAGGTCAGCCGTTCCA
39[48]	22[48]	CGTTATACAATTATCAGTACGGTGAATATTCG
13[64]	19[71]	GATTCTCCATCTACAAGGTGAGAA
33[32]	50[32]	TTGAAAACAGCCGTTTCAAGAACGGCCAGTTA
60[111]	51[111]	GGTTGAGGTAGCGTAA
36[63]	43[71]	GTGAATTAAAGAAAGACTTTTTCA
22[39]	24[32]	TATTAAATCAAAGAAACTGATTAT
		CACTAAAAAAGCTGCTTAATCTTGCATATAAC
42[79]	23[79]	TGTTTAGCTGGCATCA
35[32]	52[32]	TTAGGTTGTATCCCATCGCGCCTGCGCATTAG
14[103]	18[96]	AAATAATTGTAATGGGTTAATGCC
12[95]	29[95]	ACCGTGCAAATCACCAGGAGAGGGTCAGAAGC
8[95]	26[88]	GCATGCCTAATAGTAGTTAGCAAACCCAATTCTGCTGAAT
10[31]	28[24]	CCAGCCATGGATTTAGGAGCACTACGTCAGATAGAAACAA

24[95]	42[88]	CAAATGGTTTTGAAAGTGACCTTCAAGTACAAAAGAGGCA
15[48]	0[40]	GTAAACGTATTAAAGAACGTGGAC
24[71]	41[63]	TATATTTTCATTTGGGCGGTCAATCGGATATTGTACCCCC
29[32]	34[32]	AGGCGAATGAGAAGAG
37[88]	44[88]	GAATAAGGCTTGAGATAAACGGGTAACGAGGG
2[39]	11[39]	AAGGGAGCAAAGCGAAGCAGATTCGTCTGAAA
53[48]	36[48]	AAGAATTGAGAGAATACAATAGATCCTTATGT
4[39]	9[39]	GTGTAGCGTACTATGGTATTACCGCCTTGCTG
39[104]	39[111]	TGAACGGT
63[40]	49[47]	TCATAGCCTAGCAGCAATCCTGAA
54[47]	39[47]	GAAACAATAGGCATTTACCAGTATATCATATG
48[95]	63[111]	ATTTTTTCCGGAACCAGAGCCACCACCGGAAC
19[24]	30[24]	CAAATCAACTTGCTGATCGCGCAGAAGAAGAT
1[40]	15[63]	CCGTAAAGCACTAGTTTGCCCCAGAGTCCACTTAATATTT
13[48]	2[40]	GAGTAACACTGAATCGGAACCCTA
51[24]	62[24]	TTTGTTTACAAAATAACAGCAAAAAGTAGCGA
56[63]	54[48]	ATTAGCGGCAATAATACATATAAAAAGAGCAA
20[47]	6[40]	TCTAAAATTGGATTATCAGAACAATTGCTTTGAGGCCGAT
59[72]	54[72]	TGGAAAGCGTTTTAACAGAACCGCGCCACCCT
0[71]	14[64]	GGAACAAGCAGGCGAACTTTCATC
31[64]	46[64]	TTTTGCCAAGCGAGAGACTAATGCCATAACCG
20[95]	35[95]	CCTCATATTTGCTCCTACTTCAAAAGGACGTT
39[96]	55[95]	AGGACAGACGAAATCCGCGACCTGTCGAGAGG
19[96]	27[103]	TCAATATGCCCGAAAGTTTGATAA
41[96]	56[96]	CGGAGATTACCGTACTGTTGATATAAGTATTA
22[47]	7[47]	ACAACTCGGTAATATCTTAACCGTAAAAGAGT
33[24]	47[31]	TAGAATCCAGTGAATAATATAGAA

51[88]	62[88]	AGACAGCCAGACGTTACCACCACCAGAACCGC
16[31]	32[32]	CAGCAGAACAATTTCATTTGAATTTATATGTG
25[24]	37[31]	CTGAATAATTTGCACGTTAATTTC
45[16]	30[16]	TCTTTCCTGAATTTATTTTTCCCTGATGAAAC
19[8]	20[8]	ATATCTGGTAGATTAG
36[111]	27[111]	CGAGTAGTGAGGTCAT
35[24]	46[24]	CCTCCGGCTCAATAGTTATCATTCTTATTTTC
47[64]	62[56]	TTAATTGTAAAAAAAGTTTGCTAAACCCGTCACCAATGAA
5[72]	11[95]	TCGTGGGGTGCCTAATGAGTGAGCGTCGGGAAGCCGGAAA
21[96]	38[96]	AGAAGCCTAGCTTAATTGCGAACGAGGCTGGC
16[47]	30[32]	TAACCGAACGAACCACCACGCTGACTGAGCAA
11[80]	3[87]	CTTCTGGTACCTGTCGGGGCGCCA
58[23]	44[16]	ACAATCAAGCCAAAGAATTAACTGAACGATTTACGAGCAT
56[95]	54[80]	AGAGGCTGAGACTCCTACAGTTAATTAGTACC
34[47]	19[47]	AAGACGCTTATTCATTTACCTTTTAGGAATTG
63[64]	49[79]	CCATCTTTTCATAATCGAGCCACCACAACTTT
33[56]	47[63]	CACATTCAGCTTTTGCAGGAGCCT
58[103]	57[111]	GATACAGGGCCTATTTCGGAACCT
62[87]	48[80]	CACCCTCAAAAATCACACGTTGAA
49[8]	50[8]	TTAGTTGCATTATTTA
38[87]	20[80]	ATCAAGAGCATTCAGTATAATGCTACCTTTAAATTTTAAA
33[80]	16[80]	AACGCCAACCCCCTCAAATAGTAAGAAAAGCC
61[40]	43[47]	AGCACCATACGGAAATAATGAAAACAGGGAAGTTTATCAA
14[111]	1[111]	GCCATCAAAAATCCCT
14[23]	0[8]	TTGAATGGATAGCCCTGAAAAACCGTCTATCA
31[16]	16[8]	ACATTTAAGATAAAACAGAGGTGA
5[56]	12[56]	GTATAACGGAATCGGCACTCCAGCCAGTATCG

53[32]	57[39]	CAGAGAGAATAAGTTTTACATAAA
52[71]	58[64]	CAGTACAACCACCCTCGGGGTCAG
18[87]	14[80]	TAGCTATTAGAGAATCGCCTTCCT
52[63]	59[71]	GAGAATAAGAAATTAAAGCCAGAA
63[8]	62[8]	AGACTGTAAGTTTGCC
56[111]	55[111]	AAACATGAAAGTATAG
37[8]	38[8]	TTCAAATAAATAAGAA
48[111]	47[111]	GGAATTGCTCTTAAAC
57[8]	56[8]	ATGTTAGCACTCCTTA
10[111]	5[111]	AGGCTGCGATTAATTG
25[8]	24[8]	TGTTTGGAATCAATAT
32[111]	31[111]	TCATAACCAGCGTCCA
11[8]	10[8]	ATACCTACGAAAAACG
47[8]	46[8]	ATAGCAAGAATCATTA
1[8]	2[8]	TCACCCAAGACGGGGA
52[111]	43[111]	CCAATAGGTAATGCCA
4[71]	23[71]	GCATTAATTGCTTTCCCTTCGCTAAAGGCGATTCAGAGCATGAAAAGG
2[111]	20[96]	ACAGCTGATTGCCCTTTTTCTTTTGCATCGTACCAGGCAATTTAGAAC
57[72]	41[87]	CCGTATAACAAGAGAAAGGCGGATAAGTGCCGCTCCATGTGCGAAACA
42[111]	23[111]	CACCAACCGACGAGAAAGGCGCATAGTAGATTCATTAGATACATCCAA
39[80]	10[80]	TGACCAACCAATAACCAGTTGATTATTAAGCAGTAATACTCGATCGGT
48[79]	29[79]	AATCTCCAATCGGTTTCGCCCACGAGATACATAAAGATTCACCCTGAC
31[96]	50[96]	GACTGGATCTCGTTTAACGAGGCATGCGCCGATTTGCGGGGTCTTTCC
21[8]	7[23]	TAGATAATATTAATTTGAGTAGAAAATAACATAAGTGTTTTTATAATC
41[8]	25[23]	TATTTAACTTAATTGAGAATCATAATTACTAGGGCAATTCTTATACTT
60[23]	47[23]	ATTATCACATTAGAGCACAGCCATTATTTTGCATCGTAGGCAAATCAG
1[24]	14[40]	TTTTGGGGCAAAGGGCAAAACATCGCCATTAAAAATAATTGAATACGT

4 spacer Ts were added to all the strand termini (5’ or 3’ or both) that end at the edges of DN2.

S3.2.3 DN3

S3.2.3.1 Schematic for DN3

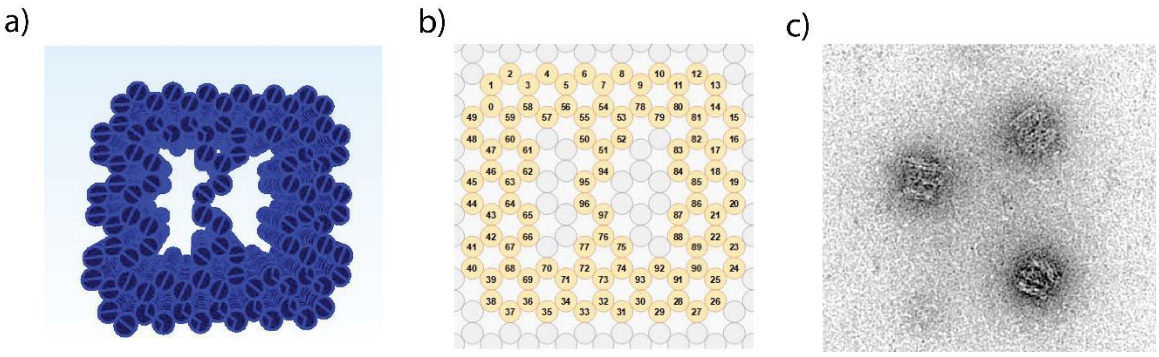

Figure S3.5: DN3. a) Cartoon b) arrangement of double helices constituting DN3 c) TEM image (scale bar = 50 nm).

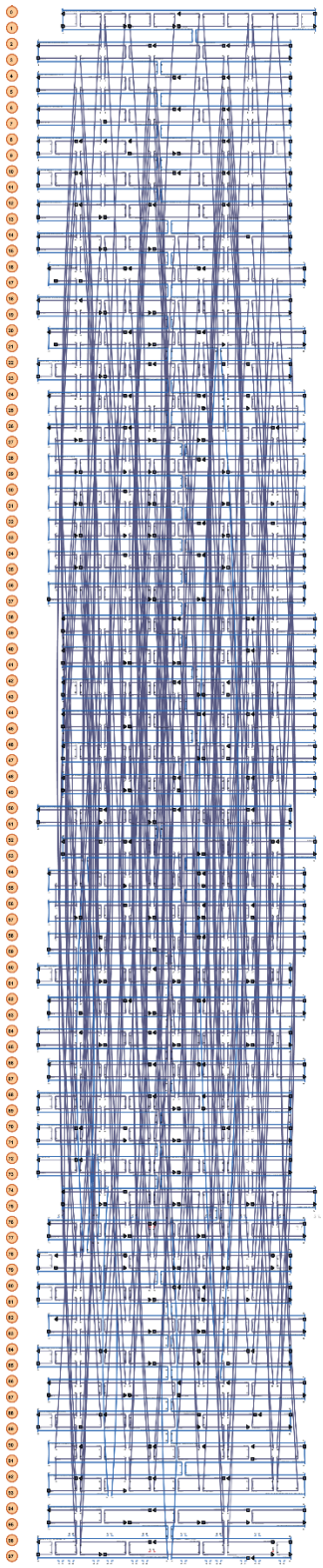

Figure S3.6: caDNAno schematic showing individual strands and scaffold for DN3.

S3.2.3.2 Sequences for DN3

Start	End	Sequence
56[78]	55[78]	TTTTGTTAAGCCTTCCTG
79[56]	12[56]	ATAAGGGCCTGCTCAGTTTGAGACAACT
10[74]	7[74]	TTTTGCGGAACAATGGCAATAATCCTAAAATTATTTGC
78[74]	79[74]	CAACTCTGAC
72[13]	72[2]	TCAGTGAGGCCA
78[69]	56[63]	TTGAAAGCGTGGGATTCATCAGCGTCTGATCAGCT
17[14]	15[20]	GAACAAGTGTTTATAGACGAC
22[55]	24[49]	ATCGGAAAAGGCCGGGTCGCT
64[34]	65[41]	TTTTGCACCAATACTGCGGGC
73[2]	31[13]	CCGAGTAAAAGAAAGAGCAAGTCAGA
93[5]	29[13]	TTATAAATCACCCTGATAGCAGC
92[34]	27[34]	TGATGGTTGCCCCAAACGATTATTATTT
15[2]	16[5]	GTAATTCTGTCCCAACAATAG
16[48]	83[48]	AACAGTTCTAAAGCACAAAGTACGAAAG
44[81]	43[81]	AGTAAGCGTCATAGTGCCTTGAGT
6[55]	54[49]	AAATTGCGAACCTAATGTGAG
66[48]	42[42]	ATTTTAACTGTAATCCCATTA
79[7]	12[14]	TGCAAGGCGATTAACGTTGTATACCAGTGAGAATC
65[2]	66[5]	AGTAAAATGTTTCCCTCAAAT
57[35]	4[42]	AAGAACTGTAGTAAATGTTTAACGTCAGGCCTGAT
4[41]	51[34]	TGCTTCTGAGAGACGATGCAAATTGGGCCGAGAAAACCGCTTTTGGGAA
22[74]	89[74]	CTCAGCAGCGAACCAGTAATAAAA
1[9]	0[9]	CTTGCATAAC
81[35]	15[34]	GAGGAAATACAGTAATAAGAGAACAACA
88[48]	22[35]	ACCCTTCTGCCAACGCGCGGGGACGGGCAACAGTGAGAAGCA
53[9]	55[27]	CGCCAGCTCATCAAGAGTAATCAACGGCCCTGA
65[21]	44[9]	ATAGCGTAAAGAAGAGCCAGCGGCCGGAAACGTCACCAAT
59[5]	62[5]	GTTAATAAATTAGGAAAACTAATCATAACCCT
49[9]	2[2]	CAGAGCCACCACTGAGTGATTCTGTAGCTTAGATTAAGACGCTGA
32[78]	31[78]	AGCCCTCATATTTTCTGT

53[49]	9[41]	CCCGTCGGGTGTAGATGGGCGCATCGGCCAAGAACGACCAGGTAATCAT
15[21]	79[27]	GACAATAAATATAAGCAGGTCGTCACGAGTTGGGT
86[78]	21[78]	TGAATGGCTAAACATCGC
24[48]	28[49]	GAGGCTTGATACCGTATTTACAACATTGCAACAGGGAAAATC
20[27]	87[27]	CGAGAACCATTACCGCTCACTAGCTGCA
96[74]	97[74]	CTAAAAAGCA
1[42]	62[49]	TTCCCTGATGAAACTTTTTTATACCCCGGTAAAACTGCCTGAAGATCTA
35[14]	72[14]	GAGGAAACGAACAAAACCAGAGATATAA
12[13]	12[2]	GCCATATTTAAC
85[2]	84[2]	TAAAGAAGTG
75[9]	75[20]	TGAGTGTTGTTC
43[56]	61[62]	GTTTTAAGCCGGAGCGTTCTATTTTGAGGAGTCTG
34[48]	35[55]	TCACCTTAACACCACCCTCAT
41[9]	64[14]	GATTGAGGGAGGCGACTTGGAATTAGTTTTGCC
12[55]	16[49]	CGTATTATTTGAGGATTAGAGAGGAAGGGCAAATC
31[56]	31[55]	ACGTTAGCAACTTTCAACAGTTTCAGAATATCGTCTTTCCAG
58[20]	4[2]	GGGAAGAGTGAATTTTAACCTCCGGCTTAGGTT
71[2]	70[2]	AGCTTATTCG
65[63]	44[63]	TAAAGATGAGAAAGCGGGGTCACATGGC
19[2]	20[5]	TCTTTCCTTATCCCGTTTTTA
84[48]	85[34]	ACCAACCTAACAATTCCACACGCTAACT
72[74]	71[74]	CAAATGGTCAATATTCTACTAATA
8[55]	79[55]	TGGATTACTGATTAATGAACGGTCAATC
42[81]	67[78]	AACAGTGCCCGTATTTCAACG
54[48]	57[48]	CGAGTGAACACGCCTAGGAGAGGTAAAC
43[9]	42[9]	TTTGGAGCCA
84[62]	81[62]	GCCACTAAGAATACATACCAAATCGCCT
62[27]	45[27]	AAGAGCAATAAAAAGTCAGACAGCAGCA
90[34]	26[28]	TGCCCTTCCTGAATCTAACGA
82[78]	17[78]	TTGACCCCCTATCAAACC
94[34]	95[27]	TAGCGGTCACGCTGGCCGCTA
88[74]	88[65]	GGGACATTCT
40[62]	42[56]	CAAGAGAACCTATTGTTAATG
17[7]	18[2]	AAGTCCTAATAATCGGCTG
37[35]	69[41]	GTGGCAAGAACTGGGACAAAG
34[27]	38[9]	AGATAGCCGCAATAAAGACTCATACATAAGACACCACGGAATAAGTT

61[21]	48[9]	CATAACGTCATCAGTCGGTCATAATCAAAATCACCGGAAC
33[35]	73[41]	GAAGCCCCCACAAGACGAACG
54[78]	53[81]	TAGCCAGCTACAAACGGCGGA
6[74]	5[74]	ACGTAAAACAGAACAGTACCTTTT
88[64]	86[56]	GGCCAACAGATACGTGTTTAATG
31[35]	92[35]	AGAGAGAGCGCATTTAATAACTCCTGTT
52[20]	52[9]	TCTTCGCTATTA
20[78]	87[78]	CATTAAAAATACCGAAAGCCCTAATTAGTCGCACAGACAATATTTT
21[35]	20[28]	ATAGCCAAATACCGCACTCAT
56[27]	49[27]	TTGAGATCCTTATGGGACGTTAACGGAAATATATGCGGAACC
38[81]	37[78]	CGAGAGGGTTGAGCCACCCTC
77[49]	32[49]	TCATTTTTTAGCTATTAGTTTTCTAAAG
71[42]	33[34]	CGAGCTGATACAGGCAAGGAGCCCGAAACAAACTCAGTAAGCTCTTACC
22[62]	19[74]	AGACAGCAACTGATCGAACCAAGTATTAACACCGCCTGCA
68[34]	71[41]	AAATCAGTTAAGAGCATGATTATAACGGAATACCCTAAGAAACAGGGCG
76[78]	75[81]	GCTGAATATACTAAAGTACGG
22[34]	89[48]	AATCAGACCGACTTGCGGGAGGGAGTTACGAGGGTGCAGATT
90[78]	26[70]	CATTTTGACACAACCATTATCAG
51[35]	50[42]	GGTAACCGTGCATCGCCAGCT
85[35]	19[34]	CACATAGAAAATTTACGAGCATATTAAA
96[34]	96[35]	TTGCTTTAGGAGGCCGATTAAAGGGCGACCGATTTAGTATGG
48[81]	47[81]	AGAGCCGCCACCGACGATTGGCCT
95[49]	77[48]	GGGAAAGGGAGCCCAAAACCGACTGGACTCCAACGTAAGAGG
7[21]	1[27]	TTCATCTAGACAAAAAATGCTTACCTTTTATCAAAAGCGATAAATCGTC
70[13]	33[13]	CGTTTTACAAAGCGAGTTACCACAATGA
55[49]	95[48]	ATCAAAACACTCCATGCCAGTGCGCTAGGGCGCTGCTTGACG
19[21]	84[21]	GAACGGGTGTAGAATGAGTGAAACATAC
14[74]	81[74]	GAGCACTAACAAGATAAATTGTGT
57[49]	6[56]	GTTAATATTTTGTTCATTTTTTACAGTAAATAAAG
38[62]	65[62]	ATAGCCCCTCAGTACGGTTGTCGGGAGATAGAACCGTGTAGG
11[2]	10[2]	TATACTGCGT
79[2]	78[2]	TGTGCGGGGA
4[74]	3[74]	ACATCGGGAGAAGAGGCGAATTAT
15[35]	80[42]	TGTTCAAGGAATTGCCGTCAACGGAGATCTTAGCC
48[41]	1[41]	TTGCCATTCAGAGCCAGTACAATTAATT
87[5]	26[5]	GGAAACCTGGTATTGGGGTTTTTGAGAGAGTGCACCCCCTAATTTG

52[81]	52[70]	TTGACCGTAATG
13[2]	14[2]	AACGCCAACATGACAAAAGGTAAA
66[34]	41[27]	TCATAAATATTCATAAAACGACCGTCACGAAGGTA
14[62]	13[74]	CTAATAGATTTAGAAGTATTAGACTT
84[20]	13[20]	GAGCCGGTTCCTGTAATTCGTCATGCCTAGTACCGTAATTTA
61[63]	48[63]	GAGCAAAGATGAACCAGGTCAAGAACCA
83[49]	21[55]	AGGCAAACGAAGGCCATGAGGCGGCTTTCAGAGCG
5[2]	50[2]	GGGTTATATAACTTTCAACAGTGAATCAGGCAAAGCGC
77[5]	97[20]	CTGAGAAGTGTTTTGTACGGTACAGCGGGA
12[74]	11[74]	TACAAACAATTCGTAACATTATCA
69[42]	38[42]	AATTAGCACATTATTTAGCGGGGTTTTGGGAATAGGTGTATA
79[42]	53[48]	GCAGACGGTGTACACGAACAA
40[81]	39[81]	TTAAGAGGCTGAGATAAGTGCCGT
87[42]	90[49]	CTGAAAGCGTAAGAAGATAGACACCAGTAATGGAT
18[74]	85[74]	ACAGTGCCACGCCATTAAACGGGT
9[42]	8[28]	CATATTCTACTTCTGAATAAATTTAATG
41[28]	37[34]	AATATTGCAAAGACGAAAATTAACGCAACATAAAG
84[74]	84[63]	AAAATACGTAAT
51[2]	94[5]	CATTCGCCATTCCCACCACAC
2[34]	57[34]	AAAACATATCATAGCCAGTCACGATTTT
25[49]	27[48]	ATAGTTGGAATTTCTTAAACATCAAAAA
85[56]	15[74]	AAGTTTCTGAGAGCTGCTGAATCAGTTGTTATCTAAAATATCTTTAG
48[62]	2[56]	CCACCAGCCGCCACAATTACCAAACATCCCTGAGC
83[35]	16[28]	CGCTCAAACTCCCCGGGTACCATATCCCATCCTATGAAGCTAATGCAGA
64[74]	65[74]	AGGGTTCAAA
59[35]	2[35]	ATTACAACATTATAGTTGAATACCAAGTGATTAGAATCCTTG
10[55]	80[49]	CACCAGATTTTAAACATGTTA
8[74]	9[74]	CAATATTCAT
57[63]	49[81]	AAAATTCGATTGTAATCAGAATCATTTGCCTCAGAGCCACCACCCTC
32[48]	33[55]	TTTTGACTTAGTACAAACTAC
97[2]	96[2]	CGTTATTCCT
67[5]	35[13]	GCTTTAAACTATTATAAAGCGGACGCAGTAGGAAACC
24[62]	23[74]	TATATTCCTTTTGCGGGATCGTCACC
62[48]	60[35]	CAAAGGCATATGATCCAATCAAGTTTGCCTTATTATCAGGTA
7[2]	8[14]	CAAATATATTTTAGTTAATATACCGA
33[14]	74[9]	AATAGCACAATAATGTCTGTCCCGAGATAGGGT

50[74]	50[63]	ATCGGCCTCAGG
89[14]	19[20]	CTTTTCAGGCTTATTAGGAATAAGCAAGATTCCAA
50[20]	54[5]	CGGAAACAAGGCTTTAACAAAGCTGCTCAT
92[78]	27[78]	TTGCTGGTAAAATACCGAATAATATTGTATCG
70[55]	34[49]	ATAAATCAAAAGGTAGTTTCG
23[2]	22[2]	GAACGTCTAA
92[13]	27[13]	CAAAATCAGCAAGCAAAAATGAGTTACA
50[62]	8[56]	AAGATCGATAATTCACATTAACCATATCGATTGTT
77[28]	31[34]	ATTGCTCAGGTCAGCAAATTAAATTGAGTAATATC
10[13]	82[7]	TATCATAAAATTCTAAACGACAAGCTTGAATCATG
8[13]	78[7]	CCGTGTGCGTTAAAGCGAAAG
6[41]	52[28]	TTCAGCCAATCGCATCTGACCTACCCAAATCTTGAGATCGGT
23[21]	88[21]	GAACCTCTATAGAACCAGTGAGAGAGGC
26[27]	29[27]	GCGTCTTCAGCCATTTTTGTTGAGAGAA
24[78]	90[63]	GCCCACGCATAACCGAAATGACAGCTCAAT
97[21]	51[20]	GCTAAACGACGAGCACGTATATTAATGCCGCGTAAAGGCTGC
63[14]	61[20]	GACGACGACACTATGCAGATA
52[27]	50[21]	GCGGGCCGCAACTGCTGGTGC
78[27]	10[14]	GCTGGCTGACCTTGTAAGAATTGTTTAG
81[2]	80[2]	GTGCCGGCCA
62[78]	45[81]	CGGAGAGGGTAGCTATGCTGATAACAAATATCTCTGAATTTACCGTTCC
9[28]	79[41]	GGAATCACGCATAGAACGCCAGGGAGGC
45[9]	59[20]	GAAACCATCGATTGTAGCGGGCATTTTTGAGATACGAACT
37[5]	70[14]	TTAGCAAACGTAGAAACTTATTATTGCATCAATATCG
26[69]	31[69]	CTTGCTTGCCTTTAAATTTTTAACAACTTGCTAAATAAATGA
75[63]	77[78]	ATATGCAAATGCTGGGCTTAGAGCTTAATT
42[41]	64[35]	AAGGTGACCAGTAGATGAGGC
89[2]	88[2]	AGGGTGCGCC
88[20]	18[14]	GGTTTGCTCGTGCCGCCCGCTTGCCTAAACCAATC
43[49]	68[49]	GTAATAACCCCCTGACTTTTGACCAAAA
2[74]	59[78]	TCATTTCAATTAAAGAAAACAAAATTAACAATTAAGCCCCAA
52[69]	51[74]	GGATAGGGACGACGACAGT
29[56]	89[62]	AGAAAGGTCACGTTAAAAACGCGTCTGACACACGA
47[56]	4[56]	GTTGAGGGGTAATCGTTGATATAAGCAATCGCGCAACAATAA
50[41]	6[42]	TTCCGGCCACCAGATATTCATTAATGGAAGGGTTAGTAGATT
47[9]	46[9]	TCATCCGTTT

57[14]	6[2]	TGAATTAGGTTTAATATATGTGAACGCGAGAAAACTTTTT
74[27]	71[27]	AATACGCCATCACGGATTAGACCGGAAG
87[28]	21[34]	TTAATGAATCGGACAATAATTGCGTTGCGCGCCCA
76[34]	29[34]	GATTTTAGAACAAGTTGTAGCTGATTAGAGACGGGTAACATA
35[56]	97[69]	TTTCAGGAACACTGGGCATCAAACCTGTTGCGGATTAGCTCATCTATCATGCCGTA
29[14]	90[14]	CTTTACATAACGTCGGTCCACTGGCCCT
16[78]	83[78]	CTCAATCAATATCTGGCCTCAAAAGCGATTACTAAAACACTCATCT
12[34]	12[35]	AGTAGGGGCATTTTCGAGCGATAATACAAATCCTTTGCCCAC
34[78]	33[78]	GGAACCCATTCCACAGAC
83[5]	86[5]	CATAGCTGTAAGCATACCTGGGGTTCCAGTCG
68[74]	40[63]	ATAAAGCTAAATCCAGGCGGACTCCT
33[56]	75[62]	AACGCCTGTAACGAGACCATTATATAACGTTTTAA
9[2]	8[2]	TAAGGATAAA
32[69]	38[63]	AGTTAGCGTAGCATGTACCGTGATAGCAACCCTCATAGTACCTATAAGT
58[78]	57[78]	AAACAGGAAGCATTAAAT
39[9]	65[20]	TATTTTGTCACACCCTGACAGTTCAGTGAATCCAGACTGG
0[81]	1[81]	CATTTAATTA
60[74]	61[74]	GAATCCAAGA
63[35]	62[28]	AGCGACATAACGAGGCATAGT
37[49]	70[56]	GTACTCAGGAGGTTGAACCGCAGCAATAACATCCA
95[5]	76[5]	CCGCCGCGCACGTGCTGAATCAGGCCAGAATC
63[5]	64[2]	CGTTTACCAAGAGGGGGTAAT
70[27]	40[9]	GACTTCAAAAAAGAGTCTTTAATCAATAAAAAGGGCGACATTCAACC
4[55]	56[49]	CGGATTCATGAATATAACCAA
66[78]	41[81]	CAAGGATAAAAATTTTAGCCTTTATAAACAATTCTGAAACATGAAAGTA
30[27]	33[27]	AGAATTATGAGCGCTTAAGCCATAGCTA
27[35]	24[28]	ATCCCAAGCCAACGCTTACTTGCAGGTTTTGAAGC
24[27]	93[27]	CTTAAATATTTTATCACCGCCGCTGGTTGGTTCCGTATTCTT
92[55]	75[41]	ATTACCGCCAGCAAATCACTTTCCCAATTCTGCCGAGTCCAC
46[81]	63[78]	TGATATTCACAAAATTAATGC
20[48]	86[42]	AAGATAAACGGCTAGAGGACT
27[49]	25[62]	AGGCTCCAAAAGGATCGAGGTCGCCGAC
70[74]	69[74]	GTAGTAGCATTAAAGCCTCAGAGC
95[28]	94[35]	CAGGGCGCGTACAGGCAAGTG
2[55]	58[49]	AAAAGAATACAAAAATATTTA
49[42]	48[42]	CGCCACCCTCAGAAAGCCGCCGCCAGGT

91[63]	73[74]	CTCATGGATATCCAACTCAAATCATTCCAGATACATTTCG
10[41]	81[34]	GAATTATTACTAGACAACGCTTTTCCCAGACTCTA
13[21]	8[21]	GGCAGAGCTTAATTATAAAGCAAAAGCCAAACACCGTTTGAA
28[48]	29[55]	TCCAACAGGCGGAGTGAGAAT
31[14]	92[14]	GGGTAATACTGAACAAAAGAAAAATCGG
27[14]	23[20]	AAATAAATCCAGAGAGCTACACAAGATTTTTTAGC
75[42]	92[56]	TATTAAAGAACGATAGTTGATGCCTGAGTAGAAGAGAACAAT
96[69]	95[62]	TCGGAACCCTAAAGCCGGCGA
81[49]	20[49]	TTGTATCGCGCGAAATCACCTCAGCAGCGGCGGTCCCAGCAG
3[2]	57[13]	GAAGAGTCAATAAAAATCTATCATTG
94[78]	95[78]	AGGGAAGAAAGCGAAAACGTGGCGAGAAAGGA
80[41]	10[42]	GGAACGTCAGAACGTTATTAAAGGAGCG
1[28]	61[41]	GCTATTATAAATCACAACATTGAAAGATCCAAAAGGAATTTC
45[28]	66[35]	CCGTAATTTAGCAAAAAATCAATTATCAGAATGACCATAACCATAATCG
74[81]	29[78]	TGTCTGGAAGTTCTATCGGGGGATTTAAAGGAATT
61[42]	47[48]	AGGTCATTAGCATGGCCATTG
69[49]	37[48]	AAAATTACACCCTCAGAGCAACATCACC
47[49]	66[49]	ACAGGAGATTAAAGATTCAACACAGTCAGAGTAATCTCATAT
16[27]	83[34]	ACGCGCCAAAAATAGAGCTCGGTGAAATTGTTATC
58[48]	0[42]	AATTGCTTCATATGATGGAAA
94[62]	10[56]	GGAGCGGTTGAGGGTCACGTTGATTCTCAGGACAGTCAGATGAAGAAAC
80[74]	79[69]	CGAAATCCGCGAAACCGAA
44[48]	44[49]	GAGTGCCATTACCACAGTAGCGACAGAGAATGGAAGATACAG
61[2]	60[2]	CATTCTACCA
73[42]	76[35]	AGTAGATTATTTTCATTTGACCTTTTGATCAAAGG
65[42]	43[48]	AATGCCTAATCACCCATACTG
21[7]	24[5]	TTCATCGCCGGTATCGAGGCGAGTTGCTAT
75[21]	77[27]	CAGTTTGGACAGGAACCTTTA
19[35]	85[48]	CCAAGCAGAGGTGAAAATGAAACTTTTT
49[28]	63[34]	GCCTCCCCTTTTCATAGCCCCCTTTAGCCCAAAAT
36[78]	35[78]	AGAACCGCCAGCCCAATA
44[62]	46[56]	TTTTGATAGCGCAGAATCCTC
69[2]	68[2]	AAGCAGTCAG
38[41]	68[35]	TAAAAGACATATGGGAATCAA
41[42]	41[41]	TTATTTATTTCGGAAGGATTAGGATTTACCAGCGCACGGAAA
29[35]	90[35]	AAAACAGAATAAGAGCAGGCGATCTGAT

4 spacer Ts were added to all the strand termini (5’ or 3’ or both) that end at the edges of DN3.

S3.3 Annealing DN1s and Characterization

S3.3.1 Normal DNs

By ‘normal’ DN we imply the DNs formed without any stabilizing agents except magnesium. All the structures were annealed in 5 nM concentration by mixing 5 nM m13 scaffold and 10 fold excess of staples in 1X 3D buffer. The mixture was subjected to a thermal annealing program that heated the mixture initially at 95 °C and gradually cooled down to 4 °C over a period of 37 hours.

S3.3.2 Stabilized DNs

By ‘stabilized’ DNs we imply the DNs formed with at least one stabilizing agent in addition to magnesium. All the stabilizing agents used in this study are water soluble. While annealing the DN with stabilizing agents, each stabilizing agent was added to the mixture from an aqueous stock to achieve the desired concentration of the agent.

S3.4 Characterization of DNs

All the DNs used in these study have been characterized by TEM images from negatively stained samples. The detailed protocol for the TEM imaging is described below.

S3.4.1 Preparation of uranyl formate stain

0.7 uranyl formate stain was prepared following the described procedure. 7.4 mg uranyl formate was weighed in a glass vial containing a stir bar. 1 mL of hot water was added to it and stirred for five minutes in dark. After that 10 uL of 2M aqueous sodium hydroxide was added and again stirred in the dark for another five minutes. The solution turned bright yellow. The resulting solution was filtered using a spinX column. The uranyl formate stain was prepared freshly before each imaging experiment.

S3.4.2 Preparing TEM samples

All the samples used in this study were negatively stained. 2 uL of each sample was deposited on a plasma-cleaned TEM grid (cleaned for 1 minute). The sample was soaked using a Whatman 2 filter paper after 2 minutes of deposition and the grid was washed twice with 10 uL water each time. Then 7 uL of freshly prepared uranyl formate stain was deposited on the grid, kept for 3 s, removed using filter paper and another drop of 7 uL uranyl formate stain was placed on the grid. It was removed using a piece of filter paper after 15 s. The sample was dried properly in open air for 30 minutes.

S3.5 Time vs Stability Experiments

Each DN was formed in 5 nM concentration using 1X 3D buffer that contained 16 mM Mg^{2+}. The control structures were formed without any stabilizing agents while the other structures were formed using the buffer containing the maximum amount of stabilizing agent (determined previously) that allowed the formation of DNs. Then the buffer of each DN was exchanged with the physiological buffer containing 1.2 mM Mg^{2+}

along with other cations. 100 kD molecular cut off filters were used for this purpose. 6 uL of each sample was taken out at each time point and three replicate samples were prepared for TEM following the protocol described in the previous section.

S3.6 Counting of DNs

S3.6.1 Internal standard for counting

30 nM gold NPs were used as internal standards while counting the number of structures. The stock concentration as bought from the company contained 2.0 x 10^{11} particles/mL that was concentrated ten times using 30 kD molecular cut-off filter and the resulting stock contained 2.0 x 10^{12} particles/mL.

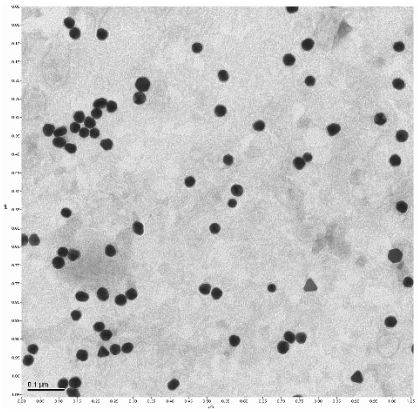

Figure S3.7: TEM image of concentrated gold NP solution (2.0 x 10^{12} particles/mL). (Scale bar = 100 nm)

S3.6.2 Preparation of TEM samples for counting

We used the concentrated AuNPs as internal standards for counting the structures. During the TEM grid preparation, there are several steps that can be broadly grouped in

the following sequence: a) deposition of sample b) washing the excess buffer c) staining. The addition of internal standard introduces another step and we had to optimize where this step could be introduced in the sequence. Following were the possibilities in hand: a) Deposit the AuNPs first before deositing the structures. We tried this, but when exposed to the physiological buffer the AuNPs got aggregated on the grid making their counting impossible. b) Deposit the AuNPs after the sample. When this was done, the AuNPs affected the staining of the particles and all the structures failed to produce properly recognizable contours when imaged. c) The AuNPs were deposited after staining, but when the excess AuNPs were removed using a piece of whatman filter paper, a part of the stain was also removed in the process and this made the structure positively stained that was not our requirement. So after all these trials, we depositied the AuNPs in between the two staining steps, that is after tha application of first aliquot of the stain, we placed 2 uL of the AuNP solution on the grid and let it deposit for 1 minute. After that the next aliquot of stain was applied and the step was completed as described in section S3.4.2.

S3.6.3 Counting procedure

We obeyed the following rules while counting: a) any structure that seemed to be deformed or did not match with the dimensions of the DN under study, were not taken into counting, b) any AuNP that aggregated beyond individual recognition were exempted from counting, c) any DN or AuNP that appeared partially on the image frame were not counted, d) there were frequent aggregates of DNs that might be due to the TEM sample making procedure or aggregation with time; for counting purposes we considered only the DNs that showed a proper contour and the full structure was recognizable. Otherwise, the whole

aggregate was left uncounted, e) the AuNPs bought from the company had some non-spherical NPs (though negligible in percentage) mixed with the spherical NPs; those particles were also included while counting the standards, f) three replicates of each sample (each structure each time point with a particular stabilizing agent) were taken into consideration, and g) more than ten images were counted for each sample.

S3.6.4 Illustration of the counting procedure

The procedure for counting one structure (DN1) without any stabiliaing agent and with one stabilizing agent (1 mM arginine) is shown below. The exact protocol was followed for all counting experiments. One point has to be kept in mind that the numbers correcponding to the TEM images below are representative only. The actual numbers that were used to construct time vs stability plots came from thirty images for each time point. The images illustrate the various situations that were encoured during the process of counting like non-homogenous AuNPs, AuNP aggregates, Dn aggregates, deformed DNs, etc. The density of DNs probably decreases with time and hence gradually they lose the capability to provide good contrast in the images.

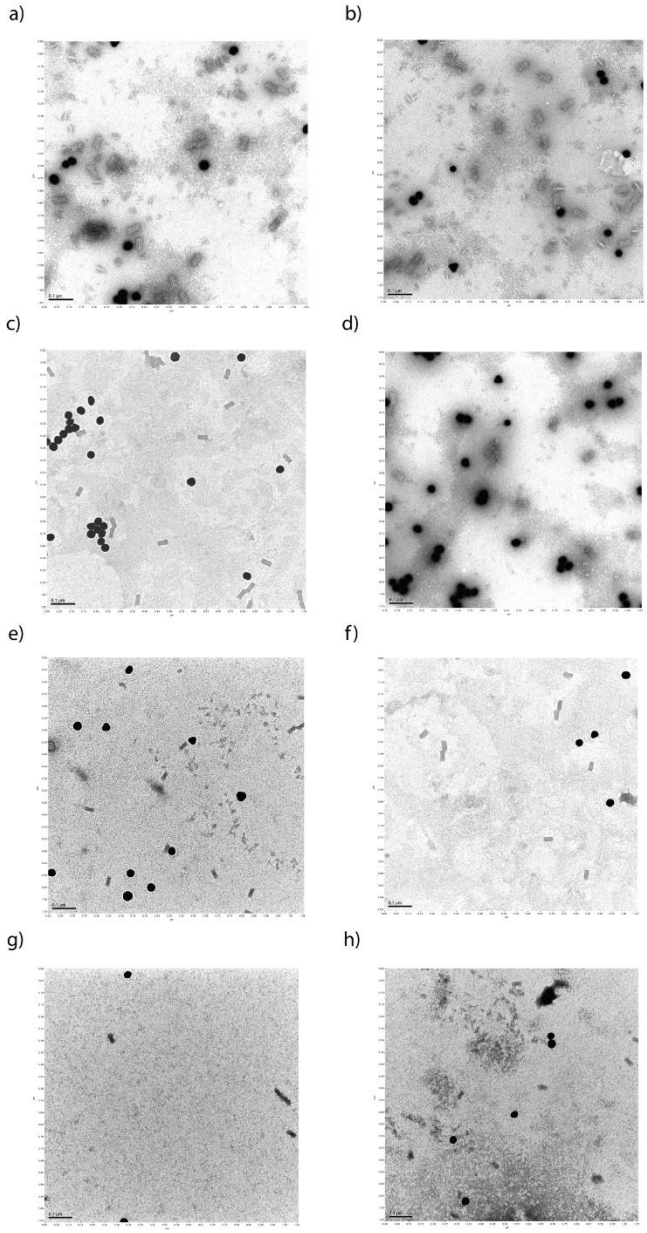

Figure S3.8: TEM counting of DN1 formed without any stabilizing agent subjected to physiological buffer. a) 0 min (19 DN1, 8 AuNP b) 20 min (17 DN1, 14 AuNP) c) 40 min (16 DN1, 26 AuNP), d) 60 min (7 DN1, 32 AuNP) e) 90 min (8 DN1, 10 AuNP) f) 120 min (8 DN1, 4 AuNP) g) 180 min (0 DN1, 1 AuNP), and h) 240 min (0 DN1, 5 AuNP) (Scale bar = 100 nm)

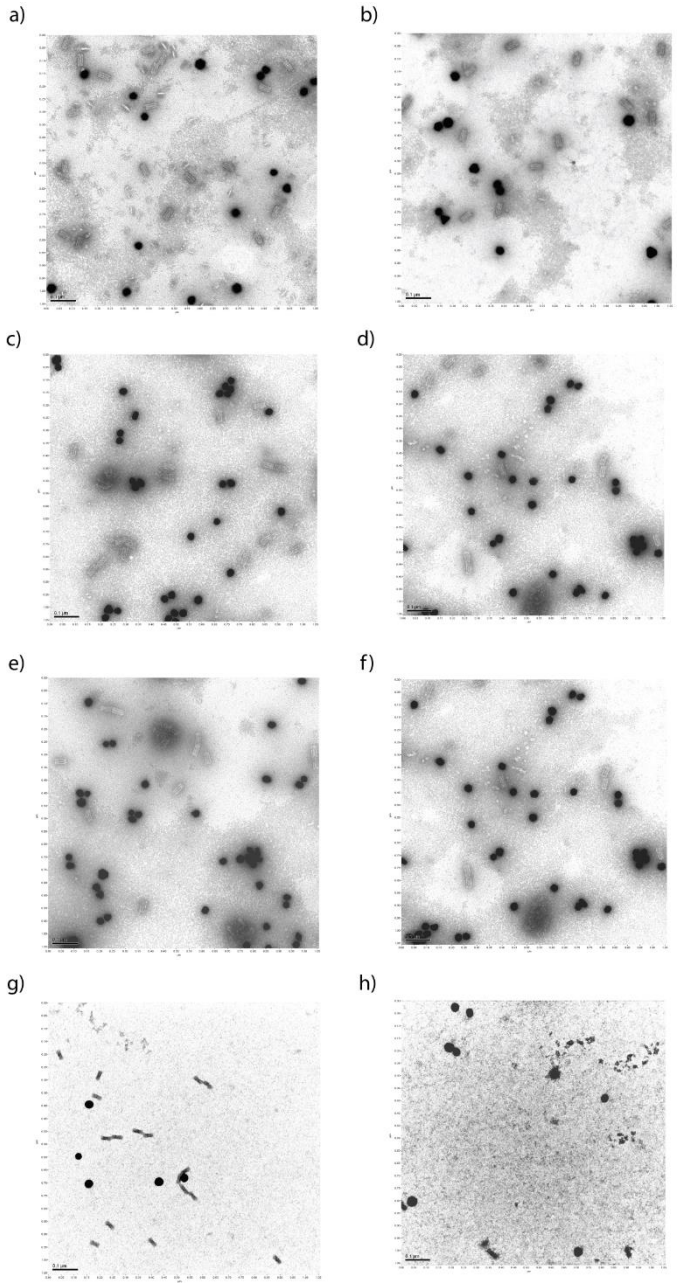

Figure S3.9: TEM counting of DN1 formed with 1 mM free arginine subjected to physiological buffer. a) 0 min (19 DN1, 14 AuNP b) 20 min (12 DN1, 11 AuNP) c) 40 min (12 DN1, 29 AuNP), d) 60 min (9 DN1, 29 AuNP) e) 90 min (11 DN1, 36 AuNP) f) 120

min (6 DN1, 37 AuNP) g) 180 min (17 DN1, 5 AuNP), and h) 240 min (0 DN1, 7 AuNP) (Scale bar = 100 nm)

S3.7 Determining half-lives of DNs

S3.7.1 Procedure for calculation

The AuNPs served as internal standards for counting and we calculated the number of intact DNs per 100 AuNPs and constructed the time vs number of each DN sample. Using Prism 5 software from Graphpad, the plots were fitted with one phase exponential decay (non-linear fitting) and the half-lives were obtained. The half-lives thus obtained provided an indication of the efficiency of each stabilizing agent and their combinations.

S3.7.2 Illustration of half-life calculation

The construction of time vs stability plots for DN1 without any stabilizing agent and all the stabilizing agents separately and their combinations are shown below.

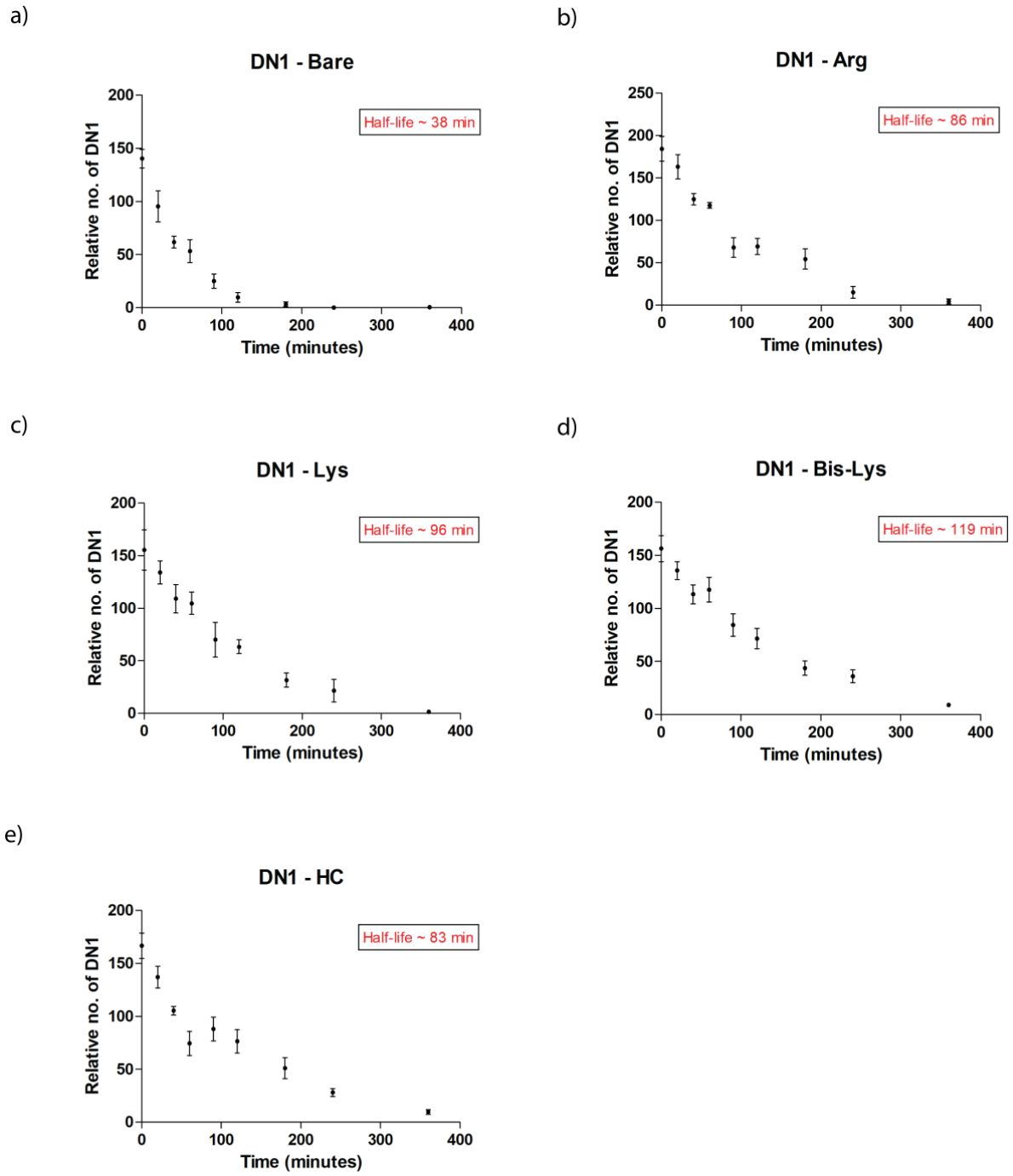

Figure S3.10: Time vs stability plots of DN1 formed with a) no stabilizing agent b) free arginine c) free lysine d) free bis-lysine, and e) hexamine cobalt.

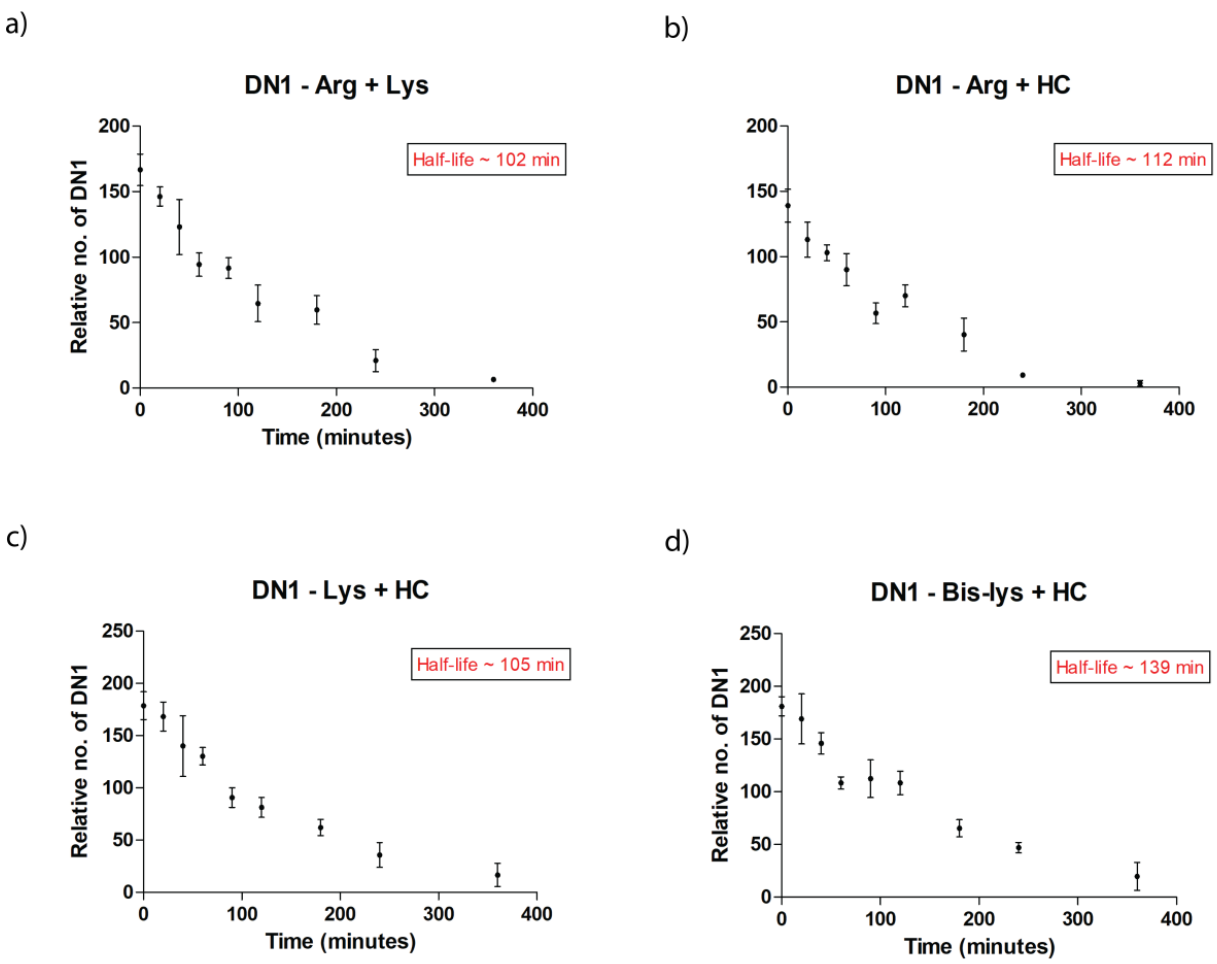

Figure S3.11: Time vs stability plots of DN1 formed with a) free arginine + lysine b) free arginine + hexamine cobalt c) free lysine + hexamine cobalt, and d) free bis-lysine + hexamine cobalt.

S3.8 Melting Temperature Study

The melting points of DNs were determined using a time vs fluorescence method using a PCR instrument. 50 uL of each DN formed with or without stabilizing agents were mixed with SYBR green (the solution is made 2X with respect to SYBR green). The mixture was first heated from 25 °C to 80 °C and then cooled to 25 °C, the complete thermal

program being of 19 hours. The plots were normalized and the melting points were obtained from the first derivative plot. Three sets of sample plots for DN1, DN2 and DN3 controls are shown below.

a)

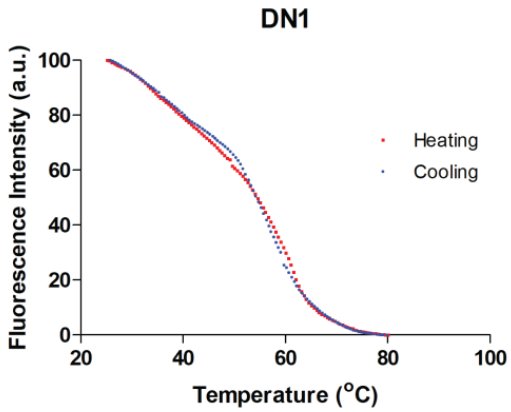
DN1
Fluorescence Intensity (a.u.)
Temperature (°C)
Heating
Cooling

b)

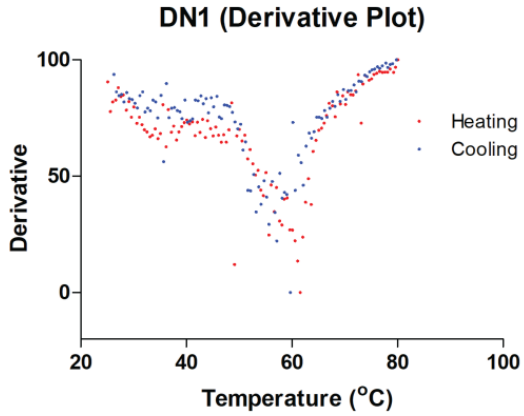
DN1 (Derivative Plot)
Derivative
Temperature (°C)
Heating
Cooling

c)

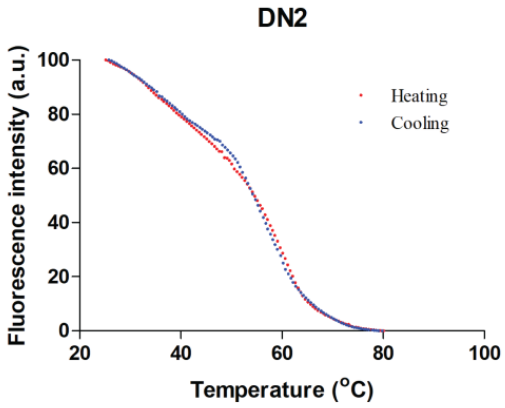
DN2
Fluorescence intensity (a.u.)
Temperature (°C)
Heating
Cooling

d)

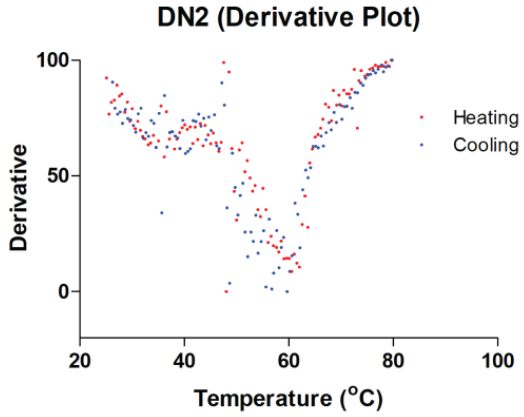
DN2 (Derivative Plot)
Derivative
Temperature (°C)
Heating
Cooling

e)

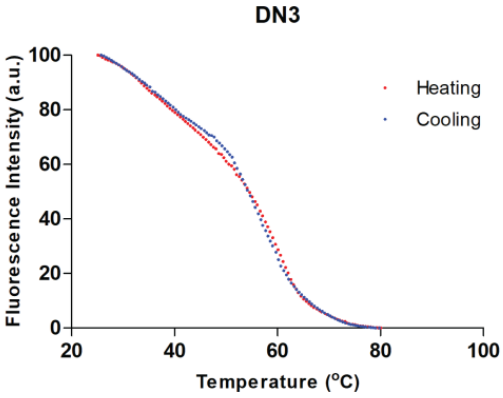
DN3
Fluorescence Intensity (a.u.)
Temperature (°C)
Heating
Cooling

f)

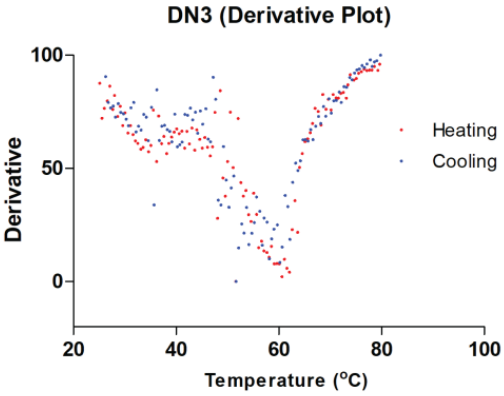
DN3 (Derivative Plot)
Derivative
Temperature (°C)
Heating
Cooling

Figure S3.12: Heating and cooling curves a) DN1 c) DN2 e) DN3. Derivative plots. b) DN1 d) DN2 f) DN3.

APPENDIX C

SUPPLEMENTAL NFORMATION FOR CHAPTER 4

BUILDING SERUM ALBUMIN-COATED DNA NANOSTRUCTURES FOR *IN VIVO* APPLICATIONS

S4.1 Materials and Instruments

All DNA strands were purchased from Integrated DNA technologies. The strands for DNO were bought in 96 well plates and used without any further purification. Rest of the strands were purified using 10% denaturing polyacrylamide gels prior to annealing structures. DBCO-NHS ester was bought from Click Chemistry Tools. Anhydrous DMSO was purchased from Life Technologies. All the linear and branched PEG-azides were bought from Creative PEGWorks. DSPE-PEG (2000) Azide was bought from Avanti Polar Lipids. Propidium iodide and CellTracker CM-Dil dye were bought from ThermoFisher Scientific. RAW264.7 cells used in the cellular uptake study were bought from ATCC. FBS that was used to supplement DMEM cell culture medium was purchased from Gibco Life Technologies. Mouse serum was purchased from Sigma Aldrich. DNase I, Bovine Pancreas was purchased from Gold Biotechnology. Recombinant Human Clusterin alpha chain protein was purchased from Abcam. All the other chemicals that are not mentioned here were bought from Sigma-Aldrich.

For the organic synthesis experiments, all solvents and reagents were obtained from Sigma–Aldrich, TCI America and Matrix Scientific and used without further purification. Analytical thin-layer chromatography (TLC) was performed on aluminum plates precoated with silica gel, also obtained from Sigma–Aldrich. Column chromatography was carried out on Merck 938S silica gel. Proton and carbon NMR spectra were recorded with a Varian 400 MHz NMR spectrometer. Spectra were referenced to the residual solvent peak, and chemical shifts are expressed in ppm from the internal reference peak. All compounds described were of >95% purity. Purity was confirmed by analytical LC/MS recorded with

a Shimadzu system. Elution started with water (95%, +0.1% formic acid) and acetonitrile (5%, +0.1% formic acid) and ended with acetonitrile (95%, 0.1% formic acid) and water (5%, 0.1% formic acid) and used a linear gradient at a flow rate of 0.2 mL/min. The molecular ions $[M]^+$, with intensities in parentheses, are given, followed by peaks corresponding to major fragment losses. Melting points were measured with a MEL-TEMP II melting point apparatus and are reported uncorrected.

Live cell confocal microscopy was done using the Confocal laser scanning microscope Leica TCS SP8. Flow cytometry studies were conducted using the S1000EXi flow cytometer coupled with the CellCapTure software from Stratedigm. The cytometry data were analyzed using the Flowjo v10 software from Flowjo, LLC and plotted using the Prism 5 software from Graphpad. For the time vs stability experiments, the band intensities of gels were measured using the ImageJ software.

S4.2 Synthesis of AAM

S4.2.1 Schematic of the organic synthesis

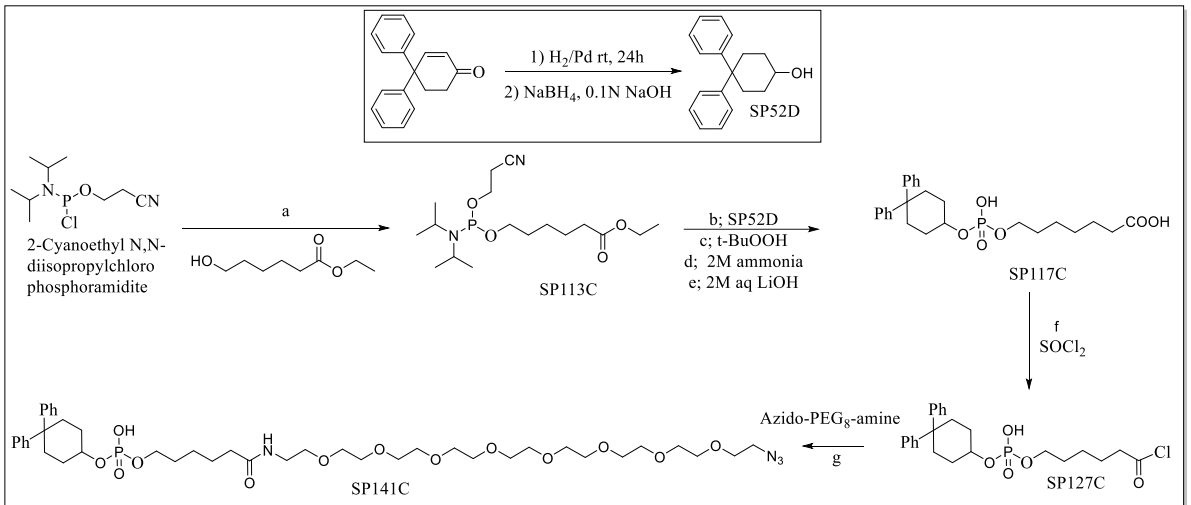

Scheme 1. *Reagents and conditions:* a) iPr_2EtN, CH_2Cl_2, 16h, rt; b) tetrazole, MeCN, 16h, rt; c) 2h, rt; d) 16h, rt; e) 12h, rt; f) 2h, reflux; g) CH_2Cl_2, Et_3N, rt, 16h.

Figure S4.1: Scheme showing the synthesis of AAM (SP141C).

S4.2.2 Synthesis and characterization of the intermediate SP52D

To a suspension of 10% palladium on carbon (25 mg) in THF (8 mL) was added a solution of 4,4-diphenyl-2-cyclohexen-1-one (500 mg, 2mmol) in THF (2 mL). The round-bottom flask was flushed with hydrogen gas, and the system was sealed under a hydrogen atmosphere (1 atm) and stirred vigorously for 24 h. The reaction mixture was filtered through Celite, and filter cake was washed with THF (2 x 5 mL). The filtrate was cooled down to 0 ^{o}C in an ice bath and was treated with sodium borohydride (20 mg, 0.52 mmol). Sodium borohydride was first dissolved in 0.1 M aqueous NaOH (2.5 mL) and cooled to 0 ^{o}C, and then added dropwise to the reaction mixture. The reaction was warmed to room temperature and stirred overnight. The reaction was cooled again to 0 ^{o}C, and quenched

with 3 M aqueous HCl (~2 mL). The mixture was stirred for additional 1 hour in ice bath, and white precipitate formed. The precipitate was filtrated, filter cake was washed with ice-cold water and dried in lyophilizator. The crude was recrystallized in absolute ethanol, yielding intermediate **SP52D** as a white solid.

4,4-diphenylcyclohexan-1-ol (SP52D)

Yield 84%, 420 mg, white solid. ^{1}H NMR (400 MHz, $CDCl_3$): δ 7.31-7.11 (m, 10H), 3.79 (m, 1H), 2.63 (d, *J* = 14 Hz, 2H), 2.09 (t, *J* = 11.2 Hz, 2H), 1.85 (s, 2H), 1.57-1.51 (m, 3H); ^{13}C NMR (100 MHz, $CDCl_3$): δ 148.5, 146.9, 128.5, 128.3, 127.5, 126.7, 125.8, 125.7, 69.7, 45.7, 33.8, 31.7.

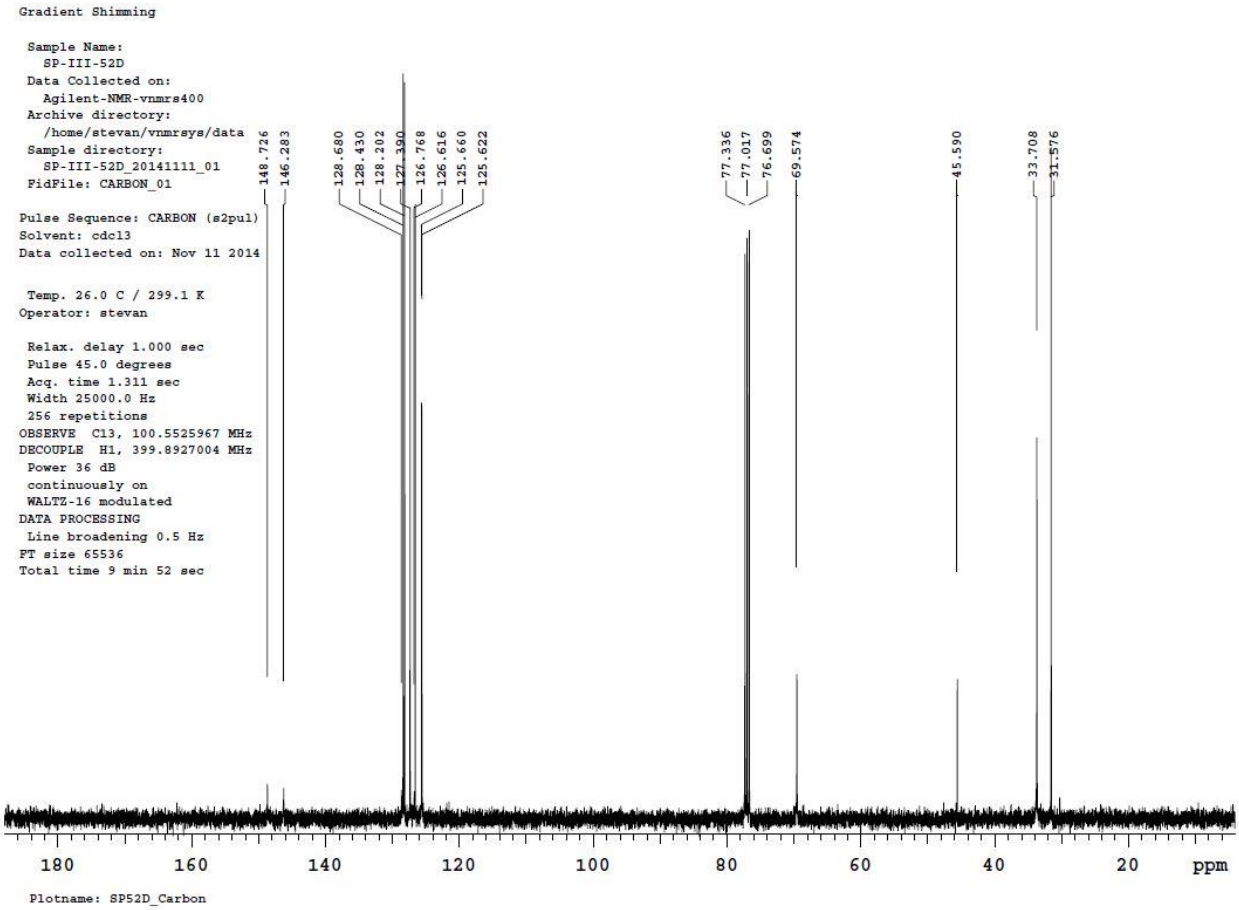

Figure S4.2: ^{13}C NMR for SP52D.

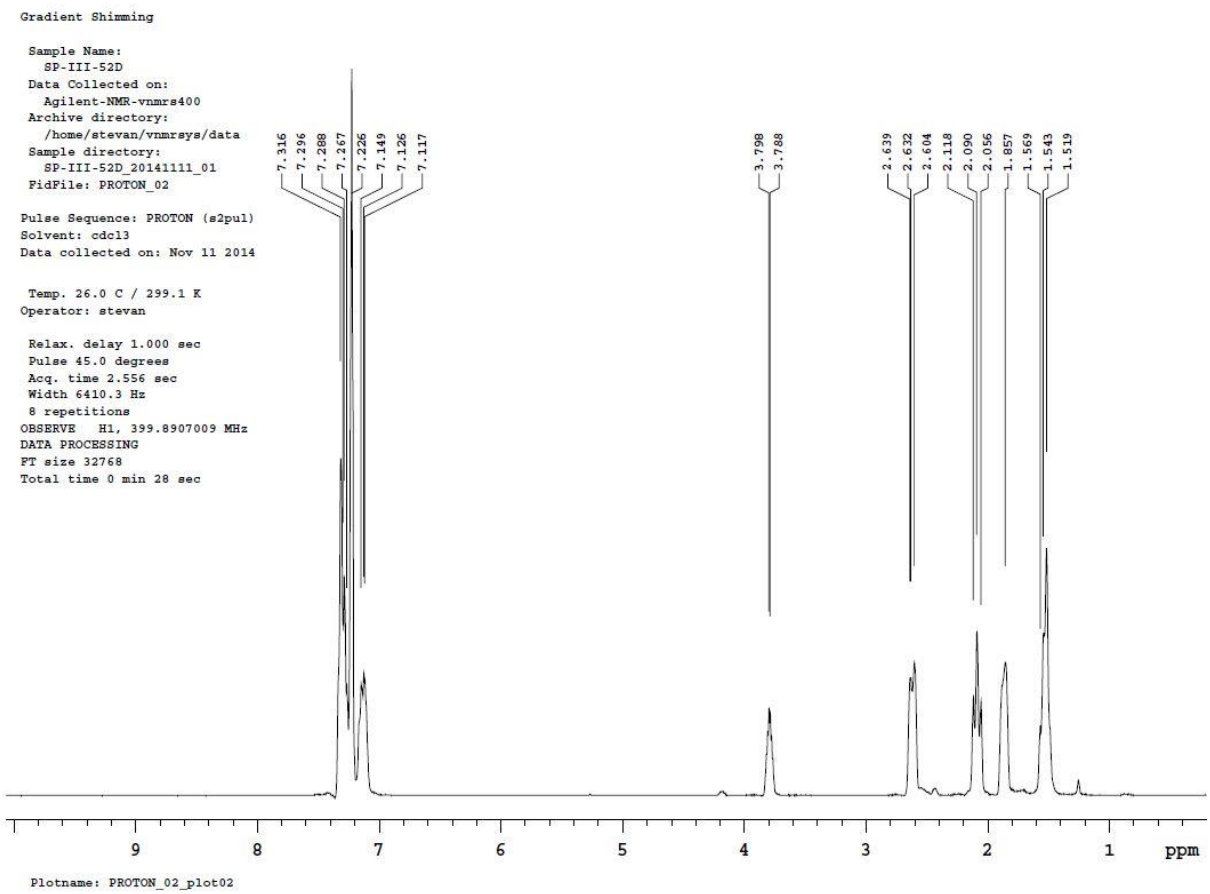

Figure S4.3: ^{1}H NMR for SP52D.

S.4.2.3 Synthesis of albumin-attracting molecule SP141C

Ethyl 6-hydroxyhexanoate (0.5 mL, 3.12 mmol) and diisopropylethylamine (1.03 mL, 6.25 mmol) were dissolved in CH_2Cl_2 (10 mL) and stirred under argon atmosphere. Dropwise was added a solution of 2-cyanoethyl-*N*,*N*-diisopropylchlorophosphoramidite (0.87 mL, 3.9 mmol) in CH_2Cl_2 (2 mL), and the reaction was stirred overnight at room temperature. The reaction was washed with saturated aqueous sodium bicarbonate (25 mL), dried over

anhydrous sodium sulfate, filtered and concentrated under reduced pressure. The crude material was purified by flash chromatography (9:1 hexane/EtOAc with 0.1% Et_3N) to yield the product SP113C as a clear liquid.

Ethyl 6-[(2-cyanoethyl)(N,N-diisopropylamino)phosphino]oxyhexanoate (SP113C)

Yield 38%, 430 mg, clear liquid. ^{1}H NMR (400 MHz, $CDCl_3$): δ 4.12-4.06 (m, 4H), 3.82-3.75 (m, 2H), 3.63-3.53 (m, 2H), 2.61 (t, *J* = 6.4 Hz, 2H), 2.30-2.25 (m, 4H), 1.67-1.58 (m, 6H), 1.41-1.35 (m, 4H), 1.29 (d, *J* = 6.4 Hz, 4H), 1.25-1.19 (m, 12 H), 1.15 (t, *J* = 6.8 Hz, 9H); ^{13}C NMR (100 MHz, $CDCl_3$): δ 173.7, 173.5, 117.7, 63.5, 63.4, 63.1, 60.3, 58.4, 58.2, 46.2, 45.9, 43.1, 34.3, 34.1, 30.9, 30.5, 25.6, 24.7, 23.6, 22.4, 20.4, 14.3, 11.6. ESI-MS: [m/z+H]: 361. (REF 1)

Ethyl 6-[(2-cyanoethyl)(*N*,*N*-diisopropylamino)phosphino]oxyhexanoate, **SP113C** (340 mg, 0.94 mmol) and 4,4- diphenylcyclohexanol, **SP52D** (250 mg, 1 mmol) were dissolved in acetonitrile (10 mL). A solution of 1*H*-tetrazole in acetonitrile (70 mg, 1 mmol) in acetonitrile (2 mL) was added, and the reaction mixture was stirred at room temperature under argon atmosphere overnight. A 70% w/w aqueous solution of *tert*-butylhydroperoxide (1.3 mL, 10 mmol) was added, and the reaction stirred for an additional 2 h, then concentrated under reduced pressure. The resulting residue was concentrated, dissolved in ethyl acetate (25 mL), transferred to separatory funnel and washed with 10% solution of $Na_2S_2O_3$ (2 x 25 mL), followed by washing with saturated aqueous $NaHCO_3$ (25 mL) and brine (25 mL), dried over anhydrous sodium sulfate, filtered and concentrated under reduced pressure. The crude material was purified by flash chromatography (1:1 hexanes/EtOAc with 0.1% Et_3N) to yield a colorless oil. This intermediate was treated with 2 M ammonia in methanol (10 mL) and stirred at room temperature under argon

atmosphere overnight. The reaction was concentrated, and the resulting oil was dissolved in THF (10 mL) and cooled to 0 ^{o}C in an ice bath. A 2M aqueous solution of lithium hydroxide (5 mL) was added, and the reaction was warmed to room temperature and stirred overnight. The reaction was concentrated and the solution was acidified to pH=2 with 2M aqueous HCl, forming a white precipitate that was extracted with ethyl acetate (3 x 25 mL). The organic fractions were combined, dried over anhydrous sodium sulfate, filtered and concentrated to yield the product **SP117C** as a clear, colorless oil. (REF 2)

7-((((4,4-diphenylcyclohexyl)oxy)(hydroxy)phosphoryl)oxy)heptanoic acid (SP117C)

Yield 30%, 125 mg, clear, colorless oil. ^{1}H NMR (400 MHz, $CDCl_3$): δ 8.73 (s, 1H), 7.24-7.20 (m, 8H), 7.13-7.10 (m, 2H), 4.44-4.43 (m, 1H), 3.96 (q, *J* = 6.8 Hz, 2H), 3.73 (t, *J* = 6.8 Hz, 2H), 2.56-2.51 (m, 2H), 2.29 (t, *J* = 7.6 Hz, 2H), 2.20-2.14 (m, 2H), 1.89-1.78 (m, 7H), 1.66-1.56 (m, 4H), 1.42-1.36 (m, 2H). ^{13}C NMR (100 MHz, $CDCl_3$): δ 178.8, 147.2, 146.7, 128.5, 128.4, 127.0, 126.9, 125.8, 125.8, 68.0, 67.2, 67.2, 45.5, 33.9, 32.7, 29.9, 29.8, 29.3, 25.6, 24.9, 24.2. ESI-MS: [m/z]: 446.

Carboxylic acid **SP117C** (64 mg, 0.14 mmol) was refluxed 6 hours in neat $SOCl_2$ (5 mL). Thionyl chloride was evaporated and acid chloride **SP127C** was used for the next step without further purification.

Acid chloride **SP127C** (46 mg, 0.1 mmol) was dissolved in CH_2Cl_2 (5 mL) and Et_3N (40 μL, 0.3 mmol) was added, followed by addition of solution of *O*-(2-Aminoethyl)-*O′*-(2-azidoethyl)heptaethylene glycol (44 mg, 0.1 mmol) in CH_2Cl_2 (2 mL). Reaction mixture was stirred at room temperature overnight under argon atmosphere. Reaction was concentrated under reduced pressure and resulting crude product loaded on column and

flash chromatography was performed in 0-5% methanol:dichloromethane solvent system. Final product **SP141C** was obtained as colorless thick oil.

1-azido-28-oxo-3,6,9,12,15,18,21,24-octaoxa-27-azatritriacontan-33-yl (4,4-diphenylcyclohexyl) hydrogen phosphate (SP141C)

Yield 38%, 33 mg, clear, colorless thick oil. ^{1}H NMR (400 MHz, $CDCl_3$): δ 7.23-7.19 (s, 8H), 7.09 (s, 2H), 4.32 (s, 1H), 3.86 (s, 4H), 3.62-3.51 (m, 32H), 3.38-3.35 (m, 4H), 2.49 (s, 2H), 2.13 (s, 3H), 1.81-1.57 (m, 6H), 1.33-1.23 (m, 2H). ESI-MS: [m/z+1]: 867.

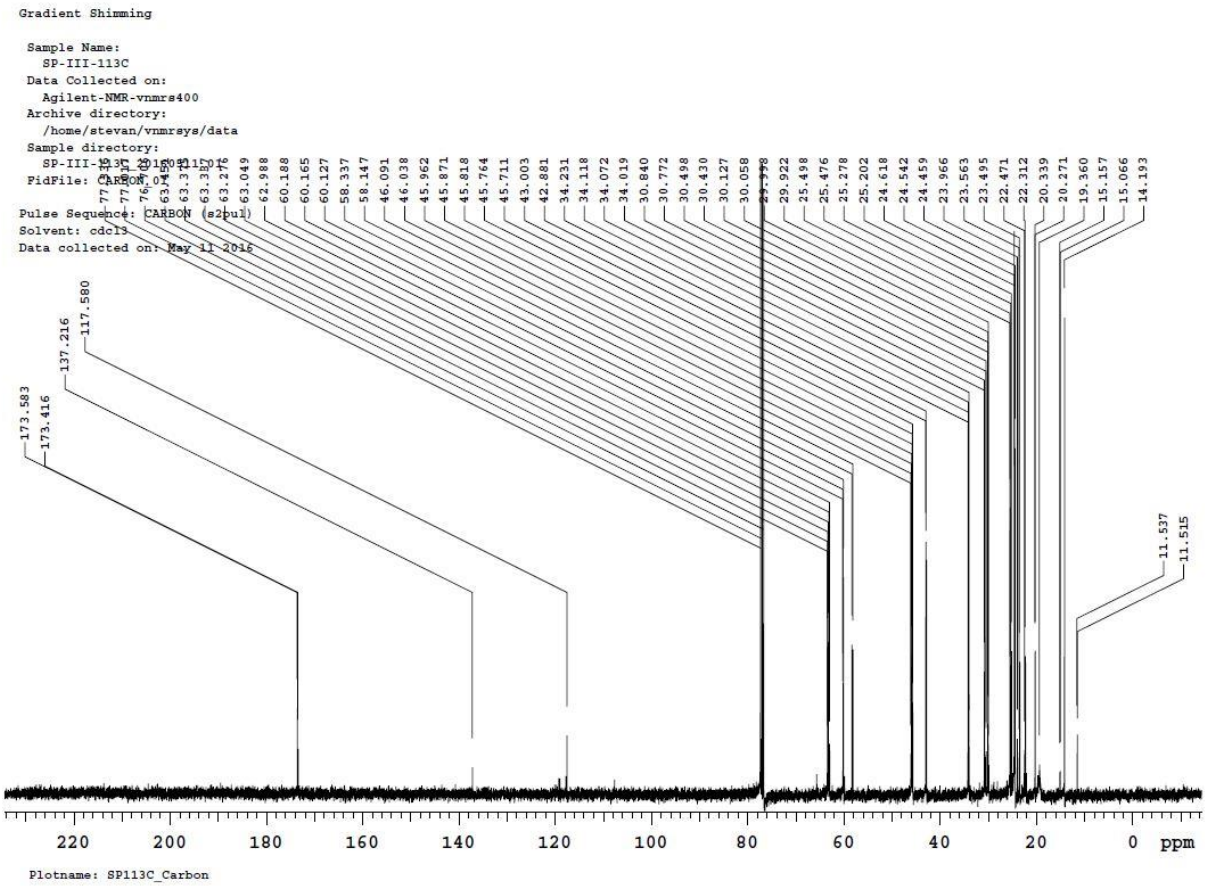

Figure S4.4: ^{13}C NMR for SP113C.

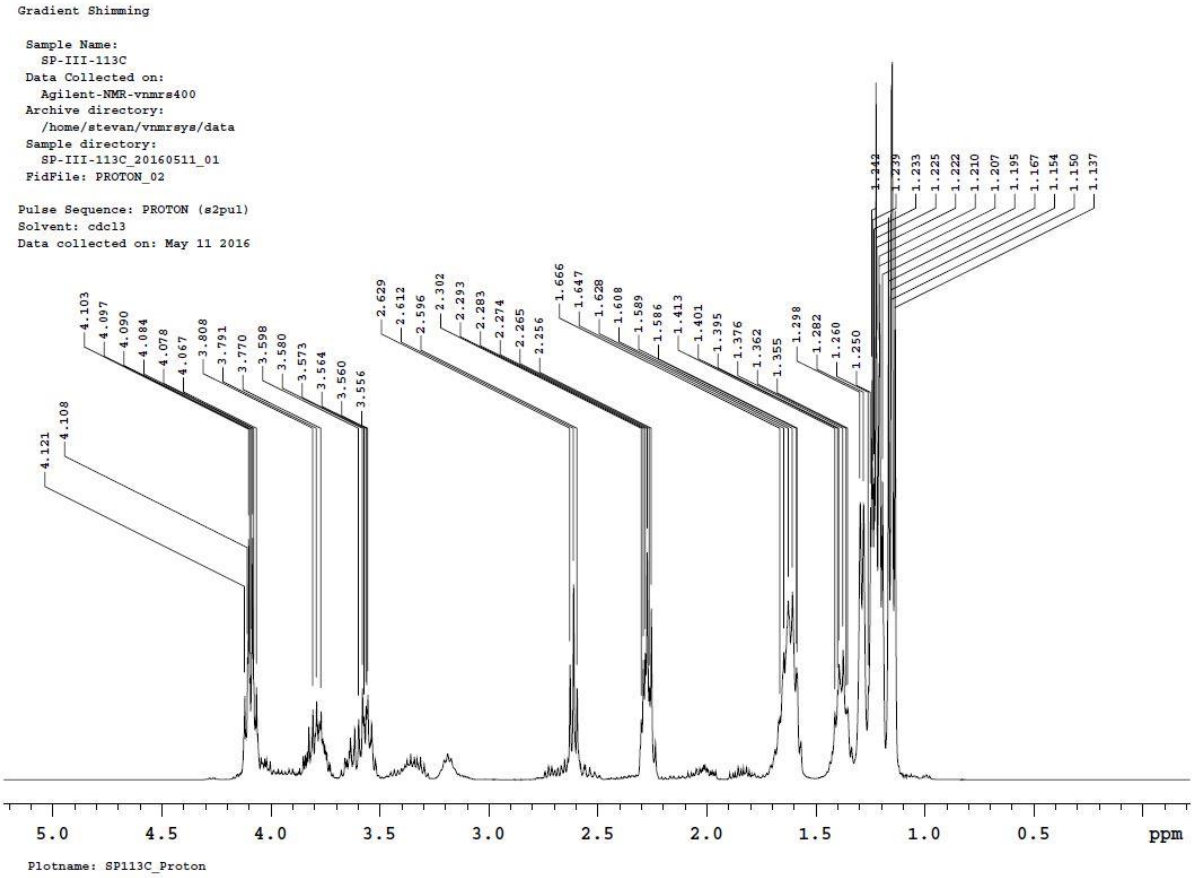

Figure S4.5: ^{1}H NMR for SP113C.

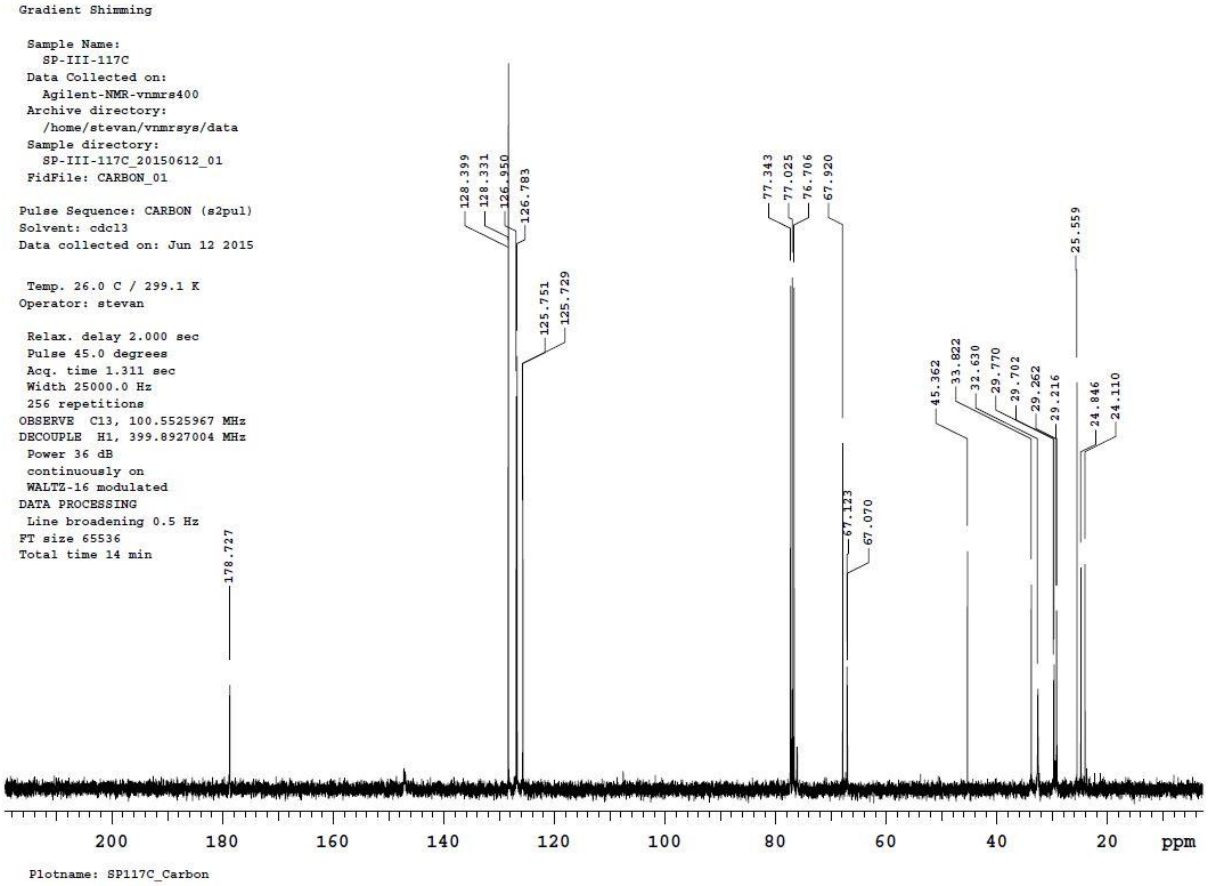

Figure S4.6: ^{13}C NMR for SP117C.

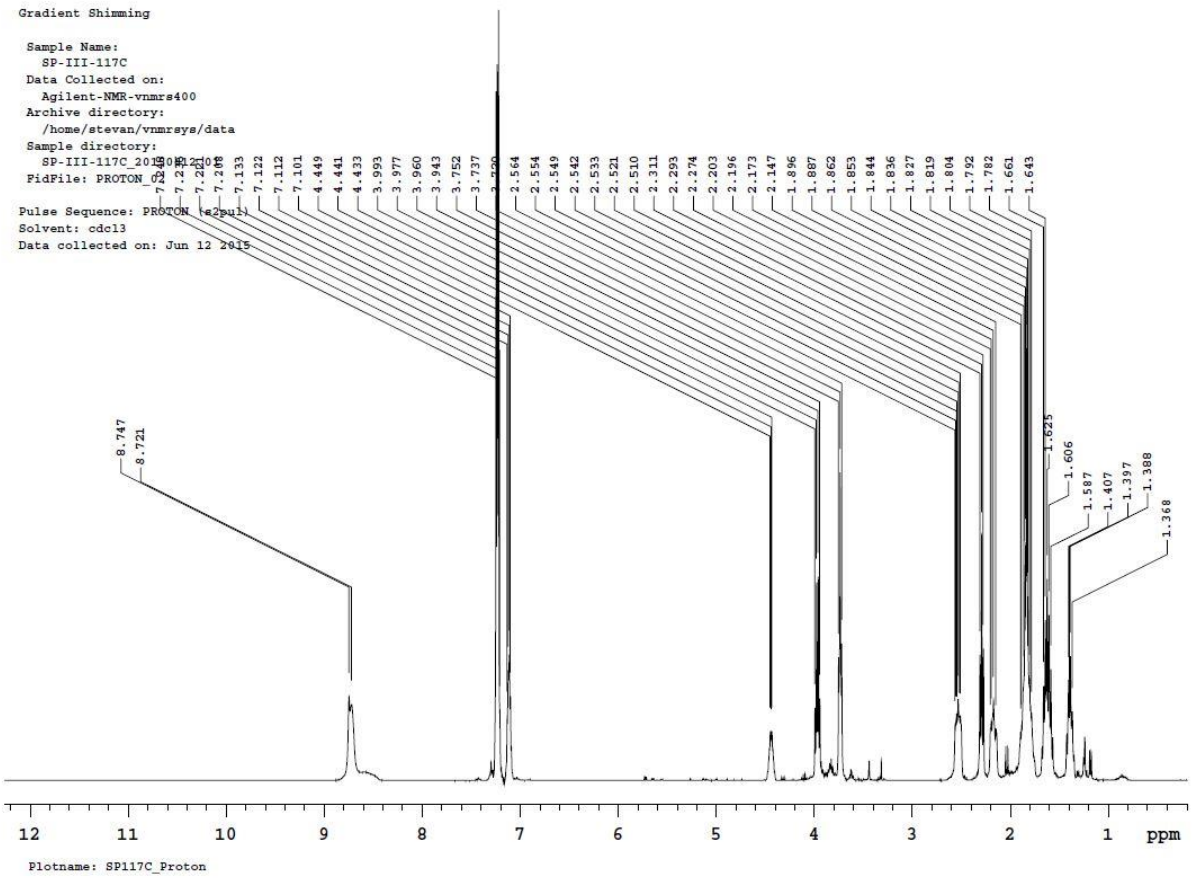

Figure S4.7: ^{1}H NMR for SP117C.

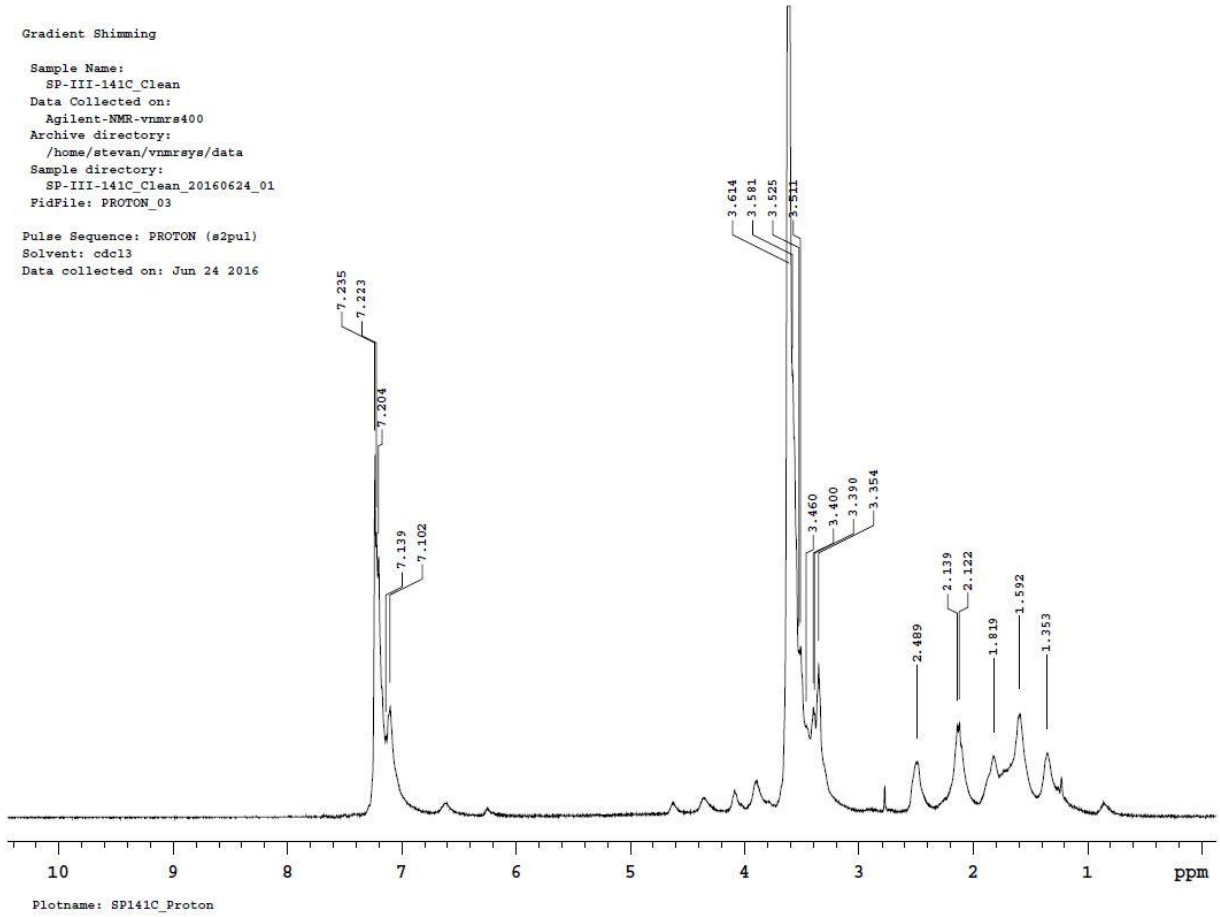

Figure S4.8: ^{1}H NMR for SP141C.

REF 1: S. Raddatz, J. Mueller-Ibeler, J. Kluge, L. Wab, G. Burdinski, J. R. Havens, T. J. Onofrey, D.Wang, M. Schweitzer, *Nucleic Acids Res.* **2002**, *30*, 4793.

REF 2: ChemMedChem. 2014 Oct;9(10):2223-6. doi: 10.1002/cmdc.201402212. Epub 2014 Jul 23.

S4.3 Details of Td and DNO structures

S.4.3.1 Td

S4.3.1.1 Strands for Td

Strand 1: AGG CAC CAT CGT AGG TTT C TTG CCA GGC ACC ATC GTA GGT TTCT TGC CAG GCA CCA TCG TAG GTT T CTT GCC

Strand 2: CAG AGG CGC TGC AAG CCT ACG ATG GAC ACG GTA ACG ACT

Strand 3: AGC AAC CTG CCT GTT AGC GCC TCT GTT TTT TCG ATC ACG TAG CAC AGC AT

Strand 4: /5Alex488N/TTA CCG TGT GGT TGC TAG TCG TT

The complementary of the single stranded handle (labeled in red) with strand 3 was named strand 5 and it had an amine modification at the 5' end.

Strand 5: /5AmMC12/AT GCT GTG CTA CGT GAT CGA

The Alexa fluor 488 dye was attached to strand 4 for flow cytometry studies. For all other experiments the unlabeled strand was used.

S4.3.1.2 Schematic for Td

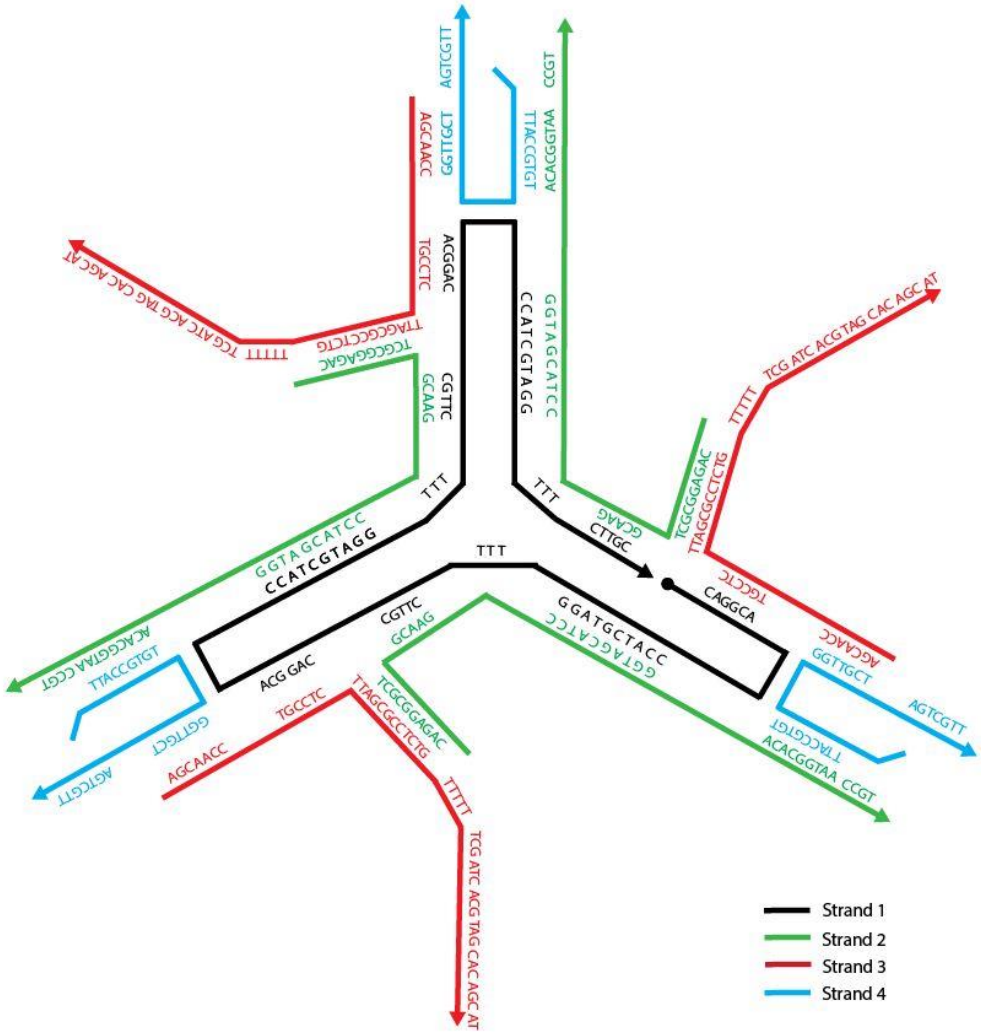

Figure S4.9: Schematic showing one unit of Td. 4 similar units assemble together through sticky end hybridization to build up the complete Td.

S.4.3.2 DNO

S4.3.2.1 Schematic for DNO

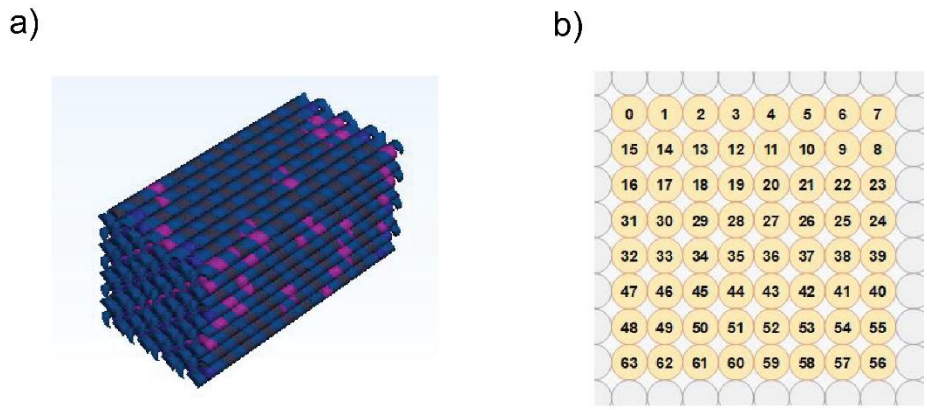

Figure S4.10: caDNAno image of DNO. a) DNO b) caDNAno image showing the arrangement of double helices constituting DNO.

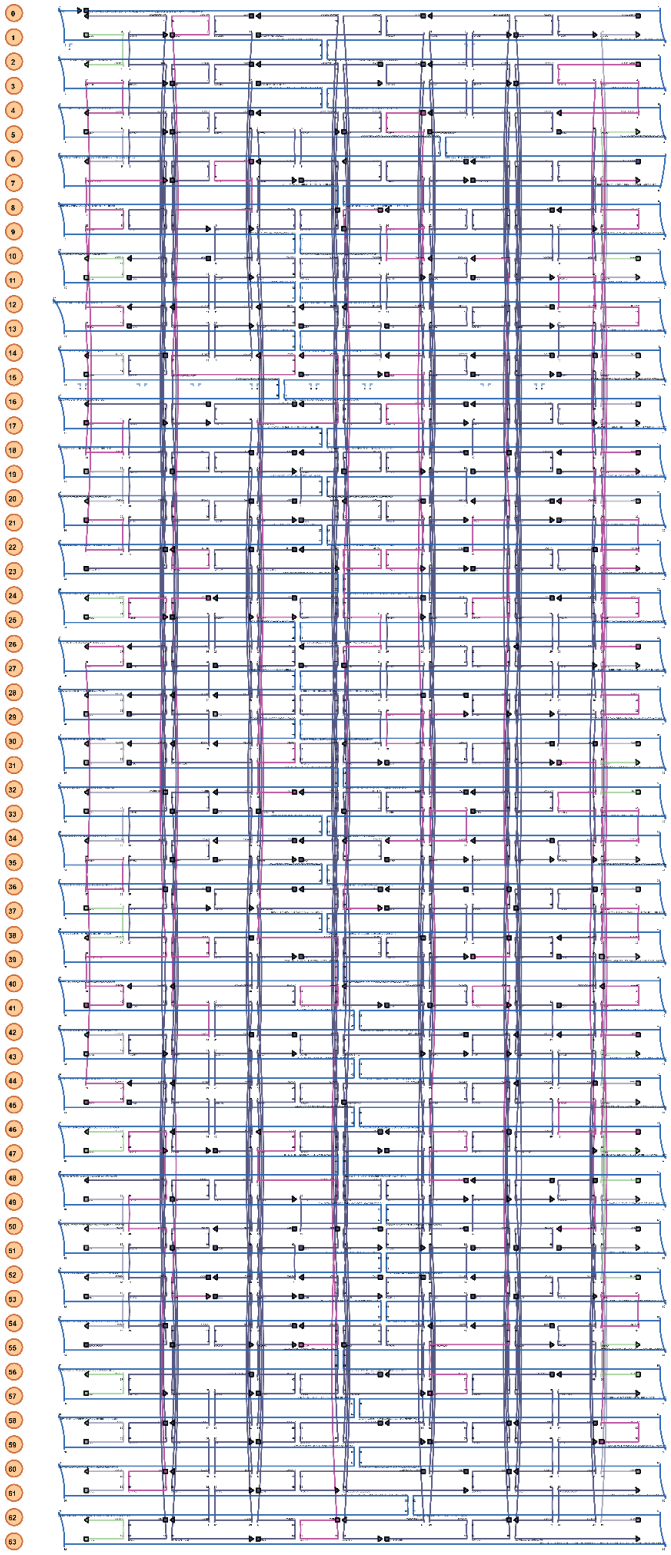

Figure S4.11: caDNAno design of DNO.

S4.3.2.2 Sequences for DNO

Start	End	Sequence
16[111]	15[111]	CATATGTATTTTAACC
20[111]	11[111]	TAAAAATTAGCGCCAT
13[16]	1[23]	AGAGATAGTAGAGCTTATCAAGTT
38[39]	40[24]	GACCGTGTTGTTTAGTAAAGCCAACGCTCAAC
50[63]	61[79]	GAGCGTCTGCAAGGCCGGAAACTCAGAGCCGC
11[16]	3[23]	ATTTTGACGCGCGTAAGAGAAAGG
58[63]	52[48]	TGCCTAACGCAAAGACGAGGGAGGCATAAAAA
44[103]	53[103]	AGCATCGGAAAATACGAACCCATGACCCTCAT
50[79]	35[79]	ATTTTCTGGCTTGCAGGCTACAGAGCTCATTA
59[8]	58[8]	TTACCAGCTAGAAAAT
29[16]	17[23]	TTACAAAAACCTCAAACCGCCTGC
60[87]	49[87]	CCTTGATACACCAGAAGTAAATGACAACAGTT
3[88]	13[95]	GGGTGGTTCACCGCCTGATTGACC
29[8]	28[8]	ATACCAAGTCGCCTGA
35[64]	51[63]	AAGAACTGGGCTTTGAGGACTTCCTTTACAGA
60[79]	43[79]	TTCACAAAGCCTGTAGTTCGTCACTGAGGAAG
60[71]	61[55]	CAAATAAATCCTCGGTAAATATTGTACCATTA
28[71]	36[64]	GAGCTTCAGTCAGGATTAATCATT
62[111]	49[111]	CAGAGCCGAGAAAGGA
51[8]	52[8]	AAATAAGAAACACCCT
20[39]	25[39]	ATCTTTAGAAGTATTACAAAATTATGGAAGGG
48[103]	61[111]	GAATAATAGTGAGAATCCACCCTCAGAGCCGCCGCCAGCA
15[80]	0[72]	AAATTTTTAGTGTTGTTCCAGTTT
2[71]	11[71]	CAGCAAGCAGGCGGTTGACGACGACAGCTTTC

53[8]	54[8]	CAGAGGGTAAGCCCTT
46[63]	63[63]	ATATACACACGCTAACGCTCCAAAAGCGTTTG
50[111]	45[111]	GTTTTGTCATCGTCAC
32[23]	32[8]	ACCTTGCTTCTGTAAA
33[40]	16[48]	ATAGCGATAGCTTTACGAGAATGATAATGGAACAAATATT
7[48]	6[56]	CTGTCCATAGCTCGAAGCGGGAGC
32[79]	17[79]	ACCAAAATGAGGGGGTAATGCTTTAGCAAACA
56[39]	57[23]	CCCAAAAGAACTGGCATGATTAAGAAACGTAG
22[23]	10[16]	CGAACGTTACATTTGATGCAACAG
42[47]	26[48]	TAAAGTACACCTAAATTTAATTACCAACTAAA
51[80]	34[80]	CATTCCACTAGCAACGGGAGTTAAACAGGTAG
19[80]	1[87]	GACAGTCATCTGCCAGAAACGGCGGGCCCTGATTGATGGT
3[24]	17[31]	AAGGGAAGCCCCGATTAACCCTTCCAATATTTAACAGTGC
55[24]	58[24]	AACAAAGTAATAGCTAAAAATACAATTTTGTC
42[39]	55[39]	CGACAAAATTAGGCAGGAAATAGCTACCAGAA
30[111]	17[111]	AATCGTCAAAAACTAG
41[64]	56[64]	AGCGATTACAGAACCGTCAGTACCGGATTAGG
36[103]	42[96]	AAATTGGGCTTGCCCTTAAAACGA
5[8]	6[8]	CTTAATGCTACGCCAG
19[56]	30[56]	TTCAAAAGAGGCTATCCAAAAATCCAGAAAAC
43[8]	42[8]	ACAACATGCCAGACGA
15[8]	14[8]	GCGAACTGCTATTAGT
62[23]	48[8]	CAGAATCAGCGCGTTTGAGGTTTTGAAGCCTT
30[103]	35[103]	TAAATATTAAAGCGGAACGGAACAGGGAAGAA
16[79]	2[72]	CCAAAAACTTCGCATTGTAGCCAGAATCCTGTGAGAGTTG
22[103]	24[96]	GCAAAGAATAGCATTAACATTTCG
38[71]	40[56]	ACAAGAACCATAAGGGCGGAACGAGGCGCAGA

2[63]	31[63]	GGTCCACGACCCGTCGAACATTAATTGCCTGATGTATAAGAAAAGAAG
18[47]	12[40]	AAATCTAAAAGCGTAATTACATTG
23[80]	6[80]	ATTCTACTGCAGGTCGGTAACGCCAAAGTGTA
27[32]	37[39]	GAATATACATGCAAATATCTTCTG
36[23]	28[16]	AAGACAAACTTTTTAATAACGGAT
36[31]	44[24]	CCAATCGCATGCAGAACCTAATTT
21[48]	4[40]	AAACACGGGCTGGCGAAAGATCGCCAAAGGGCGCTGGCAA
52[31]	60[24]	ACGGGAGACAAAAGGGAAAGGTGA
50[55]	32[48]	TTCCAGAGTCTTACCATCATCGAGTAAGAACGACAGTACA
31[8]	30[8]	AATTAATTAAACATCA
1[88]	15[95]	GGTTCCGATAGGGTTGGTTAAATC
55[8]	40[16]	AGTAAGCAGATAGCCGAGTAGGGC
51[32]	59[39]	ACGTCAAATATTCATTCGACATTC
35[48]	18[48]	AACTATATCAGACCGGCCATAAATAGGATGAA
36[87]	29[87]	GGTTTAATTACCAGTCTATCGCGTTATTATAG
50[47]	35[47]	CCTAATTTGGTATTAAAAAAATAAGGTTATAT
59[40]	53[47]	AACCGATTACCACGGATAACCCAC
5[96]	9[103]	TAACTCACCAACTGTTCCCAGTCA
41[16]	26[16]	AACGCCAAAGGCGTTATATTTTAGTAAAACAG
22[79]	7[79]	ATAAAGCCTAAGTTGGACTCTAGACATGGTCA
36[79]	21[79]	TTCAACTTTAGAGAGTGTAGCTCAATGACCCT
61[8]	60[8]	ATTTGGGACGTCACCG
18[39]	28[32]	AGCATCACCAGTTGAAACATCGGG
23[8]	5[23]	GAGTAACATTATCATTTGATTAGTGAACTCAAAGGAACGGGCCGCTAC
28[79]	10[72]	TTTAATTCAGGCCGGATGCAATGCCGGCACCGGCGGGCCT
5[24]	12[24]	AGGGCGCGGTCACGCTGCTCAATCACCAGTCA
8[55]	5[55]	CACGCAAAAAGGGGGATAAACAGGACGAGCAC

18[79]	4[72]	TTTGAGAGGTGGGAACTTTGAGGGTGCGTATTTGCCAGCT
24[47]	23[55]	TCATATTCCCACCAGAAGGAGCGG
57[40]	55[47]	GGTGGCAAACGGAATAGGAAACCG
53[88]	60[88]	GAGCCACCTACCGTAATGAATTTAACGATTGG
6[111]	8[96]	ACACAACATACGAGCCGAAATTGTCCAAGCTT
46[87]	32[80]	ACAACCATATCAGCTTCGATAAAA
15[96]	17[103]	AGCTCATTCCCCGGTTGTAATCGT
27[56]	34[56]	TCCAACAGAAGCGAACGCGATTTTAGATTTAG
3[40]	3[63]	AGGAGCGGGCGCTCGCGCGGGGAG
53[80]	43[87]	CACCCTCAAAAGAATATTTCCATT
20[71]	25[71]	CTGAGTAAAAAACATTACATGTTTTTTCATTC
7[24]	9[31]	AGTGAGGCTTTTAGACACTATCGG
47[32]	61[39]	GGCTTATCACCTCCCGACAATTTTCCGTAATCTCACCAGT
30[95]	47[103]	CATTGAATAAGGAATTCCAGACGAGCTTTCGAGGTGAATT
49[24]	63[39]	ACCCAGCTACTTGCGGTCATCGGCATTTTCGG
54[95]	58[88]	CAGGAGGTTGCCCCCTAGTGTACT
0[39]	13[39]	TCCAACGTTCGAGGTGGGCACAGATGACCTGA
55[56]	57[71]	GGTTTTGCCCAATAATAGATGAGTAACAGTGC
33[8]	34[8]	TTAATTAACAAAATCA
0[111]	1[103]	AAAGAATAGCCCGAGAAATCGGCA
7[80]	21[95]	TAGCTGTTTCCTGTGTGGAAGCATAGGGTTTTGGGAAGGGTTTGCGGG
44[111]	35[111]	CGAAAGACAAATCTAC
27[16]	12[16]	AGGTTTAAACAACTAATCAGTTGGCACGACCA
41[72]	39[79]	TACCAAGCTACTTAGCAACCGAAC
6[79]	8[64]	AAGCCTTAGAATCAGATTCGTAATGGATCCCC
45[56]	51[71]	CCGTTCGGTCGCTGAGTATGGGATACTACAAC
51[48]	34[48]	TAGCAGCCTGAACAAGACCAAGTAGAAAGATT

37[64]	53[63]	ACGTAACACACTCATCTTTGAATAAGTTAAGC
14[95]	31[95]	CGCGTCTGGATGAACGGATAATCAAATGTTTA
58[87]	52[80]	GGTAATAAGCAGTCTCCACTGAGT
27[48]	12[48]	AAGCAAACTAAGGTTAAGGAAAGAGCCTCAGG
34[95]	49[95]	ACATTATTAGGCCGCTCAATGACATCAGCGGA
36[47]	21[47]	AAATGCTGAGTAACAGTACCATATGACTTTAC
54[23]	43[23]	TCTTACCGAATTGAGCAATTCTGTTTCAGCTA
9[56]	20[56]	TGTGCTGCTTACGCCATTGTACCATGTGTAGG
51[96]	59[103]	CTCATAGTCAGGTCAGCCGTTCCA
39[48]	22[48]	CGTTATACAATTATCAGTACGGTGAATATTCG
13[64]	19[71]	GATTCTCCATCTACAAGGTGAGAA
33[32]	50[32]	TTGAAAACAGCCGTTTCAAGAACGGCCAGTTA
60[111]	51[111]	GGTTGAGGTAGCGTAA
36[63]	43[71]	GTGAATTAAAGAAAGACTTTTTCA
22[39]	24[32]	TATTAAATCAAAGAAACTGATTAT
42[79]	23[79]	CACTAAAAAAGCTGCTTAATCTTGCATATAACTGTTTAGCTGGCATCA
35[32]	52[32]	TTAGGTTGTATCCCATCGCGCCTGCGCATTAG
14[103]	18[96]	AAATAATTGTAATGGGTTAATGCC
12[95]	29[95]	ACCGTGCAAATCACCAGGAGAGGGTCAGAAGC
8[95]	26[88]	GCATGCCTAATAGTAGTTAGCAAACCCAATTCTGCTGAAT
10[31]	28[24]	CCAGCCATGGATTTAGGAGCACTACGTCAGATAGAAACAA
24[95]	42[88]	CAAATGGTTTTGAAAGTGACCTTCAAGTACAAAAGAGGCA
15[48]	0[40]	GTAAACGTATTAAAGAACGTGGAC
24[71]	41[63]	TATATTTTCATTTGGGCGGTCAATCGGATATTGTACCCCC
29[32]	34[32]	AGGCGAATGAGAAGAG
37[88]	44[88]	GAATAAGGCTTGAGATAAACGGGTAACGAGGG
2[39]	11[39]	AAGGGAGCAAAGCGAAGCAGATTCGTCTGAAA

53[48]	36[48]	AAGAATTGAGAGAATACAATAGATCCTTATGT
4[39]	9[39]	GTGTAGCGTACTATGGTATTACCGCCTTGCTG
39[104]	39[111]	TGAACGGT
63[40]	49[47]	TCATAGCCTAGCAGCAATCCTGAA
54[47]	39[47]	GAAACAATAGGCATTTACCAGTATATCATATG
48[95]	63[111]	ATTTTTTCCGGAACCAGAGCCACCACCGGAAC
19[24]	30[24]	CAAATCAACTTGCTGATCGCGCAGAAGAAGAT
1[40]	15[63]	CCGTAAAGCACTAGTTTGCCCCAGAGTCCACTTAATATTT
13[48]	2[40]	GAGTAACACTGAATCGGAACCCTA
51[24]	62[24]	TTTGTTTACAAAATAACAGCAAAAAGTAGCGA
56[63]	54[48]	ATTAGCGGCAATAATACATATAAAAAGAGCAA
20[47]	6[40]	TCTAAAATTGGATTATCAGAACAATTGCTTTGAGGCCGAT
59[72]	54[72]	TGGAAAGCGTTTTAACAGAACCGCGCCACCCT
0[71]	14[64]	GGAACAAGCAGGCGAACTTTCATC
31[64]	46[64]	TTTTGCCAAGCGAGAGACTAATGCCATAACCG
20[95]	35[95]	CCTCATATTTGCTCCTACTTCAAAAGGACGTT
39[96]	55[95]	AGGACAGACGAAATCCGCGACCTGTCGAGAGG
19[96]	27[103]	TCAATATGCCCGAAAGTTTGATAA
41[96]	56[96]	CGGAGATTACCGTACTGTTGATATAAGTATTA
22[47]	7[47]	ACAACTCGGTAATATCTTAACCGTAAAAGAGT
33[24]	47[31]	TAGAATCCAGTGAATAATATAGAA
51[88]	62[88]	AGACAGCCAGACGTTACCACCACCAGAACCGC
16[31]	32[32]	CAGCAGAACAATTTCATTTGAATTTATATGTG
25[24]	37[31]	CTGAATAATTTGCACGTTAATTTC
45[16]	30[16]	TCTTTCCTGAATTTATTTTTCCCTGATGAAAC
19[8]	20[8]	ATATCTGGTAGATTAG
36[111]	27[111]	CGAGTAGTGAGGTCAT

35[24]	46[24]	CCTCCGGCTCAATAGTTATCATTCTTATTTTC
47[64]	62[56]	TTAATTGTAAAAAAAGTTTGCTAAACCCGTCACCAATGAA
5[72]	11[95]	TCGTGGGGTGCCTAATGAGTGAGCGTCGGGAAGCCGGAAA
21[96]	38[96]	AGAAGCCTAGCTTAATTGCGAACGAGGCTGGC
16[47]	30[32]	TAACCGAACGAACCACCACGCTGACTGAGCAA
11[80]	3[87]	CTTCTGGTACCTGTCGGGGCGCCA
58[23]	44[16]	ACAATCAAGCCAAAGAATTAACTGAACGATTTACGAGCAT
56[95]	54[80]	AGAGGCTGAGACTCCTACAGTTAATTAGTACC
34[47]	19[47]	AAGACGCTTATTCATTTACCTTTTAGGAATTG
63[64]	49[79]	CCATCTTTTCATAATCGAGCCACCACAACTTT
33[56]	47[63]	CACATTCAGCTTTTGCAGGAGCCT
58[103]	57[111]	GATACAGGGCCTATTTCGGAACCT
62[87]	48[80]	CACCCTCAAAAATCACACGTTGAA
49[8]	50[8]	TTAGTTGCATTATTTA
38[87]	20[80]	ATCAAGAGCATTCAGTATAATGCTACCTTTAAATTTTAAA
33[80]	16[80]	AACGCCAACCCCCTCAAATAGTAAGAAAAGCC
61[40]	43[47]	AGCACCATACGGAAATAATGAAAACAGGGAAGTTTATCAA
14[111]	1[111]	GCCATCAAAAATCCCT
14[23]	0[8]	TTGAATGGATAGCCCTGAAAAACCGTCTATCA
31[16]	16[8]	ACATTTAAGATAAAACAGAGGTGA
5[56]	12[56]	GTATAACGGAATCGGCACTCCAGCCAGTATCG
53[32]	57[39]	CAGAGAGAATAAGTTTTACATAAA
52[71]	58[64]	CAGTACAACCACCCTCGGGGTCAG
18[87]	14[80]	TAGCTATTAGAGAATCGCCTTCCT
52[63]	59[71]	GAGAATAAGAAATTAAAGCCAGAA
63[8]	62[8]	AGACTGTAAGTTTGCC

56[111]	55[111]	AAACATGAAAGTATAG
37[8]	38[8]	TTCAAATAAATAAGAA
48[111]	47[111]	GGAATTGCTCTTAAAC
57[8]	56[8]	ATGTTAGCACTCCTTA
10[111]	5[111]	AGGCTGCGATTAATTG
25[8]	24[8]	TGTTTGGAATCAATAT
32[111]	31[111]	TCATAACCAGCGTCCA
11[8]	10[8]	ATACCTACGAAAAACG
47[8]	46[8]	ATAGCAAGAATCATTA
1[8]	2[8]	TCACCCAAGACGGGGA
52[111]	43[111]	CCAATAGGTAATGCCA
4[71]	23[71]	GCATTAATTGCTTTCCCTTCGCTAAAGGCGATTCAGAGCATGAAAAGG
2[111]	20[96]	ACAGCTGATTGCCCTTTTTCTTTTGCATCGTACCAGGCAATTTAGAAC
57[72]	41[87]	CCGTATAACAAGAGAAAGGCGGATAAGTGCCGCTCCATGTGCGAAACA
42[111]	23[111]	CACCAACCGACGAGAAAGGCGCATAGTAGATTCATTAGATACATCCAA
39[80]	10[80]	TGACCAACCAATAACCAGTTGATTATTAAGCAGTAATACTCGATCGGT
48[79]	29[79]	AATCTCCAATCGGTTTCGCCCACGAGATACATAAAGATTCACCCTGAC
31[96]	50[96]	GACTGGATCTCGTTTAACGAGGCATGCGCCGATTTGCGGGGTCTTTCC
21[8]	7[23]	TAGATAATATTAATTTGAGTAGAAAATAACATAAGTGTTTTTATAATC
41[8]	25[23]	TATTTAACTTAATTGAGAATCATAATTACTAGGGCAATTCTTATACTT
60[23]	47[23]	ATTATCACATTAGAGCACAGCCATTATTTTGCATCGTAGGCAAATCAG
1[24]	14[40]	TTTTGGGGCAAAGGGCAAAACATCGCCATTAAAAATAATTGAATACGT

The green strands are modified with a handle at their five prime end for hybridization with a strand containing alexafluor488 dye at its 5’ end. The modified sequences are:

Start	End	Sequence
63[8]	62[8]	**AAT GGC ACA CCA ACG ATC AGC AA**AGACTGTAAGTTTGCC
56[111]	55[111]	**AAT GGC ACA CCA ACG ATC AGC AA**AAACATGAAAGTATAG
37[8]	38[8]	**AAT GGC ACA CCA ACG ATC AGC AA**TTCAAATAAATAAGAA

48[111]	47[111]	**AAT GGC ACA CCA ACG ATC AGC AA**GGAATTGCTCTTAAAC
57[8]	56[8]	**AAT GGC ACA CCA ACG ATC AGC AA**ATGTTAGCACTCCTTA
10[111]	5[111]	**AAT GGC ACA CCA ACG ATC AGC AA**AGGCTGCGATTAATTG
25[8]	24[8]	**AAT GGC ACA CCA ACG ATC AGC AA**TGTTTGGAATCAATAT
32[111]	31[111]	**AAT GGC ACA CCA ACG ATC AGC AA**TCATAACCAGCGTCCA
11[8]	10[8]	**AAT GGC ACA CCA ACG ATC AGC AA**ATACCTACGAAAAACG
47[8]	46[8]	**AAT GGC ACA CCA ACG ATC AGC AA**ATAGCAAGAATCATTA
1[8]	2[8]	**AAT GGC ACA CCA ACG ATC AGC AA**TCACCCAAGACGGGGA
52[111]	43[111]	**AAT GGC ACA CCA ACG ATC AGC AA**CCAATAGGTAATGCCA

The pink strands are modified with a handle at their five prime end for further attachment of PEGs and DSPE-PEG. The modified sequences are:

Start	End	Sequence
4[71]	23[71]	**TCG ATC ACG TAG CAC AGC** **AT**GCATTAATTGCTTTCCCTTCGCTAAAGGCGATTCAGAGC ATGAAAAGG
2[111]	20[96]	**TCG ATC ACG TAG CAC AGC** **AT**ACAGCTGATTGCCCTTTTTCTTTTGCATCGTACCAGGCAATTTAGAAC
57[72]	41[87]	**TCG ATC ACG TAG CAC AGC** **AT**CCGTATAACAAGAGAAAGGCGGATAAGTGCCG CTCCATGTGCGAAACA
42[111]	23[111]	**TCG ATC ACG TAG CAC AGC** **AT**CACCAACCGACGAGAAAGGCGCATAGTAGATTCATTAGATACATCCAA
39[80]	10[80]	**TCG ATC ACG TAG CAC AGC** **AT**TGACCAACCAATAACCAGTTGATTATTAAGCAGTAATACTCGATCGGT
48[79]	29[79]	**TCG ATC ACG TAG CAC AGC** **AT**AATCTCCAATCGGTTTCGCCCACGAGATACATAAAG

		ATTCACCCTGAC
31[96]	50[96]	**TCG ATC ACG TAG CAC AGC**
		ATGACTGGATCTCGTTTAACGAGGCATGCGCCGATTTGCGGGGTCTTTCC
21[8]	7[23]	**TCG ATC ACG TAG CAC AGC**
		ATTAGATAATATTAATTTGAGTAGAAAATAACATAAGTGTTTTTATAATC
41[8]	25[23]	**TCG ATC ACG TAG CAC AGC**
		ATTATTTAACTTAATTGAGAATCATAATTACTAGGGCAATTCTTATACTT
60[23]	47[23]	**TCG ATC ACG TAG CAC AGC**
		ATATTATCACATTAGAGCACAGCCATTATTTTGCA
		TCGTAGGCAAATCAG
1[24]	14[40]	**TCG ATC ACG TAG CAC AGC**
		ATTTTTGGGGCAAAGGGCAAAACATCGCCATTAAAAA
		TAATTGAATACGT
55[48]	25[47]	**TCG ATC ACG TAG CAC AGC**
		ATAGGAAACGAAATTCTTTCGAGCCACATGGTTTGAAATACC
		TTAGAACC
59[104]	40[104]	**TCG ATC ACG TAG CAC AGC**
		ATGTAAGCGTCTTTTGATTTTCAGGGGGTGTATCTGTATCATAATTGTGT
46[111]	19[111]	**TCG ATC ACG TAG CAC AGC**
		ATCCGATAGTTAGTAAGAACGAACTATTGCATCAAGAGGA
		AGATATTCAA
26[111]	7[111]	**TCG ATC ACG TAG CAC AGC**
		ATTGGCTTAGTTATTTCACAGGCAAGCGACGTTGGGCCAG
		TGTATCCGCT
18[111]	4[96]	**TCG ATC ACG TAG CAC AGC**
		ATCTGATAAAATAGGTCAAGATGGGCCACCAGTGCACTGCCCG
		CTTTCCA

17[8]	4[8]	**TCG ATC ACG TAG CAC AGC** **AT**TATTAACATATCAAACTGGCCAACGTAATAAAAAC GTGGCCCACCACA
62[55]	46[40]	**TCG ATC ACG TAG CAC AGC** **AT**ACCATCGACCCTTATTCGAGGCGTTTTAGCGACGGT ATTCAACAAGCA
45[8]	26[8]	**TCG ATC ACG TAG CAC AGC** **AT**ATCGGCTGGTAGAAACGAGACTACGAACGCGA AGATTTTCAAATAAAG
8[63]	37[63]	**TCG ATC ACG TAG CAC AGC** **AT**GGGTACCGGCGCGAGCTAAAGCTATCTGGAAGTAAAT ATGCCAAATCA
24[31]	53[31]	**TCG ATC ACG TAG CAC AGC** **AT**CAGATGATAAAAAGCCGATAAATACATGTAATGGTAAAGT GCTAATAT
15[64]	34[64]	**TCG ATC ACG TAG CAC AGC** **AT**TGTTAAAAAGGAAGATGAGTCTGGAAACAGTTAG GTCTTTATCAGTTG
6[39]	22[24]	**TCG ATC ACG TAG CAC AGC** **AT**TAAAGGGACACCGAGTTGTAGCAATACTTCTTTTG CGGAACCTTTGCC
32[47]	14[48]	**TCG ATC ACG TAG CAC AGC** **AT**TAAATCAAACCTTTTTTCAATTACGAGCCAGCAGC AATCAATGTGAGC

S4.4 Annealing the DNs

S.4.3.1 Td

Strand 5 was reacted with DBCO-NHS ester separately and converted to DNA-DBCO. The five strands (1:2:3:4:5) were mixed in the molar ratio of 1:3:3:3:3 in 1X TAE buffer (containing 12.5 mM Mg^{2+}) and was subjected to a 12 hour thermal annealing program starting from 80°C and ending at 4°C with a regular decrease in the temperature by 1°C. The structure was characterized and purified using 1% agarose gel electrophoresis.

S.4.4.2 DNO

DNO was annealed in 5 nM concentration by mixing 5 nM m13 scaffold and 10X staples in 1X 3D buffer. The annealing program used heated the mixture of strands to 95°C and cooled them to 4°C over a period of 37 hours.

S4.5 Conjugation of DBCO to S5-amine

S4.5.1 Procedure

100 mM stock solution of DBCO-NHS ester was prepared in anhydrous DMSO. 20 uL of DBSO-NHS stock was diluted using the same solvent and reacted with 100 uM aqueous solution of S5-amine in 50 mM phosphate buffer (pH = 8.5). The volume ratio of S5-amine: DBSO-NHS (diluted with anhydrous DMSO): phosphate buffer was 1:8:3. The reaction mixture was stirred at room temperature for 30 minutes and then lyophilized overnight. The lyophilized powder was dissolved in water and purified using HPLC to obtain pure S5-DBCO. The product was characterized by mass spectroscopy.

S4.5.2 Mass spectroscopic characterization

The conjugation of DBCO to S5-amine was confirmed by MALDI. The mass shifted from ~6407 D to ~6727 D that corresponds to the attachment of DBCO to the DNA-amine.

a)

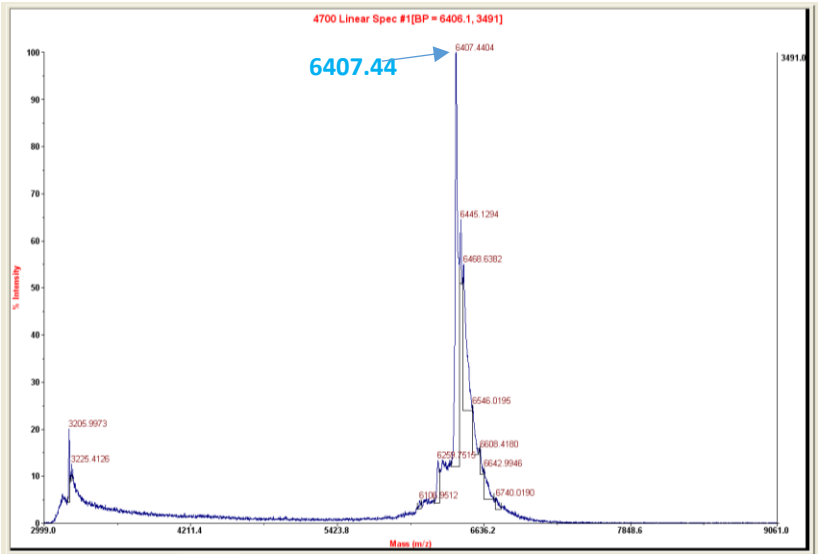

b)

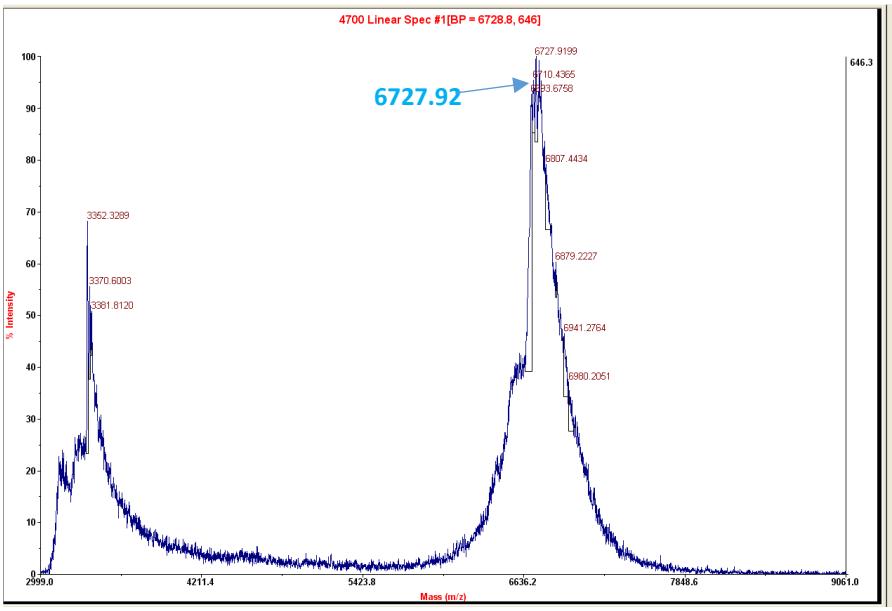

Figure S4.12: MALDI spectrum. a) S5-amine b) S5-DBCO.

S4.6 Conjugation of AAM to S5-DBCO

S4.6.1 Procedure

20 uL 100 uM S5-DBCO was reacted with 1, 2.5 and 5 equivalents of AAM in 0.1 M phosphate buffer (pH = 7.5) at room temperature for six hours. MALDI spectrum of the reaction mixtures showed that S5-DBCO: AAM = 1:2.5 led to the formation of S5-AAM. Control reaction mixtures containing S5-amine instead of S5-DBCO showed no shift in the peak from the characteristic S5-amine peak. The product was purified using HPLC.

S4.6.2 Mass spectroscopic characterization

a)

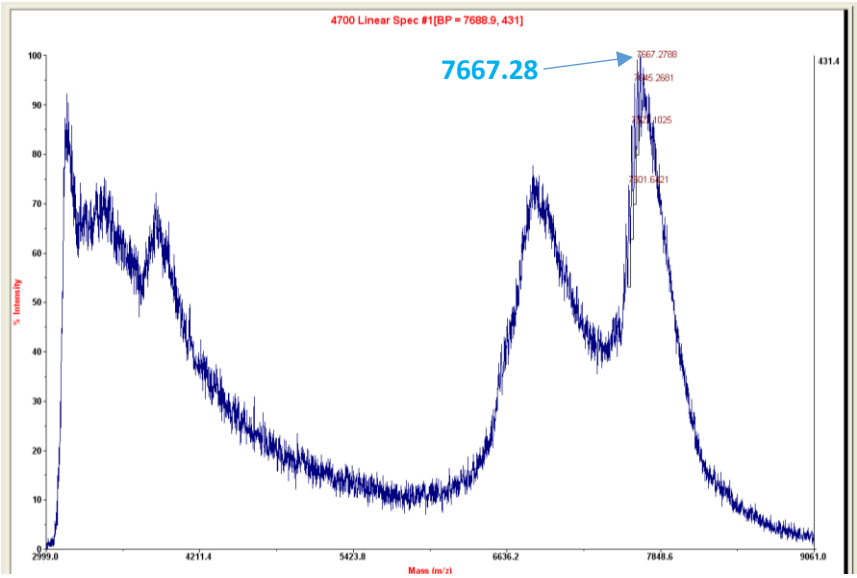

b)

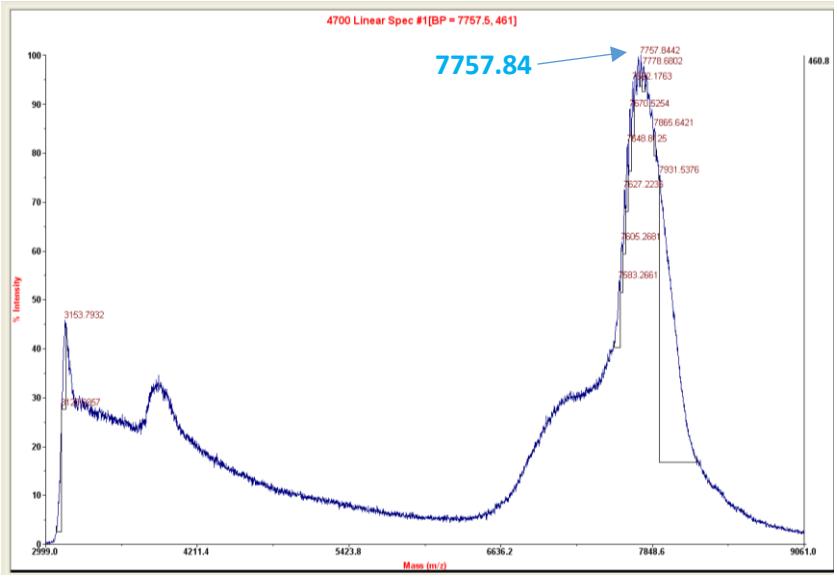

c)

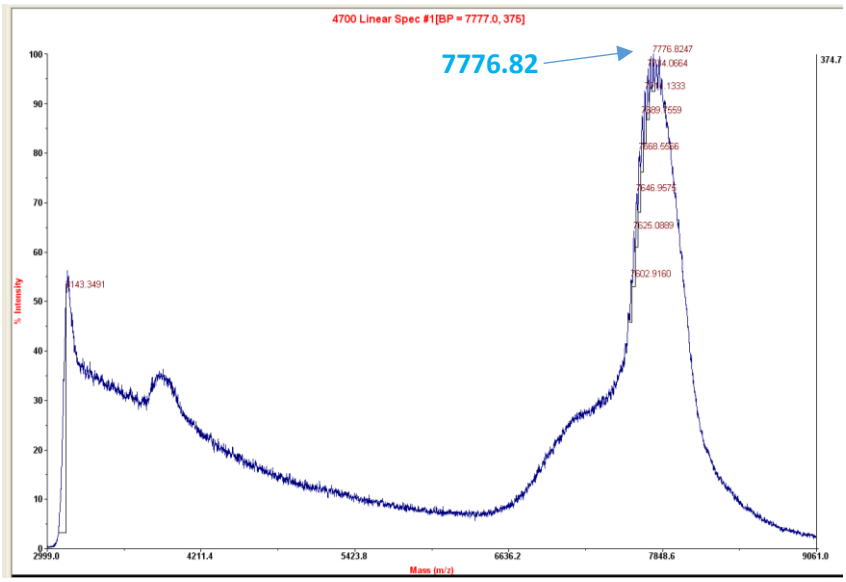

Figure S4.13: MALDI spectrum of S5-DBCO + AAM with S5-DBCO: AAM molar ratio of a) 1:1 b) 1:2.5, and c) 1:5.

a)

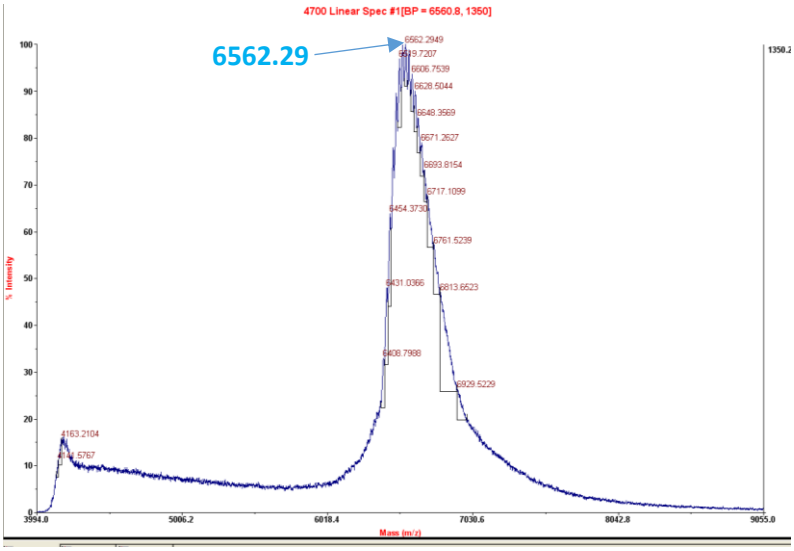
4700 Linear Spec #1[BP = 6560.8, 1350]
6562.29
% Intensity
Mass (m/z)

b)

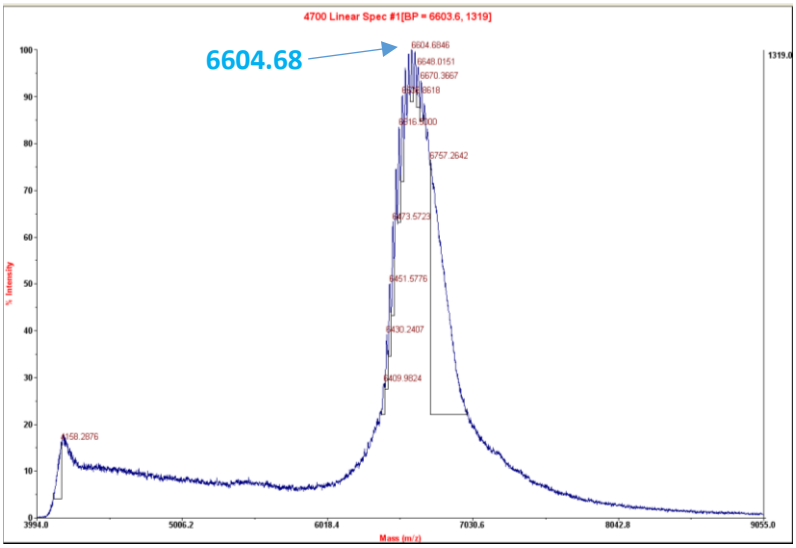
4700 Linear Spec #1[BP = 6603.6, 1319]
6604.68
% Intensity
Mass (m/z)

c)

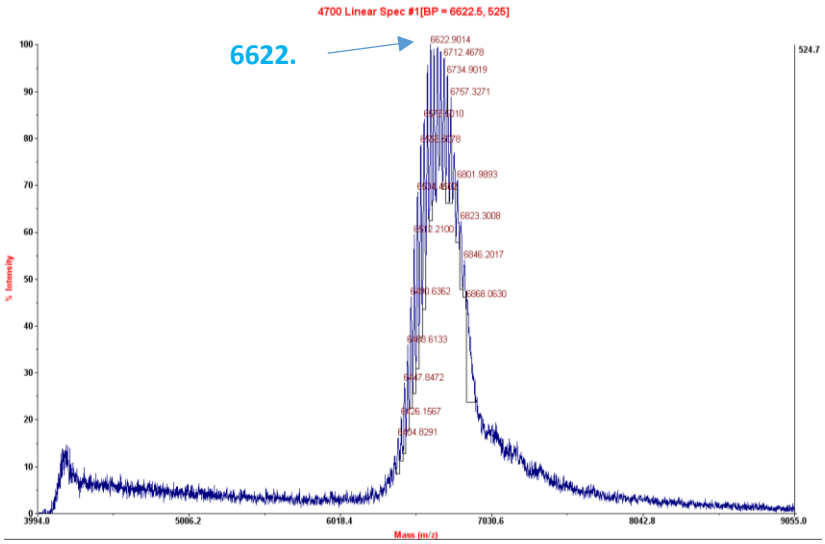

Figure S4.14: MALDI spectrum of S5-amine + AAM with S5-amine: AAM molar ratio of a) 1:1 b) 1:2.5, and c) 1:5.

S4.7 HSA Binding of S5-AAM

S4.7.1 Reaction

S5-AAM was mixed with 1, 2.5, 5, 7.5 and 10 equivalents of HSA in 1X TAE/Mg^{2+}. The reaction mixtures were left at room temperature for 4 h without shaking. The reaction mixtures were kept protected from light.

S4.7.2 Characterization

10 uL of each reaction mixture was run on 12% native polyacrylamide gel prepared in 1X TBE buffer at 45°C 30 mins under 200V for 30 minutes and then under 500V for 1

h. These conditions were used by Lacroix and coworkers to characterize HAS binding to their alkyl conjugated DNA. The gel was stained with ethidium bromide for band visualization. From the bands it was found that that showed a 1:5 ratio of S5-AAM: HSA led to decent conversion to S5-HSA.

S4.8 Time vs Stability Studies

For the time vs stability studies the Td and DNO samples were concentrated 20 fold and then diluted to DMEM + 10% FBS medium, the final concentrations being 1 uM and 10 nM for Td and DNO respectively. The Td samples were studied for 48 hours while the DNO samples were studied for 5 hours. 30 uL aliquots were taken out from each sample at different time points and were run on three separate gels (triplicate). The Td samples were run on 1.5 % agarose gel and the DNO samples on 1% agarose gel, both in 1X 3D buffer, at 4°C. After the completion of run, the gels were stained with SYBR green for band visualization.

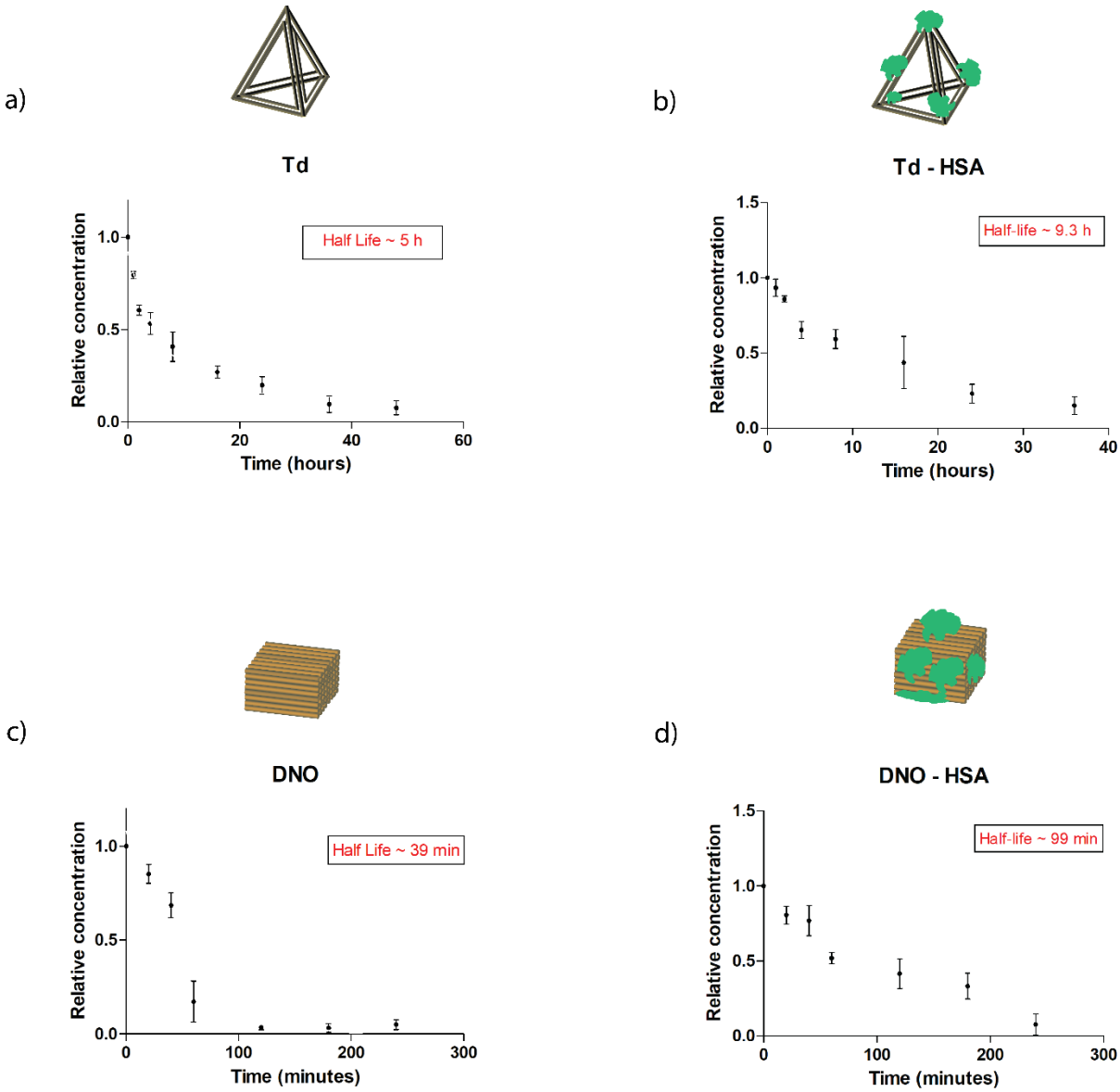

Figure S4.15*:* Time vs stability plots for a) bare Td, b) HSA coated Td, c) bare DNO, and d) HSA coated DNO.

S4.9 Confocal Microscopy

The confocal microscopy was performed on living cells in 1X PBS buffer. Cells were seeded at 3000 cells/well and grown for 24 h in a special 8 well transparent bottomed

in DMEM + 10% FBS medium. Then each well was incubated with 2 uL of the sample (dye labeled DNA or structure, their concentrations modified in a way that alexa fluor 488 concentration in each sample was always 120 nM). Incubation procedure similar to the one followed during flow cytometry studies was followed. After incubation for 1h, the cells were washed once with 1X PBS and 1 uM solution of the CellTracker CM-Dil dye in 1X PBS was added. The cells were incubated at 37°C for 5 minutes and then at 4°C for 15 more minutes. The medium was again replaced with fresh 1X PBS. In addition to imaging cells directly after incubation, we also studied batches treated with DNase after incubation, such that any DNA or DN sticking to the surface was degraded by the nuclease.

Conditions similar to cell growth were maintained during imaging. We used a 40X immersion objective and a white light laser for imaging.

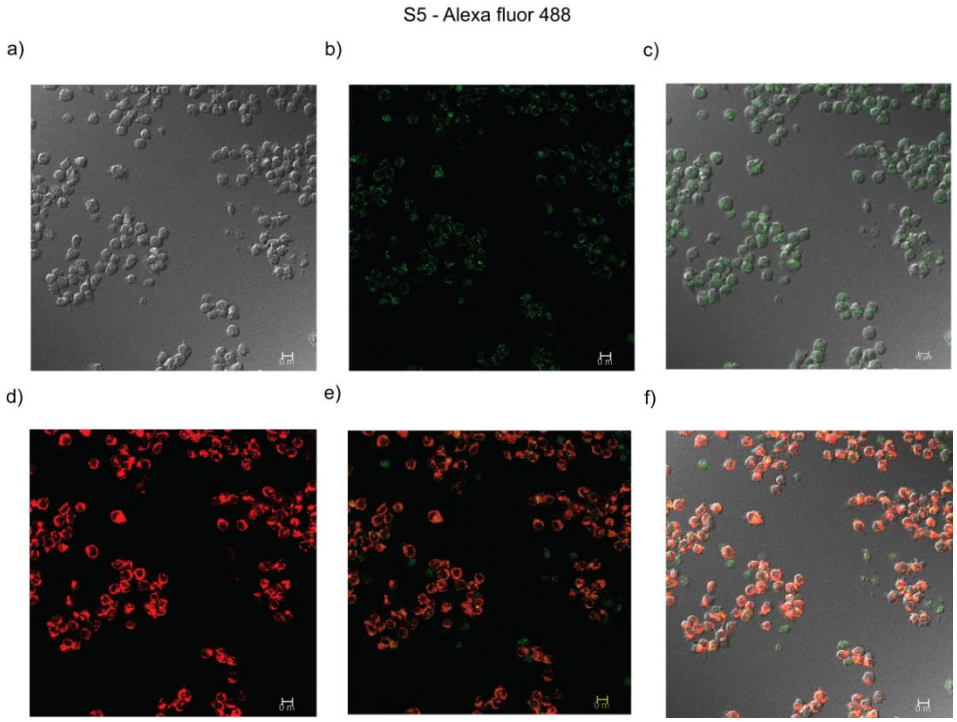

Figure 4.16*:* Confocal microscopy images of RAW cells incubated with Alexa fluor 488 labeled S5. The cell membranes were stained with CellTracker CM-Dil dye. A) Bright field image b) green fluorescence from internalized S5 c) overlay of bright field and green fluorescence d) red fluorescence from CellTracker CM-Dil dye e) overlay of green and red fluorescence f) overlay of bright field, green and red fluorescence.

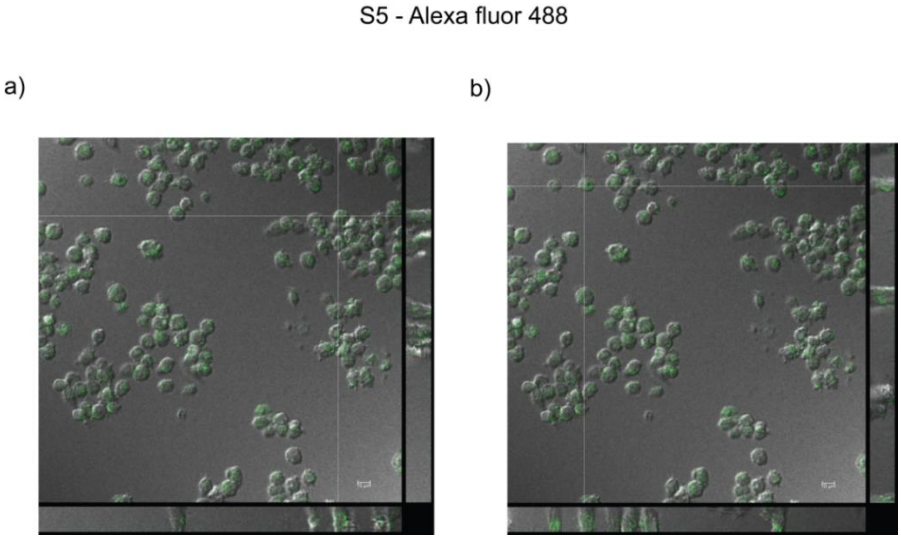

Figure 4.17*:* Z-stacked confocal microscopy images of RAW cells incubated with Alexa fluor488 labeled S5. The crosshairs indicate orthogonal sectioning. The bottom and right panels show the sectioned planes and confirm that fluorescent particles (green) are located inside the cells and not merely attached to the cell membrane.

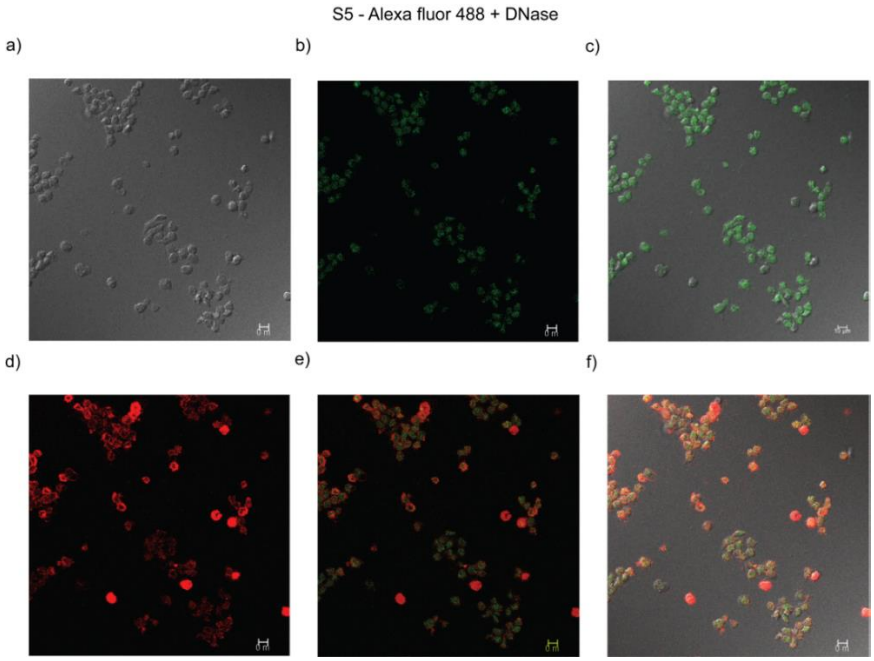

Figure S4.18*:* Confocal microscopy images of RAW cells incubated with Alexa fluor 488 labeled S5 followed by DNase treatment. The cell membranes were stained with CellTracker CM-Dil dye. a) Bright field image b) green fluorescence from internalized S5 c) overlay of bright field and green fluorescence d) red fluorescence from CellTracker CM-Dil dye e) overlay of green and red fluorescence f) overlay of bright field, green and red fluorescence.

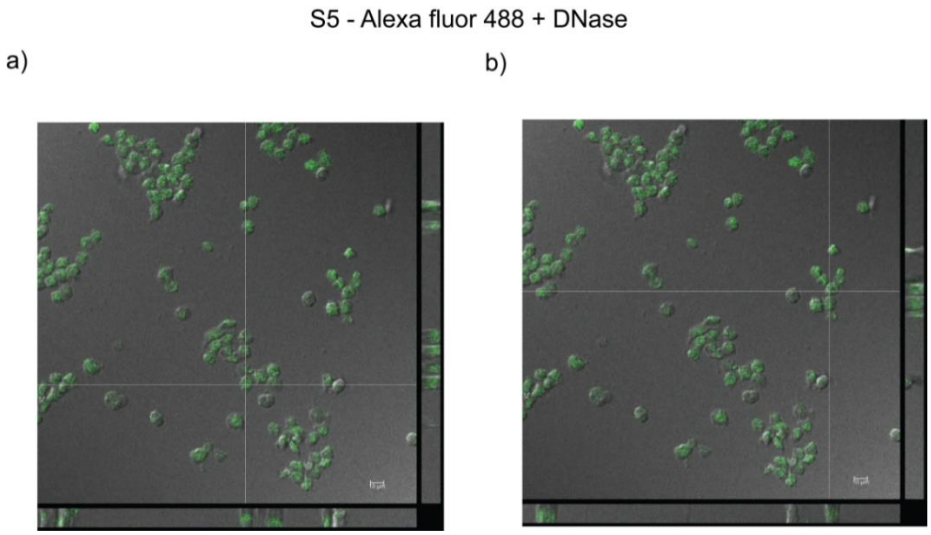

Figure S4.19*:* Z-stacked confocal microscopy images of RAW cells incubated with Alexa fluor 488 labeled S5 and then treated with DNase.

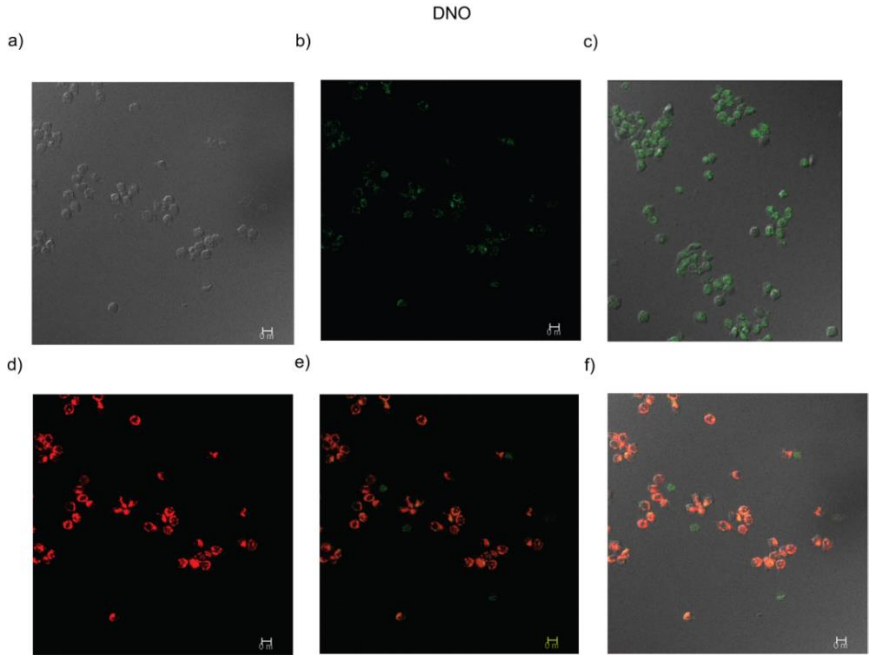

Figure S4.20*:* Confocal microscopy images of RAW cells incubated with Alexa fluor 488 labeled DNO. The cell membranes were stained with CellTracker CM-Dil dye. a) Bright field image b) green fluorescence from internalized DNO c) overlay of bright field and green fluorescence d) red fluorescence from CellTracker CM-Dil dye e) overlay of green and red fluorescence f) overlay of bright field, green and red fluorescence.

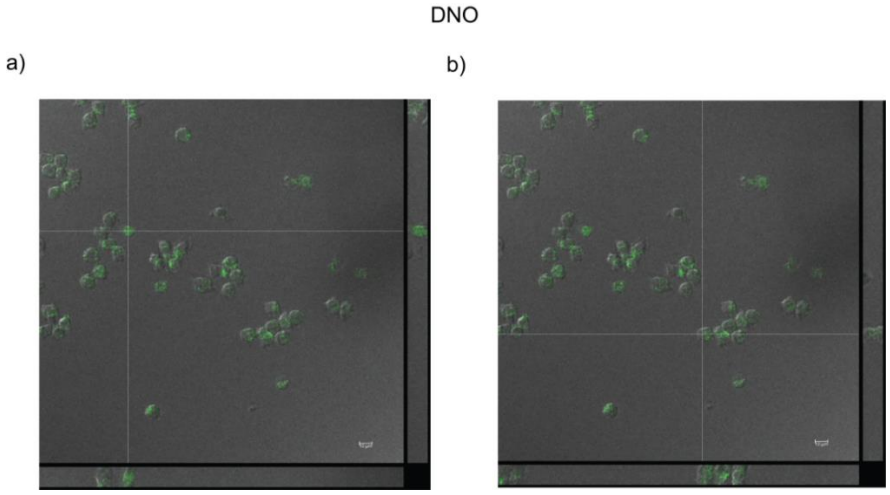

Figure S4.21*:* Z-stacked confocal microscopy images of RAW cells incubated with Alexa fluor 488 labeled DNO.

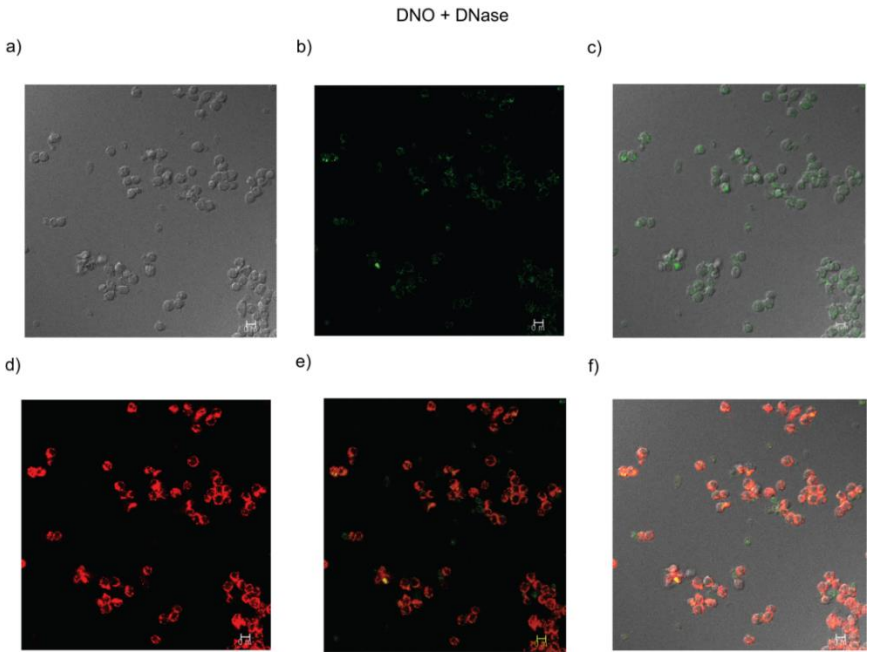

Figure S4.22*:* Confocal microscopy images of RAW cells incubated with Alexa fluor 488 labeled DNO followed by DNase treatment. The cell membranes were stained with CellTracker CM-Dil dye. a) Bright field image b) green fluorescence from internalized DNO c) overlay of bright field and green fluorescence d) red fluorescence from CellTracker CM-Dil dye e) overlay of green and red fluorescence f) overlay of bright field, green and red fluorescence.

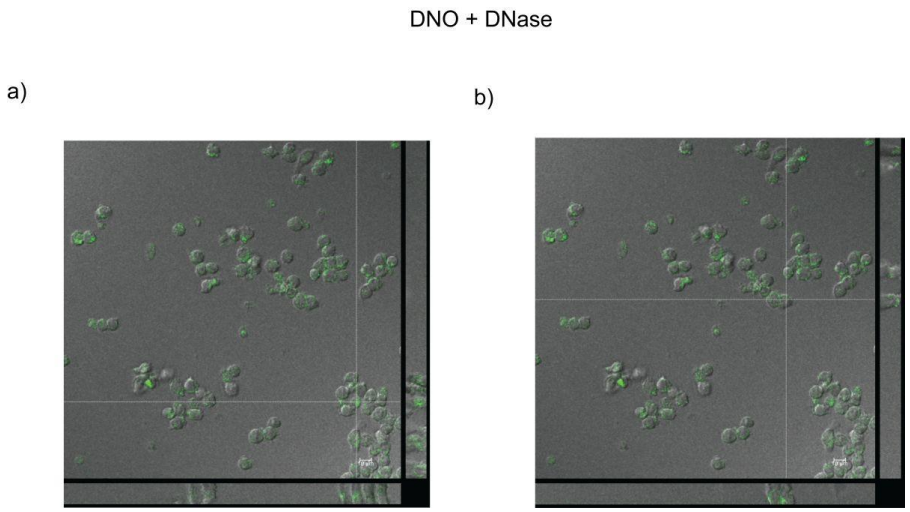

Figure S4.23*:* Z-stacked confocal microscopy images of RAW cells incubated with Alexa fluor 488 labeled DNO and then treated with DNase.

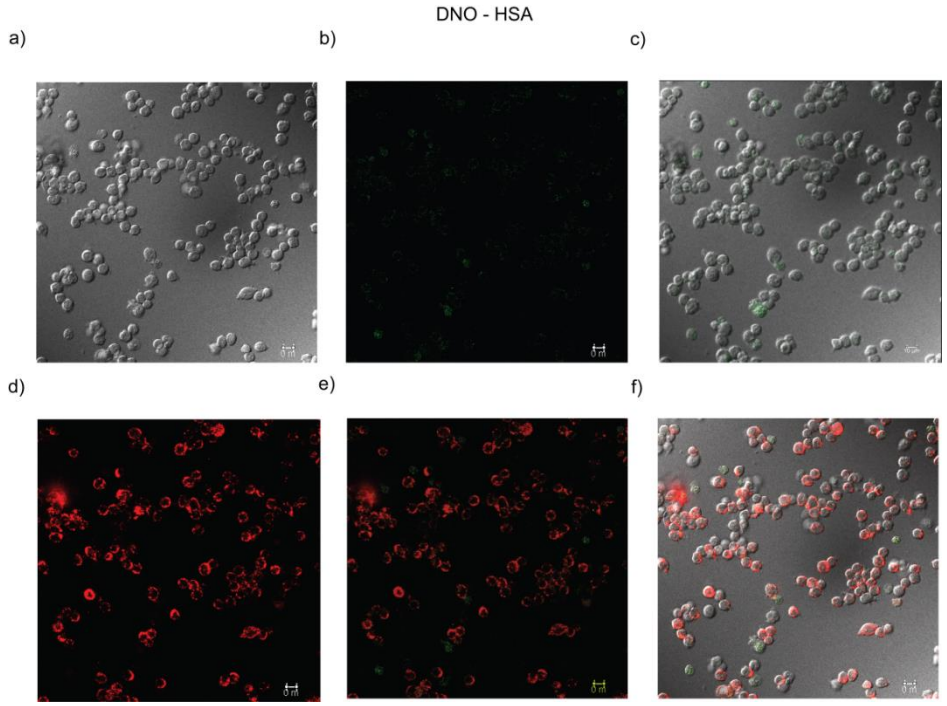

Figure S4.24*:* Confocal microscopy images of RAW cells incubated with Alexa fluor 488 labeled DNO. The cell membranes were stained with CellTracker CM-Dil dye. a) Bright field image b) green fluorescence from internalized coated DNO c) overlay of bright field and green fluorescence d) red fluorescence from CellTracker CM-Dil dye e) overlay of green and red fluorescence f) overlay of bright field, green and red fluorescence.

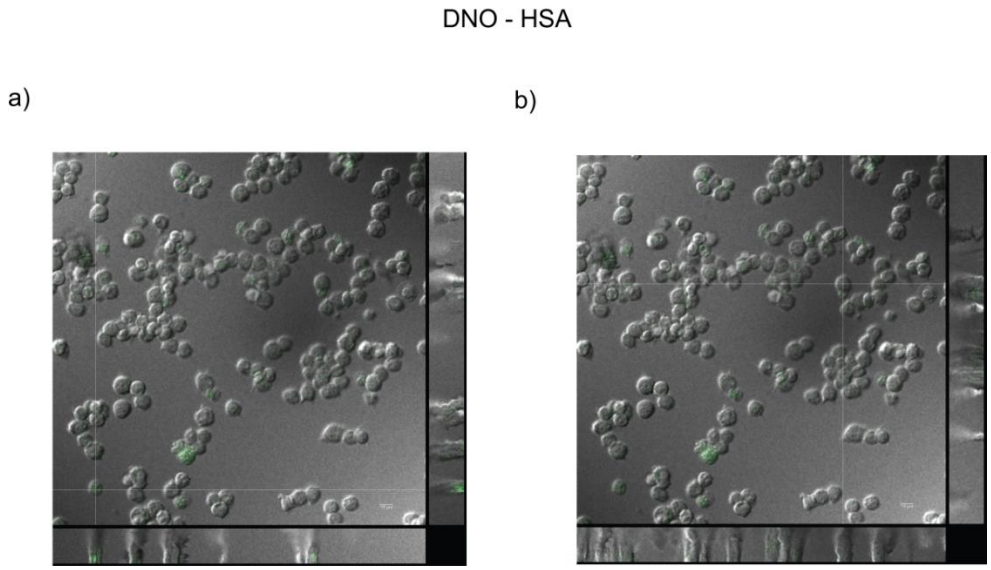

Figure S4.25*:* Z-stacked confocal microscopy images of RAW cells incubated with Alexa fluor 488 labeled HSA coated DNO.

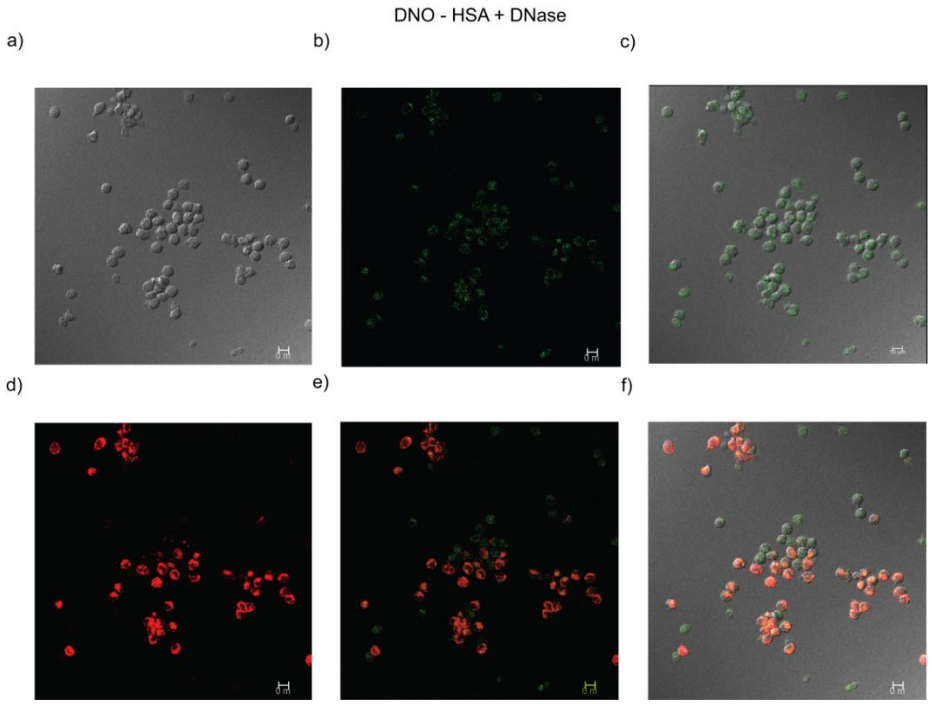

Figure S4.26*:* Confocal microscopy images of RAW cells incubated with Alexa fluor 488 labeled DNO followed by DNase treatment. The cell membranes were stained with CellTracker CM-Dil dye. a) Bright field image b) green fluorescence from internalized coated DNO c) overlay of bright field and green fluorescence d) red fluorescence from CellTracker CM-Dil dye e) overlay of green and red fluorescence f) overlay of bright field, green and red fluorescence.

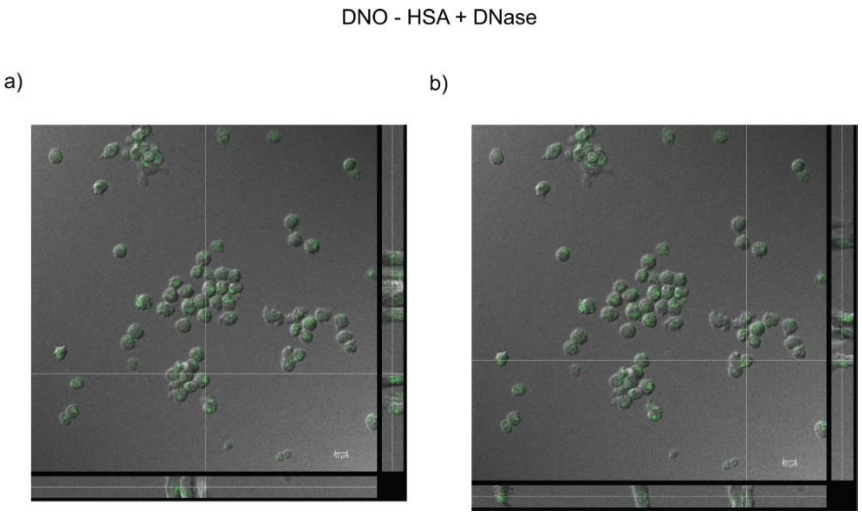

Figure S4.27*:* Z-stacked confocal microscopy images of RAW cells incubated with Alexa fluor 488 labeled HSA coated DNO and then treated with DNase.

S4.10 Flow Cytometry

S.4.10.1 Incubation with DNs

Before incubation the existing medium was replaced with fresh medium. The cells in each well were incubated with 10 uL of each sample (S5-dye or DN), the concentration of the sample was such adjusted that the concentration of Alexa fluor 488 was always 120 nM. Td was annealed in 250 nM concentration and as each Td contained 12 fluorophores, hence the concentration of the fluorophore became 3 uM. The sample was diluted 25 fold and 10 uL of the diluted sample was added to each well when required. DNO was annealed in 5 nM and then concentrated to 10 nM. As each structure contained 12 fluorophores, hence concentration of fluorophore became 120 nM.

An issue that we had to face during incubation of the cells with DNs was the instability of the structures in cell culture medium. Our previous experiments showed that Td had a half-life of about 5 h in DMEM + 10% FBS medium whereas the same was only ~39 minutes for DNO. So, if we incubate the cells with only one aliquot of the structure, there was obvious chances of the macrophages internalizing free dye labeled DNA that resulted from the degradation of DNs. Hence, we replaced the medium every 30 minutes for Td incubation and added fresh aliquot of Td (10 nM, 10 uL) and for incubation with DNO the process was repeated every 10 minutes. This minimized the chance of dye labeled DNA internalization.

S.4.10.2 Dead cell staining

Propidium iodide stock was prepared by dissolving solid propidium iodide in deionized water and the stock concentration was 1 mg/mL. While staining the cells, the stock was diluted to 3 uM by using 1X PBS buffer. 1 mL of the 3 uM dye was added to each well.

S.4.10.3 DNase treatment

DNase powder was dissolved at a concentration of 1 mg/mL in 50% Glycerol with 20 mM Tris-HCl, pH 7.5, and 1 mM $MgCl_2$. After the cells have been incubated with the DN, we replaced the medium and added 10 uL of the DNase stock per mL of the medium, incubated at 37°C for 10 minutes and again changed the medium with 1X PBS in case of confocal microscopy or with 3 uM propidium iodide solution (in 1X PBS) in case of flow cytometry studies.

S.4.10.4 Analysis of FACS data

The RFI value from RAW cells incubated 10 uL of the blank was collected each time the experiment was done and this value was subtracted from the RFI values of samples. 40,000 events were collected for each sample and each sample was studied in triplicates. A separate sample was prepared for dead cells and they were incubated with propidium iodide (PI) for 15 minutes prior to the flow cytometry experiment. RFI value from this control sample show that most of the dead cells has an RFI (form PI) higher than 10^2. This value for PI RFI was used as a gating. All the samples were incubated with PI solution prior to flow analysis and the gating was applied so that while analysis we could collect the RFI values only from living cells. This minimized the chance of false positives as dead cells have a much higher permeability in comparison to the living ones.

APPENDIX D

SUPPLEMENTAL NFORMATION FOR CHAPTER 5

PROXIMITY LIGATION ASSAY TO ESTIMATE THE STABILITY OF DNA NANOSTRUCTURES

S5.1 Methods and Instruments

All DNA strands were purchased from Integrated DNA technologies. The strands for DNC were bought in 96 well plates and used without any further purification. Rest of the strands were purified using 10% denaturing polyacrylamide gels prior to annealing structures. FBS that was used to supplement DMEM cell culture medium was purchased from Gibco Life Technologies. Human serum was purchased from Sigma Aldrich. All the other chemicals that are not mentioned here were bought from Sigma-Aldrich.

Real time PCR instrument from Qiagen was used for the PCR experiments. The time vs stability results were plotted using the Prism 5 software from Graphpad. For the time vs stability experiments, the band intensities of gels were measured using the ImageJ software.

S5.2 DNA nanostructure designs

S5.2.1 Wireframe Tetrahedron (Td)

S5.2.1.1 Sequences for TdP0:

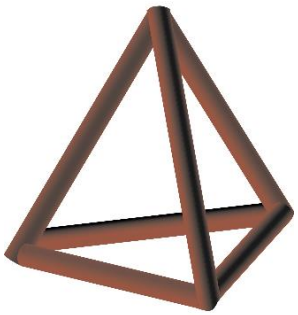

Strand 1:

ACA TTC CTA AGT CTG AAA CAT TAC AGC TTG CTA CAC GAG AAG AGC CGC CAT AGT A

Strand 2:

TAT CAC CAG GCA GTT GAC AGT GTA GCA AGC TGT AAT AGA TGC GAG GGT CCA ATA C

Strand 3:

TCA ACT GCC TGG TGA TAA AAC GAC ACT ACG TGG GAA TCT ACT ATG GCG GCT CTT C

Strand 4:

TTC AGA CTT AGG AAT GTG CTT CCC ACG TAG TGT CGT TTG TAT TGG ACC CTC GCA T

S5.2.1.2 Sequences for the antennae pair (A1 and A2)

A1: TGTG GTC TAT GTC GTC GTT CG CTA GTA GTT CCT GGG CTG CAC

A2: TCG AGG CGT AGA ATT CCC CCG ATG CGC GCT GTT CTT ACT CA

S5.2.1.3 Sequences for TdP2

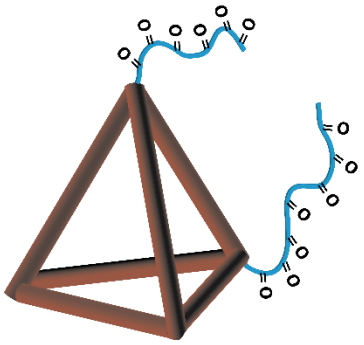

The two strands 1 and 4 were replaced with PN1 and PN2.

PN1 (Added antennae to 3’ end of Strand 1):

ACA TTC CTA AGT CTG AAA CAT TAC AGC TTG CTA CAC GAG AAG AGC CGC CAT AGT A TGTG GTC TAT GTC GTC GTT CG CTA GTA GTT CCT GGG CTG CAC

PN2 (Added antennae to 5’ end of Strand 4):

TCG AGG CGT AGA ATT CCC CCG ATG CGC GCT GTT CTT ACT CA TTC AGA CTT AGG AAT GTG CTT CCC ACG TAG TGT CGT TTG TAT TGG ACC CTC GCA T

S5.2.1.4 Sequences for TdS2

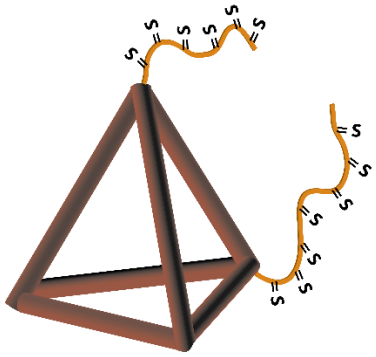

The two strands 1 and 4 were replaced with PN1S and PN2S. ‘*’ indicates phosphorothioation of the DNA backbone.

PN1S (Added antennae to 3’ end of Strand 1):

A*C*A* T*T*C* C*T*A* A*G*T* C*T*G* A*A*A* C*A*T* TA*C* A*G*C* T*TG* C*T*A C*A*C* G*A*G* A*A*G* A*G*C* C*G*C* C*A*T* A*G*T* A* TGTG GTC TAT GTC GTC GTT CG CTA GTA GTT CCT GGG CTG CAC

PN2S (Added antennae to 5’ end of Strand 4):

TCG AGG CGT AGA ATT CCC CCG ATG CGC GCT GTT CTT ACT CA T*T*C* A*G*A* C*T*T* A*G*G* A*A*T* G*T*G* C*T*T* C*C*C* A*C*G* T*A*G* T*G*T* C*G*T* T*T*G* T*A*T* T*G*G* A*C*C* C*T*C* G*C*A* T*

S5.2.2 Larger Tetrahedron (TD)

S5.2.2.1 Sequences for TDP0:

Strand 1: AGG CAC CAT CGT AGG TTT C TTG CCA GGC ACC ATC GTA GGT TTCT TGC CAG GCA CCA TCG TAG GTT T CTT GCC

Strand 2: CAG AGG CGC TGC AAG CCT ACG ATG GAC ACG GTA ACG ACT

Strand 3: AGC AAC CTG CCT GTT AGC GCC TCT

Strand 4: TTA CCG TGT GGT TGC TAG TCG TT

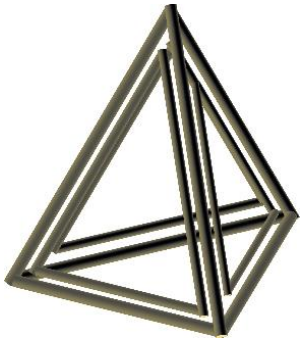

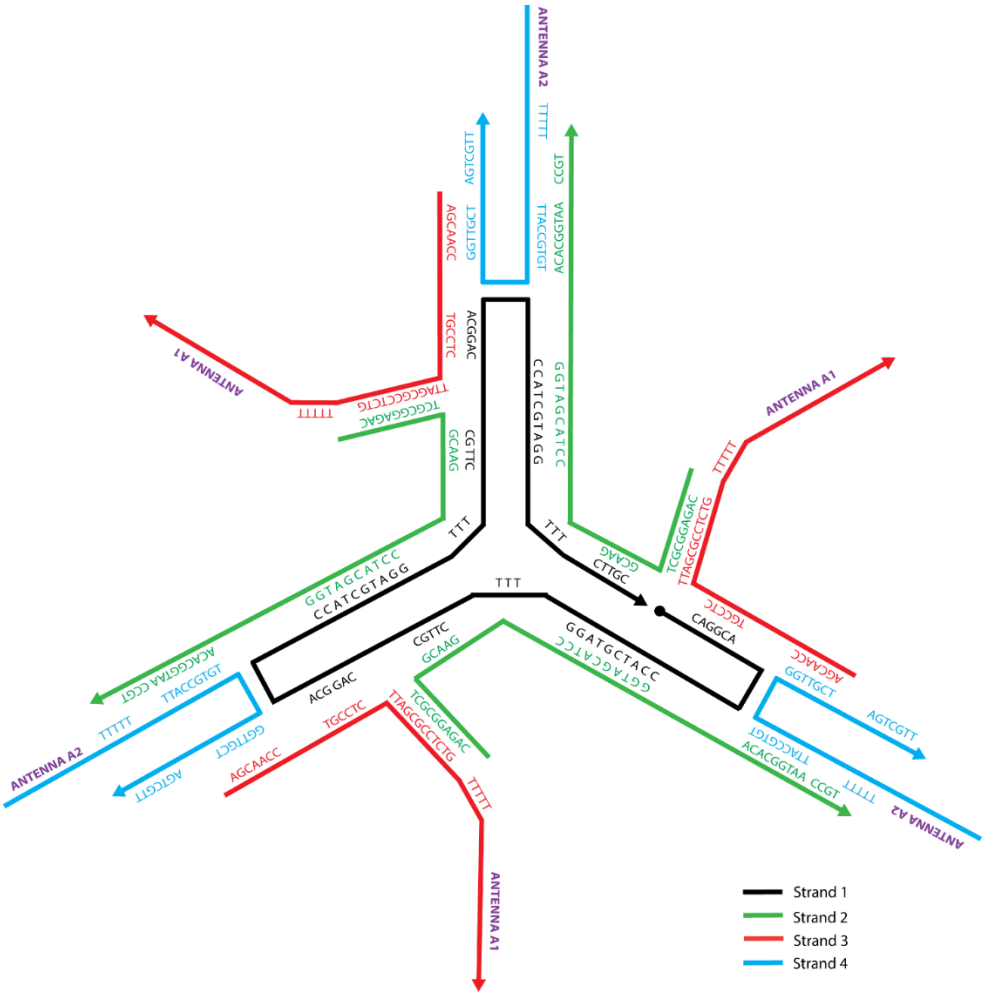

Figure S5.1: Schematic of TDP0

S5.2.2.2 Sequences for TDP24

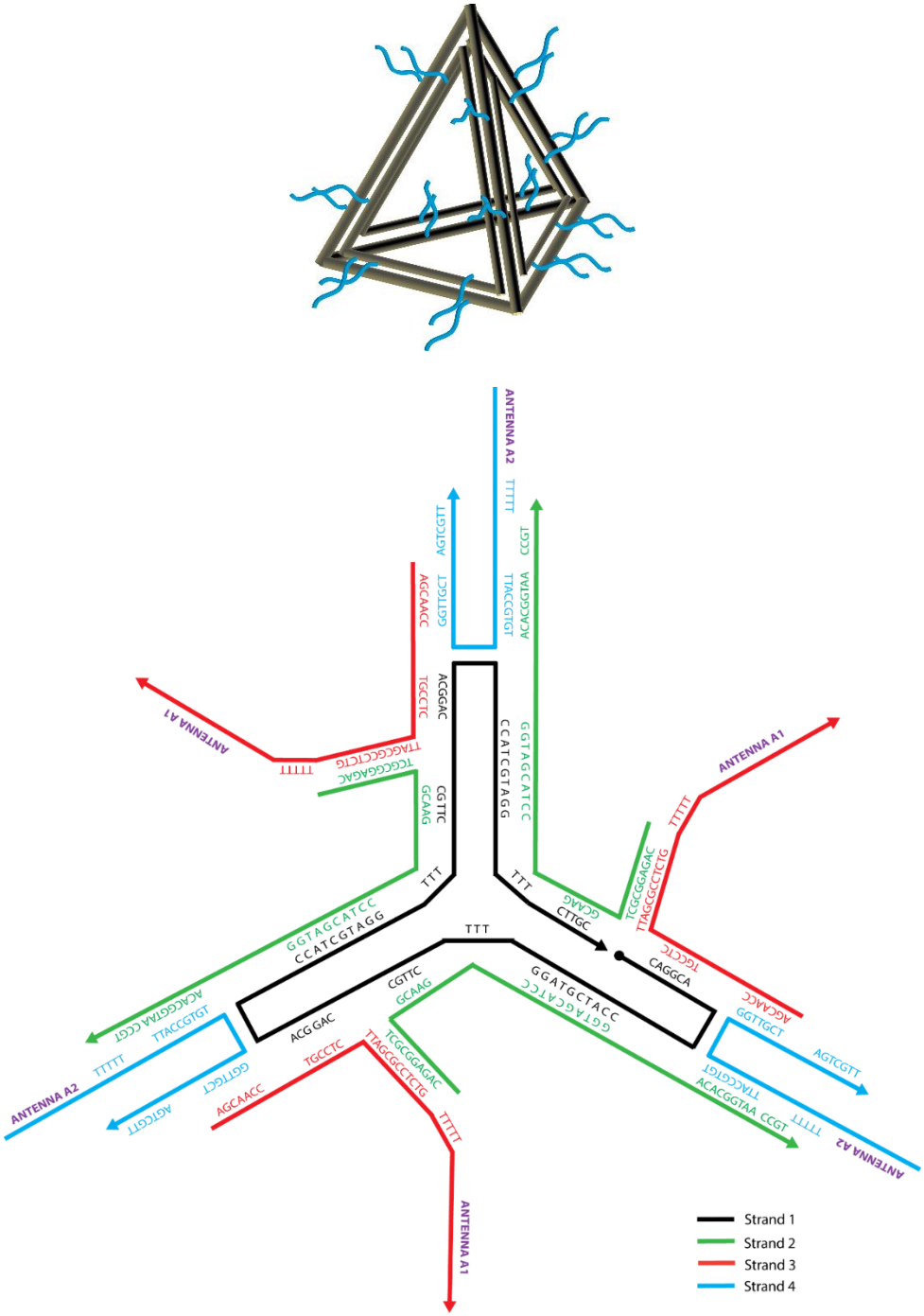

Figure 5.2: Schematic of TDP24

Antennae + Strands:

XA1 = strand 3 + 5T linker + A1:

AGC AAC CTG CCT GTT AGC GCC TCT G TTTTT TGTG GTC TAT GTC GTC GTT CG CTA GTA GTT CCT GGG CTG CAC

XA2 = A2 + 5T linker + strand 4

TCG AGG CGT AGA ATT CCC CCG ATG CGC GCT GTT CTT ACT CA TTTT TTA CCG TGT GGT TGC TAG TCG TT

While annealing TDP24, the strands 3 and 4 were replaced with XA1 and XA2 respectively.

S5.2.3 DNA Origami

S5.2.3.1 caDNAno schematic for DNCP0

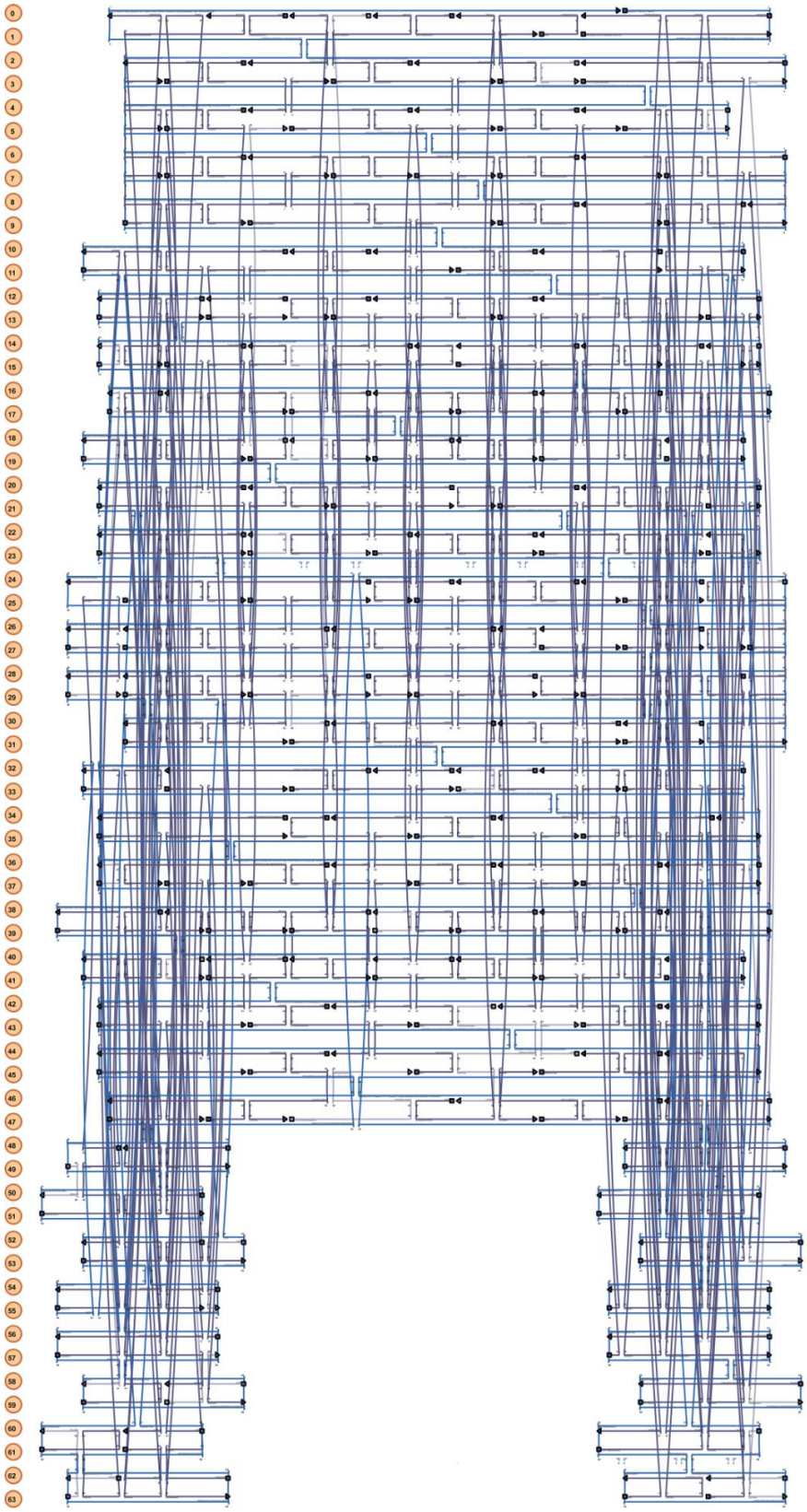

Figure 5.3: caDNAno schematic for DNCP0

S5.2.3.2 Strand sequences for DNCP0

Start	End	Sequence
0[79]	2[72]	TCGAGGTGTAGCCCGAGATAGGGTGAAAATCCTGTTTGAT
33[80]	32[80]	GAAACGCAAGTTTTGC
35[104]	33[111]	TAGAAAGACAAAAGGAATAGTAAG
7[72]	10[64]	TACATTTTCGTCTGAAATGGATTACGTGGCACTTTGAATG
45[40]	43[39]	TTAAAGCCGCATTGACAGGAGGTTCCACCGGA
10[63]	12[64]	GCTATTAGAGGAATTGAGGAAGGTATAATACA
4[39]	19[39]	AGTGTTTTTGTCCATCTCGCCTGATTGCTTTGTTATTCATTTCAATTA
36[55]	40[48]	AAGAACTGGGCGACATCATTACCACACTACGAGAACGAGG
24[127]	47[140]	ATATGCAATACAACGCTGAGAATAGAAAG
23[64]	25[71]	GTATCACCCATTTTCAAAAAAGCC
42[87]	46[80]	CTTTTTCATCAGAGCCACCGGAGTTGCAGACCCTCAGAGCGCT
		TTCGAAAAAAGGC
44[119]	45[138]	CCGATATAACCGATAGTTGCGCCGACAATGACAAC
36[119]	42[120]	GTAAATTGATTCAGTGAATAAGGCCGAGGGTA
16[119]	5[111]	CCGGTTGAGCCGGAGAGTTCTAGCTGATAAATGGTTTGCG
28[95]	41[95]	AAACCAATCTGGCTGATTGTGTCGATACACTA
34[129]	54[109]	AATGCAGATACATAACGCTTCATCAGAAATCAGGTCT
32[95]	34[88]	GCAAAAGAATAATAACGGAGAGGCATTACATACCCAAAAG
35[72]	33[79]	AAAACGAATGATTAAGAAACCGAG
45[96]	44[104]	TCTTAAACAGCTTGATTTCGGTCG
10[95]	11[119]	CCAGTCACAGGAGCACTAACGACAGTATCGGCCTCAGGAA
2[71]	4[72]	GGTGGTTCACAGGGCGCGTACTATAAGGGATT

12[47]	10[48]	TATTAGACCAAATCAACAGTTGAATCTTTAAT
6[39]	9[39]	AAACTATCCGCCAGCCATTGCAACCACCAGTCACACGACCTAGAACCC
5[48]	3[55]	TAACCGTTGTAGCAATGAACGGTACGCCAGAACGCTTAAT
9[120]	57[140]	GAGGATCCCATAGCTGAGGCAAAGCGCCACAGCTGGC
3[56]	0[64]	GCGCCGCTCGAAATCGTTATAAATCAAAAGAACCGTAAAG
47[48]	45[71]	GGTTTTGCTCAGTATAGCAAGCCCGAGCCTTTAATCAGTCAAG CGTGTATCGGTTT
42[55]	44[56]	AAAATACGCCTCAGAGCCGCCACCACCAGAGC
20[79]	17[79]	AGCCTTTACTGAGTAATATACTTCAAGGCTAT
61[16]	0[32]	ATTAATTAACCTTGCTCGGCGAACGTGGCGAGAAAGGA AGGCCCCCGA
12[63]	30[56]	TTTGAGGATATCCGGTAGACGGGA
52[31]	38[24]	AGAGAGATCTAACGAGCGTCACCA
54[34]	33[47]	CCTAAGAAAAGTAAGCAGA
33[48]	32[24]	TAGCCGAACGACTTGCGGGAGGTTTTGAAGCCTTAAATCA
37[40]	37[23]	GACAAAAGGCTCATTATACATAAGTTTATTTTGTCACAATT TCATATG
50[138]	41[135]	GGATTTTGTAACAAGCGCG
23[40]	22[40]	ATATAAGTATCCAATC
20[39]	29[39]	AGAAGATGGCGGAACAAAGTACCGAATCCTAA
45[72]	43[71]	ATCAGCTTCGCCACCAGAACCACCCTCAGAAC
24[63]	25[39]	GGGACCAGGCGGATAAGTGCCGTCGAGAGCTTATAAGAAT
59[24]	16[24]	TGCAACAGTTGCACGT
52[146]	13[138]	AAGACTTCAAACAGACCGGTGAATCCCATG
42[119]	50[107]	GCAACGGCGGGATCGTAGTTTTGTCGTCT
47[112]	24[104]	GTACAAACCTAAAGTACGGCCACC
1[96]	23[95]	GTTCCAGTTCACCCAAATCAAGTTGTACCGCC

43[104]	39[111]	GCTTTTGCTACAGAGGATCTTTGAACCGTCACAAGAGTAA
32[135]	36[120]	TACCAGACGACGATAATATCATAATAAATCAATTGAGAT TAACGAGTA
11[80]	9[87]	ATATCTTTGACGTTGTAAAATATTAGACAACGACGGCCAG
55[109]	31[111]	TTAATAGCGAGGGATAGCG
21[128]	27[135]	AAGCCTCAATTTTTGCAATTGCTC
4[103]	16[96]	GGGAGCTAGGAGAGGCTAATGCCGAGTCTGGACAATATAA
12[95]	30[88]	CTAATAGAGTAAAATGGAGAGAAT
7[56]	19[63]	CGCTCATGTCACTTGCACAGTAACACATCGGGATTTTAAA
37[104]	35[103]	AAAGGTGAGGCTTGAGATGGTTTAATTACAGG
5[112]	62[112]	TATTGGGCGCCAGGGTTTCACCAGTCTACTAAAGGAG CTGAAAAGGTG
31[112]	56[109]	TCCAATACTCTGCCAGATGGGATAACCGCTTCTGG
9[40]	7[55]	TTCTGACCTGAAAGCGTAAGAATATTTACATTGGCAGATTA GGAAAAA
0[47]	2[40]	TAAAGGGAGGAAGAAAGCGATCCCGCAAAAAAGGAGCGGG
58[146]	8[136]	CTTCGCTATTAAGTGAGCTAATTCGTA
7[24]	59[39]	AATATTACGGCCTTGCGTAGATTTTCAGGTTTAAAATTATTGCCACGC
36[138]	53[146]	AGAAGGAAGCCCGA
46[79]	24[80]	TCCAAAAGAATAGGAACCCATGTATCAGAGCC
17[48]	6[40]	ATGAATATCTGAGTAGAAGAACTC
42[138]	37[138]	CAGCATCGGAATTGCCCTGACG
24[103]	25[111]	CTCAGAACAAATTCTTACCAGTAT
31[48]	13[55]	AGAAGGCTTTTAGAAGATTAAATG
24[79]	22[72]	ACCACCCTGTACTCAGGGTTATAT
9[88]	7[87]	TGCCAAGCCTCACAATTCCTCAATGACGCACA
46[119]	47[111]	ATAATAATTTTTTCACCGTCACCA

2[39]	4[40]	CGCTAGGGACCACCACACCCGCCGTCCTGAGA
54[140]	34[130]	GATTGCATCAAAACCCTCGTTTCAACT
7[88]	19[95]	CAACATACACCTGTCGTGCCTGAGGAGAGGGTTAAAGATT
33[112]	30[112]	AGCAACACAAACCAAACCCTGACTCAGATGAA
32[79]	13[87]	CAGGAGGCAACGCAGGGGGTAATATTAGAGCCTCTCCGTG
56[34]	12[32]	GAATCAGTTGGTTTACAAA
43[40]	39[47]	ACCGCCTCTAACCCCTATAGCTGCTTAGCAAGCAACTTTG
3[88]	1[95]	TGACGAGCCAGCAGGCTGAGTGTT
20[103]	29[103]	ACCCTGTACAATTCATG
		CATGTAGATTTTTTG
10[47]	13[31]	GCGCGAACTGATAGCCCTAAAACAATATCTGGCCTCA
		AATACGCTGTA
28[63]	41[63]	CATTCCAACAGATGAACTTAGCCGAGGCACCA
16[23]	3[23]	AAAACAGAGAGGCGAAAATACCAAAAACAGTAGTGAG
		GCCGGTCACGC
32[63]	34[56]	GAACCTCCCAAAGTTACCAGAAGGACTCCTTATTACGCAG
27[96]	38[96]	AACAAGAACTGATAAACCTTCATCCGACTTGA
8[103]	9[119]	GTTATCCGTTGCATGCCTGCAGGTCGACTCTA
44[55]	47[47]	CGCCGCCAAGAATGGATCTGAATTTACCGTTCATTAGCGG
34[55]	36[56]	TATGTTAGTTGGGAAGAAAAATCTGCGATTTT
44[103]	43[103]	CTGAGGCTTAAAGGCC
47[96]	45[95]	CTGAGTTTGTTGAAAATCTCCAAAGGTGAATT
2[103]	3[103]	GTTTGCCCACGTATAA
27[112]	60[107]	TCCCAAGATACCAAAATTCGCAAACCTGTTTAGCTAT
36[87]	40[80]	TTTAATCAAAATATTGGGAATTAGGCAAAAGAAAATCCGC
33[24]	35[47]	CCCTTTTTGAATCTTAAAGACACCACGGACAGTCAGGACG

34[87]	36[88]	AACTGGCACTAACGGAACAACATTATTTCAAC
18[47]	5[47]	TAACGGATACGCAAAT
0[63]	23[63]	CACTAAATGAATAGGT
23[96]	22[96]	ACCCTCAGAACCGTGTTTAGTTTGACCTTTAA
6[143]	58[115]	AACTCACATTAATTGCGCCTAATGCGCTTCGCCATTCAGGCTGCG
4[71]	16[64]	TTAGACAGACTTCTTTTCTCTTTTAGTACACATGAATAAT
23[128]	49[143]	ATATAACATGTTTTAATGAATATACAGCGGAGGCGC TAAACAACTTTC
5[24]	63[36]	AAAGAGTCTATAATCACATAAATCAATAT
37[72]	35[71]	GGGAAGGTTTGTGAATTACCTTATACGTTAAT
28[135]	55[140]	TCCAACAGAAGCGAACTATCGCGTCAGAAGCAAAGCG
12[31]	55[31]	CAATTCGACCCAATAGAGTCAGAGTACAATTT
3[104]	2[104]	CGTGCTTTCCTCGGACGGGCAACAAGTTGCAGCAAGCG GTCCACGCTG
43[72]	39[79]	CGCCACCCTGAGGAAGCGAAAGAGAGCCAGCAAGACCAGG
5[88]	3[87]	ACGCGCGGAACAGGAGGCCGATTAGGTTGCTT
6[103]	7[119]	GTCGGGAAGAGCCGGAAGCATAAAGTGTAAAG
1[104]	1[140]	TTGGAACAAGAGTCCACTATTAAAGAACGTGGACTCC
27[136]	15[138]	CTTTTGATAAGCAAACAAT
25[16]	22[11]	ATAAATAAGAGAAAACTTTTT
48[15]	26[5]	ACTGGTAAACCGTGTGAGTACCGACAA
37[24]	42[11]	GTTTACCATTTGCCATCTTTTCATAATCA
62[15]	62[5]	TCTGTAAAACC
27[16]	20[11]	ATTCTGTCAACATCAAGAAAA
3[24]	2[16]	TGCGCGTACGCTGGCAAGTGTAGC
50[31]	44[11]	TTATTCTGCAGAGCCAGAGGCAGGTCAGACGATTGGC
63[128]	19[135]	TAGTAGTAAAAATTAATCACCATC

46[140]	43[138]	GAACAACTAAAGGTTTTCTGTCATCGCCCGCAGCGAAAGA
37[11]	36[11]	GAAAACAATA
9[16]	58[24]	TTCTGGCCAACAGAGAAGTAATAAATCACCTTAGCAGCAA
12[138]	31[127]	GGCGCATCGTAACCGTGCATGCGGAAT
43[11]	48[16]	AAATCACCGGAACCTTGAGTACCTATTTCACTAGTGT
31[16]	12[11]	TTACCGCGCAACTCGTATTAA
2[143]	62[128]	CGCCTGGCCCTGAGAGGCTGATTGAATCATAC
7[120]	18[120]	CCTGGGGTGTTGCGCTATGAACGGATTCAACC
10[119]	8[104]	AAGTTGGGCGGAAACCTTTCCTGTGTGAAATT
57[3]	10[8]	ATAAAACAGAGGTAAAAATAC
27[5]	28[5]	AAGGTAAAGTAGCAAGCCGTTT
24[143]	23[138]	GCTCAACAGTT
51[0]	40[8]	CAGTTAATGCCCCCTGACAGTGCCTTAACGGGAGCGTCAG
14[138]	59[146]	ATTGGTGCGGGCCT
61[0]	18[8]	TTTGAATTTCGTCGCTACATTTAATTTAATGGGTTACAAA
41[8]	38[3]	ACTGTAGCATCGATAGCAGCA
19[8]	16[13]	ATCGCGCAAAT
56[140]	11[135]	GAAAGGGGCCAGCTCCAGGAT
35[11]	54[3]	TAAAAGAAACGCACCAATAAGAGCAAGAAACAAT
17[13]	58[8]	AAAGAGGCGGT
4[132]	5[132]	TTCTTGGTTT
13[11]	56[3]	ATCCTTTGCCCGAATCAAACCCCACCAGCAGAAG
47[13]	24[5]	GATACAGGCCTAATTTAATGGTTTGAAATA
62[143]	3[143]	ATCCAATACCCTTCAC
55[3]	32[8]	GAAATAGCTTTTGTGCTAAAT
40[135]	39[140]	AAACAAAGATATTCATTACCC
48[143]	21[138]	AACAGTTTATGCTGTAAAGAGGTCGAG

18[135]	17[140]	AATATGATTAATCGTAAAACT
60[138]	63[143]	AGCGCATTAAC
49[5]	50[0]	GTTCGTATAAA
15[11]	14[11]	TTTGAAAAAG
38[140]	35[138]	AAATCAACGTAACAGATTAAGAACACCAGTAGGAATACCA
39[3]	52[8]	CCGTAATCAGTAGAGAATTGA
63[5]	60[0]	TTTCAATTTCA
23[11]	0[13]	CAAATATATTTTATTGACGGGGAA
38[95]	42[88]	GCCATTTGACGGAAATACTAAAGA
15[24]	49[36]	ATCATTTTATGAAACACAGACGACTAATAAGAAAACATGAAAGTA
38[23]	26[16]	ATGAAACCGCGTTTTCTTGCCTTTGTCAGTGCGAATATAA
38[63]	42[56]	AGTAGCACTCAACCGAAAACGGGT
19[40]	17[47]	CCTGAAACACCATATCAACGTCAG
41[120]	44[120]	GATTATACCGATCTAACACCCTCAACGCATAA
22[95]	47[95]	CCTCCGGCCGTTATACCGCCACCCCCGTAACA
19[96]	17[111]	CAAAAGGGTGAGAAAGTAATCAGAGCAAACAA
16[95]	26[88]	TCCTGATTGATGATGGATACTTTTAAGTCCTGAATTGAGA
51[107]	48[112]	TTCCAGACGTTAGTTCCACAG
29[104]	15[119]	TTTAACGTCAAAATTCATATTTTGAAAAACAG
17[112]	6[104]	GAGAATCGCACTGCCCGCTTTCCA
21[56]	25[63]	GTCAATAGGTAAATGCATTACTAG
16[63]	26[56]	GGAAGGGTGAGCGGAACAAGGATAATGCAGAAATGTAATT
30[55]	14[48]	GAATTAACTTACAAAACCATCAAA
14[71]	32[64]	TTAACCAATAACAACCAGCGCATTATTCTAAGGTTTTAGC
40[31]	41[31]	TAAGGAGTATCGGCAT
13[56]	29[63]	TGAGCGAGTAGGAACGTAAACAGC
39[32]	53[39]	GAACTGACGCCGGAAACGTCTTTC

57[109]	10[96]	TGCTAACGCCAGGGTTTTC
25[112]	0[104]	AAAGCAGCGAGTAGATCTGGAAGTGTCTATCAGTGAACCA
18[79]	7[71]	TTGAGAGAGATAATGAGCATTTAGTAATAACAGAAATACC
26[55]	0[48]	TAGGCAGAGAATCATATGATGCAAATAGCCCGCGGAACCC
59[115]	27[127]	CAACTGTTGGGAATATGTACCGAAGATTGATCGGTTGGTACCTTT
39[80]	21[87]	CGCATAGGCAATAATCCAATAGATGCGGGAGAATAGGTCT
19[120]	25[127]	CAGTCAAAGCAAATAATGGTCATACTGCGAACTTAATTGC
13[88]	29[95]	GGAACAAAATTTTTGTAAGAAACG
29[40]	13[47]	TTTGCCAGTGAACACCTCATCAAC
39[48]	21[55]	AAAGAGGAGAACGGGTTTCAGCTAAAAATTTTTGAGAAGA
41[32]	37[39]	TTTCGGTCTATTAGCGGCGCCAAA
53[115]	38[120]	ACGAGAATGACCAAAAGCTGC
48[36]	51[31]	TTAAGAGGCTGAGGGAACCTA
41[96]	37[103]	AAACACTCCTTTGAGGTATTCATT
15[80]	18[80]	GATTATCAGTTTGGATTGTGTAGGAGCTATTT
49[112]	20[104]	ACAGCCCTTAGCAACGCTCAACAGAGATACATACATTATG
58[39]	57[34]	TGAGAGCCGCT
39[112]	14[104]	TCTTGACATAGTCCTAATTTACGAAAAGCCCCTTAAAATT
40[79]	14[72]	GACCTGCTTTTATCAAGGCTGTCTATATTCCTCTCATTTT
13[32]	31[47]	GCCAGCTTCTGAACAACAAGCAAATCAGATAT
26[127]	46[120]	GGATGGCTCATAGTTACTGTAGCATAAATGAAAATTGCGA
60[31]	40[32]	TTAGAATCTAGCGATAGCTTAGATCGAGCCAGGACAAT AAGTCAATCA
30[111]	12[96]	AATAGCAGTGACCGTATTTGAGGGGACGACAA
14[103]	32[96]	CGCATTAACGGCGGATCCTTTACATTTAGACTAGGCTTTT
40[47]	14[40]	CGCAGACGACAACATGATTAAACCAAGAAACCAATAATTC
13[128]	31[143]	TGGTGTAGCCTCAAATCGTCATAAATATTCAT

25[40]	20[40]	AAACACCGGGCATTTTTAAGACGCTAGGCAAA
41[64]	37[71]	ACCTAAAATTTCCATTTTGAGGGA
52[39]	55[34]	CAGAGATCTAT
62[36]	23[39]	ATGTGAGTGAATAATTTTCCCTTTAGAGCGTTAATTTCATGGTTG
29[16]	15[23]	GTAGGAATTTAATTTTGTAACATT
61[107]	23[127]	ATTTTCATTTGGGGCGCGCAAGAAAAACCTTCATTCC
21[88]	26[96]	GAGAGACTACCTTATTTAGGGCTT
22[71]	40[64]	AACTATATTGAATTTAACGCCAACCGCGCCTGCCATGTTA
30[127]	52[115]	GCTTTAAAATTATAGTTTTAATTCAGAAA
14[39]	39[31]	GCGTCTGGCCTTCTTATGAGCGCTCACTCATCTCAGAACC
19[64]	29[71]	TGCAATGCTTTCAACGTTATCATCTTCCTTATCATATTAT
38[119]	27[111]	TCATTATCCCCCCAGCAGATTTGTATCATCGCAAATAATA
26[87]	0[80]	ATCGCCATATCATATGTTAGGTTGGAGGTTTATTTTGGGG
29[72]	11[79]	TTATCCCAAACAGGGACGTCGGATGTCAATAGTATCTAAA
15[48]	18[48]	ACCAGAAGTAGAACCTCCTCATATAGAAACAA
17[80]	5[87]	CAGGTCATTGCCAGCTATCGGCCA
30[87]	14[80]	AACATAAAATCCAAATTAAATCAG
25[72]	21[79]	TGTTTAGTATTTAACATCAAAATC
39[64]	38[64]	CGGTGTACAAATCACC
22[39]	47[31]	GCAAGACAAAGAACGCGGCGTTAACTGACCTACAAGAGAA
14[127]	40[120]	AAACGTTAGAGCTTCAGTCAGGATAGAACCGGTACAACGG
63[112]	4[104]	GCATCAATTGATTAGAATCAGAGC
0[140]	22[128]	AACGTCAAAGGGCGGCAAAGATCCCAATT
29[5]	29[15]	TTATTTTCATC
33[8]	30[16]	AGCTATCTTACCGAAGAGATTAGTCACCCAGCGGTAATCA
10[135]	13[127]	GTGCTGCAAGGCGATTGATCGCACTTTCCGGCGGTCACGT
21[11]	60[16]	CAAAATTAAAACACTTGAATT

53[8]	28[16]	GTTAAGCCCAATAACGAACCCACACGACAGAAGAGAACAA
16[140]	14[128]	AGCATGTCAATCAGGGCGATCTAAATTGT
11[8]	7[23]	CGAACGAACTCAATCATCGCCATTTCTAAAGCAAGGG ACATCCAGAAC
45[11]	45[39]	CTTGATATTCACAAACAAATAAATCCTCA
59[8]	5[23]	CAGTATTAACACCGCCATGAAAAAGAAATTGCTGGTAA TAACCGAGTA
20[138]	15[135]	CATAAAGCTAATATAAGCA
47[32]	46[13]	GGATTAGGCAGTAAGCGTCATACATGGCTTTTGAT
8[135]	9[143]	ATCATGGTCCGGGTACCGAGCTCG
34[47]	34[11]	CAAACGTAGAAAATACATACATAAAGGTGGCAACATA

S5.2.3.2 Strand sequences for DNCP2

For making DNCP2 (5 nm) the two red strands were replaced by DA1 and DA2.

DA1 = 10[119] + **A1**:

AAGTTGGGCGGAAACCTTTCCTGTGTGAAATT **TGTG GTC TAT GTC GTC GTT CG CTA GTA GTT CCT GGG CTG CAC**

DA2 = **A2** + 7[120]:

TCG AGG CGT AGA ATT CCC CCG ATG CGC GCT GTT CTT ACT CA CCTGGGGTGTTGCGCTATGAACGGATTCAACC

For all other structures, DA2 was always used instead of the normal strand (without antenna). For making DNCP2 (21 nm), DA2 was used. To provide the other antenna, the blue strand was replaced by DA3.

DA3 = 9[40] + **A1**:

TTCTGACCTGAAAGCGTAAGAATATTTACATTGGCAGATTAGGAAAAA**TGTG GTC TAT GTC GTC GTT CG CTA GTA GTT CCT GGG CTG CAC**

For making DNCP2 (33 nm), DA4 was used instead of DA3 (the normal green strand was replaced).

DA4 = 16[23] + **A1**:

AAAACAGAGAGGCGAAAATACCAAAAACAGTAGTGAGGCCGGTCACGC**TGT G GTC TAT GTC GTC GTT CG CTA GTA GTT CCT GGG CTG CAC**

For making DNCP2 (41 nm), DA5 was used instead of DA4 (the normal purple strand was replaced).

AAACACTCCTTTGAGGTATTCATT **TGTG GTC TAT GTC GTC GTT CG CTA** GTA GTT CCT GGG CTG CAC

S5.3 Annealing the DNs

S5.3.1 Td

All the wireframe tetrahedron structures (TdP0, TdP1, TdP2, TdP3, TdP4, TdS1, TdS2) used in this project were annealed in 1 uM concentration mixing the four constituent strands in 1:1:1:1 molar ratio in 1X TAE/Mg^{2+} buffer following a flash-freeze protocol (2 min heating at 80°C, immediately cooling down to 4°C).

S5.3.2 TD

All the larger tetrahedral (TDP0, TDP12, TDP24) were annealed in 250 nM concentration mixing the strands 1,2,3 and 4 in the molar ratio 1:3:3:3 in 1X 3D buffer following an annealing program that heated the strands to 80°C and cooled them to 4°C over a period of 12 hours.

S5.3.3 DNC

All the DNC structures were annealed in 5 nM concentration by mixing 5 nM m13 scaffold and 10X staples in 1X 3D buffer. The annealing program used heated the mixture of strands to 95°C and cooled them to 4°C over a period of 37 hours.

S5.4 Characterization of annealed DNs

S.5.4.1.Td

The annealed structures were characterized via a 3% mini agarose gel run in 5 mM borax buffer for 8 min at room temperature under 300V. 5 uL of 1 uM structures mixed with 1 uL 6X loading dye was loaded on each well. After completion of run, the gel was stained with ethidium bromide solution for 5 minutes for band visualization.

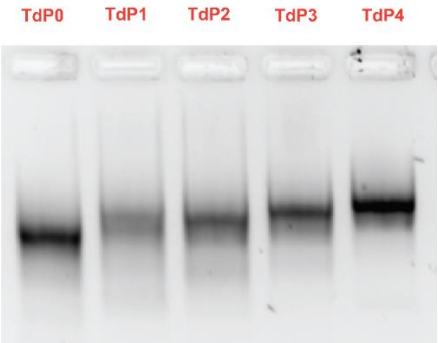

Figure 5.4: Agarose gel for characterization of TdP structures.

S.5.4.2 TD

The annealed structures were characterized via a 1.5% agarose gel run in 1X 3D buffer for 30 min at 4°C under 100V. 5 uL of 1 uM structures mixed with 1 uL 6X loading dye was loaded on each well. After completion of run, the gel was stained in ethidium bromide solution for 5 minutes for band visualization. After completion of run, the gel was stained with ethidium bromide solution for 5 minutes for band visualization.

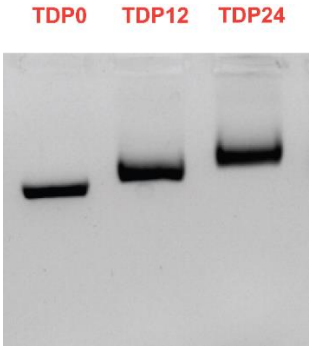

Figure 5.5: Agarose gel for characterization of TDP structures.

S.5.4.3 DNC

The annealed structures were characterized via a 1% agarose gel run in 1X 3D buffer for 1 h at 4°C under 100V. 10 uL of 5 nM DNC mixed with 2 uL 6X loading dye was loaded on each well. After completion of run, the gel was stained with ethidium bromide solution for 5 minutes for band visualization.

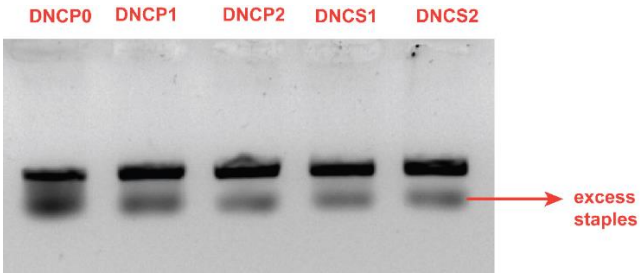

Figure 5.6: Agarose gel for characterization of DNC structures.

S5.5 Proximity Ligation

The ligation mixture contained 11.2 uL (7 uM) of the connector strand, 200 uL of 10X T4 ligase buffer, 2 uL (40U/uL) of T4 ligase, 768 uL water, thus resulting to a total volume of 1000 uL. We mixed this solution with each sample as and when required in 1:1 volume ratio and incubated for 10 minutes at room temperature prior to RTPCR.

S5.6 RTPCR

S5.6.1 Primers used during RTPCR:

P1 forward: 5'ATG TGG TCT ATG TCG TCG TTC G

P2 reverse: 5' TGA GTA AGA ACA GCG CGC AT

S5.6.2 RTPCR Protocol

We optimized the PCR conditions and obtained the finalized protocol as:

Stage 1: 95 °C 120 s Optics off

Stage 2 (Repeat 37 times): 95 °C 15 s optics off, 58 °C 20 s optics on, 75 °C 15 s optics off

Stage 3 (Melting curve): Start 57 °C end 95 °C optics Ch1, 0.2 °C/sec

S5.7 Calibration Curve

S5.7.1 PLA product for the antennae pair

A1 & A2 = A1+A2:

TGT GGT CTA TGT CGT CGT TCG CTA GTA GTT CCT GGG CTG CAC TCG AGG CGT AGA ATT CCC CCG ATG CGC GCT GTT CTT ACT CA

S5.7.2 Construction of the calibration curve

We used serially diluted concentrations of the ligated product (A1 + A2) of the antennae pair to construct the calibration curve. Log of copy number per unit volume was plotted against the threshold cycle (Ct) values. This curve was used in further experiments to fit the threshold cycle (Ct) values obtained from RTPCR experiments and obtain the particles per unit volume.

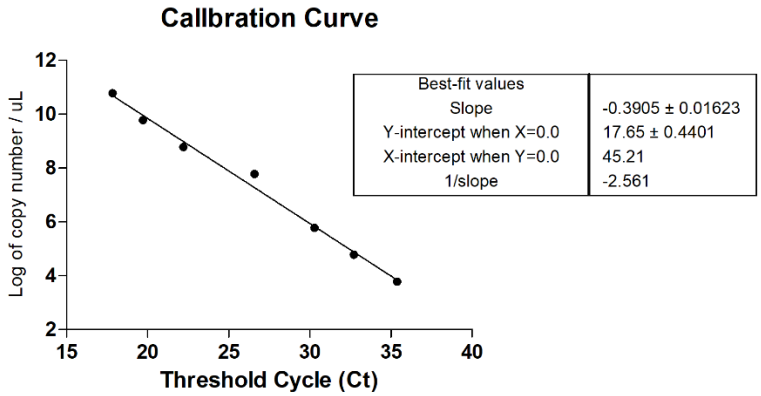

Figure 5.7: Calibration curve for PLA

S5.8 Data Analysis

All the Td, TD and SQ samples were annealed at 1 μM, 250 nM and 5 nM concentrations (of structures and not antennae) respectively. The Td samples were annealed in 1X TAE/Mg^{2+} buffer while the other two in 1X 3D buffer. Four serial dilutions (each 10 fold) were made for each sample and triplicate of each dilution was studied. The values presented here are the average values from a particular triplicate of the third dilution, which is 10^3 fold dilution. Hence, for Td, TD and SQ, we reported the values from 1 nM, 0.25 nM and 0.05 nM samples.

S5.9 PLA in Different *In Vitro* Conditions

We incubated TdP2 and TdS2 in four different media for 48 hours and collected 12 uL aliquots at different time intervals. Those aliquots were used for PLA and gel electrophoresis experiments. The gel electrophoresis was done using 1% agarose gel, in 1X 3D buffer under 90 volts and 4°C.

a)

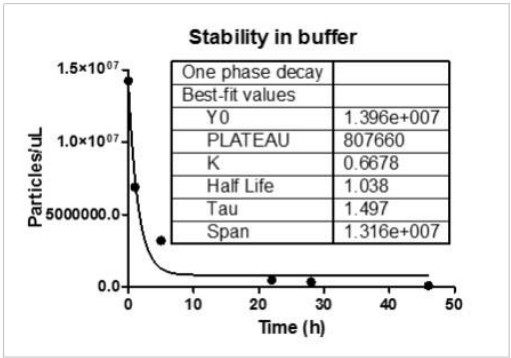

b)

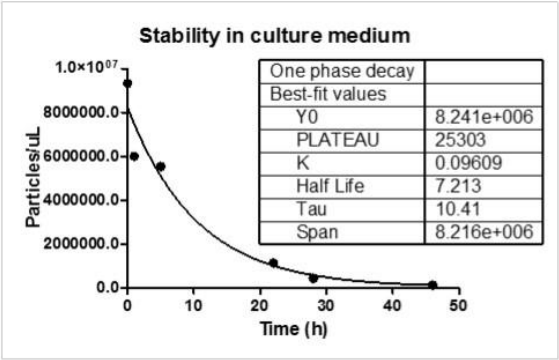

c)

d)

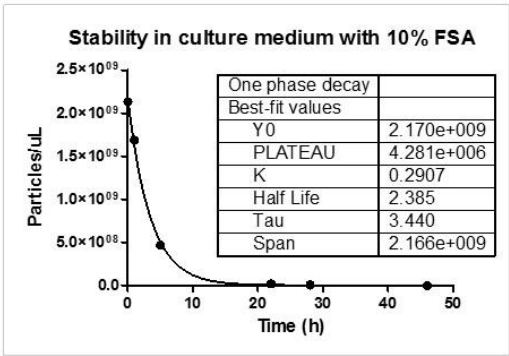

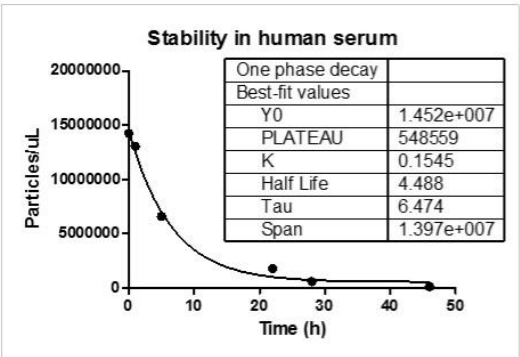

Figure 5.8: In vitro time vs stability plots for TdP2 in a) 1X 3D buffer b) DMEM c) DMEM + 10% FBS, and d) human serum.

S5.10 PLA in *In Vivo* Conditions

S5.10.1 Injection

100 uL, 1 uM of each of TdP2 and TdS2 in 1X PBS buffer were injected separately in Wister rats. A small cut was made at the tail-end of each animal and 5 uL of blood was collected at different time points for each sample.

S5.10.2 Separation of samples from blood

a) Add 3 uL of blood in 200 uL of 5% suspension of Chelex 100 in water.
b) Vortex immediately for 10 sec
c) Incubate for 30 min on 56°C
d) Vortex for 10 sec
e) 8 min in boiling water
f) Centrifugation 3 min 10000g
g) Separate supernatant for RT PCR

Then I add 1 uL of sample to 24 uL of RT PCR master mix and run it on the previously mentioned RTPCR program.